GKSS FORSCHUNGSZENTRUM in der HELMHOLTZ GEMEINSCHAFT

Investigations on the Environmental Chemistry of Atmospheric Mercury on Local, Regional and Global Scales

Vom Fachbereich Umweltwissenschaften der Universität Lüneburg als Habilitationsschrift angenommene Arbeit

Author:

R. Ebinghaus

ISSN 0344-9629

GKSS 2003/23

GKSS 2003/23

Investigations on the Environmental Chemistry of Atmospheric Mercury on Local, Regional and Global Scales

Vom Fachbereich Umweltwissenschaften der Universität Lüneburg als Habilitationsschrift angenommene Arbeit

Author:

R. Ebinghaus

(Institute for Coastal Research)

GKSS-Forschungszentrum Geesthacht GmbH • Geesthacht • 2003

ISSN 0344-9629

GKSS-Forschungszentrum Geesthacht GmbH · Telefon (04152)87-0
Max-Planck-Straße · D-21502 Geesthacht / Postfach 11 60 · D-21494 Geesthacht

GKSS 2003/23

Investigations on the Environmental Chemistry of Atmospheric Mercury on Local, Regional and Global Scales

(Vom Fachbereich Umweltwissenschaften der Universität Lüneburg als Habilitationsschrift angenommene Arbeit)

Ralf Ebinghaus

218 pages with 67 figures and 29 tables

Abstract

Mercury is outstanding among the global environmental pollutants of continuing concern. Long-range atmospheric transport, its transformation to more toxic methylmercury compounds, and their bioaccumulation in the aquatic food-chain have motivated intensive international research in this field.
The starting point of this habilitation thesis is a research study carried out to assess the mercury emissions and environmental impact from a partly demolished industrial plant in the Halle/Leipzig area as an example for the atmospheric dispersion of atmospheric mercury on a local scale. It was estimated that between 2 to 4 kg were emitted per day from the industrial complex and that about 30 % of the emissions were deposited in the local vicinity of the plant, whereas 70 % were available for long-range-transport at least on a regional scale.
Since gaseous elemental mercury has an estimated average in the atmosphere of about 1 year, it is also subject to long-range-atmospheric transport on regional, hemispherical and even global scales. Observational data on the spatial and temporal distribution of atmospheric mercury are extremely limited. Analytical capabilities have been developed to generate input data for numerical simulation models to quantify the distribution, transport and deposition of atmospheric mercury over north-western and central Europe. The data sets presented in this work are currently in use as reference data for an international model intercomparison exercise under the UN-ECE Convention on Long-Range Transport of Air Pollutants, coordinated by EMEP-Meteorological Synthesizing Centre East in Moscow, Russia.
Long-term measurements at a site located at the western Irish coast line have shown stable concentration levels of atmospheric mercury over several years despite reduced emissions in Europe. An increase of 4 % per year was detected for air masses clearly of marine origin, possibly reflecting a trend in global emissions.
A significant concentration gradient has been measured between the northern and southern hemisphere with an about 30 % higher northern hemispheric mean.
Finally, first measurements of atmospheric mercury have been carried out in Antarctica and are supplemented by data of a Canadian group obtained in the Arctic to assess the importance of polar regions as sinks in the global cycling of mercury. With the first annual time series of atmospheric mercury in the Antarctic it could be shown that the phenomenon of mercury depletion events (MDEs) do occur in the South polar region and that these events are positively correlated with ground level ozone concentrations during Antarctic spring.

Untersuchungen zum umweltchemischen Verhalten von atmosphärischem Quecksilber auf lokalen, regionalen und globalen Skalen

Zusammenfassung

Das Quecksilber ist als globaler Schadstoff nach wie vor von herausragender Bedeutung in der umweltpolitischen Diskussion. Die großräumige Verfrachtung über die Atmosphäre, die Bildung toxischer Methylquecksilber-Verbindungen und die Bioakkumulation in der aquatischen Nahrungskette haben intensive internationale Forschungsanstrengungen motiviert.

Am Beginn dieser Habilitationsschrift steht ein Forschungsprojekt, in dem Quecksilberemissionen und Umweltbeeinträchtigungen, die von einem teilweise stillgelegten Chemiekombiat in der ehemaligen DDR ausgingen, untersucht wurden. An einem Altstandort im Raum Halle/Leipzig wurde das lokale Verteilungsverhalten von Quecksilber über die Atmosphäre untersucht. Es konnte gezeigt werden, dass aus den stillgelegten Anlagen 2 bis 4 kg Quecksilber pro Tag entweichen und dass davon etwa 30 % im Umfeld der Industrieanlage wieder deponiert wurden, während ca. 70 % für eine großräumige Verteilung zumindest im regionalen Maßstab zur Verfügung standen.

Gasförmiges elementares Quecksilber hat eine durchschnittliche atmosphärische Verweilzeit von etwa einem Jahr und kann somit auf regionalen, hemisphärischen und sogar globalen Skalen verteilt werden. Messdaten zur regionalen raum/zeitlichen Variabilität zum Beispiel in Europa waren zu dieser Zeit kaum verfügbar. Im Rahmen dieser Arbeit wurden analytische Verfahren entwickelt und an verschiedenen Standorten eingesetzt, um Eingabedaten für numerische Simulationsmodelle zu erzeugen, mit denen Verteilung, Transport und Deposition von Quecksilber über Zentral- und Nordwest-Europa untersucht werden konnten. Die Datensätze werden weiterhin als Referenzmessungen für eine internationale Modellvergleichsstudie eingesetzt, die im Rahmen der UN-ECE Konvention für den grenzüberschreitenden Transport von Luftschadstoffen (CLRTAP) vom Meteorologischen Synthese-Zentrum in Moskau, Russland, koordiniert wird.

Langzeitmessungen an einer west-irischen Küstenmessstelle ergaben ein stabiles Konzentrationsniveau über mehrere Jahre, obwohl die Quecksilberemissionen in Westeuropa in dieser Zeit reduziert wurden. Im selben Zeitraum konnte jedoch ein jährlicher Anstieg von 4 % erkannt werden, wenn Luftmassen eindeutig marinen Ursprungs beprobt wurden, was möglicherweise einen globalen Trend der Emissionen widerspiegelt.

Ein signifikanter Konzentrationsgradient zwischen der nördlichen und der südlichen Hemisphäre mit etwa 30 % höheren Konzentrationen auf der Nordhalbkugel konnte experimentell nachgewiesen werden.

Abschließend werden erste Messungen von atmosphärischem Quecksilber an einer Messstelle in der Antarktis beschrieben, die, gemeinsam mit Arbeiten einer kanadischen Gruppe in der Arktis, Einblicke in die Rolle der Polregionen im globalen Kreislauf des Quecksilbers ermöglichen. Mit dem ersten zeitlich hochaufgelösten Langzeitdatensatz konnte gezeigt werden, dass das Phänomen der „atmosphärischen Quecksilberrückgänge" auch in der Antarktis auftritt und dass dieser Effekt mit Rückgängen des bodennahen Ozons gekoppelt ist.

Manuscript received / Manuskripteingang in TDB: 15. September 2003

Table of Contents

1 Introduction

Mercury is outstanding among the global environmental pollutants of continuing concern. Especially in the last decade of the 20th century, environmental scientists, legislators, politicians and the public have become aware of mercury pollution in the global environment. It has often been suggested that anthropogenic emissions are leading to a general increase in mercury on local, regional and global scales.

Mercury is emitted into the atmosphere from a number of natural as well as anthropogenic sources. There is growing body of evidence suggesting that presently mercury emissions from anthropogenic sources are at least as great as those from natural sources (Fitzgerald et al., 1998; Martinez-Cortizas et al., 1999). In contrast with most of the other heavy metals, mercury and many of its compounds behave exceptionally in the environment due to their volatility and capability for methylation.

Mercury is on the priority list of a large number of international agreements and conventions aimed at the protection of the environment including all compartments, human health and wildlife (e.g. HELCOM, OSPAR, AMAP, UN-ECE, EMEP, EU-AQFWD)*[*]

Long-range atmospheric transport of mercury, its transformation to more toxic methylmercury compounds, and their bioaccumulation in the aquatic foodchain have motivated intensive research on mercury as a pollutant of global concern. Mercury takes part in a number of complex environmental cycles, and special interest is focused on the aquatic-biological and the atmospheric cycles.

Environmental cycling of mercury can be described as a series of processes where chemical and physical transformations are the governing factors for the distribution of mercury in and between different compartments of the environment. Mercury can exist in a large number of different physical and chemical forms with a wide range of physical, chemical, and ecotoxicological properties and consequently with fundamental importance for the environmental behaviour. The three most important chemical forms known to occur in the environment are:

- elemental mercury [Hg(0)], which has a high vapor pressure and a relatively low solubility in water;
- divalent inorganic[Hg^{2+}or Hg(II)], which can be far more soluble and has a strong affinity for many inorganic and organic ligands, especially those containing sulphur;

[*] see index of abbreviations

- methylmercury [CH_3Hg^+ or $MeHg^+$], which is strongly accumulated by living organisms. Conversions between these different forms provide the basis of mercury's complex distribution pattern on local, regional, and global scales.

At the beginning of the last decade the most important European emission sources for atmospheric mercury were located in the former German Democratic Republic (GDR). For entire Europe the annual anthropogenic emission of mercury has been estimated to be about 726 tons, originating from 928 sources (Axenfeldt et al., 1991). The dominating source categories in Europe at that time were fossil fuel combustion and chlor-alkali plants. Waste incineration and non-ferrous metal smelting contributed less than 10 %. Emissions from GDR accounted for more than 40 % of the European total. The contribution of the GDR originated from a relatively small but in most cases highly industrialized areas. According to Helwig and Neske (1990), extremely high amounts were emitted in the region Halle/Leipzig/Bitterfeld, due to the burning of lignite coal in power plants without desulfurisation equipment and high losses of mercury from the chlor-alkali factories.

As a consequence of the political changes in East Germany many of the major emission sources had been shut down.

The start-off point of this work is a research study carried out to assess the mercury emission from one partly demolished industrial plants in the Halle/Leipzig/Bitterfeld area as an example for the atmospheric dispersion of mercury on a local scale.

Since gaseous elemental mercury has an estimated average lifetime in the atmosphere of about 1 year, it is also subject to long-range transport on regional, hemispherical and even global scale.

At GKSS Research Center numerical models and analytical capabilities have been developed to quantify the regional, spatial and temporal distribution of atmospheric mercury over north western and central Europe and will be described here.

Finally, first measurements of atmospheric mercury in the Antarctic have been carried out during this work and will be supplemented by data of Canadian researchers for the high Arctic to assess the importance of polar regions as receptors in the global cycling of mercury.

The following chapter will summarize present knowledge on the sources and magnitudes of natural and anthropogenic mercury fluxes to the atmosphere from various sources and their relative importance on local, regional and global scales. To characterize the main emission pathways, the Expert Panel on Mercury Atmospheric Processes (1994) defined three different terms for mercury emissions:

- Anthropogenic mercury emissions: the mobilization or release of geologically bound mercury by man's activities, with mass transfer of mercury to the atmosphere.

- Natural mercury emissions: the mobilization or release of geologically bound mercury by natural biotic and abiotic processes with mass transfer of mercury to the atmosphere.
- Re-emissions of mercury: the mass transfer of mercury to the atmosphere by biotic or abiotic processes drawing on a pool of mercury that was deposited to the Earth's surface after initial mobilization by either anthropogenic or natural activities.

1.1 Sources and Magnitudes of Anthropogenic Mercury Emissions

Mining, smelting and refining of metals and their myriad applications have resulted in the mobilization and dispersion of large amounts of heavy metals into the environment. Emissions into the atmosphere during extraction, production, fabrication, application, and their end-use have resulted in a widespread distribution of their compounds, including mercury. While the emissions in the developed countries are relatively well quantified, those in the developing world are poorly known.

The main types of anthropogenic emission sources may be categorized as follows (Porcella et al., 1996):

1. COMBUSTION

Fossil Fuels (coal, oil, gas) and wood

Wastes (municipal, medical, hazardous wastes)

Sewage sludge

Crematories

2. HIGH TEMPERATURE PROCESSES

Smelting

Coking

Ore roasting

Cement and lime production

3. MANUFACTURING COMMERCIAL

Chlor-alkali plants

Metal processing

Chemical and Instruments Industry (mercury chemicals, paints, batteries, thermometers, process reactants & catalysts)

4. GOLD EXTRACTION

5. OTHER SOURCES

Fluorescent lamps

Hazardous and municipal waste sites

Mine spoils

Land disturbance (e.g. deforestation, reservoir construction)

Pacyna and Pacyna (2000) estimated the global anthropogenic mercury emissions for the major processes mentioned above. The results are summarized in Table 1.1.

Table 1.1: Global Emissions of Total Mercury from Major Anthropogenic Sources in 1995 in Tons

Continent	Stationary combustion	Non-ferrous metal production	Pig iron and steel production	Cement production	Waste disposal	Total
Europe	185.5	15.4	10.2	26.2	12.4	249.7
Africa	197.0	7.9	0.5	5.2		210.6
Asia	860.4	87.4	12.1	81.8	32.6	1074.3
North America	104.8	25.1	4.6	12.9	66.1	213.5
South America	26.9	25.4	1.4	5.5		59.2
Australia & Oceania	99.9	4.4	0.3	0.8	0.1	105.5
Total	1474.5	165.6	29.1	132.4	111.2	1912.8

When they are produced during combustion processes, oxidized forms of mercury can be retained in modern flue gas cleaning systems (Pacyna, 1996). Mercury retained in fly-ash as well as in bottom ash is disposed of on land where it may be released by volatilization or find its way in a form of direct releases to the aquatic environment. The mercury content of coal from different parts of the world are summarized in Table 1.2. Apart from the coal and fossil fuels, a significant proportion of mercury emissions is attributed to mercury in the various raw materials used for industrial purposes. The concentrations of mercury in various raw materials are summarized in Table 1.2. Though, the concentrations of mercury in these raw materials is small, their contribution to the total emission of mercury is significant as they are used in extremely large quantities.

Table 1.2: Mercury Content in Different types of Raw Materials (adapted from Mukherjee, 1996)

Source Category	Origin	Mercury Content ($\mu g\ g^{-1}$)	Reference
Coal	various	0.04-3.3	Meji,1991 Airey, 1992
Coal		0.02-1.0	Swaine, 1990
Coal	Australia	0.01-0.25	Sloss, 1995
Oil	Former USSR	0.005	Mukherjee et al., 1995
Peat	Finland	0.01	Mukherjee et al., 1995
Wood	Finland	0.01	Mukherjee et al., 1995
Cu-ores	USA	0.5 (average)	Jaisinski, 1995
Zn-concentrate	Finland	100-500	Kuivala, 1984
Cu-concentrate	Finland (Domestic)	13	Rantalahti, 1996
	Finland (Imported)	110	Rantalahti, 1996
Cu-concentrate	Sweden	200	Dyvik, 1995
Pb-concentrate	Sweden	50	Dyvik, 1995

Historically, and today in developing countries, the caustic soda industry producing chlorine and sodiumhydroxide is a significant source of atmospheric mercury emission. As outdated Hg-consuming processes are replaced with other methods, active mercury emissions are eliminated. However, wastes from earlier operations stored nearby have been shown to emit Mercury to the atmosphere at rates which may exceed those allowed for modern mercury process alkali plants (Lindberg and Turner, 1977).

Mercury is used throughout the world for the production of gold using the amalgamation technique (Cleary, 1996). Starting in Latin America in the 1980s a revival of the use of amalgamation in gold panning has spread rapidly in tropical areas and roughly 10 million people was estimated to be engaged in this activity (Ramel, 1996). The gold/mercury amalgam is usually caught in a sluice box and then heated in an pan where the mercury

evaporates into the air and the raw gold remains. In Brazil alone, gold production comprises about 2000 sites ("garimpos") of which about 80% are located in Amazonas. It is mostly small scale activity in remote villages and the amount of mercury released to the environment is about 1.3 kg mercury for each kg of gold or an overall estimated emission of 180 tons y^{-1} (Ramel, 1996). It has been estimated that about 2 million people in Brazil alone are directly or indirectly dependent on gold extraction (Branches et al., 1993). In Tanzania, 250,000 people live in gold mining villages along river- beds (Ikingura and Mutakyahwa, 1995). Official statistics concerning gold production and use of mercury are often under-reported because of illegal use and wide spread smuggling of both mercury and gold. The current and total emissions of mercury to the atmosphere from different gold mines is summarized in Table 1.3. It is evident from the table that mercury emissions from mining activities are quite significant.

Table 1.3: Estimates of Current (t y^{-1}) and Total (tons emitted to date of original reference) Emissions of Mercury to the Environment from Gold Mining Sites

Site	Period of operation	Annual Emissions	Total Emissions	Reference
Amazon, Brazil	since 1979	180	3000	Pfeiffer & Lacerda, 1988
Hindanao Is., Phillipines	since 1985	26	200	Torres, 1992 & Craemer, 1990
Rio de Janeiro, Brazil	since 1985	0.5	3.0	Lacerda et al., 1997
Puyango River, Peru	since 1987	2.9	14	CIMELCO, 1991
Narino, Colombia	since 1987	0.5	3.5	Priester, 1992
Colombia				
Victoria fields, Tanzania	since 1991	6.0	24	Ikingura, 1994
Pando Dept., Bolivia	since 1979	7-30	300	Zapata, 1994
Dia pi Valley, China	since 1938	2.4	130	Ming, 1994
Dixing region, China	since 1992	120	360	Yshuan & Liu, 1994
Guyana Shield, Venezuela	since 1989	40-50	300	Nico & Taphorn, 1994
TOTAL	since 1938	385.3 - 418.3	4336	

1.2 Sources and Magnitudes of Natural Emissions

The assessment of truely "natural" mercury sources and their relative importance compared to direct anthropogenic emissions and indirect (re)-emissions is a fundamental problem in studying the global balance and cycling of mercury in the environment. This knowledge is critical to our understanding of the fate of mercury since so-called natural emissions cannot be reduced or controlled in most cases. Unfortunately, as discussed below, it is very difficult to differentiate between natural and indirect anthropogenic mercury emissions into the environment. Natural mercury emissions in this context are taken to include mercury transport phenomena that would take place in the absence of human existence and activity. However, once any pool of mercury has formed in an environmental compartment, it is no longer important where it originated, since all mercury is subject to the same transport and transformation processes, although it is possible that mercury from different origins may maintain a different speciation in the same compartment and thereby react differently. This chapter will demonstrate the problems associated not only with assigning relative importance of anthropogenic and natural contributions to the same flux phenomena, but also with separating and comparing different controlling processes leading to these flux phenomena. Table 1.4 summarizes the major sources and processes that could be attributed to natural inputs of mercury into the atmosphere.

Table 1.4: Natural Sources and Exchange Processes of Atmospheric Mercury

Sources:

1. Wind Erosion and degassing from mercury mineralized soil and rock formation
2. Volcanic eruptions and other geothermal activity
3. Evasion of mercury from the Earth's subsurface crust

Exchange Processes:

4. Atmospheric interactions with terrestrial compartments
5. Interactions with the oceans
6. Interactions with freshwater ecosystems

There are numerous environmental pathways exchanging mercury with the atmosphere that come to our mind when we think of "natural" processes (Table 1.4). Among these, however, only the first three are clearly and unambiguously natural and undisturbed by anthropogenic influence. They could be classified as geological sources (meaning they have their origin in the deeper regions of the Earth's crust) and are also the only ones that are exclusively sources. The other three processes are all (more or less) influenced by human activities and are both sources and sinks of atmospheric mercury. In contrast to the former, they could be characterized as "surface linked" processes because they only occur at the very surface of the Earth's crust. The big question for those interactions is: are they net sources or sinks ? In the following chapters, it will be attempted to quantify the first three processes and to evaluate the flux direction and magnitude for the three natural air-surface exchange processes.

It seems to be the general opinion that whenever elevated mercury concentrations are encountered in any ecosystem compartment in the absence of obvious local or direct anthropogenic sources, this can be interpreted as proof of an anthropogenic influence via atmospheric long-range transport and deposition. While this may be true in many cases, some of these anomalies may be caused, at least partially, by natural local emissions due to underlying geologic anomalies. For example, in the case of elevated mercury concentrations in plants, foliar atmospheric uptake of crustal mercury emissions or root uptake from geologically enriched soils are possible alternative explanations to long-range transport of pollutants (Lindberg et al., 1979). Also, surface enrichment mercury in depth profiles measured in sediment cores may be caused by upward migration due to diagenetical processes or groundwater movement rather than solely by increased discharges or atmospheric deposition to the aquatic systems (Rasmussen, 1994). However, the direct evidence for such sediment re-distribution of mercury has yet to be published. Since these features may be overlooked in ecosystem mass balances, they will be explored in more depth hereafter. The flux estimates presented in the following sections are based on limited direct measurements, simple concentration measurements, or modeling results.

1.2.1 Erosion and Degassing of Mercury From Mineralized Surface Soils

Various estimates assume mercury volatilization rates between 1 and 5 ng m^{-2} h^{-1} for background soils in the mercuriferous belts and mineralized areas compared to below 1 ng m^{-2} h^{-1} in totally un-impacted areas (e.g. Lindqvist et al., 1991). Far higher emission rates (10 – 50 ng m^{-2} h^{-1}) have actually been measured over temperate forest soils impacted by atmospheric deposition (Lindberg et al., 1992; Kim et al., 1995) and over seismic zones

(Varekamp and Buseck, 1986). Flux chamber measurements over cinnabar rich soils in Almadén, Spain, yielded much higher fluxes, on the order of 330 ng m^{-2} h^{-1} (Lindberg et al., 1979), and fluxes on the order of 50-1000 ng m^{-2} h^{-1} were recently measured over geothermal zones in Nevada (Gustin et al., 2001), so locally, these evaporation rates can be of increased importance. Estimates of global natural fluxes from continents based on lower flux estimates suggest a total of 700 t y^{-1} degassing from soils, with 500 t y^{-1} being contributed from the mercuriferous belts (Lindqvist et al., 1991). Clearly, the newer measurements may suggest larger natural emissions. Studies in Siberia reveal that the average content of mercury in ores varies from 0.06-1.2 % (Obolensky, 1996), while the mercury content in minerals of those ore deposits ranges from 0.01 to 2.700 ppm (Obolensky, 1996). From these concentration data, it has been estimated that natural emission due to surface degassing of mercury in Siberia alone (approximate surface area 10^7 km^2) amounts to about 40 t y^{-1} (Obolensky, 1996). If volcanoes and forest fires are included, the estimate rises to 1,700 t y^{-1} (Nriagu, 1989), while 1,290 t y^{-1} were calculated as the sum of soil vapor flux, volcanic and geothermal activities (Varekamp and Buseck, 1986). To put these numbers into context, the mercury pool in a 1 m deep layer of the continents (total area $1.5*10^8$ km^2, assumed density 2 g cm^{-3}, background mercury concentration 50 ng g^{-1}) is $1.5*10^7$ tons.

These estimates demonstrate that degassing from mineralisation zones (ore bodies, geothermal areas, primary and secondary geochemical haloes) is a major contribution to the total continental mercury emissions and it seems to be comparable in magnitude to emissions from volcanic and geothermal activity. Other sources like forest fires or vapor emissions from background soils also contribute significantly to natural continental mercury emissions, but it seems that particulate export in the form of dust is not one of them. The reason for that seems to be that soil particles are fairly coarse (10 µm) and although they might be re-suspended by wind, they will settle quickly and generally not be transported very far in the atmosphere. Typical concentrations of particles of this size in background atmosphere are 25 µg m^{-3} (Finlayson-Pitts and Pitts, 1986) and assuming they have an mercury content similar to background soils (50 ng g^{-1}), this kind of particulate mercury would have a global average concentration of 2.5 pg m^{-3} in ambient air, which is three orders of magnitude lower than total gaseous mercury in background air (Ebinghaus et al., 1995). This also indicates that particulate emission of mercury from mineralized soils to the atmosphere is not likely to be a major source of atmospheric mercury and is much less important than gaseous emission.

1.2.2 Volcanic Eruptions and other Geothermal Activities

Though volcanic eruptions may contribute significantly to the natural emission of mercury, there are only a few studies to report the contribution from this source. Global estimates for mercury release from volcanoes total 830 t y^{-1}, with the vast majority being contributed by active, erupting volcanoes (800 t y^{-1}) and only small amounts (30 t y^{-1}) coming from passive degassing of volcanoes (Varekamp and Buseck, 1986). The fluxes of mercury in the gases from eruptive plumes at Mt. Etna, Italy, and Kuala, Hawaii, and in fumarolic gases at Kilauea, Hawaii, and at White Island, New Zealand, have been estimated by measuring the Hg/S ratios and then correlating those to the sulphur flux from these sources (Fitzgerald, 1996).These results were scaled up globally and it was concluded that the annual mercury flux from volcanic activity is between 20 and 90 t y^{-1} and represents only a small fraction (<3%) of the annual mercury emissions from anthropopgenic sources (Fitzgerald, 1996). This result agrees well with the above mentioned emission from passive degassing volcanoes, but active volcanic eruptions appear to be responsible for the large difference between the two global estimates; thus, their contribution constitutes a large uncertainty factor and should be re-evaluated. Studies at Solfatara volcano, Italy, estimated the mercury emission at 0.9 - 4.5 g d^{-1} (0.3 - 1.6 kg y^{-1}) (Ferrara et al., 1994), which is comparable to estimates for the Kilauea volcano, Hawaii (1.5 kg y^{-1}), but much smaller than estimates for more active volcanoes, e.g. the Colima volcano, Mexico (440 kg y^{-1}), or the Etna volcano, Italy (2.7 t y^{-1}) (Varekamp and Buseck, 1986). Data for mercury emissions from other geothermal sources are even rarer than for volcanoes, but it has been measured that one volcanic geyser on Iceland alone emits 8 kg y^{-1} mercury to the atmosphere (Edner et al., 1991). Also, atmospheric mercury concentrations over a geothermal area were elevated by about a factor of 10 compared to background regions (Gustin et al., 1996), but there is a need for measurements of the contribution of geothermal sources to the global mercury emissions. Although few data are published, a recent study reported mercury emission rates in the order of 10 - 1000 ng m^{-2} h^{-1} in geothermal areas of the western U.S. (Gustin et al; in press). Global mercury emission from geothermal sources has been estimated at 60 t y^{-1} (Varekamp and Buseck, 1986).

1.2.3 Evasion of Mercury from the Earth's Subsurface Crust

It is reasonable to assume that anthropogenic influences on the Earth's geochemistry does not go deeper than the immediate surface layer (probably much less than 0.1 kilometer). However, mercury is permanently released from deeper regions of the Earth's crust and permeates as mercury vapor to the surface through faults and fractures in bedrock. This phenomenon is being explored as a potential indicator of earthquakes, since it has been observed that mercury concentrations in soil air increase dramatically directly before earthquakes occur. Crustal mercury emissions probably display extreme spatial and temporal variation. This has been demonstrated by measurements of mercury concentrations in a subterranean vault in Precambrian Shield bedrock (Klusman and Webster, 1981) where pronounced diurnal and seasonal cycles were observed. Air and soil temperature, barometric pressure and relative humidity were identified as the most important controlling factors. It has been argued that crustal mercury emission on the global scale is mainly driven by crustal heat flow rather than by bedrock mercury content (Varekamp and Buseck, 1986). From this approach, continental crustal mercury evasion from geologic sources alone has been calculated by one author as 3000 to 6000 t y^{-1} (Rasmussen, 1994). This does not include volcanic or geothermal zones, which have to be treated separately due to their much higher heat flow. Overall, this would give a generally larger natural geological mercury flux from the continents to the atmosphere then generally assumed in other mass balances. A review of earlier estimates of natural mercury sources made between 1970 to 1982 summarizes published values in the range 2500 to 30000 t y^{-1} (Lindqvist et al., 1984). A more recent work has ended up with an estimate of 3000 t y^{-1} (Nriagu and Pacyna, 1988).

Results from the geological heat flux approach suggest that mercury transfer through mid-ocean ridges could be on the order of 1900 to 3800 t y^{-1}, while the whole oceanic crust would emit 7300 to 14700 t y^{-1} mercury (Rasmussen, 1994). These results in combination with other sources of submarine mercury like hydrothermal vents, seismic activity and erosion of ocean ridges as well as submerged parts of the continents could give the impression that atmospheric deposition might be negligible in the total oceanic mercury budget (Camargo, 1993). However, other authors assume that deposition is the major source of mercury (re)emitted to the atmosphere from ocean surfaces (Fitzgerald, 1993). These findings contradict each other to a degree that two main questions have to be asked:

- is crustal degassing really the major source of oceanic mercury and
- if so, then what percentage of that mercury actually reaches the atmosphere?

These pathways (and their terrestrial counterparts) definitely have to be investigated much more thoroughly (if possible, by actual flux measurements) before the large discrepancies in global mercury budgets can be resolved. It should, however, be noted that the scientific community is beginning to develop programs for expansion of direct measurement campaigns in international collaborative studies (e.g. Gustin and Lindberg; in press).

1.3 Natural Air/Surface Exchange Processes with Soils, Oceans, Freshwaters and Vegetation

This section will attempt to generalize the common features of mercury exchange between the atmosphere and terrestrial or aquatic compartments and general parameters determining direction and magnitude of the observed fluxes. It has to be kept in mind, though, that only gaseous dry deposition and volatilization are directly comparable this way. The net emission that is usually observed as a sum of these two processes has to be balanced against particulate dry deposition (generally small) and wet deposition (generally important) in any study to finally evaluate a compartment as a source or a sink of atmospheric mercury.

The exchange of gaseous mercury at any interface is driven by a concentration gradient. If one compartment has a higher Hg(0) concentration than another, a net emission will take place, while net deposition will occur if the competing compartment is clean compared to the overlying atmosphere. Since many investigated waterbodies seem to be supersaturated with gaseous mercur compounds compared to the atmosphere, mostly evasion fluxes from waters to the air have been reported. However, under some conditions (at night and following periods of very high winds) downward fluxes to waters in subtropical Florida have been measured (Lindberg et al., 1997). This is also mostly true for soils, but there are some measurements over background soils suggesting net deposition under limited conditions, also mostly at night or over very wet soils (Kim et al., 1995). In earlier work, it has been shown that soils adsorb mercur vapor if exposed to elevated concentrations (Klusman and Matoske, 1983). Therefore, it seems appropriate to propose the existence of a “compensation point”, meaning that soils below a certain Hg(0) concentration (or probably: soil gas concentration) tend to absorb mercury, while soils above that concentration emit mercury depending on the Hg(0) concentration in the overlying air (Kim et al., 1995) (even if the mechanisms of emission and absorption may not be the same). A similar compensation point concept has also been reported for vegetation (Hanson et al., 1995).

Other properties whose gradients influence mercury transfer across the air-surface boundary include temperature, pressure and moisture. Therefore, soil temperature correlates well with mercury emission (Kim et al., 1995), higher fluxes are observed at low barometric pressure (Mc Nerney and Buseck, 1973) (the soil air is "sucked out" of the soil) and soils emit more mercury in the moist (not flooded) state compared to the dry state (Wallschläger et al., 2000). In fact, one study of forest soils demonstrated that fluxes could change from net emission to net deposition depending on the soils moisture status (Advokaat and Lindberg, 1996). In addition, any condition that favors conversion of oxidized Hg(II) to volatile mercury species in the investigated compartment, e.g. sunlight (Amyot et al., 1994; Carpi and Lindberg, 1997) or bacterial activity, increases mercury fluxes to the atmosphere. Also, processes that accelerate the transport across the boundary layer increase the mercury flux. For example, high turbulence or windspeed conditions (Kim et al., 1995) that transport the liberated mercury away from the surface produce an elevated volatilization rate. Similarly wave breaking increases the surface area and thereby the overall mercury flux from oceans to the atmosphere (Baeyens et al., 1991).

Mercury emissions from natural surfaces at various locations have been measured with different techniques or calculated by model simulations. Table 1.5 summarizes measured and calculated emission rates of mercury.

Table 1.5: Measured and Calculated Emission Rates of Mercury from Natural Surfaces

Location	Method	Emission Rate $\mu g\ m^{-2}\ y^{-1}$	Reference
Lakes, SW Sweden	Chamber measurements	18 - 180	a, b
Forest Soil, SW Sweden	Chamber measurements	< 2	a, b
Forest, TN, USA	Model and measurements	70 - 400	c, d
Equatorial Pacific	Model and measurements	4 - 80	d
Almaden, Spain (soils near mercury mine)	Chamber measurements	1140 - 2890	e
Lakes, WI, USA	Model and measurements	0.7 - 1.5	f, g

a: Schroeder et al., 1989; b: Xiao et al., 1991; c : Lindberg et al., 1992

d: Kim and Fitzgerald, 1986; e: Lindberg et al., 1979; f: Fitzgerald et al., 1991

g: Vandal et al., 1991

The role of vegetation in the overall picture seems to be ambiguous and needs further investigation, since all processes are apparently very specific to both the site and plant species. While some plants do not accumulate mercury from soils, others reflect a contaminated growth environment with elevated mercury content probably as a result of atmospheric exposure (Lindberg et al., 1979). Among the latter, some keep the mercury in the plant structure and release it back to the terrestrial environment after decay, while others transform the mercury into volatile compounds or simply transport already reduced mercury and release it to the atmosphere (Varekamp and Buseck, 1983; Hanson et al., 1995). Both types of plants have been employed for phytoremediation of contaminated sites, but at least in the second case, this re-distribution approach is very questionable. It has been shown that mercury in lichen originates predominantly from degassing from local soils (Bargagli et al.,

1989). Vegetation surveys even reflect mercury sources at depths greater than 200 m (Kovalevsky, 1986). Trees are a special case in that they continuously take up mercury with their foliage, which is then deposited on the soil as litterfall, while simultaneously taking up mercury via the transpiration stream through the roots and releasing it back to the atmosphere from the foliage. The overall budget seems to indicate that forests could be a net source of gaseous mercury, with the soils emitting more mercury than the foliage assimilates (Lindberg et al., 1992). Some fluxes from forests to the atmosphere have been calculated (Table 1.6), but litterfall and wet deposition have to be taken into account before characterizing forests as global sinks or sources of atmospheric mercury. The source of mercury in litterfall is at present not completely understood and could include both atmospheric (external) and soil (internal) sources. However, analysis of temporal trends in foliar mercury suggest an atmospheric source (Rea et al., 1996, Lindberg, 1996).

Table 1.6: Measured Mercury Fluxes over Forests and Annual Emission Estimates (adapted from Lindberg et al., 1998)

		Measured Net Emission		Estimated Net Emission	
Site	Canopy	Median ($ng\ m^{-2}h^{-1}$)	Mean ($ng\ m^{-2}h^{-1}$)	Mean Daily ($ng\ m^{-2}$)	Annual mean ($\mu g\ m^{-2}$)
Walker Branch Watershed, TN, U.S.A.	Mature hardwood	39	37	350	70
Wartburg, TN, U.S.A.	Young pines	17	18	150	30
Gardsjön, Sweden	Forest floor	1	1	9	2

The measured values in this field study included both emission and deposition fluxes, and the median was used to indicate a true central tendency weighted by the frequency of fluxes in both directions. Short-term fluxes were scaled using long term data on evapotranspiration which correlates well with mercury emissions (Lindberg et al., 2000)

1.3.1 Re-emissions of Mercury

The discussion about the relative significances of natural and anthropogenic emissions is complicated (if not rendered impossible) by processes that we classify here as indirect anthropogenic re-emissions. This term is chosen to describe secondary re-emission of mercury from anthropogenic sources following partial initial deposition of primary anthropogenic mercury emissions. Unfortunately (for our understanding of global atmospheric mercury exchange), these processes usually take place in compartments that also exhibit a natural mercury surface exchange like waters and soils, thereby making it impossible to distinguish between the two parallel ongoing natural and anthropogenically induced processes and to separate them quantitatively. Examples of these indirect anthropogenic emissions are discussed in this chapter and include emissions from soils as a result of mercury spills, re-emissions of formerly deposited mercury in the proximity of large point sources, and emissions from anthropogenically contaminated waterbodies and, their adjacent wetlands.

1.3.1.1 Re-emissions from Rivers

Little is known about mercury emissions from the waterbodies of rivers. It is well established that rivers transport mercury as a result of anthropogenic discharges and/or natural surface run-off, and both transport and deposition behavior in the river and especially in the estuaries with respect to discharges into the oceans have been studied. The few studies that investigate mercury exchange between rivers and the atmosphere all deal with the estuarine section of the rivers and are discussed in the following section on oceans. One case study (Bahlmann, 1997), however, deals with the occurrence of volatile mercury species along the transect of the highly contaminated Elbe river in Germany. This investigation shows that volatile mercury compounds (defined as purgeable within one hour; the exact speciation was not investigated but we designate them here as dissolved gaseous mercury, or DGM) in the waterbody can be detected along the course of the river. It is shown that the highest concentrations of “free” volatile mercury compounds are found in the estuarine region. However, continuous purging of the waters revealed that a much larger amount of mercury could be volatilized from the limnic samples, and this may represent in-situ production of Hg(0) by reduction of H(II). The levels of DGM found in this study are illustrated in Table 1.7, which compares DGM levels in several waters.

Table 1.7: Range of DGM Concentrations Measured in Rivers, Marine Systems and Lakes around the Globe

Location	DGM Concentrations ($pg\ L^{-1}$)	Reference
Elbe River	47 - 152	Bahlmann, 1997
Elbe River Estuary	54 - 122	Coquery, 1995
German Bight (North Sea)	18 - 284	Bahlmann, 1997
German Bight (North Sea)	17 - 87	Reich, 1995
North Sea	< 20 - 90	Coquery, 1995
Baltic Sea	14 - 22	Schmolke et al., 1997
Equatorial Pacific	6 - 46	Fitzgerald, 1986
Equatorial Pacific	8 - 65	Mason and Fitzgerald, 1991
Northern Wisconsin Lakes	7 - 70	Vandal et al., 1990
Scheldt Estuary	190 - 500	Baeyens et al., 1991
Scheldt Estuary	45 - 80	Baeyens and Leermakers, 1996
St. Lawrence Estuary	72	Cossa and Gobeil, 1996
Seine Estuary	<10 - 90	Coquery, 1995
Long Island Sound	38 - 254	Vandal et al., 1996

This process is quite likely since the suspended particles in the waterbody of the Elbe are rich in both mercury (Wilken and Hintelmann, 1991) and bacteria which have been shown to be resistant to the high mercury levels. These bacteria were shown to demethylate MeHg-compounds as a detoxification mechanism and might also be able to reduce divalent mercury compounds (Ebinghaus and Wilken, 1993). On the base of the determined concentrations and volatilization potentials, it has been calculated that the Elbe river could emit between 100 and 500 kg of mercury to the atmosphere annually (Bahlmann, 1997). As in the case of oceans, there is a severe lack of experimental flux measurements for rivers, so this estimate has to be taken with great caution. One investigative experiment failed to detect a significant mercury concentration gradient right above the water surface of the Elbe, indicating that emission fluxes (if they occur at all) might be rather small (Wallschläger, 1996). However, gradient methods exhibit a rather high detection limit for fluxes (Lindberg et al., 1996). The only direct

flux measurements over a river surface to date showed mercury emission from the St. Laurent river in Southern Quebec and came to the conclusion that fluxes were fairly small, on the order of 1 ng m^{-2} h^{-1} (Poissant and Casimir, 1996). These studies indicated that the mercury emission was photoinduced by reduction of divalent Hg(II) under the influence of sunlight. Consequently, it will be of fundamental importance for understanding air-water-exchange of mercury in rivers to determine to what extent the transported mercury is bound by suspended particles, for this parameter may have a significant effect on the availability for conversion to volatile species. The Elbe seems to represent one extreme in that respect for more than 99 % of the transported mercury has been shown to be particulate (Wilken and Hintelmann, 1991), while other contaminated rivers and streams seem to exhibit quite different behavior (Turner and Lindberg, 1978). On a global base, it has been estimated that only 10 % of the rivers' annual mercury loads originate from direct anthropogenic sources, while the remainder results from natural and indirect anthropogenic emissions (Cossa et al., 1996); however, on a regional base, there may be vast differences in those proportions.

1.3.1.2 Re-emissions from Lakes

The air-surface exchange of mercury over lakes has been the focus of some intensive studies over the last few years. Only two studies have performed experimental flux measurements over lake surfaces, and they were both conducted in Sweden. However, several studies have reported measurements of DGM in lakes, some of which have been used to model evasion. Earlier flux chamber measurements (Schroeder et al., 1992) over five Swedish lakes found fluxes between 3 and 20 ng m^{-2} h^{-1} from the lakes to the overlying atmosphere. At one occasion, a net deposition was observed, but all of these values must be questioned because those measurements were hampered by blank problems (Kim and Lindberg, 1995). It was also found that fluxes during daytime were larger than at night, indicating that sunlight, biological activity and temperature might play an important role in the mercury volatilization processes. The authors were also able to demonstrate pronounced seasonal differences in the mercury volatilization rate with fluxes in May and June being much larger than in November. This phenomenon could be due either to temperature alone or to other seasonal cycles associated with it. More recently, methods have been developed which allow mercury fluxes to be measured directly over water surfaces with the micrometeorological modified Bowen ratio gradient approach (Lindberg et., al. 1996). During June, 1994 the first measurements of mercury vapor fluxes over a boreal forest lake were made at Lake Gårdsjön, Sweden. Using highly accurate methods with multiple replicate samplers, the authors measured concentration gradients of mercury vapor, CO_2, and H_2O over the lake surface. Mercury was found to be

readily emitted from the lake surface, and there was no evidence of Hg(0) dry deposition to the lake surface. Emission rates over the lake averaged 8.5 ng m^{-2} h^{-1}, and appeared to be weakly influenced by water temperature and solar radiation. Overall, the fluxes ranged from ~2 to 18 ng m^{-2} h^{-1}, comparable to fluxes previously measured using surface chambers as discussed above. Overall, the surface water of the lake appears to be a more active zone for mercury exchange than the surrounding soils based on two independent studies (Xiao et. al., 1991; Lindberg et. al., 1998).

All other studies on mercury emission from lakes use calculations and models to estimate mercury fluxes from measured concentrations of atmospheric mercury and DGM in the waterphase. It is then assumed that all gaseous mercury in both the waterphase and the atmosphere is Hg(0) - which is a reasonable initial assumption because other volatile mercury species in the ambient atmosphere or in water occur only at very low concentrations (e.g. Stratton and Lindberg, 1995; Bloom et al., 1996) - and that this Hg(0) partitions between water and atmosphere according to Henry's law. With regard to that, most surface lake waters seem to be supersaturated in Hg(0), which is assumed to give rise to an evasional flux. The difference between the concentrations of Hg(0) measured in the lake water and back-calculated from the atmospheric concentration is fit into a thin film model and combined with wind speed and other meteorological parameters to estimate the mercury flux from the lake to the atmosphere. It is evident that this calculation is based on pure phase thermodynamical properties and therefore unlikely to reflect reality in all natural ecosystems. Although, it is undetermined for many systems to what extent theoretical calculations and experimentally determined fluxes disagree, one study in a contaminated lake experimentally measured both DGM and fluxes simultaneously (Lindberg et al., 1997). This study found measured fluxes exceeded those modeled from DGM using reported values of the exchange coefficients in other lakes.

The majority of studies on mercury exchange between lakes and the atmosphere have been conducted using modeling approaches in a set of seven lakes in Northern Wisconsin as part of the MTL (mercury in temperate lakes) project. All investigated lakes are seepage lakes (meaning they have no permanent surface water in- or outflow) and are not directly impacted by anthropogenic mercury sources. Consequently, the general finding was that atmospheric deposition was the major source of mercury for these lakes, which represent net sinks for atmospheric mercury since the modeled volatilization rates were always significantly smaller than the total deposition from the atmosphere (consisting of measured wet deposition through rain and snow and estimated particulate dry deposition). Even though two out of three parameters in this mass balance are not determined experimentally, it still seems reasonable to conclude from these studies that lakes are net mercury sinks on an annual basis. In contrast,

studies in anthropogenically contaminated lakes like the Davis Creek Reservoir in Northern California show the opposite behavior with the evasion flux being at least twice as big as the atmospheric mercury deposition (Porcella, 1994). This is reflected in the fact that dissolved Hg(0) concentrations in a contaminated lake (Mason et al., 1995) are five times higher than in remote lakes (Vandal et al., 1995). Some studies suggest that DMM may be directly formed from inorganic mercury under suboxic/oxic conditions and could, by decomposition, be the actual source of MMM observed in freshwaters (Mason et al., 1995).

The ratio between atmospheric deposition and volatilization varied greatly between the individual MTL lakes, apparently due to differences in the water chemistry between the lakes (Watras et al. 1994). Between 10 and 50 % of the mercury deposited from the atmosphere were re-emitted, and the revolatilization was correlated positively with pH, DOC and residence time in the upper water column. Calculated flux rates range from 1 to 5 µg m^{-2} y^{-1} (0.11 to 0.57 ng m^{-2} h^{-1}). All mercury not re-emitted was usually removed from the water column via sedimentation. It was also observed that $MeHg^{+}$ was wet deposited from the atmosphere (about 1 % of the total mercury deposition), and all deposited $MeHg^{+}$ was removed by sedimentation. It has to be noted that the calculated flux rates on an hourly basis are much smaller than those measured at the Swedish lakes mentioned above. Since both, the American and Swedish study lakes should be fairly comparable and also receive comparable atmospheric mercury inputs, it cannot be ruled out that the model calculations underestimate mercury volatilization considerably, which could make them less important sinks or even - in the worst case - alter the overall role of lakes in regional mercury budgets from sinks to sources. In the Lake Gårdsjön study, it was estimated that the lake could be a net source of Hg(0) during warm dry summer months, but is a net sink the rest of the year (Lindberg et al. 1996).

The mechanism of mercury volatilization from lakes remains unclear. In contrast to oceans, information on DMM in lake waters is not known to the authors. Thus, Hg(0) is the only volatile mercury species contributing to the quantification of the emission flux. Since it is known that Hg(II) reduction can occur both through biotic and abiotic reactions, attempts have been made to further elucidate the formation of Hg(0). It has been found that mercury reduction is lower in heat sterilized lake water, suggesting that the reduction process might be biologically mediated (Vandal et al., 1995). This is in agreement with studies in Upper Mystic Lake, MA (Mason et al., 1995), who found that both the concentration of Hg(0) and its production rate are highest in the surface waters and then decrease sharply down the water-column. They were able to identify heterotrophic bacteria as the primary source of Hg(II)-reduction, while minor contributions were made by abiotic processes and possibly by phytoplankton and cyanobacteria. On the other hand, there is strong evidence that mercury

volatilization from lakes is induced by sunlight (Amyot et al., 1994), but this could either be due to photochemical reactions or to light-induced biochemical processes, so it does not necessarily contradict findings that favor biotic reduction of reactive Hg(II).

Another way of obtaining information on the processes that form Hg(0) in the watercolumn is by looking at its depth concentration profiles and seasonal variations in the water columns of lakes. During studies in Onondaga Lake, an industrially polluted lake in near Syracuse, NY, USA, maximum concentrations were observed in April and August near the surface, while the lowest concentrations were found in the hypolimnion during periods of anoxia (Jacobs et al., 1995). This matches with observations in Pallette Lake, Wisconsin, U.S.A., where it was also found that Hg(0) concentrations are highest in the epilimnion and decrease with depth through the thermocline and the hypolimnion (Vandal et al., 1995); this observation was taken as an indication that mercury reduction only occurs in the mixed layer (Porcella, 1994). Finally, in wind sheltered parts of the lake, the Hg(0) concentrations in the epilimnion were elevated compared to wind exposed regions. This finding strongly suggests that wind is an important driving force behind gas exchange at the lake surface; thus, mercury fluxes to the atmosphere are temporarily increased by windy conditions and waves.

Reactive Hg(II), the most likely precursor for Hg(0), showed variable seasonal concentration depth profiles. Its concentration was highest in the epilimnion in the early summer with low concentrations in the thermocline, but exactly the opposite in late summer. Since this parameter seems to be influenced by numerous and more complex processes, it is not surprising that two relevant sources of reactive Hg(II) were identified in these studies, one being atmospheric deposition and the other being re-mobilization from the sediments. Rain events increase reactive Hg(II) in the epilimnion, either by direct wet deposition of reactive Hg(II) or by deposition of particulate mercury that gets transformed to reactive Hg(II) in the epilimnion. Since it has been shown that both reactive Hg(II) and particulate mercury are major fractions in wet deposition (Fitzgerald et al., 1994), a mixture of both processes seems to be the most likely source of reactive Hg(II) in the watercolumn. Although Hg(0) concentrations in sediment pore waters are comparable to those in the epilimnion, they are lower than in the overlying lake water and it was concluded that Hg(0) export from the sediments is not an important source of Hg(0) in the water column. On the other hand, Hg(II) concentrations are higher in pore waters than in lake water and it also exceeds Hg(0) concentrations in pore water by at least one order of magnitude. Thus, it was concluded that export of Hg(II) from the sediments is a significant source of Hg(II) in the water column and, consequently, of Hg(0) evasion to the atmosphere (Fitzgerald et al., 1994).

1.3.1.3 Re-emissions from Marine Systems

The distribution, transport and fate of mercury at the earth's surface is critically dependent on the biogeochemical cycling and atmospheric exchange of mercury in the marine environment since, by its shear size, the ocean is both a significant source and sink for atmospheric mercury (Mason et al., 1994; Mason and Fitzgerald, 1996). A number of studies have measured volatile mercury species well above saturation levels in ocean waters primarily as DGM. Hence, the emission of mercury from the oceans to the atmosphere is certainly occurring. However, since deposition is also occurring at the same time, a major question is whether or not emissions exceed deposition. As even the direction of the net mercury flux between oceans and atmosphere has not been determined conclusively, it is only natural that the size of that flux is even more doubtful. As a matter of fact, up to date no field experiments have been attempted to actually measure air-surface exchange of mercury over oceanic waters despite the existence of proven methods for smaller water bodies. All we know is that elemental mercury seems to commonly occur in surficial ocean waters in supersaturated concentrations. From this observation, it is frequently derived that there is a net mercury emission (Vandal et al., 1991, Fitzgerald et al., 1991, 1994), but we have to keep in mind that this assumption is based on physical chemical theories whose applicabilities to the water-air-system in oceans have not been proven for mercury beyond doubt. All available flux data were obtained by this model and must therefore be seen as rough estimates rather than exact values. Estimated net mercury emissions range from average hourly fluxes of 0.4 to 16 ng m^{-2} h^{-1}. The concentrations of elemental mercury and its modeled evasional flux to the atmosphere in various oceanic regions are given in Table 1.8. From these data, the global mercury emission from oceanic sources has been estimated at 2000 t y^{-1} (Mason et al., 1994). Another important factor is that all these flux calculations are based on calm sea and moderate wind conditions (under which also all of the sampling campaigns were probably performed). It has been modeled, though, that fluxes may increase by a factor of up to 25 during storms and rough sea conditions (Baeyens et al., 1991), so this estimate may be systematically low. However, such fluxes would be very short lived while the system re-equilibrated with ambient Hg(0), and the overall effect of these pulses on annual fluxes has not been assessed.

Table 1.8: Concentrations of Elemental Mercury Measured in Various Ocean Regions and the Estimated Associated Evasional Flux to the Atmosphere (adapted from Mason and Fitzgerald, 1996)

Region	Conc. Range ($pg\ L^{-1}$)	% Hg(0)/ React. Hg	Potential Flux ($ng\ m^{-2}\ h^{-1}$)
EPO* 1990	10 - 72	14 ± 10	1.3 - 9
EPO 1984	6 - 46	5 ± 3	0.5 - 9.2
1500 W, 100 N - 120 S	8 - 18	--	0.8 - 2.8
N. Pacific	6	--	0.2
N. Atlantic	50 - 250	15 - 100	15.2 ± 10.4
Mediterranean	< 26	< 20	

EPO * : Equatorial Pacific Ocean

Both elemental mercury and DMM are found in oceanic waters in the DGM fraction. A number of studies (Mason et al., 1994, Fitzgerald et al., 1994) suggest that direct reduction of ionic mercury is predominant in low oxygen waters (Mason and Fitzgerald, 1993). Generally, both volatile species are found in comparable concentration ranges, although there always seems to be more Hg(0) than DMM.

In contrast to terrestrial systems, dry deposition of mercury does not seem to be an important process in marine ecosystems although no attempts have been made to measure it. Thus, deposition estimates are derived from precipitation measurements only. Reported results range from 0.04 to over 800 ng $m^{-2}\ h^{-1}$. The consequence of this enormous range seems to be that while on a global basis emission and deposition over oceans seem to equalize approximately, there are large regional differences depending on both the regional emission activity and the regional deposition as a result of precipitation rates and degree of local contamination. In the Arctic, for example, deposition was estimated to be five times larger than emission, while the ratio is exactly opposite in the Equatorial Pacific, leading to the conclusion that air-sea-exchange of mercury actively contributes to the global mercury transport from mid-latitude to Arctic shelves. On the basis of the existing data, it would, however, be more than daring to characterize either the oceans or the oceanic margins as

either absolute sinks or sources of atmospheric mercury until more detailed and larger scale studies have been done.

Studies in the Northern Pacific Ocean show that mercury volatilization and deposition in the tropical Pacific Ocean are pretty much equal, but while the evasional flux was fairly constant at different latitudes, deposition varied significantly, thus making the equatorial Pacific Ocean a source of atmospheric mercury while the higher latitude regions turn out to be a sink (Mason et al., 1994). Since the equatorial part of the Pacific Ocean is an upwelling area, it was suggested on the base of model calculations that reactive Hg(II) supplied by the upwelling process is the source of the observed increased Hg(0) concentrations and thus leads to the inferred atmospheric emission flux. Studies in the Northern Atlantic Ocean also identify this region as an atmospheric mercury source, with emission fluxes averaging 139 ± 95 µg m^{-2} y^{-1} (Mason and Fitzgerald, 1996). The same trend has also been observed for coastal regions. While mercury evasion in remote arctic shelf areas was very small (3.7 - 5.8 µg m^{-2} y^{-1}), it was shown to increase in more polluted oceanic boundary regions (7.3 - 22 µg m^{-2} y^{-1}). The authors conclude from these data that net atmospheric transfer of mercury from lower latitudes to arctic regions is going on despite a net global balance for emissions and depositions. Somewhat higher atmospheric mercury evasion fluxes have been reported for estuaries (3.7 - 51 µg m^{-2} y^{-1}), and the emission seems to be correlated to the rivers' mercury content (Cossa et al., 1996). In a very detailed review of studies on mercury biogeochemistry in coastal regions (Cossa et al., 1996), the authors propose the following semiquantitative budget for coastal areas. Overall, imports and exports of mercury to ocean margins seem to neutralize within the range of error. The major source of mercury is particulate matter transported in rivers. However, this amount seems to be deposited in the estuaries via sedimentation under the influence of the salinity gradient. Exchange between ocean margins and their sediments as well as with the open ocean also seem to balance. Atmospheric exchange in general seems to be a net emission process. They also attempted a mass balance for methylmercury in ocean margins and came to the conclusion that no boundary exchange process had significant impact on the $MeHg^+$ pool in coastal zones, except for upwelling processes that imported about half of the annual biomass uptake of $MeHg^+$ into ocean margin areas, with the other half being produced in situ.

Considering the enormous part of the earth's surface covered by oceans, it is of vital importance to understand if oceans only re-emit mercury that is transported by rivers or deposited from the atmosphere, or if they actually contribute actively to the global mercury budget as a net source. There is evidence that mercury from oceanic sediments is released to the overlaying water during diagenetic processes (Cossa et al., 1996). These investigations suggest that Mn-oxides bind most of the mercury in oceanic sediments, and as these oxides

get reduced and dissolved during bacterial degredation of organic matter, mercury concentrations in sediment pore waters are elevated by one order of magnitude compared to the overlying waters. Fluxes calculated from these concentrations based on molecular diffusion equal 26 ng m^{-2} d^{-1} (9.5 µg m^{-2} y^{-1}). Although this flux apparently only accounts for 3 % of the total input into these system (Cossa et al., 1996), when scaled to the total ocean sediment surface area of 3.6 * 10^{11} km^2 (= 71 % of the earth's total surface area) (Fairbridge, 1966), it yields over 3* 10^6 t y^{-1}. It is therefore vital to investigate if this flux estimate is accurate and globally representative, how it compares to direct sedimentation (i.e. if there is a net release of mercury from oceanic sediments to the water column) and to what extent this flux is carried through the water column to lead to atmospheric emission.

1.3.1.4 Re-emissions from Terrestrial Systems and Wetland Areas

Compared to the seas, there are more data available regarding mercury exchange between the atmosphere and several types of soils with respect to both the origin and the level of their mercury contamination. Beginning with impacted sites, studies in the vicinity of a strong industrial point source of mercury in eastern Germany revealed wet deposition fluxes of 1,200 µg m^{-2} y^{-1} to the soils surrounding the factory premises. For comparison, the combined source strength of the four individual production sites (one active, three shut down) including their highly contaminated vicinity was backmodelled to be 800 to 1600 kg y^{-1} and the model indicates that as much as 30 % of the total annual emission is deposited within 5 km from the spot of emission (Ebinghaus and Krüger, 1996). So, soils located close to large atmospheric mercury sources are clearly sinks while these sources are active. In the long run, however, these soils may turn into important sources when the original emissions are discontinued and therefore direct flux measurements will be important at such sites.

The first direct flux measurements of mercury at an industrially impacted site used a laboratory flux chamber (Lindberg and Turner, 1977). Emissions were measured over waste deposited in holding ponds from a former chlor-alkali plant in Virginia. The mercury concentrations in the surface waste deposits averaged 160 µg g^{-1}. The authors reported the highest fluxes yet published, on the order of 120,000 ng m^{-2} h^{-1} to 170,000 ng m^{-2} h^{-1} at 35° C and estimated an annual atmospheric emission from this one area alone of about 40 kg y^{-1}. Fluxes increased exponentially with surface temperature, and resulted in ambient air concentrations near the area of over 950 ng m^{-3} in summer. Globally, hundreds of such sites still exist and their contribution to regional mercury emissions could be significant.

Elevated mercury emissions have also been reported for soils near the Almadén mercury mine in Spain (Lindberg et al., 1979). Emission rates over naturally mercury enriched soils (concentrations averaged 97 µg g^{-1}) ranged from 600 to 750 ng m^{-2} h^{-1} at 35° C and also increased exponentially with soil temperature. For the first time direct plant uptake of this emitted airborne mercury was measured. This pathway lead to elevated levels in leaves, although root uptake from the soil pool was limited.

More recently mercury fluxes from highly contaminated mill tailings from former gold and mercury mines in the Western U.S. have been crudely estimated from atmospheric concentration gradients combined with a simple one-dimensional diffusion model. Fluxes were estimated to be 5 - 120 µg m^{-2} h^{-1}, and, surprisingly, no clear correlations with any meteorological parameter could be identified; only total mercury content in the soil samples seemed to always correlate with the estimated fluxes. The largest fluxes were usually derived from early morning measurements, but sometimes increased fluxes were obtained at nighttime or in the afternoon. Such results may indicate that some of the measured gradients were artifacts of advection of contaminated air from local sources, and cannot be used to derive fluxes. Scaling of the results to the whole Carson River Superfund site, Nevada, USA, yielded emissions on the order of 150 to 400 kg y^{-1}. These studies also showed elevated atmospheric mercury concentrations over a naturally mercury-enriched geothermal area, but these were much smaller than over the mine tailings and no fluxes were derived (Gustin et al., 1996). More extensive measurements over a nearby geothermal site confirmed air concentrations as high as 50 ng m^{-3} while fluxes measured with portable soil chambers ranged from approximately 10 to 1000 ng m^{-2} h^{-1}, much lower than seen over the mine tailings (Gustin et al., 2001). More data will be necessary to confirm that fluxes over naturally enriched soils are generally below those over contaminated soils.

Another type of mercury contaminated soils are wetlands adjacent to contaminated waterbodies which have stored large amounts of mercur as a result of sedimentation of contaminated particulate matter during periodic floodings. It is a well established remediation technique to construct wetlands in order to remove contaminants from polluted river systems due to the wetlands high organic carbon accumulation (Patrick, 1994). In the case of mercury, however, there are indications that floodplains are not only initial sinks of deposited mercury, but also long term diffuse sources of atmospheric mercury since the high water content and high productivity of wetlands seem to generate ideal conditions for the transformation of non-volatile into volatile mercury species (Wallschläger et al., 2000). There are two prominent case studies for this kind of diffusely mercury polluted wetlands, namely East Fork Poplar Creek (EFPC) in Tennessee, USA (Lindberg et al., 1995) and the river Elbe in Germany (Wallschläger et al., 2001). The former is a small waterbody that was contaminated directly

from a single large industrial point source, while the latter is the third largest river in Germany and comprises a much larger area that became contaminated by much larger absolute amounts of mercury discharges from the entire industrial area along its course. However, both study areas are relatively similar in that they are floodplain ecosystems which show similar degrees of mercury contamination. Therefore, it seems appropriate to compare the results of investigations on air-soil exchange of mercury at both sites.

The EFPC floodplains has an area of 250 ha and is estimated to contain a total mercury pool of 80 t. Soil mercury concentrations range from 4 to 60 μg g^{-1} in less contaminated and 50 - 200 μg g^{-1} in more contaminated areas (Lindberg et al., 1995). Solid phase speciation experiments seem to reveal that most of the deposited mercury is present in the forms of HgS (cinnabar and meta-cinnabar) with minor amounts of elemental Hg(0) (Barnett et al., 1995). Mercury volatilization from these floodplain soils was studied by the first micrometeorological approach to be developed for mercury, the "modified Bowen-ratio method" (MBR) (Lindberg et al., 1995). Naturally, a net mercury emission from these soils was observed, and fluxes were found to be between 10 and 200 ng m^{-2} h^{-1} over the study site containing an average of 4.3 ± 0.3 μg g^{-1} mercury. Since the applied technique has a fairly large "footprint area" (i.e. is representative of a large area surrounding the actual measurement site), these fluxes are partially influenced by air masses passing over more contaminated areas of the floodplain. Higher fluxes were correlated with wind directions coming from the more contaminated parts of the floodplains, and lower fluxes came from the less contaminated regions. The total annual emission from the EFPC floodplains to the atmosphere was estimated to be between 1 and 10 kg.

The Elbe floodplains have an estimated area of 1,100 km^2 and total deposited mercury amount of 1,500 t (Wallschläger and Wilken, 1996). Average mercury concentrations in the soils range from 1 to 10 μg g^{-1} and most of the mercury is bound by high molecular weight organic matter (Wallschläger, 1996). In these studies, flux chamber measurements were employed to estimate mercury volatilization, but they were also compared to the MBR method by measuring the concentration gradient of atmospheric mercury in the soil atmosphere boundary layer and adopting the micrometeorological parameters from the EFPC floodplains (Lindberg et al., 1995). Additionally, mercury volatilization was estimated from soil air concentration data assuming laminar diffusion. Results for mercury emissions from soils containing 10 μg g^{-1} range from 28 to 260 ng m^{-2} h^{-1} and are thus comparable to the fluxes measured at EFPC. However, it was noted that the individual applied techniques did not agree very well due to their inherent methodological differences, and, that there is a need for intercomparison studies (Wallschläger et al., 2001). The overall annual emission of mercury from the Elbe

floodplains to the atmosphere was estimated to be on the order of 1 t y^{-1}, thereby representing a significant, but not dominant mercury source on the regional scale.

Micrometeorological studies over background forest soils at Walker Branch Watershed (WBW), Tennessee, USA led to the conclusion that these soils can act both as sources and as sinks of atmospheric mercury, although emission events were observed more frequently and had a larger magnitude (Kim et al., 1995). Considering the wet deposition inputs, it appears that background soils may not significantly change the atmospheric mercury pool, but small variations in the mass balance could have large impacts on the global scale. Emission rates measured averaged 7.5 ± 7.0 ng m^{-2} h^{-1} over soils containing 0.35 - 0.82 µg g^{-1} total mercury. These concentrations, however, are slightly elevated compared to the background concentrations generally assumed today, indicating that true background soils may indeed be neutral towards surface exchange of atmospheric mercury. Studies over background forest soils in Sweden (Xiao et al., 1991) found fluxes of lower magnitudes, but these flux chamber measurements were somewhat hampered by blank problems (Kim and Lindberg, 1995). However, it was noted that net mercury emissions occur during summer at a rate of 0.3 ± 0.4 ng m^{-2} h^{-1}, while net deposition was observed in winter at a rate of 0.9 ± 0.4 ng m^{-2} h^{-1}. Unfortunately, no mercury soil contents are given to correlate with the flux magnitudes. In a related study using flux chamber methods, background forest soils in Tennessee, USA showed mercury emission fluxes between 2 and 7 ng m^{-2} h^{-1}, while open field soils in the same region exhibited greater volatilizion rates of between 12 and 45 ng m^{-2} h^{-1}, although the open field sites had a smaller mercury soil content than the forest sites. This difference was attributed to increased solar irradiation over unshaded soils. These results give an estimate of 1,000 tons mercury y^{-1} which are emitted globally from all background soils to the atmosphere, with two thirds coming from sunlight-exposed open field soils (Carpi and Lindberg, 1998).

It has been noted that vast areas of open field agricultural soils in the world are treated with municipal sewage sludge as fertilizer. In studies of sewage sludge amended soils, it was found that sludges containing 7.3 ± 2.5 µg g^{-1} mercury when applied to background soils result in a release on the order of 25 ± 10 ng m^{-2} h^{-1} when kept in the shade. However, this emission increased dramatically when soils were exposed to sunlight and emissions rose to an average of 460 ± 120 ng m^{-2} h^{-1}. In these experiments, solar radiation was shown to induce mercury emissions more directly than indirectly via soil temperature changes (Carpi and Lindberg, 1997), and that the Hg(II) contained in the sludge must be reduced in situ to Hg(0) when exposed to sunlight, perhaps by photoreduction reactions. It was calculated that in the EU and the USA alone, sludge amended soils release 5 t of mercury on an annual basis to the atmosphere making them a small source on the global scale, but important on a regional scale

in otherwise uncontaminated areas where this practice is common. In addition, during the same studies, it was shown that the sewage sludge amended soils also release methylated mercury compounds to the atmosphere at a rate of 12 to 24 pg m^{-2} h^{-1}, identifying the first ever emission of gaseous $MeHg^+$ to the atmosphere (Carpi et al., 1997). If up-scaled, sewage soil treatment in the EU and USA would liberate 1 kg of $MeHg^+$ annually. Considering that vast areas outside the western world may be impacted by sludge applications, these soils could have an important regional or global contribution.

All studies show that the mercury emission flux is more complex than simple phase transfer of Hg(0), because the necessary phase transfer enthalpy (derived from temperature dependencies) is always twice as high as for the pure compound, indicating that formation and/or transport processes slow down the volatilization rate. The whole process has been suggested to be a combination of volatilization of existent elemental Hg(0) and reduction of Hg(II) in soil solutions or in water layers on soil minerals (Lindberg et al., 1998). Observations of increased Hg volatilization from contaminated floodplains during rain events led to the suggestion of a two step mechanism comprising the same reactions: a small initial displacement of soil air containing Hg(0) and DMM (Wallschläger et al., 1995) followed by formation of volatile mercury compounds in the liquid phase as a result of reduction of Hg(II) and dismutation of $MeHg^+$ (Wallschläger et al., 2000). These studies also calculated that direct reduction of wet deposited Hg(II) is not likely to be a major source of mercury volatilization. Soil moisture may play a role in mercury emissions, however. Using a roof to eliminate rainfall over soils at Walker Branch Watershed (WBW), a strong decrease in soil mercury emissions was measured after 6 weeks of no rainfall (Advokaat and Lindberg, 1996). In fact these soils became a net sink, exhibiting consistent mercury uptake compared to continued mercury emission from adjacent control soils. Rainfall was not the source of the mercury however, as the authors once again induced mercury emissions by simply irrigating the treatment plot with distilled water.

Over the last couple of years, there has been increasing interest in understanding the driving forces behind air-surface exchange of mercury, especially over soils. In these numerous investigations, several key factors besides mercury content and speciation were identified as influencing the emission rates from soils. At EFPC, it was demonstrated that mercury fluxes increase exponentially with both soil and air temperature (Lindberg et al., 1995). Annual and diurnal cycles were observed with highest fluxes in summer and in the afternoon and lowest fluxes in winter and at night (Lindberg et al., 1995; Kim et al., 1995). These observations are probably coupled to temperature cycles, but also indirectly to biological cycles associated with them. Positive correlations were observed between emission rates and wind speed as well as relative humidity and turbulence (Kim et al., 1995). Solar radiation, temperature, and

soil moisture were identified as key parameters affecting mercury emissions from soils, and it was shown that solar radiation induced the formation of elemental Hg(0) in surface soils (Carpi and Lindberg, 1997). Rain events also increase mercury flux to the atmosphere, supporting that soil moisture is one important parameter in the formation of volatile species, probably in liquid phase reactions (Wallschläger et al., 2000).

1.4 The Atmospheric Mercury Cycle

The atmospheric cycling of mercury is determined by natural and anthropgenic emissions, a complex atmospheric chemistry, and wet and dry deposition processes. Atmospheric chemistry and especially the deposition of mercury are strongly linked to the nature of the mercury species (speciation) released into the atmosphere by different types of sources.

The linkage between the atmospheric and biological cycles is manifested in the deposition of atmospheric mercury species. Schroeder and Lane (1988) illustrated the most important processes in the emission and deposition cycle of atmospheric mercury (Figure 1.1). The deposition pathway is dominated by the flux of emitted Hg(II) compounds (formal reactive gaseous mercury or RGM), the oxidation of elemental mercury vapor to Hg(II), and subsequent wet and/or dry deposition. Mercury species attached to particles can be removed from the atmosphere by precipitation or dry deposition, but these fluxes are generally less important.

Once deposited, the formation of volatile gaseous mercury, especially the formation of highly toxic methylmercury, its enrichment in organisms and nutritional chains, and finally destruction (demethylation) of methylmercury are the main features of the biological cycle of mercury.

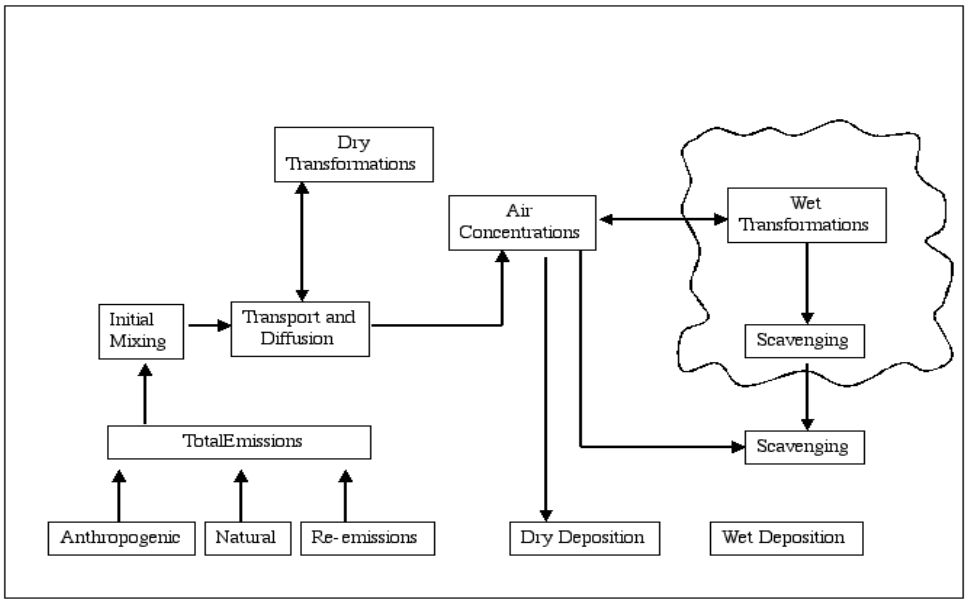

Figure 1.1: Mercury emissions-to- depositions cycle (adapted from Schroeder and Lane, 1988)

1.4.1 Speciation of Mercury Emitted into the Atmosphere

On a global scale, the atmospheric mercury cycle is dominated by elemental mercury vapor (generally >95 % of the total airborne mercury). However, the speciation of mercury emitted into the atmosphere is determined by the source characteristics and consequently shows a large regional variability.

Together, these last two pathways are also designated mercury emissions from natural surfaces, and they represent large uncontrolled area source emissions which must be taken into account by global models.

1.4.2 Mercury Species Emitted by Anthropogenic Sources

Fuel combustion, waste incineration, industrial processes, and metal ore roasting, refining, and processing are the most important point source categories for anthropogenic mercury emissions into the atmosphere on a worldwide basis. Besides elemental mercury an important and variable fraction can be emitted as reactive gaseous mercury (RGM) or particulate Hg(II) (Expert Panel, 1994).

The major portion of mercury emissions from combustion of fuels is in the gaseous phase. In the combustion zone, mercury present in coal or other fossil fuels evaporates in elemental form and then most likely a portion of it is oxidized in the flue gas (Prestbo et al., 1995). Emitted mercury species into the environment depend on the nature of the source of emission. Mercury emitted from high temperature processes such as coal combustion and pyrite roasters will probably be converted to the elemental form, Hg(0). However, in flue gases, where the temperature drops, Hg(0) may be oxidized by hydrochloric acid (HCl) and O_2 in the presence of soot or other surfaces (Hall et al., 1991; Prestbo et al., 1995). In modern combustion plants equipped with flue gas cleaning facilities such as wet scrubbers, the oxidized and particulate forms should be removed easily. Hence the primary emission will be Hg(0). Table 1.9 summarizes the speciation of mercury emissions from flue gases and other industrial emissions.

Table 1.9: Speciation of Emitted Mercury in Major Global Anthropogenic Sources in 1995 in Tons (and percent) (based on Pacyna and Pacyna, 2000)

Speciation	Stationary combustion	Non-ferrous metal production	Pig iron and steel production	Cement production	Waste disposal
Hg(0)	737.6 / (50 %)	132.4 / (80 %)	23.3 / (80 %)	106.1 / (80 %)	22.2 / (20 %)
Hg(II) gas	589.6 / (40 %)	25.0 / (15 %)	4.5 / (15 %)	19.9 / (15 %)	66.8 / (60 %)
Hg(II) part	147.3 / (10 %)	8.2 / (5 %)	1.3 / (5 %)	6.4 / (5 %)	22.2 / (20 %)

1.4.3 Mercury Species Emitted from Natural Sources and Re-Emissions

The mercury that evades from natural sources is generally entirely in the elemental form (e.g. Lindberg et al., 1998, 1996). Natural sources are, for example, the evasion from surface waters, from soils, from minerals, and from vegetation located in terrestrial or wetland systems. Volcanism, erosion, and exhalation from natural geothermal and other geological crevices also mainly emit elemental mercury.

Global volcanic emissions were estimated from the Hg/S ratio and account for approximately 20 to 90 t y^{-1}, which is about 1-5% of the annual emissions from human activities (Fitzgerald, 1996).

Generally speaking, the distinction between natural and "quasi-natural re-emissions" of mercury (that fraction, which was formerly deposited from the atmosphere to surfaces) is difficult to discern and may be regarded as an unresolved problem. In addition, the so-called natural emissions also include mercury that was previously deposited from natural sources.

Another example of a quasi-natural emission source are frequently occurring forest fires. Forest biomass is known to be a large pool of temporarily stored mercury. These emissions are of interest with respect to the emission speciation since some partially oxidized mercury species may be emitted as particulate or gas-phase species in addition to elemental merucry (Porcella, 1995). An extensive Amazon monitoring network showed that the annual atmospheric mercury emissions from slash and burn deforestation in the Amazon was 2-9 t y^{-1}. This is relatively small compared to mercury emissions from gold mining in the Amazon, which are estimated to be about 140 t y^{-1} (Lacerda et al., 1995).

However, a recent study gave first evidence that mercury emissions originating from forest fires may have been significantly underestimated (Brunke et al., 2001). During mid-January 2000 the plume from a fire, which destroyed 9000 ha of mixed vegetation in the southern part of the Cape Peninsula (South Africa), passed over a Global Atmospheric Watch (GAW) station at Cape Point where TGM and other trace gases are routinely monitored. The smoke plume was characterized by a CO/CO_2 emission ratio (ER) of 0.0602± 0.0017 mol/mol, typical for biomass burning (Hao et al., 1996; Koppmann et al., 1997). Measurements of TGM made during this episode provided an Hg/CO emission ratio of (2.10 ±0.21)*10^{-7} mol/mol. Based on the presently accepted CO source estimate for biomass burning of 621 * 10^3 kTons/y^{-1}, this ER suggests that the global TGM contribution from biomass burning amounts to approximately 0.933 ±0.93 kTons annually. This would represent 14 - 32 % of the total and 42 - 93 % of natural TGM emission globally (Brunke et al., 2001). From this study it is evident, that biomass burning might be a significant source of atmospheric mercury however, further measurements in other plumes elsewhere in the world are needed to substantiate this proposition (Brunke et al., 2001).

Photochemical and photobiological processes play an important role in the re-emission of mercury from aquatic systems. Nriagu estimated that an important fraction (10-50 %) of dissolved mercury in lakes is in the elemental form (Nriagu, 1994). However, more recent estimates in surface waters place this fraction closer to 5-10 % (Amyot et al., 1995; Fitzgerald and Mason, 1996; Schmolke et al., 1997) and new flux measurements in Sweden indicate that the emitted mercury is also in the elemental form (Lindberg et al., 1996).

Globally, it has been suggested that there exists an important re-emission of elemental mercury from marine surfaces (Mason et al., 1994). Recent data from forested areas suggest

first evidence that a similar process of Hg(0) emission may be globally important for terrestrial plants as well (Lindberg, 1996).

1.5 Mercury Species in the Atmosphere

Vapor-phase mercury is the predominant physical state in relatively clean ambient air, where both vapor-phase and particulate-phase mercury generally coexist. When speciating the vapor-phase fraction, elemental mercury nearly always constitutes also all of the mass with only minor amounts of other volatile species normally being detected (Brosset and Lord, 1991; Stratton and Lindberg, 1995; Ebinghaus et al., 1999). The speciation of mercury emitted to the atmosphere is of great importance for the atmospheric fate of mercury. Hg(0) will add to the global background and will significantly deposited only after atmospheric transformation processes or through plant surface interactions such as stomatal uptake at elevated concentrations (Hanson et al., 1995). However, particulate-phase mercury (Hg_{part}), also referred to as total particulate-phase mercury (TPM) and reactive gaseous mercury (RGM) will deposit more rapidly on a local or regional scale (Lindberg et al., 1992). Estimates by Slemr et al. (1985) based on the relations between vapor pressure and the ratio of particulate concentrations to gaseous concentrations of different species in the atmosphere (Junge, 1977) suggest that inorganic gaseous mercury species will be predominantly found on aerosols and thus will share their atmospheric fate, i.e. will have a residence time of about 5 days (Prospero et al., 1983) and cannot be transported over large distances. According to Junge, another consequence is that concentrations of Hg(II) should not be too different from particulate phase concentrations of mercury because the particulates encompass Hg(II). However, recent measurements of RGM using newly designed techniques including treated filters, denuders, and refluxing mist chambers all show that RGM generally exceed Hg_{part} concentrations (Xiao et al., 1997; Lindberg and Stratton, 1998; Ebinghaus et al., 1999).

Measurements of operationally defined Total Gaseous Mercury (TGM) are being made on a routine basis at a number of sites in Europe and North America. A recently conducted field intercomparison of measurements of atmospheric mercury species shows good comparability of the commonly accepted methods for TGM, but less so for RGM and Hg_{part} (Ebinghaus et al., 1999). Detailed results of the intercomparison study and quality assurance aspects will be discussed in chapter 3.

Long-term studies suggest that atmospheric TGM concentrations were increasing on a hemispheric or a global scale until the early 1990s; a decrease has been suggested for the period 1990-1994 (Slemr and Langer, 1992; Fitzgerald, 1995; Slemr, 1996).

Our own measurements at Mace Head, a remote marine location on the Irish west coast have shown a fairly constant average TGM level between September 1995 and December 2000 (see chapter 5). These findings are in good agreement with results obtained in the high Canadian Arctic (Schroeder, 2000) and for a monitoring station at Cape Point, South Africa (Baker et al., 2001).

Fewer data are available for particulate-phase mercury or inorganic gaseous mercury species. Table 1.10 summarizes background concentrations of these species at Mace Head, Ireland. The measurements had been performed by a number of different laboratories taking part in the field intercomparison study mentioned above (Ebinghaus et al., 1999).

In addition to the inorganic species, both methylmercury and dimethylmercury have been detected in ambient air at background and urban sites (Bloom et al., 1996). However, the concentrations are far below those of the inorganic species.

Table 1.10: Background Concentrations of Atmospheric Mercury Species detected at Mace Head, Ireland (Ebinghaus et al., 1999)

TGM (ng m^{-3})	Hg_{part} (ng m^{-3})	RGM (ng m^{-3})
1.3 - 3.8[a]	0.005 - 0.026[c]	0.013 - 0.023[e]
1.2 - 2.1[b]	0.028 - 0.115[d]	0.041 - 0.094[d]

[a]Measured with manual methods. [b]measured with automated analyzers. [c]Collected on disk filters. [d]Collected on quartz, wool plugs or Au coated glass beads. [e]Defined as reactive gaseous mercury. [f]Defined as divalent gaseous mercury.

Naturally occurring species distribution of atmospheric mercury as it can be detected at remote locations is significantly influenced by the presence of emission sources. The emitted species are dependent on the source characteristics. Depending on the atmospheric residence time and the deposition properties of the individual species, the relative proportions of the atmospheric concentrations are related to the distance of the sources. For central Europe it has become clear that several "hot spots" of anthropogenic Hg(0) emissions are located at industrial sites in the former German Democratic Republic. Annual atmospheric emissions

from this relatively small but highly industrialized are were estimated at 330 tons for 1988. A comparison with the emission of entire Europe, estimated at 726 tons for the same year, shows the significance of this locally limited but strong source of Hg(0) for central Europe (Helwig and Neske, 1990).

1.6 Atmospheric Deposition of Mercury Species

Mercury in all of its forms can be readily deposited on the Earth's surface. However, because of its reactivity and solubility, deposition of the RGM forms of mercury are generally favored. Although Hg(0) can be directly absorbed by soils and plants (e.g. Lindberg et al., 1979), these processes are most important near local sources (e.g. Hanson et al., 1995).

The major atmospheric deposition process for elemental mercury vapor in background air is the aqueous oxidation by ozone followed by an in-droplet adsorption primarily onto soot particles (Munthe, 1992; Petersen et al., 1995). It is important to be aware of the fact that the relation between emissions and depositions may be nonlinear. Consequently, deposition rates cannot be derived directly from emission rates because they are strongly influenced by secondary pollutants such as ozone and soot (Iverfeldt, 1995).

Because a small but significant fraction of the atmospheric mercury consists of vapor phase RGM or Hg(II), gaseous $MeHg^+$, and Hg_{part}, these forms must also be included in regional deposition models because of their shorter atmospheric residence time relative to Hg(0). Of the three forms, RGM or Hg(II) is of major importance for the total deposition of mercury from the atmosphere according to a Eulerian model (Petersen, et al., 1995). Although these species are typically present at less than 10 % of the total atmospheric mercury, they appear to influence the deposition flux significantly (Petersen et al., 1996; Pai et al., 1997).

Any oxidized mercury species will be subject to wet and dry deposition because of its significantly higher deposition velocity compared with elemental mercury (Lindberg et al., 1992; Lindberg and Stratton, 1998).

A major fraction of the total mercury in precipitation is associated with particles, at least in urban and industrialized areas (Ferrara et al., 1988; Iverfeldt, 1991), although it is not clear if this association occurs before or after rain formation. The particulate fraction in precipitation varies between less than 10 % at remote sites to more than 90% at polluted sites (Iverfeldt, 1991; Ebinghaus et al., 1995).

Gaseous methylmercury will not influence the total deposition of mercury to any great extend (Petersen et al., 1995). It may, however, constitute an important contribution to the overall

loadings of methylmercury in terrestrial and aquatic ecosystems (Hultberg et al., 1995). Methylmercury is present in precipitation at concentrations generally corresponding to around 5 % of the total mercur (Bloom and Watras, 1988; Hultberg et al., 1995; Munthe et al., 1995; Petersen et al., 1996) however, the sources of this methylmercury are still not known. Bloom et al. (1996) and Carpi and Lindberg (1997) have each presented evidence for gaseous $MeHg^+$ emissions from marine and continental sources, respectively.

2 Analysis of Mercury and its Compounds in the Atmospheric Environment

During recent years new analytical techniques have become available that have contributed significantly to the understanding of mercury chemistry and behavior in the atmospheric environment. In particular, these include ultra sensitive and specific analytical equipment and contamination-free methodologies. These improvements presently allow for the determination of total and major species of mercury to be made in the atmosphere. Whereas methodologies for the determination of TGM in the atmosphere were in principal available for about the past 20 years, this was not the case for mercury species such as RGM and Hg_{part}. During the past 10 years the development concerning TGM has very much focused on the improvement of precision and on methods with better time resolution. For RGM and Hg_{part} international effort has been focused on the development of generally accepted new standard methodologies with better accuracy, that allow for the comparability of measurement results obtained in different regions of the world.

In general, determination of mercury in air samples involves the following steps:

a. sample collection,

b. separation of mercury species of interest,

c. sample enrichment,

d. liberation from the sampling material,

e. conversion into elemental mercury vapor,

f. quantification.

By applying selective adsorber materials and combining them in sampling trains, steps a–c can usually be combined in manual methodologies to quantify TGM and Hg_{part}. Recently, automated analyzers for TGM determinations can be preceded by automated denuder systems for the determination of RGM additionally.

In the following, manual and automated methods for the determination of the most relevant mercury species in ambient air will be described.

2.1 Manual Methods for Sampling and Analysis of TGM and Particulate-Phase Mercury

The method described here combines separation and enrichment of TGM and Hg_{part} or TPM (Total Particulate Phase Mercury) during sample collection. The air-stream is pulled through a sampling train that retains particulates at the front end, before the total gaseous fraction is collected on solid gold or gold coated solid surfaces. Collected mercury species are usually thermally desorbed, converted into the elemental form and detected by Atomic Fluorescence or Absorption Spectroscopy in an inert carrier gas stream such as high purity Argon (pur. >99.998 %)

The sampling train is depicted in Fig. 2.1.

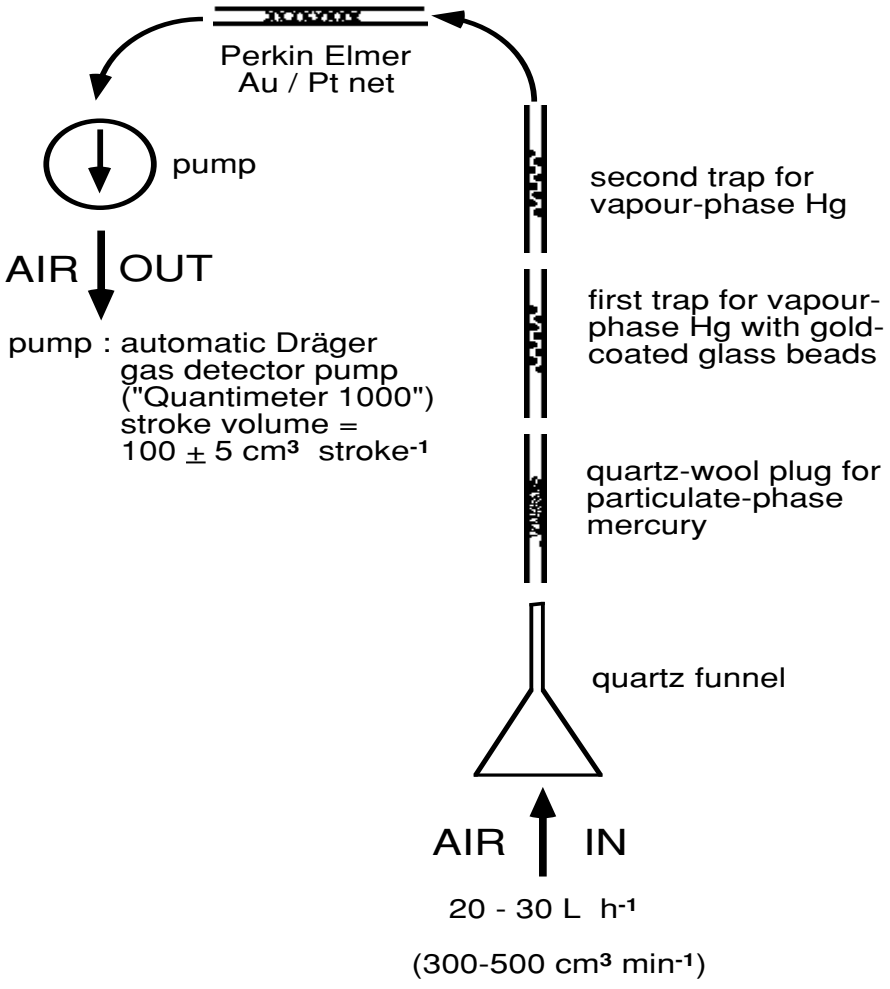

Figure 2.1: Sampling train for TGM and TPM

A quartz funnel at the sample inlet prevents co-sampling of raindrops which may effect sampling efficiency or spectroscopic detection. Approximately 20–30 L of ambient air are pulled through the sampling train with a flow-rate of 300–500 mL min^{-1}. At the front of the sampling train dust particles and particulate matter containing mercury are filtered by a quartz wool plug. TGM is then quantitatively removed from the sample-air stream by two subsequent traps consisting of gold-coated glass beads. Compared with solid gold adsorbers or gold-coated quartz sand, the gold beads technique combines several advantages that have been discussed in detail by Ebinghaus and Kock (1996). A third gold trap is placed between the sampling train and the pump to prevent contamination of the analytical traps by back-diffusion.

Calibration of the Atomic Fluorescence Detector Unit is usually carried out according to a method published by Dumarey et al. (1985). Mercury saturated air is kept under stable conditions in a specially designed calibration-unit shown in Fig 2.2. The unit is kept at a constant temperature of 20 °C±0.1 °C. For highly precise calibrations it is necessary, that the calibration-unit is operated on a very constant level below ambient temperature, for example inside a water bath, to avoid condensation effects inside the syringe or at other surfaces.

Through a septum mercury saturated air can be taken with a gas-tight syringe. At 20 °C and 1013 x 10^2 Pa 10µL saturated air contains an absolute amount of 131 pg Hg(0) (Dumarey et al., 1985). A standard deviation of 3% is achievable for the individual calibration points under these conditions. For a typical calibration between 0.1 and 3 ng Hg(0) absolute, a correlation coefficient for the calibration curve of > 0.9 can usually be achieved. Studies on the reproducibility reveal a variation coefficient of about 1 %.

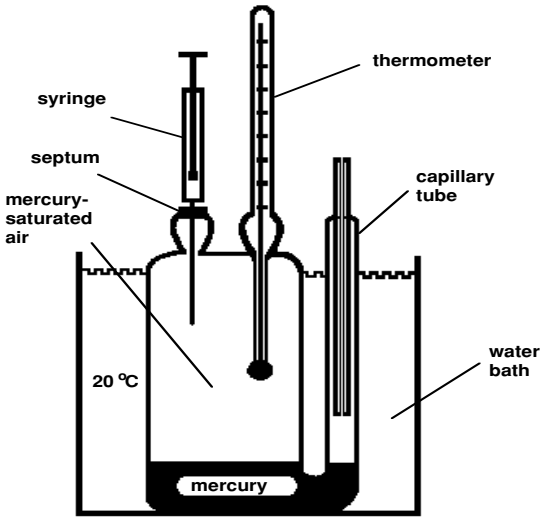

Figure 2.2: Calibration-unit according to Dumarey et al., (1985)

Determination is carried out according to the so-called "double-amalgamation technique" published by Fitzgerald and Gill (1979). However, we have modified this classical approach for the quantification of TGM in ambient air samples (Ebinghaus and Kock, 1996). The sampling traps contain 0.5 g of gold-coated glass beads with a diameter of 0.5 to 0.7 mm. The active sampling surface in one of these traps is approximately 15 to 20 cm^2. Compared with previously published sampling traps gold coated glass beads are advantageous under several aspects such as

- low costs for production,
- low flow-resistance during sampling,
- low memory effects,
- low blank values,
- quantitative desorption of sampled TGM at low temperatures.

Before sampling the traps are flushed with high-purity Argon at approximately 500 ºC for 3 to 4 minutes resulting in typical blank values of about 10 pg absolute (Ebinghaus and Kock, 1996).
The sampling trap is schematically shown in Fig. 2.3.

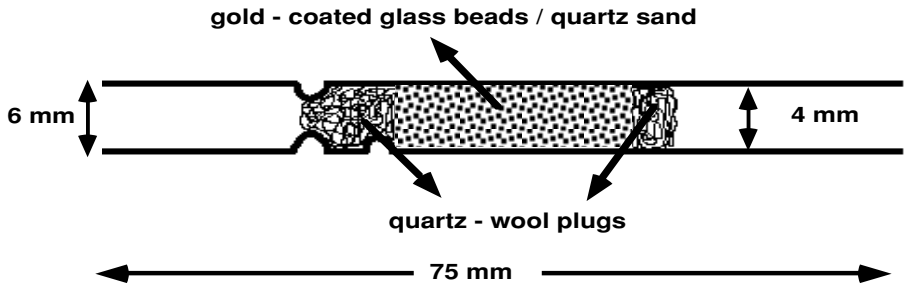

Figure 2.3: Sampling trap for TGM in ambient air

After sampling, the traps were sealed with plastic caps and stored in a firmly closed glass container. To prevent contamination during storage, approximately 1 g of silver wool are stored together with the sampling traps. To check the blank performance of sampling and storage 3 to 4 traps are treated in a similar manner as the sampling traps without plastic caps being removed at the sampling location. These blank-controls are analyzed together with the field traps and give typical blank values of 5 to 20 pg Hg(0) absolute. Therefore the entire procedure (sampling, storage, determination) has a method blank of approximately 100 pg.

Consequently, absolute amounts of 0.5 to 2 ng of mercury should be sampled on the field traps to achieve optimal results for the quantification of TGM in ambient air samples.

Field traps (gold coated glass beads and quartz wool plugs) are transferred into the desorption and detection unit as depicted in Fig. 2.4 and Fig 2.5. Quartz wool plugs are heated to 1200 °C for 1.5 minutes to release mercury from the particulates sampled. Gold coated glass beads are heated to 500 °C for 3 to 4 minutes to release the sampled the TGM fraction. In both cases, desorbed elemental mercury is transferred by an Argon carrier gas stream to another, previously calibrated gold trap ("double-amalgamation"). From this analytical trap mercury is again thermally desorbed and transferred into the AFS detector. The second amalgamation step results in a sharp AFS-signal for the desorbed mercury which is normally not achieved when TGM is directly transferred into the detector from the field trap, probably due to co-sampled organic contamination.

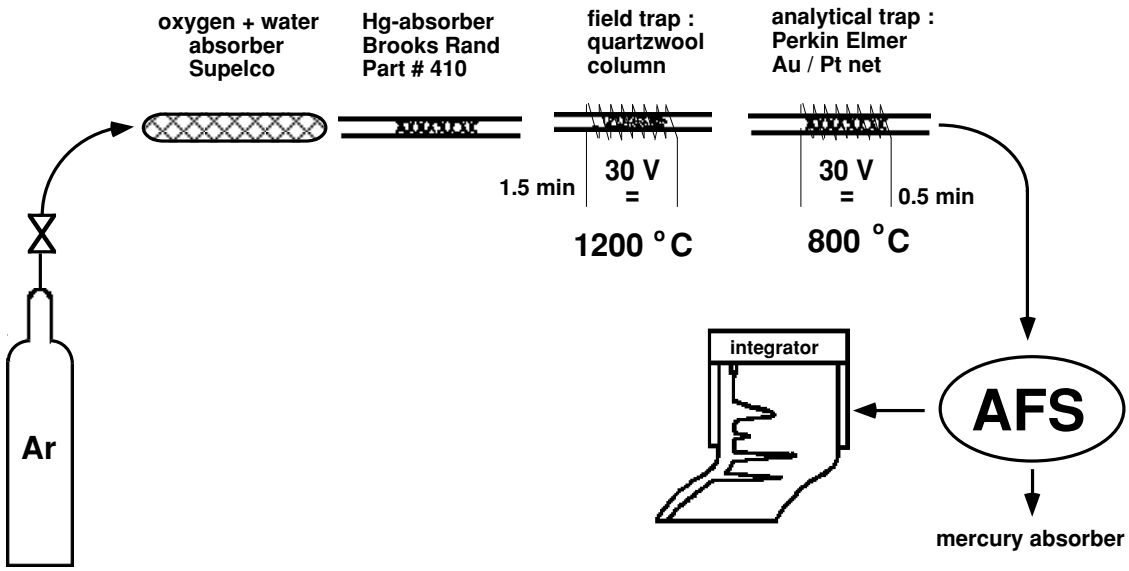

Figure 2.4: Set-up for the determination of Hg_{part} (TPM)

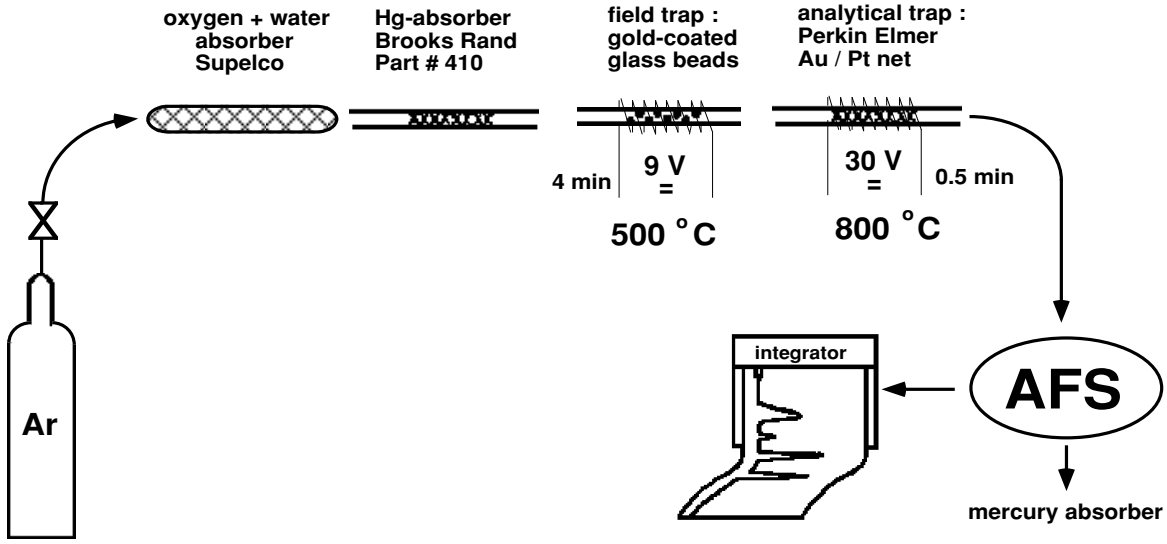

Figure 2.5: Set-up for the determination of TGM

2.2 Automated Method for Sampling and Analysis of TGM

An automated mercury vapor analyzer for the determination of mercury in ambient air has been developed, tested and marketed by a Canadian company in 1993. This instrument is based on similar basic operational features as the traditional manual methods. This instrument (Tekran Gas Phase Mercury Vapor Analyzer Model 2357A) also uses the gold amalgamation technique. The pre-filtered air stream is pulled through solid gold cartridge, then thermodesorbed and detected by Atomic Fluorescence Spectrometry (AFS) (Tekran, 1998). The instrument uses two gold cartridges in parallel, with alternating operation modes (sampling and desorbing/analysis) on a predefined time base of 5 min. A sampling flow rate of 1.5 L min^{-1} is used. Under these conditions, a detection limit of roughly 0.3 ng m^{-3} can be achieved (Schmolke et al., 1999). A 47 mm diameter Teflon pre-filter protects the sampling cartridges against contamination with particulate matter. On a predefined time base an automated two-point calibration can be performed by using an internal permeation source with a span value of approximately 17 ng m^{-3}, and a zero air reference point.

A flow-diagram of this instrument is shown in Fig. 2.6.

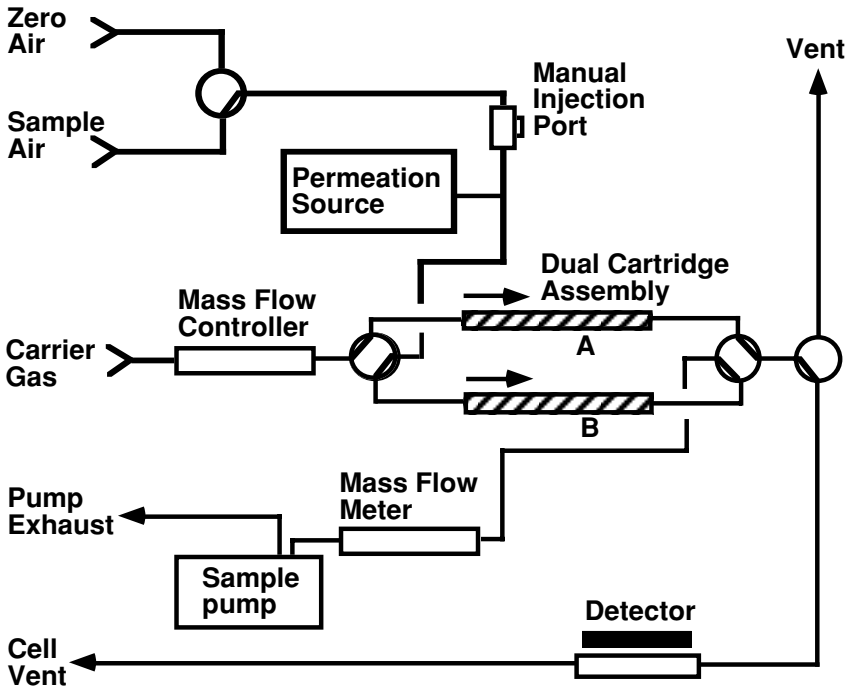

Figure 2.6: Schematic flow-diagram of Model 2537A Mercury Vapor Analyzer (Tekran, 1998)

In the meantime, other automated analyzers are available for the determination of TGM in ambient air samples. Technical details, operational features and possible applications are presented and discussed by Ebinghaus et al., (2000). Measurement uncertainty of this method is estimated in chapter 5.

2.3 Method for Total Particulate Phase Mercury in Ambient Air

Because particulate mercury generally constitutes only a small percentage of the total amount of airborne mercury, the potential importance of TPM (or Hg_{part} alternatively) in the atmospheric chemistry has long been underestimated or largely ignored (Lu et al., 1998). Recent research has shown the important role of particulate phase mercury in determining the dry deposition flux of this toxic trace metal (Keeler et al., 1995).

Because of its extremely low concentration in ambient air and the small amount of sample generally available for analysis, accurate determination of total particulate phase mercury (TPM) is extremely difficult to perform, and chemical speciation of TPM is an even more challenging task. Conventionally, airborne particles are collected using membrane or fibrous filters made from different materials (e.g. Ebinghaus et al., 1999). The exposed filters, loaded with the collected particles, are then transported to the laboratory and are digested with an acid mixture, followed by detection of total mercury. This technique is currently the most widely used procedure for TPM determination (e.g. Lu et al., 1998; Ebinghaus et al., 1999). To collect enough particulate matter for a reliable determination of associated mercury, a filter surface area as large as possible and a long sampling period (usually days) have traditionally been used. Disadvantages of the conventional technique are that it involves several filter/sample handling steps. Therefore, ultraclean mercury-free facilities are required to minimize contamination effects. Additionally, the time required for sample preparation is usually long (hours or days) resulting in high costs for analysis.

One option to have a more cost-effective methodology for TPM analysis could be the approach of using quartz wool plugs for sampling and subsequent thermal desorption that has been described above and was used in the sampling train. This method, since no extensive sample treatment is necessary, has a low risk of contamination and analysis can be carried out under normal laboratory conditions in a comparably short time. However, beside these practical advantages of quartz wool plugs in a quartz tube, adsorption of gaseous elemental mercury and other airborne species, such as dimethylmercury, reactive gaseous mercury and monomethylmercury have been reported (Lu et al., 1998; Xiao et al., 1991; Brosset and Lord, 1991; Slemr et al.; 1985).

Additionally, the pore size of these traps is not defined and the retention efficiency may vary from trap to trap. Field intercomparisons have shown that this methodology gives usually higher results for TPM compared with disc filter sampling followed by acid leaching, possibly due to co-sampling of other airborne species (Ebinghaus et al., 1999).

Nevertheless, methodology for sampling and analysis of TPM without sample transfer and sample preparation steps is preferable due to the above mentioned reasons. Furthermore, with continuing development of chemical/analytical technology, instrumentation with better sensitivity and selectivity is now available, so that reliable determination of TPM in the picogram range is now feasible, allowing sampling for a shorter period of time and/or at a lower flow rate. Thus, existing sampling protocols for TPM should be re-examined in the light of the newer technology. The use of pyrolysis, that means heating in the absence of oxygen or air, in the determination of different (operationally defined) mercury species in samples of soil and sediment has been previously reported in the literature (Biester and

Scholz, 1997; Windmöller et al., 1996). Pyrolysis of airborne particulate matter for the determination of TPM has been used by some researchers (Kvietkus et al., 1995; Ebinghaus et al., 1995; Schroeder et al., 1995b; Fitzgerald et al., 1991). If the sampling apparatus is properly designed, the trapped particles can be directly pyrolyzed in the sampling device without transfer or handling, and since no time consuming sample preparation is required, the time required for analyzing one sample can be less than 10 minutes.

Therefore an approach combining a defined and reproducible sampling methodology for TPM with low risk of contamination, short sampling intervals and short time for analysis has been developed by Lu et al. (1998) and modified in this work. This is essentially a device that serves as both particulate trap and pyrolyzer and is shown in Fig. 2.7.

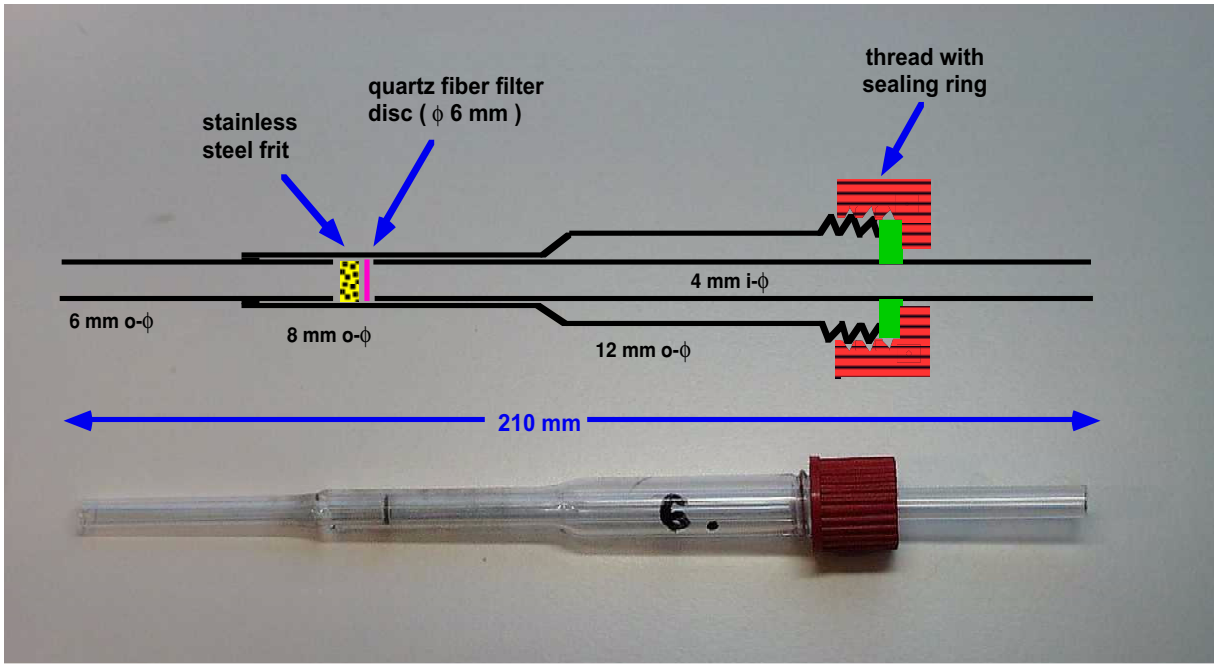

Figure 2.7: Modified version of the AES Mini Sampler for Total Particulate Phase Mercury (TPM)

2.4 Methods for the Analysis of Reactive Gaseous Mercury (RGM)

One of the major questions in the biogeochemical cycling of mercury is the extent of which gaseous Hg(II) species exist in ambient air (Schroeder and Munthe, 1998). Such species have been postulated to exist but it has been assumed that they are only a small fraction of the total atmospheric mercury. Nevertheless, this small fraction is important to the geochemical

cycling of mercury (Lindberg and Stratton, 1998). Modeling results to date have indicated that modeled fluxes are highly sensitive to the assumed fraction of total mercury that is Hg(II) (Petersen et al., 1995; Pai et al., 1997). Thus, measurement of gaseous Hg(II) is crucial to an understanding of the atmospheric transport and deposition of atmospheric mercury. This gaseous Hg(II) fraction, termed as reactive gaseous mercury (RGM), is generally assumed to consist primarily of $HgCl_2$ and/or other mercury halides, but might also include HgO, $Hg(OH)_2$, (Stratton et al., 2001). Recent studies with simulated flue gases has revealed strong evidence that $Hg(NO_3)_2 \cdot H_2O$ may be the major species emitted from coal combustion plants, especially in plants using low-chlorine coals (Centre for Toxic Metals, 1999). This species is characterized by its volatility and unusual stability.

Reliable measurements of RGM in ambient air are difficult for two reasons: the concentrations are extremely low and RGM is a very reactive substance. Two different approaches for the selective sampling and enrichment of RGM from ambient air samples have been described in the literature and have been tested and applied for field measurements within this work. These techniques are commonly referred to as (i) the denuder technique and (ii) the mist chamber approach.

Larjava (1993) introduced a KCl coated denuder for the collection of gas phase Hg(II) from flue gas at a concentration level of several tenths of mg m^{-3}. This method has been adopted and refined by Xiao et al. (1997) for the sampling and analysis of RGM in ambient air.

Brosset (1987) tried to determine ambient RGM by bubbling air through water solutions. The use of mist chambers in atmospheric studies of water soluble gases has been described by Talbot (1990) and others. This approach has been adopted by Stratton and Lindberg (1995) who have developed a high flow refluxing mist chamber, which has been modified and applied during this work. The chamber is schematically depicted in Fig. 2.8.

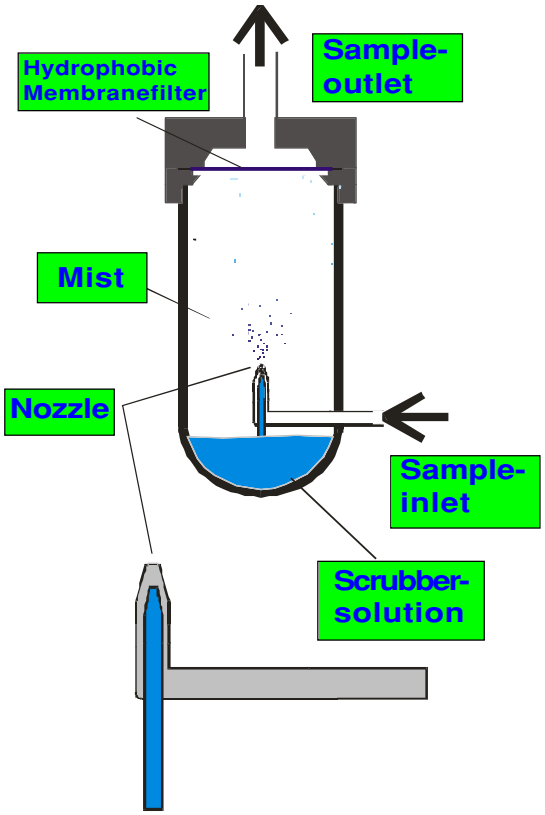

Figure 2.8: Refluxing mist chamber for the determination of RGM in ambient air

The mist chambers consist of a specially manufactured Pyrex glass body. They are partially filled with a small volume (20–30 mL) of an appropriate RGM-absorber solution. The solution consists of 0.5 g KBr/L, 0.25 g Ascorbic Acid/L in a 0.01 molar HCl. Ambient air is pulled in through the bottom at a flow rate of 10–15 L min^{-1}. A total sample volume between 0.5–3.5 m^3 is collected resulting a time resolution of 1–8 hours.

A nebulizer nozzle (orifice < 1 mm) produces a fine mist of the absorbing solution, with aerosol sized droplets. In this fashion, water soluble species are extracted from the air stream. A hydrophobic Teflon membrane filter is fixed on the top of the chamber in front of the outlet to retain the water droplets so that the solution drains back and is continuously refluxed. When sampling is completed a stannous chloride solution is added to the absorbing solution resulting in a reduction of RGM to elemental mercury. Hg(0) is then removed from the solution by an Argon carrier gas stream, preconcentrated on a gold cartridge and subsequently quantified by Cold Vapor Atomic Fluorescence Spectroscopy (CVAFS) as described in section 2.1.

Denuder techniques have been successfully used in the measurement of gas phase species in the atmosphere such as ammonia, sulphur dioxide, nitric acid, nitrogen dioxide and

chlorinated compounds (Xiao et al. 1997 and references therein). Gold- or silver coated denuders have been developed and applied for measurements of particulate and gas-phase Mercury in the air

In general, two different types of denuders are in use for the determination of RGM in ambient air however, as a common feature they are both using KCl coatings to retain gaseous ionic mercury species whereas elemental mercury is passing the denuder (Larjava, 1993, Xiao et al., 1997). First results have been published on the basis of tubular denuders by Munthe et al. (1990) and Xiao et al. (1991). Presently, the use of annular denuders in manual and automated methodologies has come up for the more precise measurement of RGM (Munthe et al., 2001). In this work we have used an automated system that has become recently available, the so called Mercury Speciation Unit Model 1130 manufactured by Tekran Inc., Canada.

Fig. 2.9 schematically shows the principle of operation of the Model 1130 Mercury Speciation Unit.

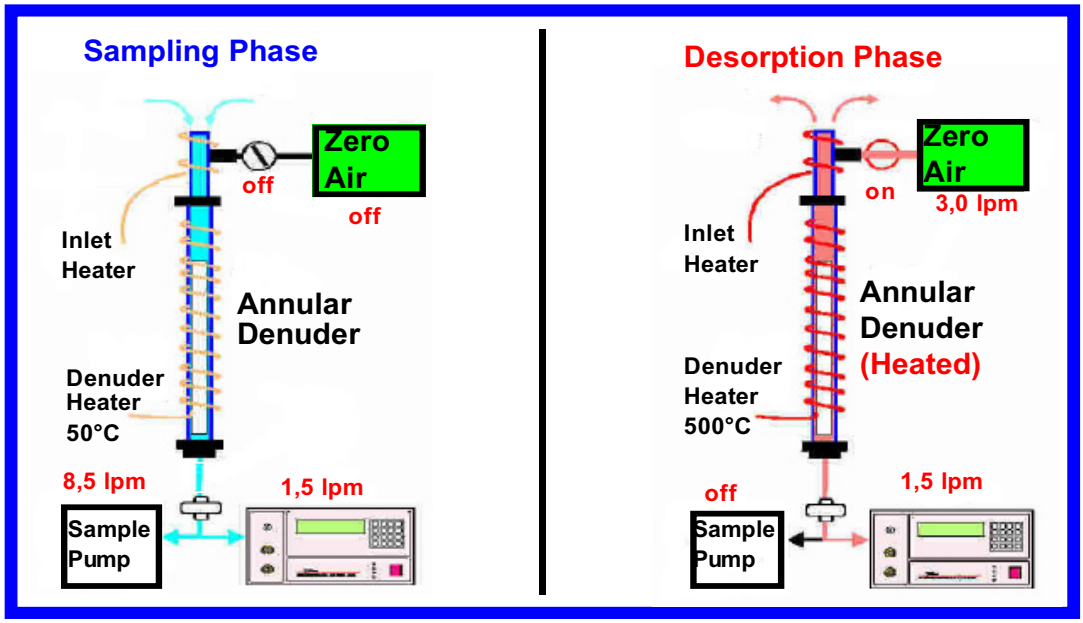

Figure 2.9: Model 1130 Mercury Speciation Unit; principles of operation (Tekran, 1998)

The instrument has an annular denuder consisting of two axial quartz tubes with about 1 mm spacing and sandblasted annulus walls. The effective KCl-coated length of the denuder is 25 cm. The denuder can be periodically re-coated, as required. The analyzer consists of a denuder heating device and a pump unit. For sampling air is pulled through the denuder (flow rate 6–8 L min^{-1}) which captures reactive mercury while allowing elemental mercury to pass

through. The denuder is kept at a temperature of 45 °C. Sampling time is 0.5–6 hours. After sampling the denuder is first flushed with zero-air to remove traces of co-trapped elemental mercury. For analysis the denuder is heated twice to 450 °C for 10 min and the species trapped on the denuder are desorbed and can be subsequently detected with an on-line connected Tekran mercury vapor analyzer (2537A). A heated line is used to minimize losses while carrying sample air and zero air between the speciation unit and the Tekran analyzer. The limit of determination is 3 pg Hg m^{-3} with a sampling volume of about 1 m^3.

Due to the fact that no reference materials or adequate standards for the collection part of the RGM analytical systems are available, intercomparisons are essential to validate this method. This need has also been pointed out by Stratton et al. (2001) who have intensively evaluated the mist chamber approach for the measurement of RGM.

2.5 Simultaneous Measurements of the Most Relevant Atmospheric Mercury Species in Ambient Air and Precipitation

As shown in the previous chapters, analytical methods have been developed for the most important mercury species in ambient air that have a direct influence on the transport and deposition of the toxic metal in the environment. Depending on the species of interest, the amount and quality of available data may vary significantly. Whereas tremendous amounts of high quality data exist for TGM, the situation is different for RGM and TPM.

Furthermore, data sets obtained from simultaneous measurements of all these species are extremely rare however, knowledge on the fractionation of these species under background conditions is of high importance for the parameterization of the boundary conditions of transport and deposition models.

In June 1998 within the framework of the Convention on Long-Range Transboundary Air Pollution, UN-ECE countries signed the protocol on restrictions of heavy metal emissions into the atmosphere. In this context Meteorological Synthezising Centre East of the European Monitoring and Evaluation Programme (EMEP - MSC-East) in Moscow is responsible to provide an operational model for the calculation of heavy metal airborne transport and deposition, including mercury. The well-known peculiar properties of mercury including physicochemical transformations during atmospheric transport make the problem of mathematical simulations of its airborne transport extremely complex (MSC-E, 2001). Besides, there is an obvious lack of experimental data which could be used for the verification of models of regional and global scale.

In accordance with recommendations of EMEP/WMO meetings MSC-East has initiated an intercomparison study for mercury models. The intercomparison study is divided in to four stages and parts of the work presented here are strongly linked to this international study.

- Stage 1: Comparison of chemical modules for mercury transformations in a cloud/fog environment with prescribed initial concentration values and input parameters. The absolute concentration values and temporal variations of selected parameters will be intercompared.
- Stage 2: Comparison of modeling results with observations during short episodes. The measurement data obtained during two Transect studies at four sites between Berlin and Stockholm will be used for this comparison. Additionally, other measurement data obtained in the model domain during these periods can be applied. Hourly/daily averaged concentrations in air and in precipitation will be compared.

- Stage 3: Comparison of the modeling results with observations for the entire year 1997. Available monthly and annual measurement data from European monitoring stations in 1997 will be used. Concentrations in air and precipitation and wet/dry deposition fluxes of different mercury species will be compared.
- Stage 4: Comparison of atmospheric mercury budgets of different mercury species in the entire EMEP domain and for some selected countries (UK, Poland and Italy). The items include the amounts of dry and wet deposition within the area as well as the amounts transported outside the area.
- The first stage is focussed on the comparison of chemical modules for mercury transformations in a cloud/fog environment with prescribed initial concentration values and input parameters.
- EMEP/MSC-East and supporting bodies have decided to use appropriate measurement results as input parameters to make modeling systems more realistic. The data presented here were selected and used as initial values for stage 1 of the model intercomparison study, because they correspond to an essential degree to the conditions of the modeled systems (MSC-East, 2001).
- Other studies presented in this work (see chapters 4 and 5) will be used during the intercomparison study as reference data for the stages 2 and 3.

Measurements have been carried out between July 6 to 27, 2000 at GKSS Research Centre Geesthacht. The study area is a rural site located in a wooded area. Metropolitan Hamburg is located approximately 30 km west of GKSS. Prevailing winds are coming from south west.

The following species have been measured

in ambient air:

- gaseous elemental mercury (GEM),
- reactive gaseous mercury (RGM),
- total particulate mercury (TPM),

in precipitation:

- total mercury,
- reactive mercury.

Gaseous elemental mercury was detected with a Tekran gas-phase mercury analyser (Model 2537A). The instrument uses the gold amalgamation technique. The pre-filtered air stream is pulled through gold cartridges, then thermodesorbed and detected by Atomic Fluorescence Spectrometry (AFS). The instrument uses two cartridges in parallel, with alternating operation modes (sampling and desorbing/analysing) on a pre-defined time base of 5 minutes. A sampling flow rate of 1.5 L min^{-1} was used. Under these conditions a detectetion limit of approximately 0.3 ng m^{-3} can be achieved. A 47 mm diameter Teflon pre-filter with a pore size of 0.2 µm protects the sampling cartridges against contamination with particulate matter.

In general, this system samples and analyses all gaseous fractions of atmospheric mercury, i.e. Total Gaseous Mercury (TGM). However, during this study the gold traps were preceded by an annular denuder which removes divalent inorganic mercury species. Therefore, under background conditions it can be assumed that the remaining and measured fraction is elemental mercury only.

Two different approaches have been used for the determination of inorganic oxidized gaseous mercury species, operationally defined as Reactive Gaseous Mercury (RGM): The Tekran mercury speciation unit (Model 1130) and the refluxing mist chamber. The methodology has been described above.

Total Particulate Mercury has been sampled and analysed according to the method published by Schroeder and co-workers (1998). Since no sample preparation, no manual sample transfer or sample handling and no addition of chemicals or reagents is required, this method has a very low risk of contamination. The procedural detection limit of this method for a typical 24 h sample is ~ 2 pg m^{-3}.

Precipitation samples were taken using the GKSS bulk sampler (Teflon, 35 cm diameter) and brown glass bottles. Sampling intervals were 48 hrs, starting at 9:00 a.m. Sampling and analysis were carried out according to the OSPAR guidelines for the sampling and analysis of mercury in precipitation. Total mercury in precipitation was determined after an oxidative digestion with Cold Vapor Atomic Fluorescence Spectrometry (CV AFS). 10 mL of precipitation sample was treated with 0.25 mL of BrCl solution (0.1 mol/L). The digestion was completed after 1 hour by addition of ascorbic acid.

For AFS-determination, dissolved ionic mercury was reduced to Hg(0) by a stannous chloride solution. The blank performance of the entire method was 2.4 ng L^{-1} with a standard deviation of 0.17 ng L^{-1} (n=10) and the limit of determination was 1.2 ng L^{-1}. Reactive mercury in precipitation was determined after direct reduction of the acidified sample with stannous chloride solution. The limit of determination is 0.6 ng L^{-1}.

Table 2.1 and 2.2 are summarizing the average concentration values, the observed minimum and maximum concentrations and the number of samples for the individual species measured between July 6 to 27, 2000. Table 2.3 gives an overview on the meteorological parameters air temperature, relative humidity and precipitation rate for the study period.

Table 2.1: Summary of average concentrations of airborne mercury species

Species	Average concentration	Minimum concentration	Maximum concentration	Number of samples
Elemental Hg (GEM)	1.59 ng m^{-3}	1.0 ng m^{-3}	2.4 ng m^{-3}	Ca. 5000
RGM; Denuder	4.0 pg m^{-3}	0.3 pg m^{-3}	90 pg m^{-3}	122
RGM; Mist Chamber	9.0 pg m^{-3}	below detection limit	20 pg m^{-3}	25
TPM	40 pg m^{-3}	below detection limit	275 pg m^{-3}	27

Table 2.2: Summary of average concentrations of mercury species in precipitation

Species	Average concentration	Minimum concentration	Maximum concentration	Number of samples
Total mercury	7.2 ng L^{-1}	5.0 ng L^{-1}	11.0 ng L^{-1}	7
Reactive mercury	2.2 ng L^{-1}	1.3 ng L^{-1}	3.5 ng L^{-1}	4

Table 2.3: Meteorological conditions

Parameter	Average value	Minimum value	Maximum value	Number of samples
Air temperature	15.4 ºC	9 ºC	27.5 ºC	
Rel. humidity	77 %	31 %	96 %	
Precipitation rate	3.5 mm / 48 hrs	0.9 mm / 48 hrs	5.9 mm / 48 hrs	8

On the basis on the information summarized in the previous tables, the following initial concentration values were adopted by EMEP (MSC-East, 2001). Because of the application in numerical simulation models for Europe, no measurement uncertainty is given, since model simulations can not handle this important analytical parameter appropriately (Ryaboshapko, 2002):

TGM: 1.7 ng m^{-3}; RGM: 5 pg m^{-3}; TPM: 40 pg m^{-3}.

3 Quality Assurance of Measurement Methods for Mercury in the Atmospheric Environment

Long-range atmospheric transport of mercury, its transformation to more toxic methylmercury compounds and their bioaccumulation in the aquatic foodchain have motivated intensive research on mercury as a pollutant of global concern. In the course of this research, mercury in air and precipitation has been increasingly measured at a multitude of different sites on a global scale and techniques have been developed for the speciation of mercury and its compounds. To achieve a scientifically sound synthesis of already available data of different origin with data to be obtained in the future, for the purpose of formulating a more comprehensive and consistent picture of the biogeochemical cycling of mercury, knowledge of the accuracy and precision of these data is imperative.

Collaborative methodology intercomparisons are an effective way of testing the accuracy, reliability and ruggedness of sampling and analytical protocols (Schroeder et al., 1995b, Youden and Steiner, 1975). In September 1995 we have initiated and carried out an international field intercomparison exercise on measurement methodologies for different atmospheric mercury species at a marine background location (Ebinghaus et al., 1999).

Previous field intercomparison measurements for TGM have been carried out at an urban/industrial site in Windsor, Ontario during the autumn of 1993 (Schroeder et al., 1995b) and at a remote continental location in North-Central Wisconsin, U.S.A. during September 1994 (Schroeder et al., 1995c). During the Windsor study two conventional manual methods were intercompared with two instruments of a new Canadian automated analyzer (Schroeder et al., 1995b). For the Mace Head intercomparison study described in this paper, 4 laboratories from North America and 7 laboratories from Europe participated. The sampling and analytical methodologies are representative to those common in use for atmospheric measurements of mercury in air and in precipitation. To our knowledge, this was the first international field intercomparison of measurement techniques for atmospheric mercury species in ambient air and precipitation at a marine background location.

3.1 International Field Intercomparison Measurements of Atmospheric Mercury Species

11 laboratories from North America and Europe met at Mace Head, Ireland for the period September 11–15, 1995 for the first international field intercomparison of measurement techniques for atmospheric mercury species in ambient air and precipitation at a marine background location. Different manual methods for the sampling and analysis of total gaseous mercury (TGM) on gold and silver traps were compared with each other and with new automated analyzers. Additionally, particulate-phase mercury ($Hg_{part_{rf}}$) in ambient air, total mercury, reactive mercury and methylmercury in precipitation were analyzed by some of the participating laboratories. Since some of the available techniques, especially for the determination of TGM in ambient air, have been used for more than 20 years (Fitzgerald and Gill, 1979; Slemr et al., 1979), some participants were asked to use their "customary" or better "traditional" manual methodology during the intercomparison exercise. In addition, automated analyzers only recently available, were also used during this study (Atomic Absorption Mercury Analyzer Model GARDIS-1A and Tekran Model 2537A-Mercury Vapor Analyzer).

The Mace Head field research station, operated by the Atmospheric Physics Research Group at University College Galway, is located on the west coast of Ireland, approximately 88 km west of Galway city, near Carna, Co. Galway (53^{o}, 19' N; 9^{o}, 54' W). The station has a clean sector zone between 180^{o} and 300^{o}, with open access to the Atlantic ocean, representing marine background conditions for atmospheric mercury and other trace gases (Jennings et al., 1993; Oltmans and Levy, 1994; Ebinghaus et al., 1995). Frequency distribution measurements of wind directions between 1990 and 1994 have shown that more than 50 % of the arriving air masses are within the clean sector (Spain, 1995).

3.1.1 Intercomparisons and Sampling Protocol

The following atmospheric mercury species were measured by a variable number of the participating laboratories:

- total gaseous mercury,
- particulate-phase mercury,
- inorganic oxidized gaseous mercury,
- total mercury, reactive mercury and methylmercury in precipitation.

Due to the limited number of participants who measured reactive gaseous mercury species, or reactive and methylmercury in precipitation, these results will only be reported in this work without being intercompared. However, these data are of great interest since only a few concentration measurements of these species exist for marine background locations in Europe. A protocol with fixed time intervals for all atmospheric mercury measurements was proposed in order to harmonize sampling. Three daily sampling intervals redundant were proposed for TGM: from 9:15 a.m. to 3:00 p.m., from 3:15 p.m. to 9:00 p.m. and from 9:15 p.m. to 9:00 a.m. next morning. All other species were collected over a 24 hour-period. Table 3.1 summarizes the measurements carried out by the participating laboratories.

Table 3.1: Measured Atmospheric Mercury Species and the Corresponding Laboratory Code

Ambient Air		Precipitation				
Lab. Code	TGM	Hg_{part}	RGM	Total Hg	Methyl Hg	"Reactive" Hg
1	X					
2	X					
3	X	X		X		
4	X					
6	X	X		X		X
7	X	X	X	X	X	
8				X		
9	X					
10	X			X		
11	X	X	X			
12	X					

3.1.2 Methods for Total Gaseous Mercury

Unlike other heavy metals, mercury occurs in the atmosphere primarily in the gaseous phase. Elemental mercury is the predominant atmospheric species in rural or remote locations. Measurements for TGM were intercompared by 10 laboratories during the Mace Head study. 4 different manual methods were used by 7 laboratories and 2 different types of automated analysers were used by 4 laboratories. The method differences were not major ones, as all the methods used used Cold-Vapor Atomic Fluorescence Spectroscopy (CVAFS) detection except one, which used Cold-Vapor Atomic Absorption Spectroscopy (CVAAS). In general, the methodology can be summarized as follows: TGM is collected by pulling ambient air through a precious metal trap. The amalgamated mercury is released by heating the trap to temperatures between 400 and 700 ^{O}C depending on the metal used. Released mercury is transferred to the detector unit directly (single amalgamation procedure) or amalgamated once more on a second trap. From this trap it is thermally desorbed and transferred to the detector (double amalgamation technique). The detectors are calibrated by the injection of small volumes of mercury-saturated gas at defined temperatures. Fundamental work on this technique has has been carried out by Braman and Johnson (1974), Dumarey et al. (1985), Fitzgerald and Gill (1979) and others.

Table 3.2 summarizes the main operational features of the intercompared methods for total gaseous mercury: They differ in using different sorption media, air flow-rates and in the number of amalgamation steps. Some of the participating laboratories filter the air sample before amalgamation of TGM, others do not use filters at all. Since the particulate mercury fraction represents only a few percent of the total mercury content in regions unaffected by local sources (Fitzgerald et al., 1983; Brosset and Lord, 1991) these methodical differences should not lead to substantial differences in measured TGM concentrations. However, little information is present in the literature regarding the effects of allowing particulate matter to build up on the TGM traps over multiple uses.

Table 3.2: Intercompared Methods for Total Gaseous Mercury (TGM)

Lab. code	Sampling trap	Method	Flow-rate [L min^{-1}]	Detection
1	Solid gold gauges	automated	1.5	CVAFS
2	Gold coated glass beads	manual	0.4	CVAFS
3	Gold coated silica sand	manual	0.75	CVAFS
4	Solid gold wool	automated	1	CVAAS
6/1	Gold coated glass beads	manual	0.4	CVAFS
6/2	Solid gold gauges	automated	1.5	CVAFS
7	Gold coated silica sand	manual	0.35	CVAFS
9	Solid gold gauges	automated	1.5	CVAFS
10	Gold/Platinum gauges	manual	0.5	CVAFS
11	Gold coated glass beads	manual	0.75	CVAFS
12	Silver coated quartz wool	manual	5–7	CVAFS

3.1.3 Methods for Particulate-Phase Mercury

The particulate mercury fraction relative to the total gaseous mercury present in ambient air is usually 4 % or less (Horvat, 1996; Schroeder and Jackson, 1987). Compared with elemental mercury vapor, particulate-phase mercury is rapidly removed from the atmosphere (average residence time of a few days). Four laboratories measured particulate-phase mercury compounds using four different methods. Sampled air is flown through particulate filters of different designs. Two laboratories used common PTFE or quartz fibre filters, two other laboratories used quartz wool plugs or gold coated glass beads. The last one was preceded by a gold-coated denuder which scrubbed all gaseous mercury from the sampled air. The filters were leached by acid and mercury was determined in solution by techniques similar to those described for the analysis of precipitation samples. From the quartz wool plug and gold trap, mercury was thermally released and de tected by CVAFS. Table 3.3 summarizes the methods for measurements of particulate-phase mercury:

Table 3.3: Intercompared Methods for Particulate-Phase Mercury

Lab. code	Collection	Flow-rate [L min^{-1}]	Desorption	Detection
3	Teflon disc filters[*1]	Not reported	Acid leaching	CVAFS
6	Quartz wool plugs	0.6–1.2	Thermal desorption	CVAFS
7	Whatman quartz fibre filters	9–10	Acid leaching and digestion with BrCl solution	CVAFS
11	Au traps preceded by Au denuders	0.2	Thermal desorption	CVAFS

*[*1] (pore size 0.45 µm)*

*[*2] (99,9 % retention effectivity for particles > 0.1 µm)*

3.1.4 Methods for Measurements of Reactive Gaseous Mercury Species in Ambient Air

Knowledge of the concentrations of reactive gaseous mercury (RGM) is of great interest because, relative to Hg(0) the wet and dry deposition fluxes are currently believed to be quite high for these compounds. Experimental data on RGM are still fairly limited however, Lindberg and Stratton (1998) have recently published a very extensive data set on vapor-phase Hg(II). Mason et al. (1997) concluded that RGM exists in ambient air based on measurements of Chesapeake Bay precipitation.

Hg(II) compounds are much more soluble in water and have a lower vapor pressure than Hg(0) and are therefore more effectively removed via wet and dry deposition. By direct stack testing of sources of atmospheric mercury species, Prestbo et al. (1995) have shown that oxidized Hg(II) can be a large percentage of all mercury species emitted. In general, the relative proportion of gaseous atmospheric Hg(II) in the TGM load is higher in the vicinity of industrial and some natural sources, compared to background locations. Due to the specific deposition behavior of Hg(II), Fitzgerald and Mason have used the terminology of "regionalizing" the relationship between sources and receptors (Fitzgerald and Mason, 1996). However, wit-

hin the framework of global cycling of mercury, information on the atmospheric residence time of Hg(II) derived from experiments is still lacking (Pacyna et al., 1996). Estimates by Slemr et al. (1985) based on Junge's relationship (Junge, 1977) are discussed later. Reactive gaseous mercury species were measured by two laboratories using two different methods: Laboratory 7 used a series of two ion exchange filters which are loaded behind a quartz fibre filter. Digestion in the laboratory consisted of refluxing the ion exchange filters with an oxidizing acid solution. The entire digested sample was analyzed by reduction with stannous chloride solution, dual gold amalgamation and CVAFS quantification. Laboratory 11 used KCl coated denuders for the sampling of gaseous Hg(II). The average collection efficiency of these denuders for Hg(II) is reported to be 98 % whereas elemental mercury is passing it (Xiao et al., 1997). Hg(II) trapped in the denuder was extracted with hydrochloric acid and analyzed with CVAFS after reduction with stannous chloride solution. Table 3.4 summarizes the applied methods for reactive gaseous mercury.

Table 3.4: Applied Methods for Reactive Gaseous Mercury (RGM)

Lab. code	Collection	Flow-rate [L min^{-1}]	Sample preparation	Detection
7	Ion-exchange membranes preceded by a particulate filter	9–10	Digestion of Ion-exchange membranes with BrCl solution	CVAFS
11	KCl denuder	0.7	Leaching of denuder wit HCl	CVAFS

3.1.5 Methods for Measurements of Mercury Species in Precipitation

Measurements of wet deposition of mercury are nowadays carried out worldwide. Mercury concentrations in precipitation collected at Mace Head during previous measurements in 1991 and 1992 cover a relatively small range of values: from 5 to 38 ng L^{-1}. The arithmetic mean of the measured concentrations is about 17 ng L^{-1} (Ebinghaus et al., 1995). At Mace Head, the percentage of operationally defined reactive mercury (HgIIa: fraction directly reducible with stannous chloride solution) of the total mercury is rather high compared to other results reported for precipitation and ranges from 25 to 79 % with a mean value of 7.5 ng L^{-1} (Ebinghaus and Krüger, 1996). Five laboratories analyzed total mercury in precipitation collected with bulk samplers. Two of them additionally measured methylmercury or reactive

mercury. Except for laboratory 8, all participants carried out ground-based sampling, i.e. approximately 1 to 1.5 meters above the soil surface. Samplers of laboratory 8 were mounted on top of a 20m-tower. Samples were acidified and shipped to the laboratories for analysis, which generally consists of

- a digestion step, for example with an acid solution of BrCl,
- a pre-reduction step, for example with hydroxyl ammonium hydrochloride solution,
- reduction of Hg(II) to elemental Hg(0) with stannous chloride and
- dual gold amalgamation followed by CVAFS quantification.
- Operationally defined reactive mercury was measured in the undigested sample, starting with the direct reduction of Hg(II).

Methylmercury in rainwater was analyzed by one of the participating laboratories. Laboratory 7 added HCl to selected samples and distilled to isolate $MeHg^+$ into a simple water matrix (Horvat et al., 1993). In the rainwater distillate, $MeHg^+$ was analyzed using aqeous phase ethylation, purging onto carbotrap, thermal desorption onto an isothermal gas chromatography column and quantified with CVAFS as described by Bloom (1989). Table 3.5 summarizes the applied methods for mercury species in precipitation.

Table 3.5: Intercompared Methods for Mercury in Precipitation

Lab. code	Collection	Sampling surface	Sample Volume	Species
3	Pyrex crystallizing dishes	610 cm^2	Not reported	Total Hg
6	PTFE funnels	962 cm^2	0.09–0.93 L	Total Hg/reactive Hg
7	PTFE funnels	78 cm^2	0.008–0.14 L	Total Hg/methyl-Hg
8	Polymethylpentane funnels*	716 cm^2	0.06–0.62 L	Total Hg
10	Pyrex crystallizing dishes	610 cm^2	Not reported	Total Hg
	**Mounted on a 20 m tower*			

3.2 Results for Total Gaseous Mercury

All data reported for total gaseous mercury measurements are summarized in Table 3.6:

Table 3.6: Reported Measurement Data for TGM by the Individual Laboratories and Related Sampling Intervals

Sample no.	Lab. No: 1	Lab. No: 2	Lab. No: 3	Lab. No: 4	Lab. No: 6/1	Lab. No: 6/2	Lab. No: 7	Lab. No: 8	Lab. No:10	Lab. No: 11	Lab. No: 12
Sampling interval											
11/1	1.71		7.4	1.7	15.7	2.49	2.04	1.66	4.2	10.89	3.3
Time	13:55-15:00		09:00-21:00	09:00-21:00	09:00-15:00	09:00-15:00	09:25-09:00*	13:55-15:00	09:00-15:00	09:25-14:59	09:00-15:00
11/2	1.95	2.2		1.7	7		2.04	1.82		3.08	1.77
Time	15:15-21:00	15:20-21:00		09:00-21:00	15:15-21:00		09:25-09:00	15:15-21:00		15:15-21:00	15:15-21:15
11/3	1.93	0.9			3.6	1.69	2.04	1.73	1.98	2.5	1.92
Ti,me	21:45-09:00	21:15-09:03			21:15-09:00	21:15-09:00	09:25-09:00	21:45-09:00	21:15-09:00	21:00-09:00	21:30-09:45
12/1	1.8	1.5	1.6	1.8		1.84	1.52	1.62	1.82	3.65	3.01
Time	11:40-15:00	09:15-15:00	09:15-15:00	09:00-21:00		09:15-15:00	10:10-09:00	11:40-15:00	09:15-15:40	09:23-15:35	10:00-16:00
12/2	1.65	1.9		1.8	1.3		1.52	1.47		1.83	1.44
Time	15:15-21:00	15:15-21:00		09:00-21:00	15:15-21:00		10:10:-09:00	15:15-21:00		15:40-20:56	16:15-22:15
12/3	1.61	3.8			1.3	1.44	1.52	1.49	1.60	1.79	1.75
Time	21:40-09:00	21:15-09:05			21:15-09:06	21:15-09:06	10:10-09:00	21:40-09:00	21:15-09:00	20:58-08:58	22:30-08:06
13/1	1.71	2.1		1.92	4.1	1.64	1.54	1.57	1.92	2.38	1.46
Time	09:45-15:00	09:15-17:00		09:00-15:00	09:15-17:00	09:15-17:00	09:38-17:02	09:45-15:00	09:50-17:30	09:15-17:32	09:35-16:59
13/2	1.67	2.2			1.3	1.48	1.57	1.56	1.82	1.76	1.52
Time	15:15-09:00	17:15-09:10			17:15-09:10	17:15-09:10	17:15-09:00	15:15-09:00	17:30-09:00	17:34-09:00	17:18-09:03
13/3											
Time											
14/1	1.65	3.1	2.1	1.8	2.6	1.84	1.66	1.63	1.7	2.65	1.56
Time	09:45-15:00	09:17-15:00	09:15-15:00	09:00-15:00	09:15-15:00	09:15-15:00	09:45-21:00	09:45-15:00	09:20-20:30	09:15-15:00	09:15-15:00
14/2	1.66		1.8		1.6	1.7	1.66	1.81	1.7	1.92	1.54
Time	17:40-20:25		15:15-21:00		15:15-21:00	15:15-21:00	09:45-21:00	17:40-20:25	09:20-20:30	15:58-20:55	15:15-21:00
14/3	1.92		2.2		1.8	1.85	1.82	1.92	2.08	1.72	1.82
Time	21:40-09:00		21:15-09:00		21:15-09:00	21:15-09:00	21:05-09:00	21:40-09:00	20:30-09:00	21:00-09:00	21:15-09:00
15/1	2.07			1.75	2.6	2		1.84		2.16	2.078
Time	09:40-15:00			09:00-15:00	09:15-15:00	09:15-15:00		09:40-15:00		09:10-14:40	09:15-15:00

**9:a.m. next morning*

The following procedure was used in order to intercompare the TGM measurements of the different groups: Since the sampling intervals were not absolutely identical during the entire experiment and because some of the laboratories had sampling gaps due to contamination and/or technical reasons, the calculation of the arithmetic mean as well as the use of weighted individual concentration measurements was not deemed to be useful. Therefore it was decided to use a 24 hour time-window and all data reported for that period (i.e. 9:15 a.m. until 9:00 a.m. next morning). The median of the reported data was calculated because it should be less affected by missing data and outliers caused by contamination problems. Reported data for September 11 (i.e. samples 11/1; 11/2 and 11/3) have not been considered for intercomparison purposes because some results had obviously been affected by a contamination event observed the night before (see Table 3.6).

Figure 3.1 shows the box and whisker plots for intercompared total gaseous mercury determinations.

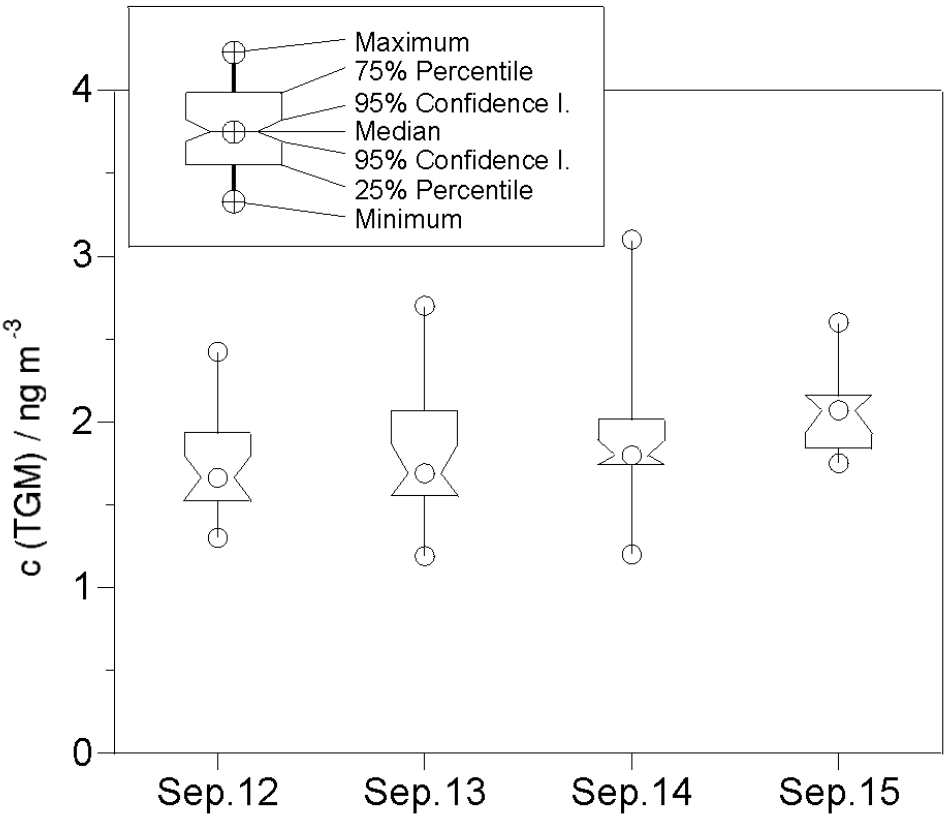

Figure 3.1: Box and Whisker plots for total gaseous mercury determinations

The boxes represent the interquartile range (mid-range) of all values. The upper and the lower limits of the boxes display the 75 and the 25 percentiles, the circle within the box gives the median of the reported results and around the median the 95 % interval as a notch. The range between the upper and lower circles (whiskers) represents the span between the minimum and the maximum values reported. Due to the above-mentioned assumptions, the height of the boxes (50 % area) is determined by method-related or methodological differences of the intercompared methods and the natural variations of the TGM concentrations that can be resolved by the shortest sampling period, i.e. 6 hours. However, due to the fairly constant mercury concentrations at Mace Head, the range of the notch boxes (0.4 to 0.6 ng m^{-3}) should mainly represent differences between the individual methods. At the same time as the intercomparison exercise was conducted at Mace Head, continuous TGM measurements were started there using an automated analyzer with 5 minute time resolution. For the period of interest, no peak concentrations, i.e. higher than 3 ng m^{-3}, were observed with this instrument (Ebinghaus et al., 1996). In addition, the standard deviations of the concentration values measured over 5 minutes integration time was calculated for the individual sampling periods. This number gives an indication for the short term variations of Hg-concentrations during the sampling intervals which could not be resolved by most intercompared techniques. The lowest variability in ambient air concentrations was observed during sampling period 12/2 with 1.46 ± 0.06 ng m^{-3}, the most pronounced variability could be detected during sampling period 14/1 with 1.63 ± 0.24 ng m^{-3}. Except for sample 14/1 and 14/3 all calculated standard deviations were less than 0.2 ng m^{-3} indicating that the variability of Hg-concentrations within the 6- or 12-hours sampling periods is insignificant. However, a systematic problem may occur regarding the 95 % confidence interval, if an outlier of a 6 hr sampling period is followed by a gap for the same laboratory. In this case the calculated notch box would be too small, because the influence of the outlayer will be under-repesented in the 24-hour window. The median values calculated for four individual days are between 1.7 and 1.95 ng m^{-3}, reflecting background conditions. Therefore all reported data for TGM concentration measurements during the period of September 12 to 15 were combined to calculate an "overall-median".

In Figure 3.2 individual laboratory results were compared with this "overall-median " depicted in the left part of the Figure. The solid bars represent the mean value of the results reported by each laboratory; the error bars indicate the minimum and maximum concentrations.

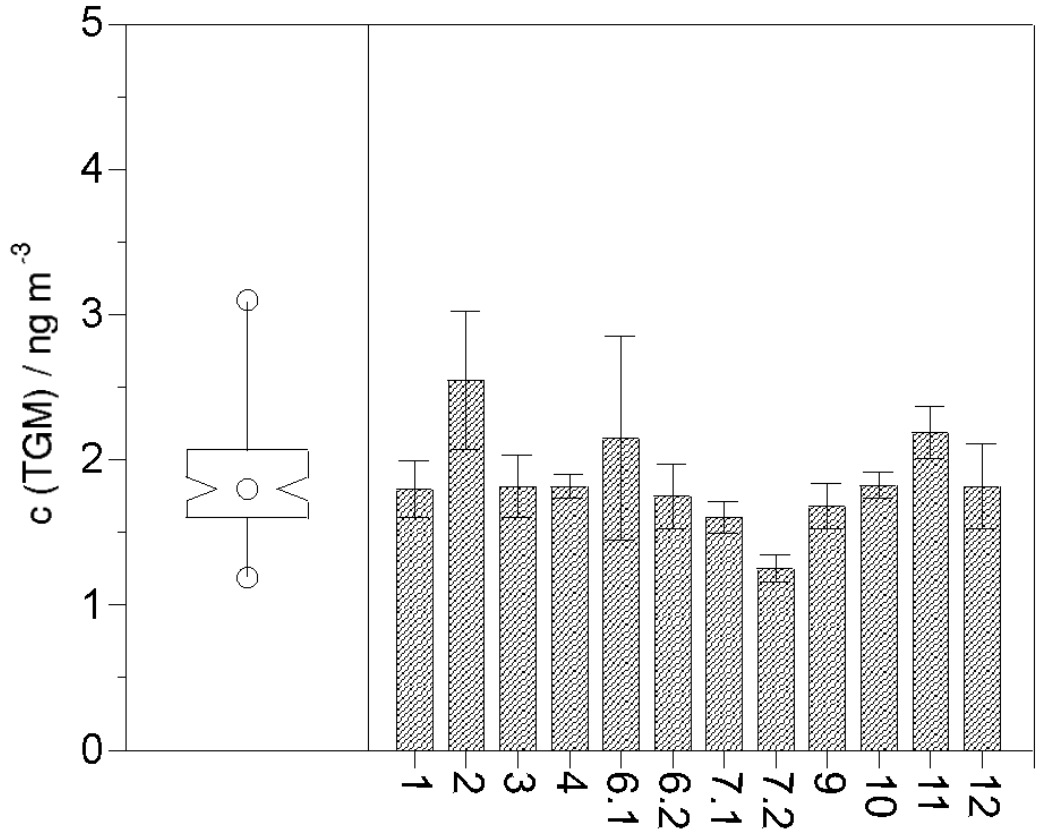

Figure 3.2: Intercomparison of individual laboratory results for TGM with the overall-median value

3.3 Results for Particulate-phase Mercury

Particulate-phase mercury concentrations (TPM or Hg_{part}) were measured by laboratories 3, 6, 7 and 11. In accordance with the sampling protocol, four 24-hour samples were taken by each laboratory. The results are shown in Figure 3.3.

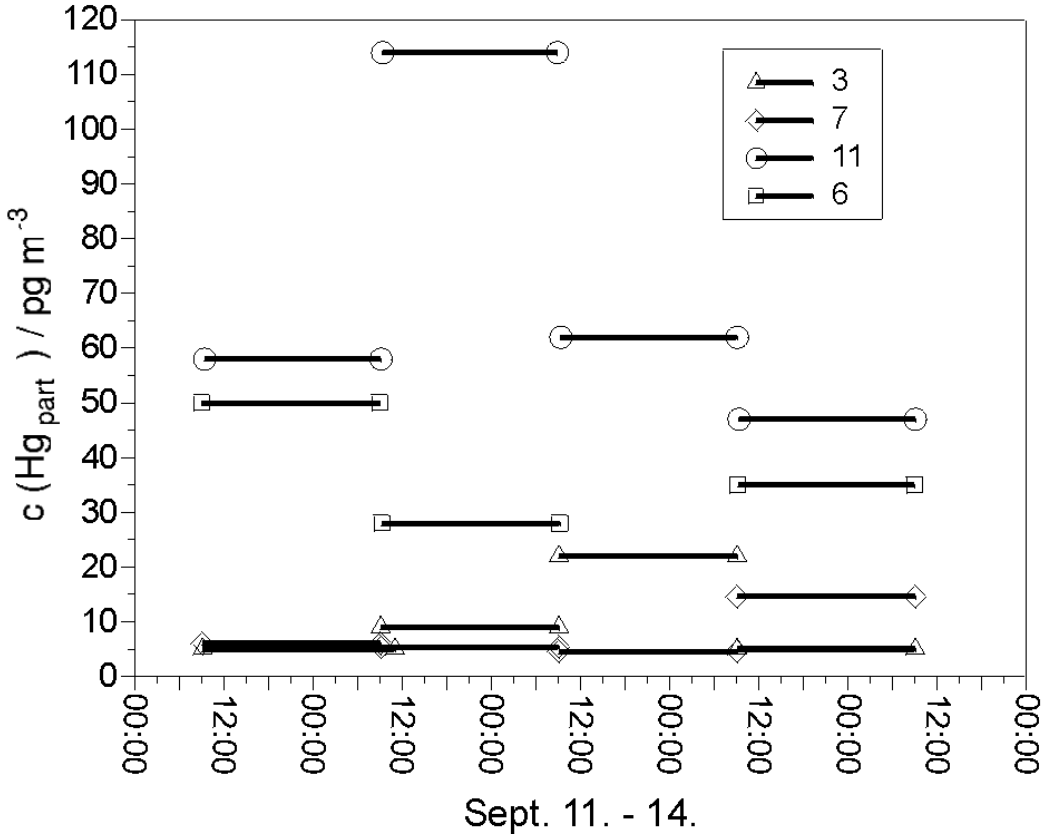

Figure 3.3: Intercomparison of individual laboratory results for total particulate-phase mercury (Hg_{part})

The range of all measured concentrations is between 4.5 and 115 pg m^{-3}. However, if only the results obtained by the use of disc filters followed by acid leaching, as used by two laboratories, are taken into account, the range is much smaller: between 4.5 and 26 pg m^{-3}. If only results are taken into account from methods in which quartz tubes filled with quartz wool or gold-coated glass beads (preceded by Au-denuders to remove TGM) followed by thermal desorption were used, the measured concentrations range from 28 to 115 pg m^{-3}. The differences in the sampling flow-rates are remarkable. Whereas laboratory 7 used flow-rates of 9 to 10 L min^{-1}, laboratory 11 sampled with 0.2 L min^{-1} resulting in absolute amounts mercury on the traps of less than 100 pg. In general it can be concluded that the collection of particulate-phase mercury on disc filters followed by acid leaching gives lower concentrations with a smaller variability. Under the conditions prevailing at Mace Head during the intercomparison study (fairly constant soot and TGM concentrations) a low variability of Hg_{part} seems to be more plausible than more pronounced variations. Some very interesting results relevant to this intercomparison have recently been obtained in a laboratory which participated in the Mace Head intercomparison, but did not sample particulate-phase mercury (Schroeder, 1997).

Using gold-coated denuders available commercially from a North American supplier, experimental results (scanning electron spectroscopy) showed that tiny flakes of gold, not visible to the naked eye, are released ("eroded") from the interior Au surface during the sampling step and end up on the particulate filter situated downstream of the denuder. Such specks of gold would have gaseous-phase mercury species (mainly elemental Hg(0)) amalgamated to them and would bias the particulate-phase mercury determination, which is based on chemical analysis of all materials on the filter (or Au traps) located downstream of the denuder. These observations provide a plausible explanation of why the "denuder method for particulate-phase mercury" tends to give results which are higher than those obtained with "filter methods". It should be kept in mind that the Canadian work involved Au denuders from one supplier, and hence their results should be independently verfied by others who use Au-coated denuders for the determination of particulate-phase mercury.

3.4 Results for Reactive Gaseous Mercury Species

Figure 3.4 shows the results for RGM obtained by 2 of the laboratories which participated in this field intercomparison project.

The results of laboratory 7 for RGM are in the range of 13 to 23 pg m^{-3}. The results for IOGM reported by laboratory 11 are in general higher and range from 41 to 94 pg m^{-3}. Estimates made by Slemr et al. (1985), based on the relationship between vapor pressure and the ratio of gaseous concentrations to particulate concentrations of different chemical species in the atmosphere derived by Junge (1977), suggest that inorganic oxidized mercury species will be predominantly found on aerosols and thus will share their atmospheric fate, i.e. will have a residence time of about 5 days (Prospero et al., 1983) and are generally not transported over large distances. According to Junge, another consequence is that concentrations of Hg(II) should not be too different from particulate-phase concentrations of mercury because the particulates encompass Hg(II).

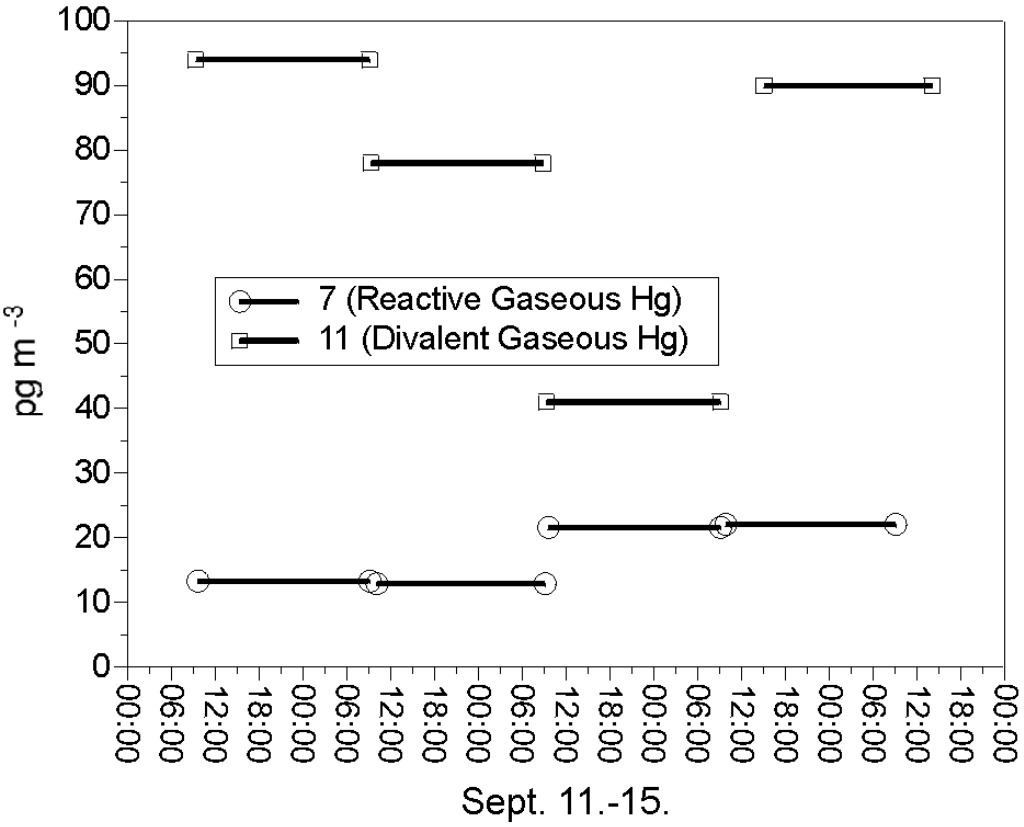

Figure 3.4: Reported results for reactive gaseous mercury species

3.5 Results for Mercury in Precipitation

The results for total mercury in precipitation measured by 5 laboratories are in the range from 4 to 12.2 ng L^{-1}, clearly representing background conditions for the time period of the inter-comparison exercise. Due to the low variability, the volume-weighted mean of all reported concentrations was calculated in order to compare the individual laboratory results against this calculated overall-mean. The volume-weighted mean was calculated by using the following equation:

$$\overline{C}v = \frac{\sum ViCi}{\sum Vi}$$

Vi represents the individual sample volume with the measured concentration *Ci*. The calculated volume weighted concentration is expressed as *Cv*.

Four rain events occurred during the intercomparison exercise and sampled volumes were in the range of a few mL to about 1 L as shown in table 3.5. Again statistical treatment of availa-

ble data should be done with great care. Figure 3.5 shows a comparison of the overall mean for total mercury in precipitation, along with the volume-weighted individual laboratory results. The calculated mean of all reported concentrations for total mercury in precipitation is 7.9 ng L^{-1} with a span between 4 and 14 ng L^{-1} as depicted in the left part of the Figure. The wide, solid bars represent the mean value of the reported results from each laboratory, the error bars indicate the minimum and maximum concentrations. However, it should be noted that the number of concentration measurements by each laboratory is very limited, i.e. only 3–4 samples were taken and analyzed. Concentration data of laboratory 8, conducting tower-based measurements, are in good agreement with the mean value. Laboratories 3 and 10, using open crystallizing dishes for sample collection, reported consistently lower numbers, whereas laboratories 6 and 7, using ground-based teflon funnels, obtained slightly higher concentrations. However, taking into account that the reported concentrations not only include different sampler designs and efficiencies, but also individual ways of storage, shipping and analysis, the intercomparability is acceptable but needs further improvement. Due to the limited number of individual measurements no error bars are given in Fig. 3.5. Laboratory 6 measured operationally defined "reactive mercury" in two samples and reported concentrations of 1.2 and 1.9 ng L^{-1}. Methylmercury in precipitation was measured by laboratory 7 at concentrations of 75 and 98 pg L^{-1}.

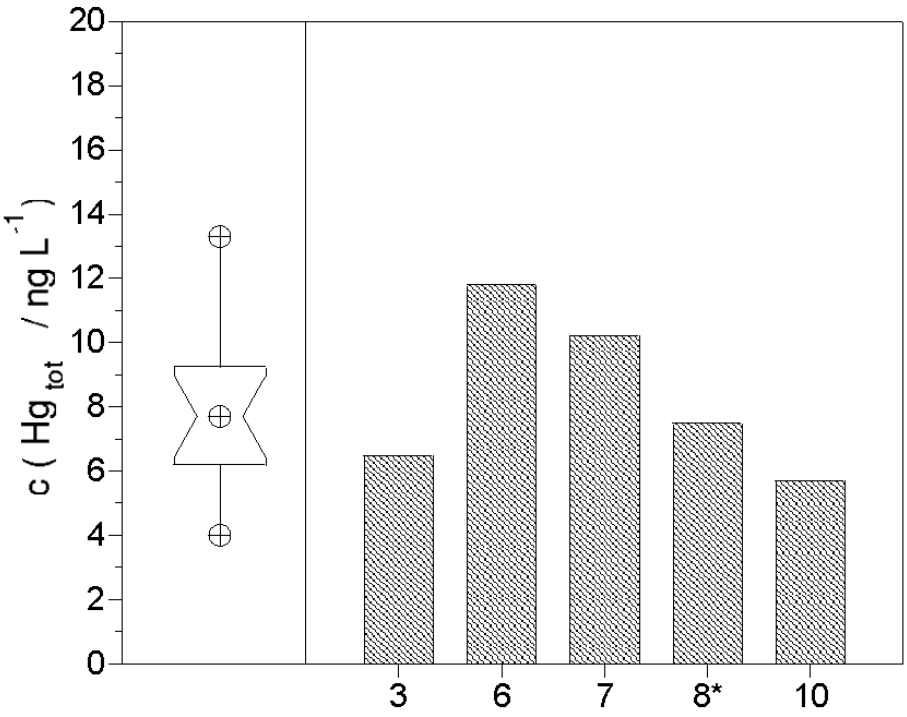

Figure 3.5: Intercomparison of individual laboratory results for total mercury in precipitation with the overall-mean value. Samplers of laboratories 3, 6, 7 and 10 were groundbased, sampler of laboratory 8* was mounted on a 20 m tower

The intercomparison results have shown the maturity of available techniques for the determination of TGM under background conditions. These techniques are based on the two-step amalgamation of TGM on gold or silver surfaces followed by CVAFS detection. Results reported for recently marketed automated analyzers are in good agreement with the traditional manual methods. Intercompared methods for the determination of total mercury in precipitation have also been shown to give fairly good agreement. However, for the implementation in monitoring networks the comparability would certainly benefit from the harmonization of the sampler design and standard operating procedures. The intercomparability of the applied methods for particulate-phase mercury is not yet satisfactory. However, the results suggest that concentration data based on collection on disk filters and subsequent acid leaching or digestion are possibly closer to reality than data based on the retention of Hg_{part} on traps containing quartz wool plugs or on coated glass beads (preceded by one or more denuders) and subsequent thermal desorption. In any case, an internationally accepted standard methodology for particulate-phase mercury is required, one that will give reproducible and comparable data. Laboratory 7 and 11 have clearly shown, that inorganic oxidized mercury species are present at Mace Head in the low pg m^{-3} range.

The GKSS laboratory was involved in the intercomparison exercise as code number 6. TGM measurements were carried out with the traditional manual method (6/1) and additionally with the Tekran Analyzer (6/2). Our own measurement data compare very well with the calculated overall median value. The Tekran data are, on an average slightly lower with a lower standard deviation compared with our manual method.

TPM values measured by GKSS are on an average higher than the results obtained by disc filter sampling methods followed by acid digestion. Laboratory 11 has applied Au-traps preceded by a KCl-coated denuder and obtained substantially higher TPM values than all other laboratories. The development of an internationally accepted and validated methodology for TPM (Hg_{part}) is a clear need for future research.

The GKSS results for total mercury in precipitation are in good agreement with the other data. In general, the GKSS data are slightly higher. To ensure comparability of mercury measurements in precipitation for example in monitoring networks, the design, shape and material of the precipitation samplers seems to be at least of similar importance as the analytical method applied.

In general it could be concluded that the observed good agreement of the TGM concentrations in air determined by different laboratories using different techniques makes a combination of data sets from different regions of the world feasible.

4 Studies on the Local Distribution of Atmospheric Mercury in the Vicinity of a Contaminated Industrial Site

For entire Europe the annual anthropogenic emissions of mercury has been estimated to be about 726 tons, originating from 928 sources by base year 1988 (Axenfeldt et al., 1991). The dominating source categories in Europe are fossil fuel combustion and chlor-alkali plants. Waste incineration and non-ferrous metal smelting contribute less than 10 %. Emissions from the former German Democratic Republic (GDR), including the different species of elemental mercury, divalent inorganic mercury and particulate-phase mercury, accounted for more than 40 % of the European total. The contribution of the GDR originated from a few relatively small but in most cases highly industrialized areas. According to Helwig and Neske (1990), extremely high amounts were emitted in the region Halle/Leipzig/Bitterfeld, due to both burning of lignite coal in power plants with flue gas desulfurisation equipment and high losses of mercury from the chlor alkali factories.

An important emitter of air- pollutants in this region was the former Chemische Werke Buna (now Buna Sow Leuna Olefinverbund GmbH; hereafter referred to as the BSL Werk Schkopau), located near Halle/Saale. Before 1989, the company produced per year 1000kT calcium carbide, 300 kT acetylene, 420 kT chlorine, 300 kT polyvinylchloride (PVC) and 120 kT synthetic caoutchouc (Krüger et al., 1999). As a consequence of the reunification of Germany, about 50 production installations which were considered to be ecologically harmful were closed at the BSL Werk Schkopau in the period between 1990 and 1992. Among them were three chlor-alkali production facilities (hereafter denoted as L66, I54 and H56), one factory still producing chlorine and sodium hydroxide (denoted P156) and one acetaldehyde factory (denoted F44). In these facilities, mercury was used as an electrode for chlorine and and sodium hydroxide production and as a catalyst for acetaldehyde production. All production sites consisted of partly demolished buildings or buildings with openings (Ebinghaus and Krüger, 1996).

The fate of mercury that has been applied at this plant for these two production pathways over the entire production period of approximately 50 years has been recalculated in a mass balance (Richter-Politz, 1991). Although this mass balance contains substantial uncertainties, it can be derived, that emissions into the atmosphere are likely to occur and, that a large pool of mercury contamination has to be expected at the site. The following table summarizes applied amounts and estimated fate of elemental and inorganic mercury at the plant for the time period 1939 to 1989.

Table 4.1: Mass Balance of Elemental and Inorganic Mercury at BSL Werk Schkopau, Recalculated for the Time Period 1939 to 1989 (Richter-Politz, 1991)

Production	Applied amounts (tons)	Fate	Estimated amounts (tons)
Sodium hydroxide	3623	Contamination in Products	45
		Recycled	35
Acetaldehyde	3479	Solid wastes	1021
		Waste water	260
		Waste air	Not known
Sum	7102	Sum	1361
		Loss	5741

Since these buildings were continuing to release gaseous mercury into the atmospheric environment, the main problem related to mercury at the BSL Werk Schkopau was the redevelopment of the contaminated site including buildings and production facilities. Furthermore, the magnitude and variations of mercury concentrations in the local atmosphere and the potential risk this posed for human health were unknown after the major mercury emission sources were closed. Therefore, in order to obtain an implication about the amount of mercury in air an important task was to estimate the quantity of mercury emissions originating from the specified sources at the factory premise.

The following three figures are used to illustrate the situation during the transition after production was stopped and before the demolition of the contaminated production halls and facilities was started.

Figure 4.1 shows a photograph of the biggest chlor alkali production facilitiy, the so-called hall L 66, Figure 4.2 shows a view inside L 66 with the iron made electrolysis cells and finally, Figure 4.3 illustrates the apparent mercury contamination inside the fabrication halls.

Figure 4.1: Chlor-alkali production facility L 66 at BSL Werk Schkopau before demolition was started

Caustic soda production in L 66 has been started in 1939. The dimensions of the hall were 100 m (length), 30 m (width) and 20 m (height). Among the NaOH production facilities L 66 was the biggest. Acetaldehyde production with mercuric sulfate as a catalyst was carried out in facility F44. This plant was of similar dimensions as L 66 however, not a closed building but an open construction.

Figure 4.2: Iron-made electrolysis cells inside L 66 for caustic soda production at BSL Werk Schkopau

In L 66, one hundred cells were in operation. Each cell contained 1 ton of elemental mercury as an electrode. Temperature of the cells during electrolysis was between 80 and 90 °C. During operation the electrolysis cells were closed with an iron-made cover.

Figure 4.3: Elemental mercury contamination on the ground level floor between the electrolysis cells

In the following, the actual situation in 1994 at the industrial site BSL Werk Schkopau will be evaluated. Emission source strength estimations based on measurements and model calculations have been derived.

The estimate was carried out in three steps:

1. measurements of TGM in the vicinity of the sources at different locations,
2. back-calculation of the mercury source strengths using the local atmospheric transport model MODIS,
3. estimation of the deposition of mercury near the sources based on modeled concentration fields.

In the following section measurements and concentrations of atmospheric mercury in the local atmosphere around the BSL Werk Schkopau are presented.

4.1 Measurements of Total Gaseous Mercury at the BSL Werk Schkopau

In October 1993, more than two year after production was stopped, indoor concentrations of the production halls of around 200 µg m^{-3} were measured inside hall F44. Inside the chlor-alkali production facilities of I54 values of 100 µg m^{-3} were detected. Close to heavily contaminated soil surfaces peak values in ambient air concentrations of 100 µg m^{3} were frequently detected (Krüger et al., 1999).

Due to the specifics of the production pathways at the BSL Werk Schkopau, it was assumed that elemental mercury was the major emitted species into the atmosphere (Ebinghaus and Krüger, 1996). Therefore, besides elemental mercury, other species which might also be of interest with regard to different behaviors in the atmosphere, i.e. RGM and dimethylmercury, were not separately measured during the field experiments. However, when applying the double amalgamation technique, both species will contribute to TGM in a quantitative way.

The purpose of the in-situ measurement was to obtain information on the horizontal distribution of TGM approximately 1.5 m above ground level. The area within a maximum distance of 5000 m from the sources was of main interest. All measurements were made within the expected plume of mercury, which was developed in the main direction of the wind and shaped by the wind shear and temperature profiles.

As an example for the results of a series of measurements, TGM-concentration data obtained during the very early morning hours of June 14, 1994 (4:30 a.m to 10:30 a.m) are depicted in Figure 4.4. The single points were sequential measurements with a 10 L sample volume of ambient air, i.e. a sampling time of 15 minutes each. The numbers within the circles are representing TGM concentrations in ng m^{-3}. The prevailing winds during these measurements were originating from the north.

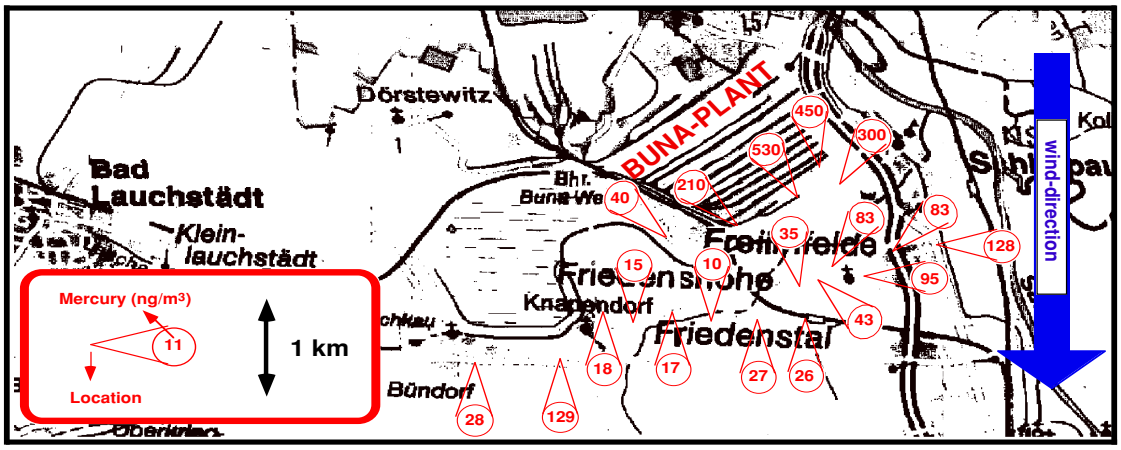

Figure 4.4: Exemplary results of concentration measurements of TGM in the vicinity of the BSL Werk Schkopau. Sampling locations are indicated by red arrows, measured concentration values in ng m^{-3} are given in the circles

As shown in Figure 4.4 the dispersion plume of mercury could be detected with this analytical approach. In this case (June 14, 1994) at the perimeter of the plant, the center of the plume is approximately 1 km wide and shows a peak concentration of 530 ng m^{-3}. All measurements showed a sharp decrease of atmospheric mercury downwind with increasing distance. At a distance of 1000 m the maximum values are around 130 ng m^{-3} and the center of the plume has broadened to approximately 1.5 km.

In order to obtain data for different atmospheric conditions during the sampling period from December 1993 to June 1994, several measurement campaigns were carried out on event basis. The reason for this was to include the influence of seasonal and temperature-related variations. During a four-day field campaign in summer, the German Weather Service (Deutscher Wetterdienst; DWD) carried out radio soundings and measured several vertical profiles of potential temperature, wind speed and direction per day.

Table 4.2 gives a summary of concentration measurements relative to the location of the source area (Distance in m / TGM in ng m^{-3}).

Table 4.2: Summary of measurements in the surroundings of the factory premises of BSL Werk Schkopau in mean distance from the source areas L66, I54/H56 and F44

Wind -	Location:	Location:	Location:	Location:	Location:	Location:	Location:	Location:
Direction:	N	NE	E	SE	S	SW	W	NW
	Dist. [m] / TGM ($ng\ m^{-3}$)	Dist. [m] / TGM ($ng\ m^{-3}$)	Dist. [m] / TGM ($ng\ m^{-3}$)	Dist. [m] / TGM ($ng\ m^{-3}$)	Dist. [m] / TGM ($ng\ m^{-3}$)	Dist. [m] / TGM ($ng\ m^{-3}$)	Dist. [m] / TGM ($ng\ m^{-3}$)	Dist. [m] / TGM ($ng\ m^{-3}$)
N	500 / 6.5			1500 / 128	800 / 530	1200 / 18		
N	1000 / 8.5				800 /450	1200 / 35		
N					800 / 415	1200 / 40		
N					1000 / 35	2000 / 129		
N					1000 / 43	2000 / 16		
N					1000 / 83	2000 / 17		
N					1000 / 95	2000 / 18		
N					1000 / 83	2000 / 15		
N					1000 / 261	2500 / 17		
N					1000 / 210	2500 / 28		
N					1000 / 152			
N					1200 / 26			
N					1200 / 300			
N					1200 / 193			
N					1500 / 235			
N					3000 / 91			
N					6000 / 11			
S	1500 / 63	1000 / 8.8	1000 / 33	1000 / 4.8	1000 / 6.0		2000 / 6.5	1000 /8.5
S	4000 / 6.8	2500 / 5.5					2500 / 8.2	3500 / 4.4
S								4000 / 4.5
SW		1000 / 62	5000 / 7.0		1500 / 32			1000 / 6.3
SW		2000 / 56			3500 / 5.3			
SW		3000 / 72			4000 / 7.5			
SW		3500 / 10						
SW		4000 / 44						
SW		5000 / 2.6						
SW		12000 / 3.2						
W		1000 /161	800 / 41					
W		1500 / 5.7	800 / 25					
W		7000 / 5.4	800 / 35					
W			1000 / 66					
W			2500 / 6.3					
W			10000 / 4.0					
W			12000 / 6.0					
NW			500 / 8.8	1200 / 38	1200 / 20			
NW			1000 / 11	1500 / 46				
			1500 / 23	1500 / 79				
NW			5000 / 4.6	1500 / 39				
NW				1500 / 7.9				
NW				2000 / 9.0				
NW				4500 / 3.8				

4.2 Dispersion Modeling of the Local Atmospheric Transport of Total Gaseous Mercury at the BSL Werk Schkopau

The local atmospheric transport originating from emissions at the BSL Werk Schkopau was calculated for a distance of a maximum of 10 km. A numerical model for simulating transport from point sources was applied (Krüger et al., 1999). Earlier results of this transport model compared well with measurements of an inorganic tracer (SF_6) within a spatial range of a maximum of 100 km (Eppel et al., 1991). The model, which is an extension of the elementary Gaussian model, essentially is an Eulerian model, whose parameterizations are more closely related to the transport properties of the atmosphere. It has been shown by Eppel et al. (1991) that the model also performs a quite realistic dispersion for episodes with a temporarily evolving boundary layer. In the model the transport equation,

$$\frac{\partial}{\partial t}C + U(z,t)\frac{\partial}{\partial x} + V(z,t)\frac{\partial}{\partial y}C - W(x,t)\frac{\partial}{\partial z}C = k_y(x,z,t)\frac{\partial^2}{\partial y^2}C + \frac{\partial}{\partial z}Kz(x,z,t)\frac{\partial}{\partial z}C - RC + S$$

which describes the concentrations $C = C(x,y,z,t)$ of a pollutant above flat terrain, is solved numerically using a momentum reduction in cross-wind direction in order to reduce a three-dimensional problem along the wind and vertical directions. The equation includes the following parameters.

C: concentration

U: wind velocity in the main wind direction

V: wind velocity in the cross-wind direction

W: deposition velocity

R: removal parameter including dry and wet deposition

K: diffusion coefficient

S: source strengths

x, y, z: spatial dimensions

t: temporal dimensions

This procedure preserves a high resolution of the plume structure especially for simulating the transport at distances far from the sources. As the numerical grid is oriented vertically in the mean wind direction, the cross wind resolution can be chosen very high for the entire domain of the model (Krüger et al., 1999). This advantage contrasts to grid models, which either

highly resolve only the source region, while distances far away from the sources are not covered by the grid, or the model domain is adequate to simulate transport far from the source, but the grid spacing is too crude to resolve the structure of the plume close to the emission source.

Besides the removal parameter *R*, which represents dry and wet deposition processes, a negative sink velocity *W* is defined in the model, which enables taking into account the effect of buoyancy of the plume centerline. Sources of pollutants are denoted by *S*. The vertically variable wind velocities *U* and *V* in the main- and cross-wind direction of the plume enable the simulation of a sheared wind field in the boundary layer. For stable and neutral atmospheres the diffusion coefficients K_y and K_z are determined from horizontal and vertical velocity variances (e_h and e_v) and the time scales t_y and t_z:

$K_y = t_y \, . \, e_h$
$K_z = t_z \, . \, e_v$

The time scales t_y and t_z were determined by fitting the horizontal and vertical extent of calculated plume cross-sections to in-situ measurements carried out during the previously described field measurements of TGM at the BSL Werk Schkopau. The velocity variances are calculated from dynamic equations for the time derivatives of e_h and e_v which contain the effects of diffusion, shear, buoyancy, re-distribution and dissipation. These equations are solved by the input of vertical temperature profiles in addition to velocity profiles.

Convective conditions are parameterized by a phenomenological approach (Lenschow and Stevens, 1982), which superimposes on the standard model a separation of the plume in an updraft and a downdraft branch. A detailed description of the procedure is given by Eppel et al. (1991).

4.3 Inverse Modeling of Mercury Source Strengths with MODIS

A reliable estimation of source strengths of gaseous mercury exclusively from concentration measurements in the local atmosphere near the sources is not possible without numerical modeling. The strong variability of the meteorological parameters determining the dispersion can only be taken properly into account using a numerical model. On the other hand, results of a dispersion model based on very uncertain and roughly estimated emission data most likely do not reflect the real atmospheric conditions. Therefore, we decided to combine both methods.

The strategy was to use the measurements as constraints in fitting the model to the emission source strengths. This procedure can be described as an inverse modeling approach, because the model is applied oppositely to the usual way, in which the transmission is calculated from known emission sources. Applying inverse modeling can be described as follows:

In the surroundings of an ensemble of emission sources, n measurements of the concentrations $c_i(x_i,y_i)$ of gaseous mercury at different point sources exist. The location of the measurements in a model grid, here in a downwind and cross-wind direction of the plume, is given by x_i and y_i. Uncertainties of the measurements are denoted by ∂c_i. The dispersion model calculates the concentrations $C_i(x_i,y_i) = f(x_i,y_i,)$, where α is the vector of free parameters being fitted. In this case, α represents the source strengths of the emission sources at the BSL Werk Schkopau, which are treated variably in the procedure. In order to minimize the differences between in-situ measurements and model results, a multiparameter function is

$$\chi^2(\alpha) = \sum_{i=1}^{n} \frac{\left[f(x_i, y_i, \alpha) - c_i \right]^2}{\partial c_i^{\,2}}$$

defined for a least-squares fit as X square:

For the minimum, which is found at $X^2 = X^2(\alpha_{min})$, a statistical test for a X^2 distribution with [n-dim(α_{min})] can be made to check the performance of the fit. The parameter vector α can usually be estimated by applying different methods for minimizing X^2. This genuine multidimensional minimization procedure has the advantage that no accurate start parameters have to be estimated, different ranges of parameters can be defined and it is even rather robust with respect to cross fluctuations in the function value (Krüger et al., 1999).

MODIS is an iterative procedure, whereby the source strengths are varied in the model simulations until the differences between the air concentrations resulting from the model and those measured during the field measurement campaigns are minimal. Thus the calculations give a solution for minimizing the problem based on TGM-measurements and meteorological input data, such as vertical profiles of wind velocity and potential temperature. Figure 4.5 shows the flow chart of the inverse modeling procedure (Ebinghaus and Krüger, 1996; Krüger et al., 1999):

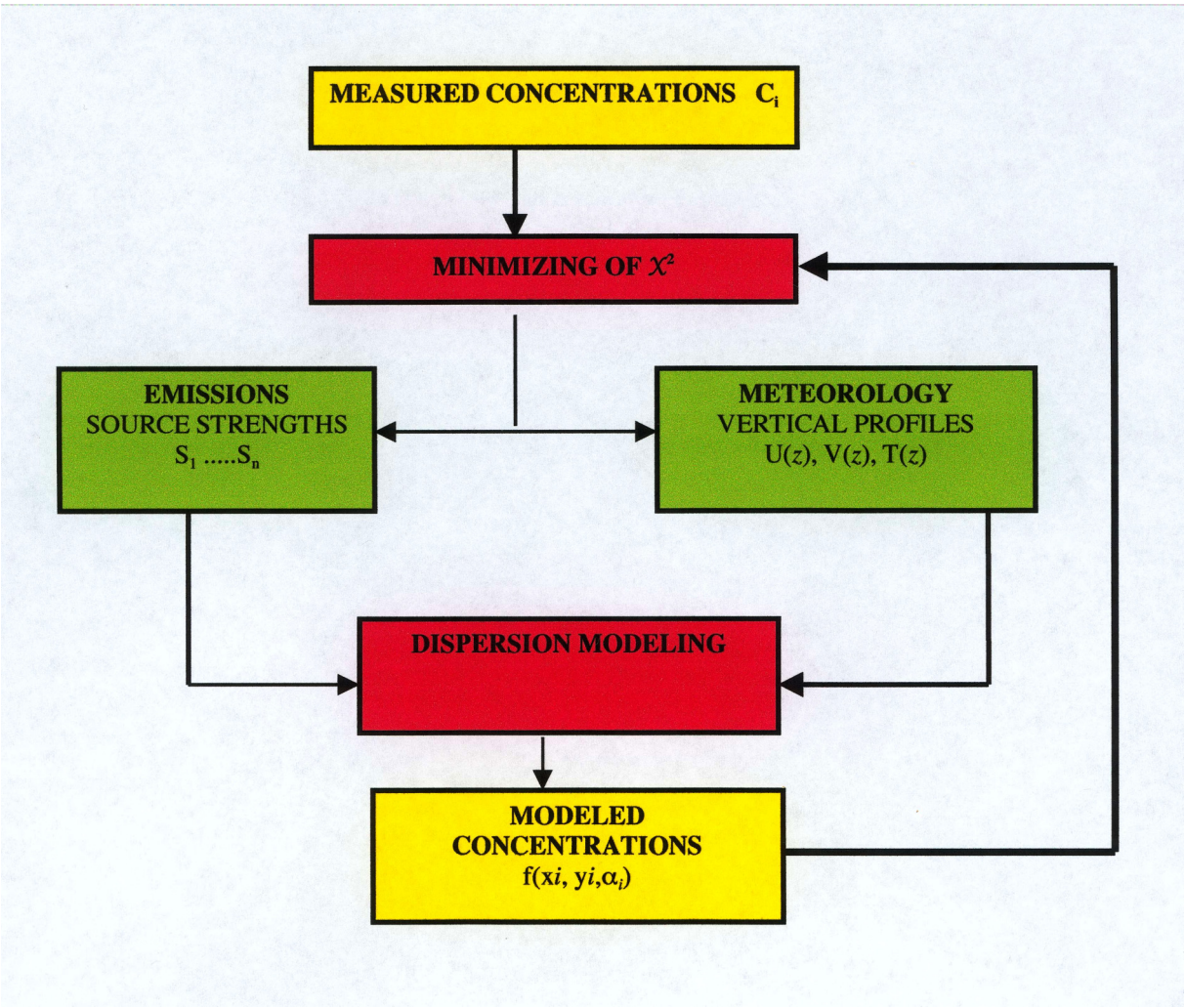

Figure 4.5: Flow chart of the inverse modeling procedure

The resulting modeled concentrations compared well with the in-situ measurement data. All differences were within a range of 25 %. The following two figures show the mercury plume for a night inversion and developing convective conditions respectively. One measurement point is based on replicate samples and was carried out every 30 minutes in the vicinity of the factory premises with respect to changing meteorological conditions and thus some values only are compared in the instantaneous pictures of the atmosphere. The meteorological input data for the model runs were measured by the German Weather Service DWD directly at the study site.

As described before, the model uses the back-calculated source strengths of the individual point sources in order to calculate the local pollutant transport and resulting concentration fields based on the prevailing meteorological conditions. Figure 4.6 shows the modeled concentration fields as a dispersion plume for a typical nocturnal inversion situation.

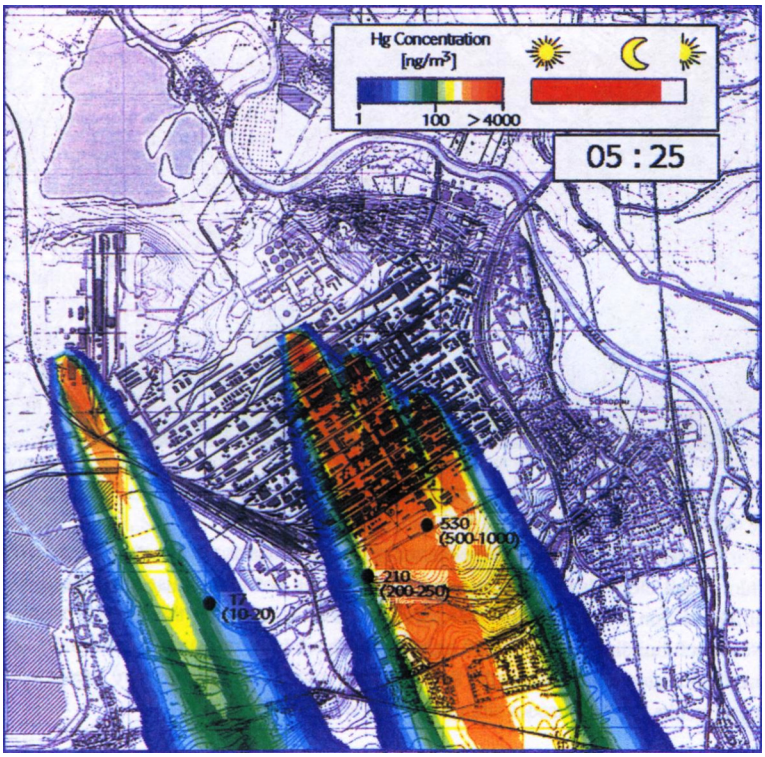

Figure 4.6: Mercury dispersion plume during night inversion

Within the nocturnal boundary layer high mercury concentrations in the center of the individual plumes build up downwind the factory. The figure shows highest measured concentrations up to values of 530 ng m^{-3}. The corresponding modeled concentration ranges are given in brackets. From Figure 4.6 it can be seen that measured and modeled concentrations are in very good agreement. It can also be seen that 4 individual sources could be identified by the inverse modeling procedure.

Figure 4.7 shows the modeled mercury dispersion plumes approximately 2 hours later after the nocturnal boundary layer broke up and more intensive vertical and horizontal mixing took place.

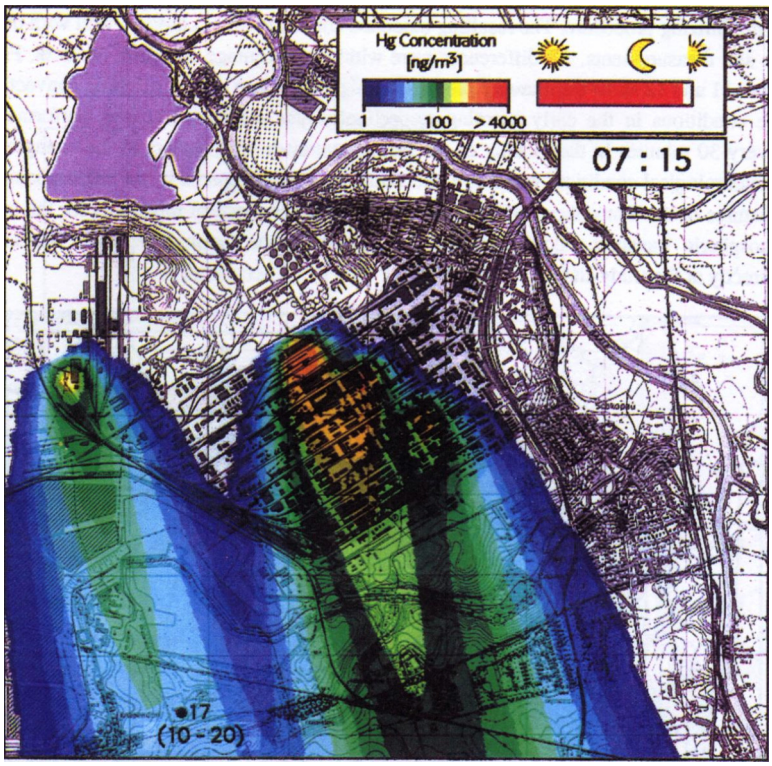

Figure 4.7: Mercury dispersion plume during convective conditions

Figures 4.6 and 4.7 show the dispersion plumes at 5:25 and 7:15 UTC. With beginning convective conditions the dispersion plume of mercury gives a different picture. High concentrations are restricted to a much smaller area closely around the main emission sources. In a distance of about 1 km from the perimeter of the plant measured and modeled concentration values are comparable to "normal" urban values.

It can be seen that three source areas, including all inactive plants, are relatively close to each other, while a fourth emission source, which was still in operation, is 1000 m further away from the others. The source strength of this plant was calculated separately from measurements in a second dispersion plume. Since the source strength of this factory was independently measured directly at the low stack of the source by the same amount of 0.3 kg day^{-1}, which was estimated by inverse modeling, a high accuracy of all other source strength estimates can be expected.

Using measurement data and modeled concentration fields, the source strength estimates for the individual sources were carried out by inverse modeling as described above. The results are given in Table 4.3.

Table 4.3: Back-calculated Source Strengths of TGM for Identified Point Sources

Hall	L 66	I 54/H 56	F 44	P 159
Source strength	1 kg d^{-1}	0.6 kg d^{-1}	0.3 kg d^{-1}	0.3 kg d^{-1}

An uncertainty of a factor of 2 should be taken into account for these estimates. Because the inverse modeling approach demands for the input measured mean concentrations in the model grid, defined here as 50 by 20 m, the uncertainty is assumed to be mainly due to the proper representation of a grid element by a few or only one measurement point inside the grid cell. The uncertainties of the emission source strength estimates are strongly dependent on the representation of a grid element by the measurements, which, in turn, is connected to the number and the locations of the measurement point.

Generally, higher source strengths were calculated for the chlor-alkali plants (L 66, I 54/ H 56; P 159). The total emission of the entire factory area in 1994 was about a factor 50 lower compared to earlier estimates and before the production was terminated (Ebinghaus and Krüger, 1996).

4.4 Estimation of Mercury Deposition in the Vicinity of BSL Werk Schkopau

Deposition estimates were carried out based on the modeled concentration field as, for example, depicted in Figures 4.6 and 4.7. The estimation of wet deposition is based on the assumption that the deposition process can be described by a scavenging coefficient for TGM in ambient air (Petersen et al., 1994). Atmospheric ozone and soot concentrations are the most important factors for the scavenging of elemental mercury vapor by rain or cloud water. Consequently, they are determining the mercury concentration in precipitation at a given Hg concentration in ambient air.

While the measured ozone concentrations in the area of interest were fairly constant at around 40 µg m^{-3}, the soot values showed a distinct daily variability with a mean of 500 ng m^{-3}. Thus, following Petersen et al. (1994), a scavenging coefficient of 10^3 was applied. For the deposition estimates, mercury concentration fields were modeled for characteristic meteorological vertical profiles dependent on 8 directions of the wind (N, NE, E, SE, S, SW, W, NW). The frequencies of the wind for the year 1993 were taken into account. The annual wet deposition flux of airborne mercury is depicted in Figure 4.8.

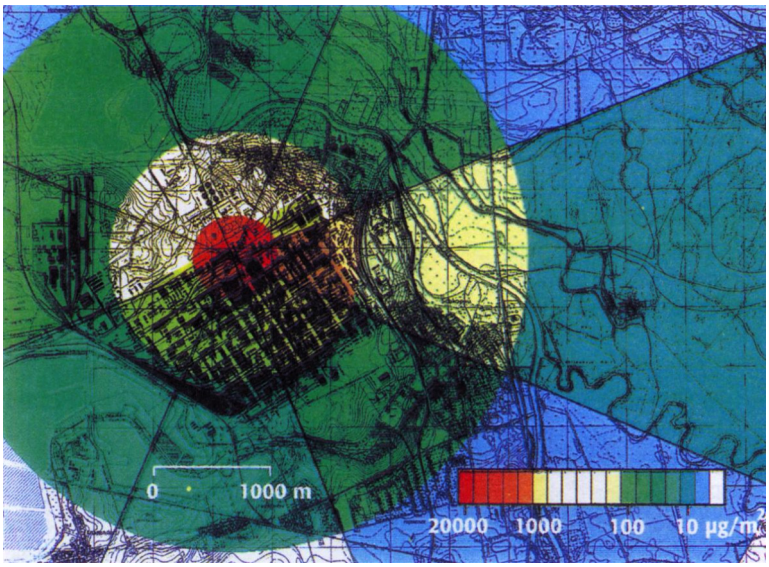

Figure 4.8: Modeled mercury wet deposition fluxes in the vicinity of the factory site, 1993

In order to estimate which fraction of the emitted mercury originating from the identified point sources is deposited locally or available for long-range atmospheric transport respectively, a simple mass-balance approach was used. The following estimate of the local atmospheric mercury budget is based on the assumption that the deposition flux is dominated by wet scavenging processes as described above. It has to be considered that, especially for industrialized areas, dry deposition might play a more pronounced role for the local mercury mass balance compared to remote regions or sea surfaces. Under these boundary conditions it can roughly be estimated, that a minimum of about 30 % of the emitted mercury is expected to be deposited within a distance of 5 km from the BSL Werk Schkopau on an average annual basis. That means that distinct point sources are slowly transformed into larger diffuse area sources because wet deposited mercury can be converted into volatile species again and re-emitted afterwards. The remaining fraction of about 70 % of the mercury emissions is, in principal, available for long-range atmospheric transport.

5 Long-term Measurements of Total Gaseous Mercury at a Remote Marine Location in Western Europe

One of the major questions connected with the present mercury research worldwide is that of trends:

- have the sources of mercury, its long range transport and deposition increased substantially increased in comparison with pre-industrial times ?
- how do they reflect the control measures adopted to control and reduce anthropogenic mercury emissions ?

Almost all information on historical trends in atmospheric mercury concentrations and subsequent deposition has been derived from analysis of dated soils, sediments and peat cores (e.g. Lockhart, 1995; Coggins, 2000). These data suggest that the present mercury deposition is 2 to 5 times higher than the pre-industrial ones. Inventories of natural and anthropogenic mercury sources suggest that the present anthropogenic mercury sources are in the same order of magnitude as the natural ones (Nriagu and Pacyna, 1988). Although these inventories are influenced by large uncertainties, they imply an increase in mercury deposition by about a factor of 3 compared with pre-industrial times, which is in fairly good agreement with experimental data derived from sediment, soil and peat analyses (Slemr, 1996).

Because of an atmospheric residence time of about 1 year (Slemr et al., 1985; Lindqvist and Rodhe, 1985), long term monitoring of atmospheric mercury concentrations may provide direct evidence of temporal trends. Slemr (1996) has reviewed the few existing publications starting with early data published by Stock and Cucuel (1934) and concludes, that the reconstruction of trends by combining data of these reports is hardly possible for several reasons:

- the quality of the reported TGM concentration measurements is mostly unknown,
- mercury monitoring has only rarely been accompanied by supporting measurements of chemical tracers that will allow to eliminate locally influenced data,
- most of the reported measurements of TGM in air are very limited in time and space.

Based on these uncertainties and the systematic gaps in knowledge behind, Fitzgerald (1995) has proclaimed the need for a global monitoring network.

Continuous measurements of total gaseous mercury (TGM) concentrations with 15 minutes time resolution have been carried out between September 1995 and March 2001 at the atmospheric research station at Mace Head, western Irish coast line. Together with a Canadian

site in the high Arctic (Alert, Nunavut, NWT), Mace Head was the first research station generating highly time resolved concentration measurements of TGM on a routine basis.

Mace Head is located in County Galway near Carna on the west coast of Ireland at 53°20' N, 9°54' W, as shown in Figure 5.1. It is exposed to the North Atlantic Ocean having a wide clean sector between 180° and 300°. It is ideally situated to study atmospheric composition under Northern Hemispheric background conditions and also under European continental conditions, generally when the air masses are originating from easterly direction (Jennings et al., 1993; Oltmans and Levy, 1994; Ebinghaus et al., 1995). The meteorological records show that on average over 50 % of the air masses arriving at Mace Head are within the clean sector (Spain, 1995). Climate at Mace Head may be classified as maritime. The underlying bedrock is granite (biotide granodiorite), outcrops of which is visible in the peat formations at the site. Peat is found in depths ranging from a few centimeters to several meters as one moves from the hill slopes to the hollows. There is no industrial activity which would influence measurements at the station within about 90 km of the site, where the nearest major conurbation of Galway city is located east of Mace Head.

The main source of income to the community in this area is fishing and agriculture. Agriculture activity in the area mainly consists of low level sheep and cattle grazing. Occasionally the burning of gorse and heather by local farmers may influence measurements at the site, but disruption of this kind can be monitored through aerosol measurements at the site (Coggins, 2000).

Figure 5.1: Location of the Mace Head Atmospheric Research Station

Continuous measurements of TGM have been carried out at Mace Head for the period September 1995 to July 1997 within the framework of the German-Irish collaboration

program in Science and Technology and from May 1997 to March 2001 in the course of an European Union funded project (MOE: Methylmercury over Europe – Relative importance of depositional methylmercury fluxes to various ecosystems; Environmental and Climate Programme, DGXII, Contract ENV4-CT97-0595).

Recently, the Irish Environmental Protection Agency (EPA) has approved the funding for a continuation of atmospheric mercury monitoring at Mace Head at least until the end of 2004.

5.1 Trend in the TGM Concentration Measurements at Mace Head from September 1995 to March 2001

Measurements of TGM at Harwell, a rural site in southern central England using a similar instrumentation between June 1995 and April 1996 revealed an average concentration of 1.68 ng m^{-3} (Lee et al., 1998). Measurements at Alert, a monitoring station in the Canadian high arctic during 1992 and 1993 showed a mean concentration of 1.63 ng m^{-3} (Schroeder and Schneeberger, 1996). Burke and Keeler, (1996) measured TGM concentrations at a number of rural sites in the Great Lakes region of North America and found a mean TGM concentration between 1.59 and 1.93 ng m^{-3}. This consistency in the TGM concentration range would suggest that TGM is well mixed in the troposphere at least on hemispherical scale and has a long atmospheric residence time.

At Mace Head, the daily averaged concentration values in Fig. 5.2 show a short-term variability on the scale of a day to a few days. This short-term variability may be explained by short pollution events associated with different air masses. This effect was also observed by Slemr and Scheel, (1998) at the Wank Mountain in Bavaria and also in the data of Schroeder and Schneeberger, (1996) at Alert, Canada. The incidence of occurrence of short-term variability in the TGM concentration data is reduced in the more recent data obtained between 1998 and 2001, which may indicate a decreasing trend in anthropogenic mercury emissions into the atmosphere on a regional scale.

Average TGM-concentrations measured at Mace Head between September 1995 and January 2001 are of value 1.75 ng m^{-3}. Highest daily average concentrations are of value 4.3 ng Hg m^{-3} whereas highest monthly average is 2.4 ng m^{-3}. The highest monthly means were recorded for the months of January 1996, March 1996 and November 1996 and are 2.4 ng m^{-3}, 2.4 ng m^{-3} and 2.2 ng m^{-3} respectively. The lowest monthly mean was recorded during February 1996 at 1.5 ng m^{-3}. Trend analysis of TGM data obtained during the first two years of the entire measurement period shows a weak decrease of 4% in the TGM concentrations, as shown in Figure 5.2.

At Mace Head, pollution events with elevated TGM concentrations may be influenced by local or regional sources as indicated by back trajectory analysis, and supporting wind direction, black carbon mass concentration, and condensation nuclei measurements recorded at the site (Cooke et al., 1997). High hourly mean values of up to 8.0 ng m^{-3} have been observed during pollution events in January 1996.

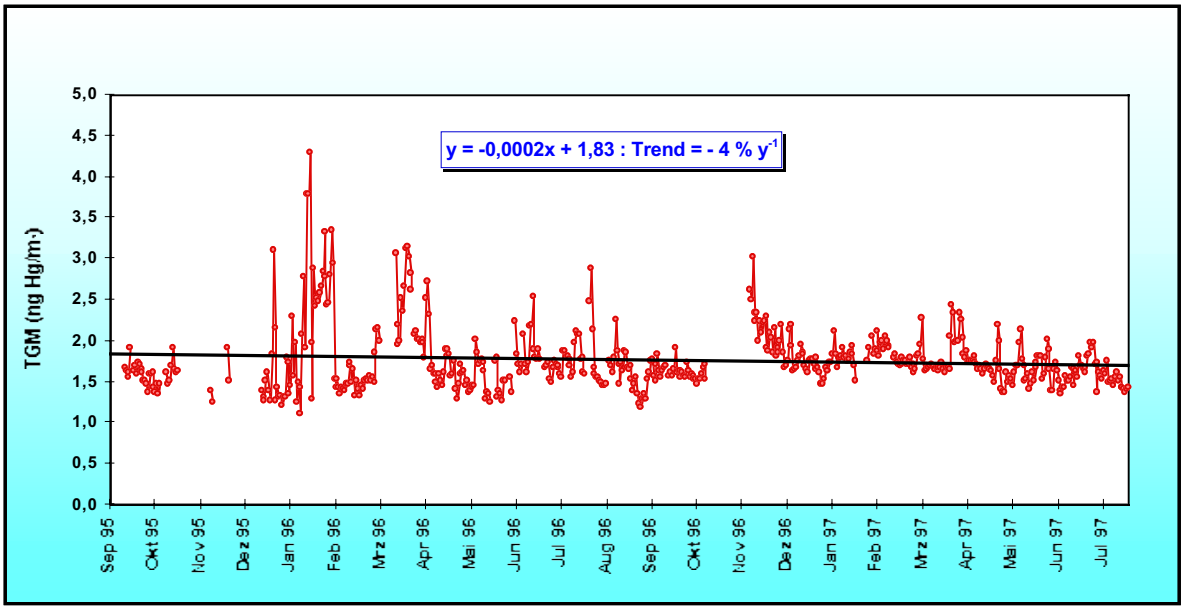

Figure 5.2: TGM concentrations measured at Mace Head from September 1995 to July 1997 (24 hour averages)

The measured TGM concentrations clearly reflect northern hemispheric background values. However, several pollution events have been observed with elevated concentration over a 24 time period. These events could be caused by local sources such as peat and coal burning and/or by long-range transport of air masses of continental origin. For an assessment of possible trends in the concentration data it is imperative to exclude these data with appropriate methods. The most pronounced variability of concentration data could be detected between December 1995 and April 1996. Due to technical problems no measurements could be carried out between October and November 1996.

During the first period of continuous mercury concentration measurements a slight decrease of 4 % in the 24 hour average concentrations could be detected. Maximum concentrations have been measured in January 1996 and are of value 4.5 ng m^{-3}. The average concentration for this period is 1.84 ng m^{-3}.

In August 1997 measurements were interrupted due to technical problems and lack of external funding sources after the German-Irish cooperation program had been terminated.

In April 1998 the Mace Head monitoring work was embedded in a EU Environment and Climate project dealing with the regional distribution of atmospheric mercury species over Northwestern Europe. In this project Mace Head served as a reference site reflecting the western inflow boundary conditions of the atmospheric mercury burden.

Daily average TGM concentrations for the second period of the long-term study are given in Figure 5.3.

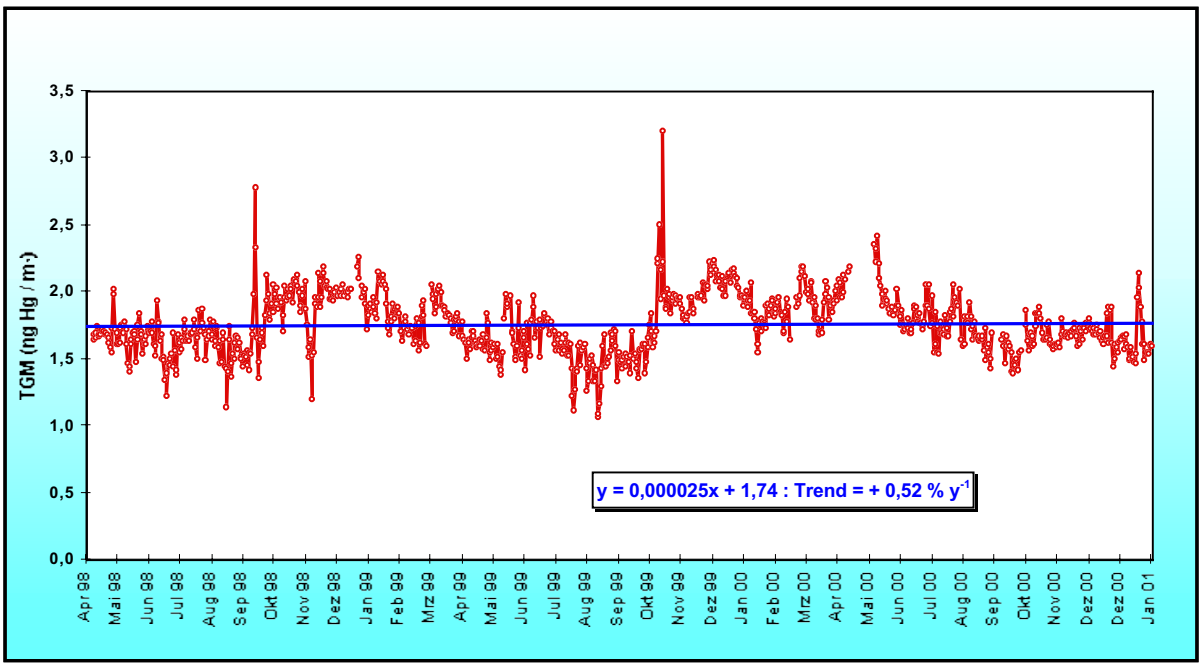

Figure 5.3: TGM concentrations measured at Mace Head from April 1998 to January 2001 (24 hour averages)

In the second period of continuous TGM measurements at Mace Head the variability or scattering of daily averages is low compared with the earlier measurements. Only very few days with average concentrations > 2.5 ng m^{-3} have been observed over a period of almost three years. Trend analysis shows an almost constant TGM average concentration level, with an increase of 0.5 % per year. Due to technical advancement, gained experience and better trained personal on the site, the data set shows only one small gap in May 2000. Between April 1998 and January 2001 the instrument was in operation for more than 95 % of the measurement period.

The combination of both measurement periods for trend analysis is shown in Figure 5.4. The data set presented is one of the very few highly time resolved data sets worldwide, allowing an estimate on the short term variability and long term trends of atmospheric mercury and remote marine background conditions.

This also shows that longer time periods have to be taken into account when trend estimates should be derived. The two individual periods show opposite trends with a decrease at the beginning and a slight increase later. By combining both periods a very stable concentration level with no significant trend between 1995 and 2001 could be seen as depicted in Figure 5.4.

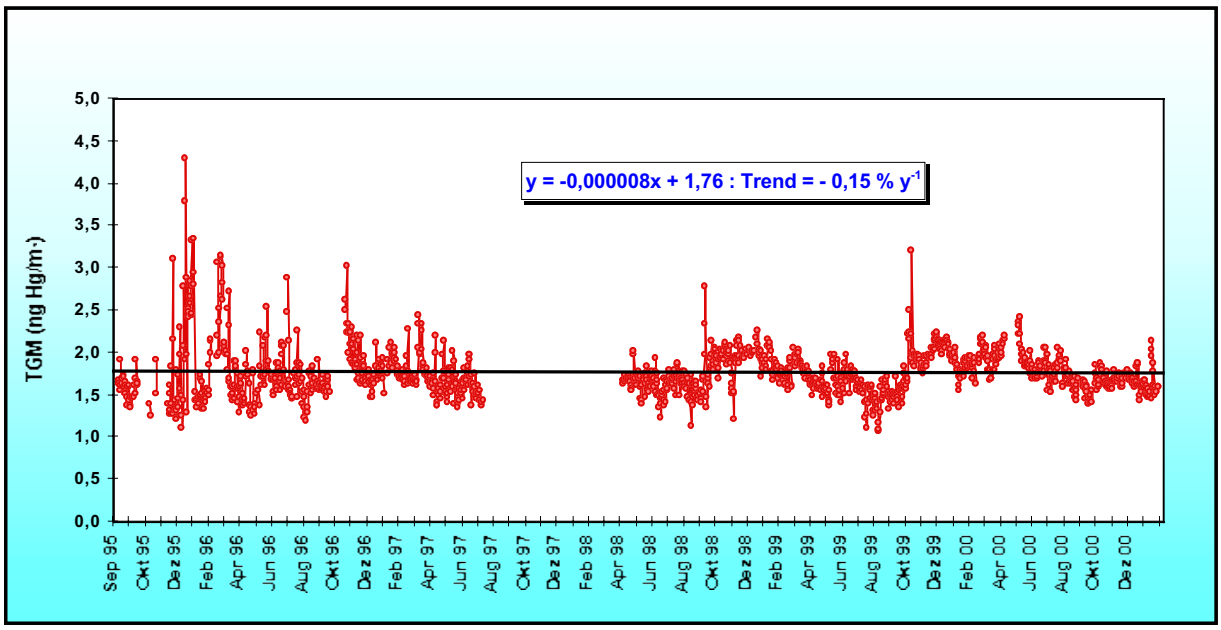

Figure 5.4: TGM concentrations measured at Mace Head from September 1995 to January 2001 (24 hour averages)

From Figure 5.4 it can be seen that the variability of daily average concentrations (scattering) was more pronounced in the beginning of the long-term study. Between September 1995 and July 1997 higher concentrations (i.e. > 2.5 ng Hg m^{-3}) have been detected much more frequently compared with the second period of the study from April 1998 to January 2001. Between 1995 and today no significant trend in the atmospheric mercury concentrations has been observed (decreasing rate about 0.15 % yr^{-1}).

Between 1990 and 1996 Slemr and Scheel (1998) observed a decreasing trend of 7 % in yearly TGM mean concentrations at the Wank Mountain in Southern Germany reducing from 2.97 ng m^{-3} in 1990 to 1.82 ng m^{-3} in 1996. Iverfeldt (1995) observed a decreasing trend in TGM measurements made in Sweden from a mean TGM concentration value of 3.2 ng m^{-3} for the period of 1985 to 1989 to a mean concentration of 2.7 ng m^{-3} for the period 1990 to 1992.

These cited studies report measurements taken during earlier time periods compared to those at Mace Head started in September 1995. Significant reductions in the total anthropogenic

mercury emissions into the atmosphere have been calculated for the time after 1990 in the course of the political changes in eastern Europe. Emissions were reduced from 726 tons annually before 1990 (Axenfeldt et al., 1991) to 246 tons per year in 1995 (Pacyna and Pacyna, 2000). Further emission reduction to about 200 tons $year^{-1}$ has been calculated since then however, the percentage is relatively small compared with previous decreases (Pacyna, 2001). This estimates are in good agreement with the TGM data set obtained at Mace Head for the years between 1995 and 2001. Similar results have been obtained for the same time period in the high Canadian Arctic (Schroeder, personal communication).

One major question related to long-term data sets is if seasonal patterns possibly overlap a constant trend. The results of the X-11 (Census method II) seasonal adjustment procedure is shown in Figure 5.5. The purpose of seasonal decomposition and adjustment is to isolate the trend, seasonal, cyclical and irregular components, that is, to de-compose the series into the trend effect, seasonal effects, and remaining variability. The black line in Figure 5.5 represents the seasonally adjusted time-series of the monthly averages at Mace Head from September 1995 – December 2001. Missing data were computed by interpolation from available adjacent points. The gray dashed line shows the final trend-cycle component after being smoothed via a variable moving average procedure and the corresponding linear regression (dotted line). As already shown before no significant trend between 1995 and 2001 can be derived even after seasonal decomposition. The remaining cyclical component reveal higher concentrations during winter months compared with the summer months. The difference between a cyclical and a seasonal component is that the latter occurs at regular (seasonal) intervals, while cyclical factors usually have longer duration that varies from cycle to cycle; therefore, not being removed in this method.

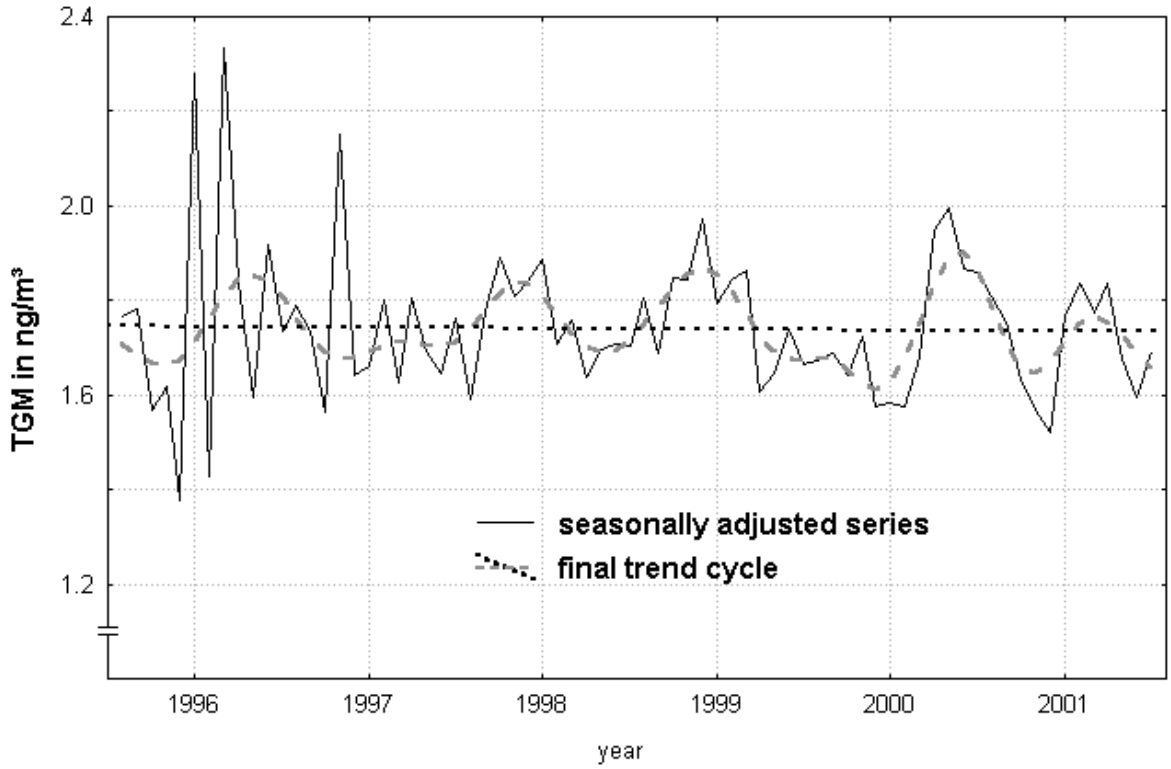

Figure 5.5: Results of a X-11 (Census method II) seasonal adjustment procedure applied to the monthly averaged TGM concentrations measured at Mace Head from September 1995 to December 2001

5.2 Seasonal Variations of TGM Data Measured at Mace Head

Between 1995 and 2001 average TGM-concentrations are remaining fairly stable at a concentration value of 1.75 ng Hg m^{-3}. However, on an annual basis (averaged monthly means) the winter months show higher concentrations compared with the summer months. Monthly averages for the individual months have been used to evaluate seasonal variations in the TGM background levels. Although the number of data points (based on 5 years) is still fairly limited, a seasonally dependent TGM background concentration can be derived with higher levels in winter compared with the summer months. Lowest TGM-concentrations have been observed in summer (April to September), with approx. 1.6 ng m^{-3}, whereas the average concentrations during wintertime (October to March) are around 1.9 ng m^{-3}. The seasonal variability of the averaged monthly means at Mace Head is shown in Figure 5.6.

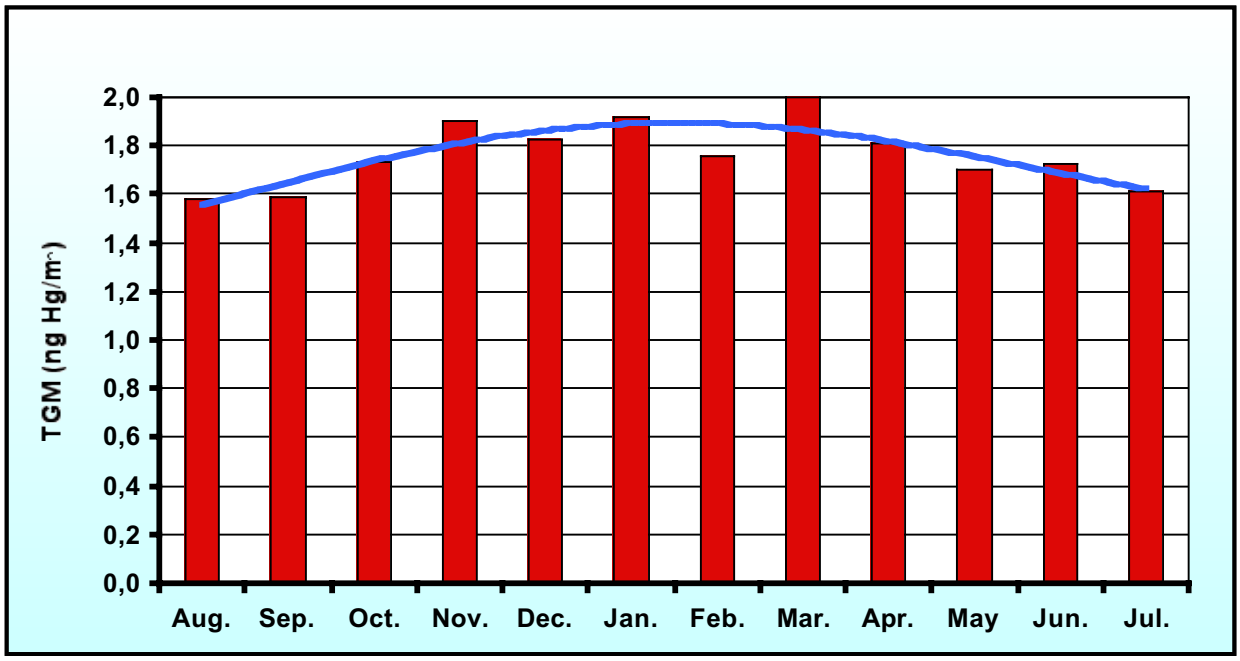

Figure 5.6: Averaged monthly means of the TGM-concentrations at Mace Head, Ireland

The peak to peak amplitude, that is the difference between the seasonal average for the winter/spring periods and summer/autumn periods is approximately 0.3 ng m^{-3}. This difference corresponds to approximately 20 % when referred to the overall TGM average concentration of 1.75 ng m^{-3}.

Summer minimum TGM concentrations have also been observed by Slemr (1996) at the Wank Summit and by Brosset (1982) in Sweden.

TGM measurements at the Wank Mountain in Southern Germany increased from a minimum during December and January to maximum concentration in February, March and April. From April onwards, concentrations decreased towards a minimum. The peak to peak amplitude of seasonal variation observed at the Wank summit was 0.75 ng m^{-3} which corresponded to 30 % of the average TGM concentration observed at the site. A spring maximum is also consistent with TGM measurements made by Brosset, (1982) between October 1979 and September 1980, in Sweden. However a second maximum in September and October was also observed in this data. Brosset, (1987) observed another seasonal variation in measurements again in Sweden between July 1983 and June 1984 in which TGM concentrations were at a maximum between October and December.

These two types of seasonal variation are explained by Slemr, 1996. The seasonal variation, with summer minimums observed at the Wank Mountain, and in Sweden (Brosset, 1982), is

characteristic of the majority of trace gases of which almost all are removed from the atmosphere by oxidation processes (Warneck, 1988). The major oxidation species in the troposphere is the OH radical which has a pronounced seasonal cycle at middle and higher latitudes (Fourth report of the Photochemical oxidants review group, 1997), (Warneck, 1988), (Logan et al, 1981). Higher OH concentrations in summer lead to faster removal by oxidation and to a summer minimum in pollutant concentrations. Polluted air masses move in regions with low photochemical activity (Beine, 1997).

A seasonal cycle in washout out of mercury has also been observed in many studies (Jensen and Iverfeldt, 1994). Maximum washout occurs in summer, and may result from greater oxidation of to Hg^0 to more soluble species.

It is also possible that the trend observed in the Mace Head data may be due to the seasonal cycle in the burning of fossil fuels. Fossil fuel combustion for domestic heating is greatest during the winter and spring period (Cooke et al, 1997).

A different seasonal cycle in TGM concentration measurements with a summer maximum was observed at a rural site in Tennessee by Lindberg et al, (1992). The seasonal cycle in TGM concentration observed by Lindberg, 1992, is probably due to the influence of local mercury sources and the its dependence on air and soil temperature, with higher summer temperatures increasing mercury fluxes.

5.3 Differentiation between Air Masses of Marine or Continental Origin

Evaluation of TGM concentration data obtained during different episodes of the entire long term measurement period has been accomplished in the course of a PhD thesis at the National University of Ireland in Galway (Coggins, 2000), which was co-supervised by the author of this work. One of the major purposes of this work was, to evaluate different parameters to be used for the differentiation of clean oceanic air masses from continentally influenced ones.

5.3.1 Wind Direction Measurements as a Clean Sector Filter for TGM Data

Mace Head is exposed to air masses from the North Atlantic in the sector between 180° and 300° (Jennings et al., 1993; Oltmans and Levy 1994; Ebinghaus et al., 1995). European continental air masses arrive at the site between $45° < \text{wind direction} < 135°$. The

meteorological records show that on average over 50% of the air masses arriving at Mace Head are within the clean sector, as depicted in Figure 5.7. 96 - hour air mass back trajectories, calculated using the ECMWF (European centre for medium range weather forecasting) global trajectory model also aid in identifying clean sector air masses. Air masses at Mace Head with black carbon mass concentrations less than 75 ng m^{-3} are used to identify air masses of marine origin (Cooke et al, 1997). Air masses with condensation nuclei concentrations < 700 cm^{-3} are used as an additional criterion for air masses of marine origin (Cooke et al, 1997).

Figure 5.7 illustrates the frequency distribution of incoming air masses at Mace Head for the time period 1997 to 1998. The mean TGM concentration for clean sector air masses is 1.72 ng m^{-3}. For the same period, 20 % of the air masses are in the continental sector 35° <WD< 145° and had an average TGM concentration of 1.83 ng m^{-3}.

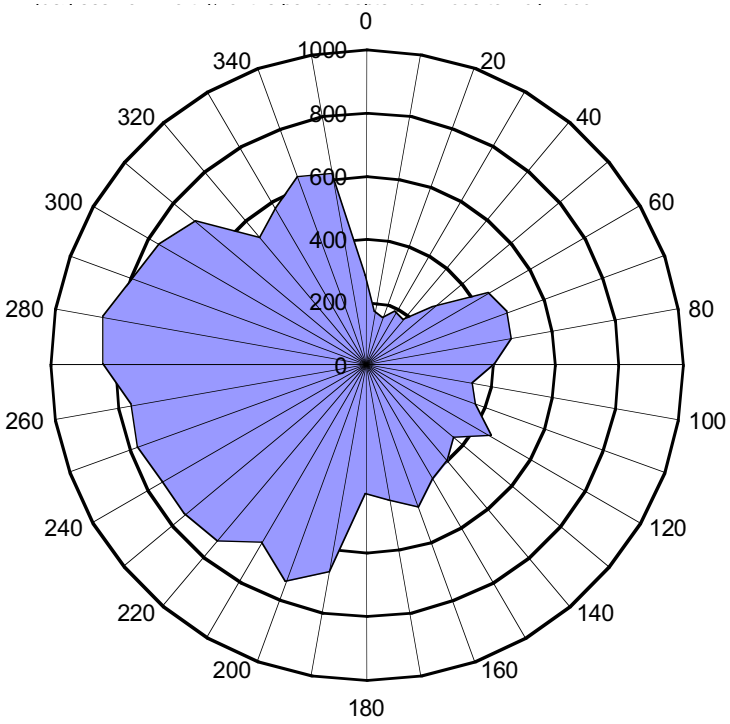

Figure 5.7: Frequency distribution (in hours) of wind direction showing air masses at Mace Head (degrees from North), for the period September 1995 to May 1999

The distribution of TGM mean concentration for the clean sector and continental air masses is summarized in Table 5.1.

Table 5.1: Summary of Wind Direction Measurements as a Clean Sector Filter for TGM Data from September 1995 to May 1999 (n = 18806)

	Clean Sector $180^o < WD < 300^o$	Continental Sector $35^o < WD < 145^o$
% of total hours	50	20
Mean TGM concentration (ng m^{-3})	1.72 ± 0.3	1.83 ±0.5
% of hourly mean TGM < 2 ng m^{-3}	59 %	19 %
% of hourly mean TGM > 2 ng m^{-3}	41 %	30 %

Table 5.1 reveals that 59 % of air masses, which had a mean TGM concentration lower than 2 ng m^{-3} were of marine origin and arrived within the clean sector, while 19 % were of continental origin.

In contrast to this, only 41 % of the air masses with TGM mean concentration > 2 ng m^{-3} arrived through the clean sector, whereas 30 % of the continental sector data showed these elevated concentrations. However, it is obvious that wind direction measurements only are not sufficient to identify air masses that clearly of marine origin and are not affected by anthropogenic sources.

5.3.2 Black Carbon Aerosol Measurements as a Clean Sector Filter for TGM Data

Black carbon aerosol (soot) measurements in the air have in previous studies been positively correlated with airborne TGM measurements (Ebinghaus et al., 1995). Other studies on black carbon aerosol mass concentration measurements have observed higher mass concentrations early in the year at the site (Cooke et al., 1997). Industrial emissions would be expected to remain fairly constant throughout the year, but emissions of black carbon aerosol from domestic processes such as burning of fossil fuels will be the highest in the winter months (Jennings et al., 1993). Additionally, coal, oil and wood combustion are all sources of atmospheric mercury (Pirrone et al., 1996; Ebinghaus et al., 1999).

The TGM concentrations from September 1995 to May 1999 have been classified in different groups of air masses according to simultaneously measured concentrations of black carbon aerosol. It could be derived that lower soot concentrations in the sampled air masses are not reflected in the TGM concentration levels which remain fairly constant at around 1.75 ng m^{-3}. Examining the monthly data, it is observed that for measuring periods where the monthly mean exceeds the average concentration for the entire measuring period (i.e. 1.75 ng m^{-3}), black carbon aerosol concentrations are also elevated above the clean sector value of 75 ng m^{-3}. This may indicate a similar source for the higher TGM and black carbon aerosol concentrations.

When both parameters, i.e. wind direction and black carbon aerosol measurements are combined and different soot concentration levels of less than 70 ng m^{-3} are used as a cut off point for the clean sector ($180^{o} < WD < 300^{o}$) TGM data, a reduction in hourly mean TGM concentrations can be observed as depicted in Figure 5.8.

Lower soot concentration do not reduce TGM average values to any greater extent and the total number of hours where these two boundary conditions were fulfilled between September 1995 and May 1999 was a little less than 2000 hours. A further decrease of the soot cut off level to 10 ng m^{-3} for example will reduce TGM averages from 1.59 ng m^{-3} to 1.57 ng m^{-3} only however, the number of observation hours is reduced to 279. Additionally, the accuracy and precision of the automated aerosol black carbon analyzer may be doubted at these very low soot concentration levels.

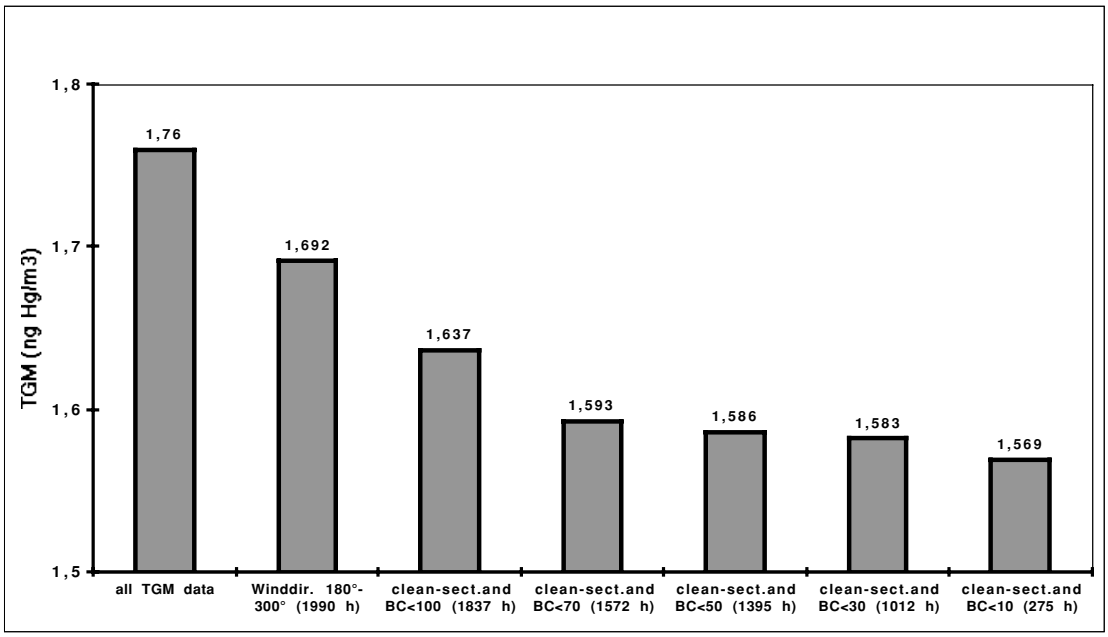

Figure 5.8: Average TGM concentrations (ng m^{-3}) within the clean sector as indicated by the clean sector parameters of wind direction (WD) and black carbon aerosol mass concentrations (ng m^{-3})

Based on this result it may be concluded, that the combination of the two filter parameters wind direction (180^o < WD < 300^o) and black carbon aerosol (< 70 ng m^{-3}) is a simple and applicable approach to successfully identify air masses of marine origin that are not biased by local or regional anthropogenic emissions of mercury.

5.4 Long-term Trend of Clean Sector TGM Data

The entire data set has been treated according to the strategy explained above to evaluate any trends in the TGM measurements when clean air masses of oceanic origin arrive at the site. This would allow to estimate trends in the global background concentration of atmospheric mercury, when only long-range transport processes and no local or regional effects are reflected in the measured concentration level at Mace Head.

The results are shown in Figure 5.9.

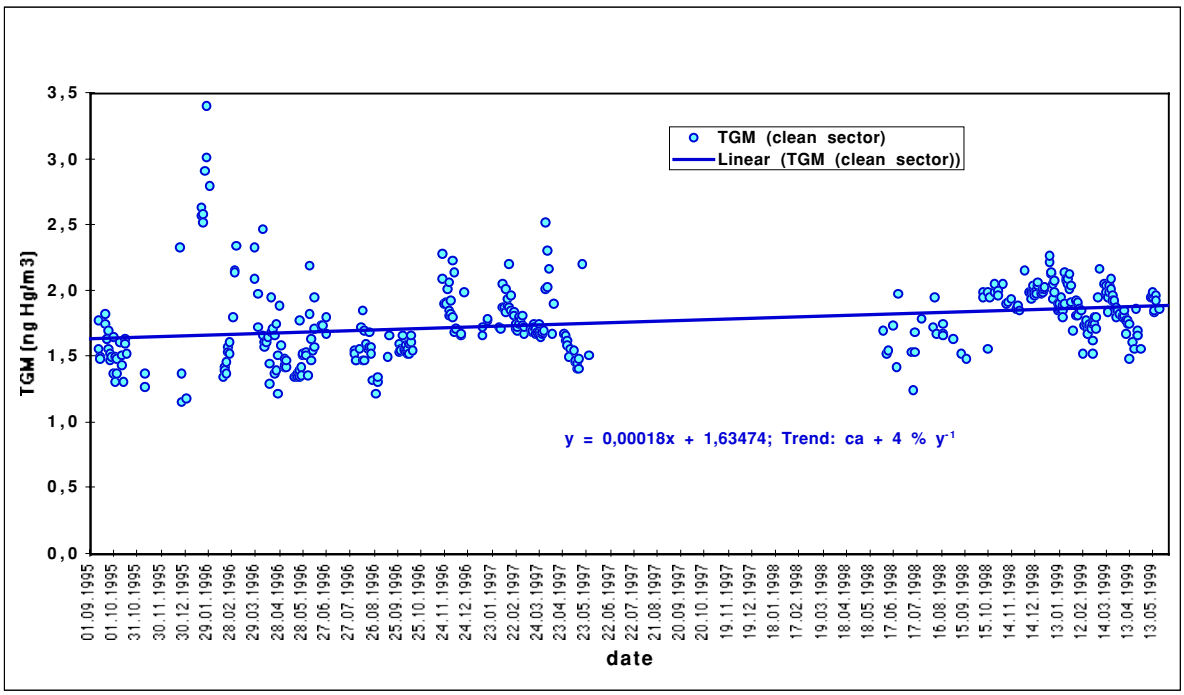

Figure 5.9: Trend of clean sector TGM concentration data (hourly averages) for the period September 1995 to May 1999

From Figure 5.9 an increasing trend in the clean sector data between September 1995 and May 1999 of approximately 4 % per year may be derived. Only few data worldwide exist to compare this finding on trends in global background concentrations of TGM with other results. For the period 1977 to 1980 Slemr (1996) has reported an annual increase of atmospheric mercury concentrations of about 1.4 % in the northern hemisphere derived from ship cruises over the Atlantic Ocean. However, the same methodologies revealed a decreasing trend in atmospheric mercury levels of about 4 % per year for the years 1990 to 1994 (Slemr, 1996). The observed trends are believed to reflect the trends in major anthropogenic mercury sources, i.e. burning of coal and mercury emissions from waste incineration. Slemr also claims that further increase in TGM concentrations is to be expected after the exhaustion of the reduction potential for the reduction of mercury emissions (Slemr, 1996).

5.5 Seasonal Variations in the Clean Sector TGM Concentration Data

The entire TGM data set shows a seasonal variability with elevated levels in the winter months, as discussed above.

Seasonal variations in the clean sector data were also investigated. The difference between the seasonal average for the winter/spring period and the summer/autumn period is reduced to approximately 0.16 ng m^{-3}, corresponding to about 10 % when referred to the overall TGM average concentration of 1.75 ng m^{-3}. The differences in monthly averaged clean sector data were statistically tested to see whether or not it is statistically significant (Chatfield, 1984). Auto correlation coefficients were calculated which measure the correlation between monthly TGM concentration measurements a distance of one month apart. When calculating the correlation coefficient and the lag, a slight pattern occurs. However, the correlation is limited by lack of data and is not statistically significant, i.e.

$$< \pm 2 / \sqrt{N}$$

When analyzing the polluted sector data only (35^o < WD < 145^o), no seasonal trend has been observed.

6 Studies on the Regional Distribution of Atmospheric Mercury in North-western and Central Europe

Since almost all our knowledge on the regional distribution of atmospheric mercury is derived from ground-based measurements at single locations for different time periods, little information is available on the vertical and horizontal distribution in the troposphere. Based on the generally accepted view that elemental mercury with an atmospheric residence time of about 1 year is by far the dominating component of total atmospheric mercury (Lindqvist and Rodhe, 1985; Slemr et al., 1985; Schroeder and Jackson, 1987), rather even vertical and horizontal distribution of atmospheric mercury in the troposphere of a hemisphere is expected. Since all other gaseous mercury species and those attached to aerosols have a much shorter atmospheric residence time of up to a few days, enhanced mercury concentrations and pronounced concentration gradients are expected only in the vicinity of sources. These general suppositions are supported by model simulations of transport and chemistry of mercury in the atmosphere (Mason et al., 1994a; Pai et al., 1997; Petersen et al., 1998).

The regional distribution of atmospheric mercury in Central Europe before 1990 was characterized by a strong south-to-north decreasing gradient from the main emission area in Germany to Scandinavia. In 1995 and 1997 we have carried out two south-to-north transect measurement campaigns to obtain an up-dated picture on the regional distribution of atmospheric mercury in Central Europe.

6.1 Simultaneous Ground-Based Measurements on the Regional Horizontal TGM Distribution on a 800 km Transect between Stockholm and Berlin

Due to it's long atmospheric residence time, atmospheric mercury is subject local, regional and global transport. Among the airborne mercury species elemental mercury is the most predominant (approximately 90 % of total) form. A distinct pattern in Total Gaseous Mercury (TGM) concentration is not to be expected at remote places unless a local mercury source, diffuse emissions or long-range transport have direct influence on the site of observation.

There have been only a few attempts to investigate the spatial distribution of mercury on a regional scale. A 15 % increasing gas phase mercury concentration gradient was observed from the southern to northern part of Michigan USA (Keeler et al., 1995). In the Scandinavian countries a deposition network of eight sites was installed in the mid nineties. A clear north to south increasing gradient in wet mercury deposition fluxes was found (Iverfeldt, 1991).

Atmospheric dispersion models are currently used to describe the atmospheric distribution and deposition of mercury on regional scales, for example for Europe and North America. Experimental input data are needed for the parameterization of the chemistry scheme and for the verification of the model results. However, most of the available information is based on measurements at single locations for different time periods from days to several years. Very few attempts have been made to investigate the distribution of atmospheric mercury during field experiments at simultaneously operated measurement sites on a regional scale. Extremely valuable information has been generated during the Nordic Network for Scandinavia in the late 80's. During the Scandinavian study manual methods for the analysis of atmospheric mercury with a time resolution of several days have been applied. A north to south increasing gradient of aproximately 15 % in the annual average TGM concentration was established (Iverfeldt, 1991a). This effect was attributed to an increasing impact of the major atmospheric mercury source areas in eastern Germany.

No experimentally derived information on the regional distribution of atmospheric mercury for Central Europe was available for the time after 1990. In the following the results from two field experiments carried out for two weeks in summer 1995 (June/July) and three weeks in winter 1997 (March/April) at four European sites along a 800 km line between Berlin and Stockholm will be described. Measurements were carried out with a new automated technique with a time resolution of 5 minutes. A total number of more than 30,000 individual concentration measurements has been carried out during these two campaigns representing the most comprehensive data set on the regional horizontal TGM distribution in Europe. An overview about the geographical arrangement of the Transect sampling sites is given in Figure 6.1.

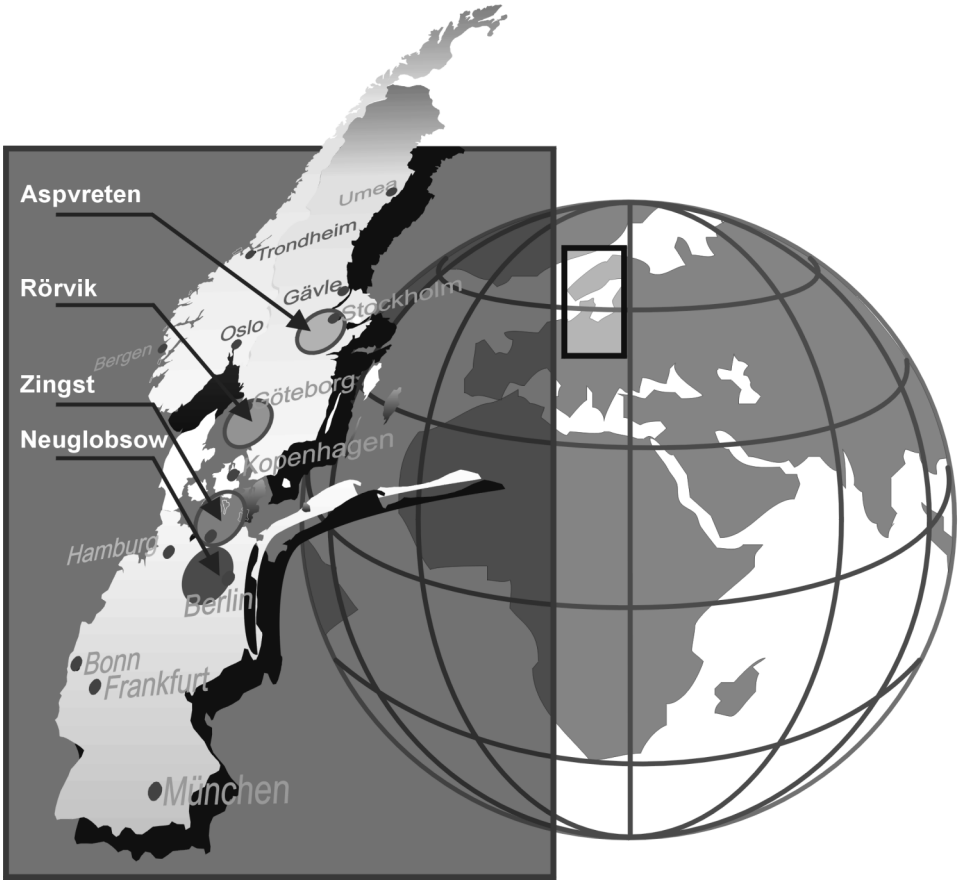

Figure 6.1: Location of the study sites during the two transect experiments

6.1.1 Experimental Strategy of the Transect Experiments

The aim of the South-to-North Transect Experiment was on one hand to get new information about the regional horizontal distribution and transboundary transport of mercury in middle-northern Europe. On the other hand it was an effort to improve the knowledge about the short time variability of TGM and the influence of the main meteorological and atmospheric chemical factors on its diurnal pattern.

- The sampling site Neuglobsow is located about 50 km north-west of Berlin, close to the lakes of the Müritz river, in a wooden area. Neuglobsow is the most southern sampling site, about 150 km north of the heavily industrialised region between Halle and Leipzig. Considering the area of the former GDR as important source area for atmospheric mercury (Berdowskie et al., 1997), Neuglobsow is expected as the site with the most elevated TGM back ground concentration.
- Zingst, the second German sampling site is located adjacent to the southern shore line of the Baltic Sea.

- The third sampling site is located on the west coast of Sweden approximately 40 km south of Gothenburg and 1km east of the shore.
- The most northerly sampling site, Aspvreten, an EMEP monitoring station as well, is located south east of Stockholm.

At all four sites TGM was detected with Tekran Gas Phase Mercury Analyzers (Model 2537A). To achieve the best possible comparability between the four sites the instruments and internal permeation sources were calibrated before and after the experimental work by manual calibration. The procedure was adopted from Dumarey et al. (1985). Additionally all instruments were subjected to intensive two days intercalibration exercises in the GKSS laboratory before the beginning and after the completion of the measurements. The TGM concentrations measured during these periods ranged from 1.5 to 8 ng m^{-3}. A maximum bias of less then 5% was detected between the instruments. To foster the direct comparability of the measurements at the four sites, correction factors were computed from the intercalibration exercises and used to correct the systematic differences between the instruments. All TGM values measured during the experimental phase were corrected by these factors for further examination to eliminate the bias between the individual analyzers.

6.1.2 Results of the 1995 Transect Experiment

Figure 6.2 summarizes the TGM time-series measured at the four sampling sites. The sites are arranged from the most northerly site at the top of the graph to the most southerly at the bottom. The data points represent the 5 min average concentrations.

Due to a power failure at Asprveten, a loss of data occurred between 29 June 11:00 p.m. and 30 June 11:00 a.m. At the two Swedish sites the mercury concentrations remained nearly constant at about 1.5 ng m^{-3}. Concentrations higher than 2 ng m^{-3} were only infrequently detected. On three occasions concentrations of approximately 1.0 ng m^{-3} were detected in the early morning hours. The time series measured at Rörvik and Aspvreten are characterized by almost the same pattern, with relatively low TGM concentrations. Median TGM concentrations of 1.54 and 1.53 ng m^{-3} were observed at Asprveten and Rörvik respectively.

The decreasing amplitude of the variability in the diurnal TGM cycle at the four sites from the more southerly (German) to the northern (Swedish) locations is obvious (Figure 6.2). In contrast to the Swedish sites, a certain number of peak events with significantly elevated TGM concentrations were observed at Zingst and Neuglobsow. The classification significant

relates to the "regional background concentration" which is less than 2 ng m^{-3} at the German sites. The background concentration is characterized here by the median 0.5 h average concentration at each site.

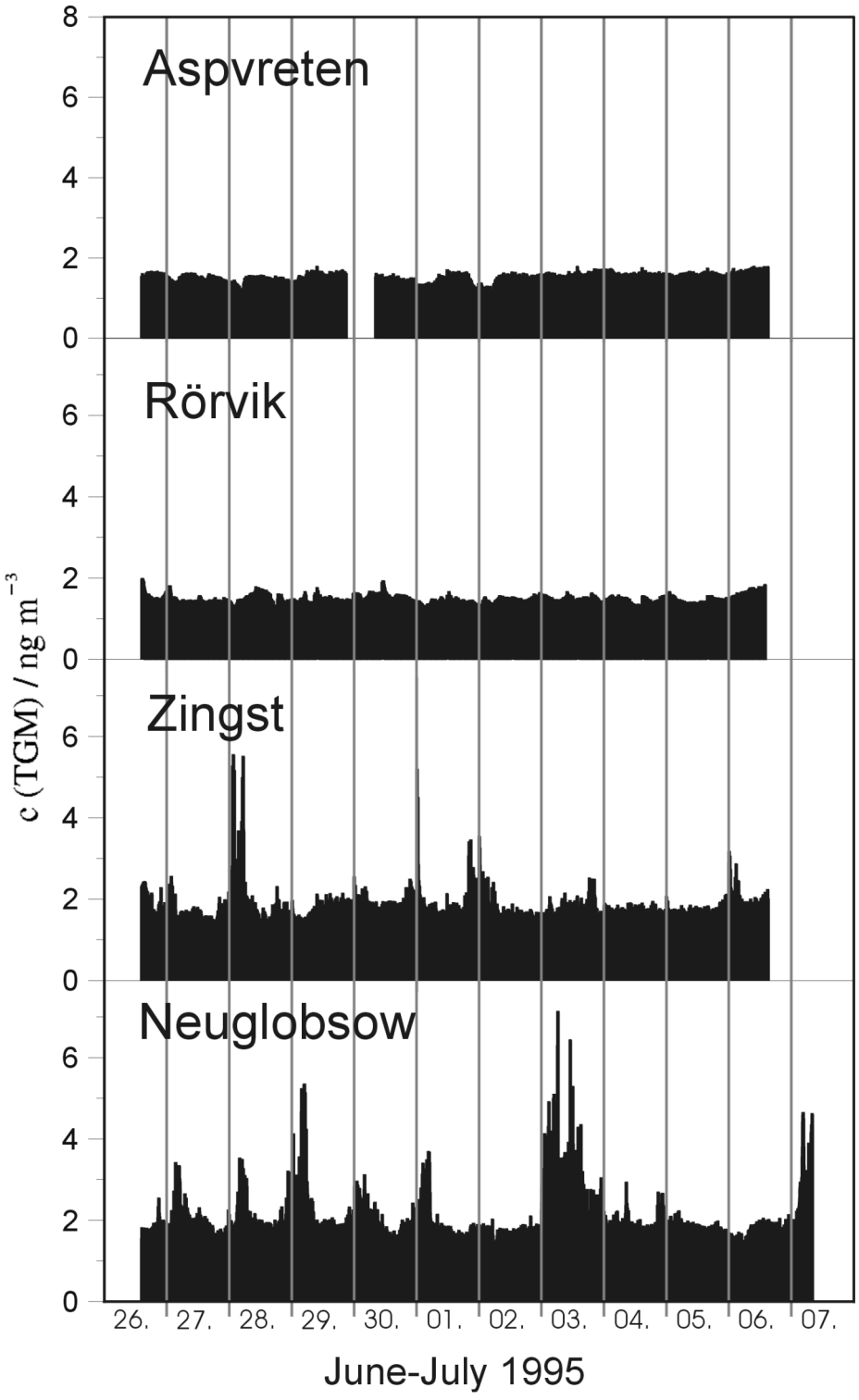

Figure 6.2: Time series of the 5 min average concentrations observed during the 1995 Transect Experiment, separately displayed for each sampling site

During a rain event at Neuglobsow TGM concentrations increased by a factor of 2 -3. As rainfall started at Neuglobsow on July 03, the TGM-concentration increased from the typical regional back ground level of approximately 2 ng m^{-3} to a value of about 6 ng m^{-3}. The rain continued during the whole day. After the initial "jump", TGM leveled out at an average value of about 3.5 ng m^{-3}, a factor of 1.7 higher than the background value. The following day rain activity declined, and the TGM concentration decreased again to the usual background level of approximately 2 ng m^{-3}. Similar TGM concentration behavior was observed by Wallschläger (1996), Wallschläger et al. (2000) during a field experiment carried out on the Elbe river flood plain. At Zingst a much less pronounced effect was observed. At the Swedish sites rain events had no apparent effect on the ambient TGM concentrations. In particular the obvious TGM peak during the rain event in Neuglobsow on July 07 was mainly due to changing air masses during the day, as the analysis of the meteorological situation shows. However, also increasing diffuse emissions from soil, induced by rain fall could contribute to the observed effect.

Figure 6.3 shows the combined graphical representations of the frequency distribution and the diurnal cycle of the 1 h average TGM concentrations measured during the 1995 Transect Experiment at each individual sampling site.

The frequency plot groups the TGM concentrations measured during the 1995 Transect Experiment cases into 0.2 ng m^{-3} classes. Additionally a fitted Gaussian probability plot is superimposed. The diurnal cycle depicted as box and whisker plot. All TGM observations are collected in hourly daytime groups on a 24 hour scale. Each box displays the following basic statistics minimum and maximum concentration, 25 %–75 % quartile and median concentration.

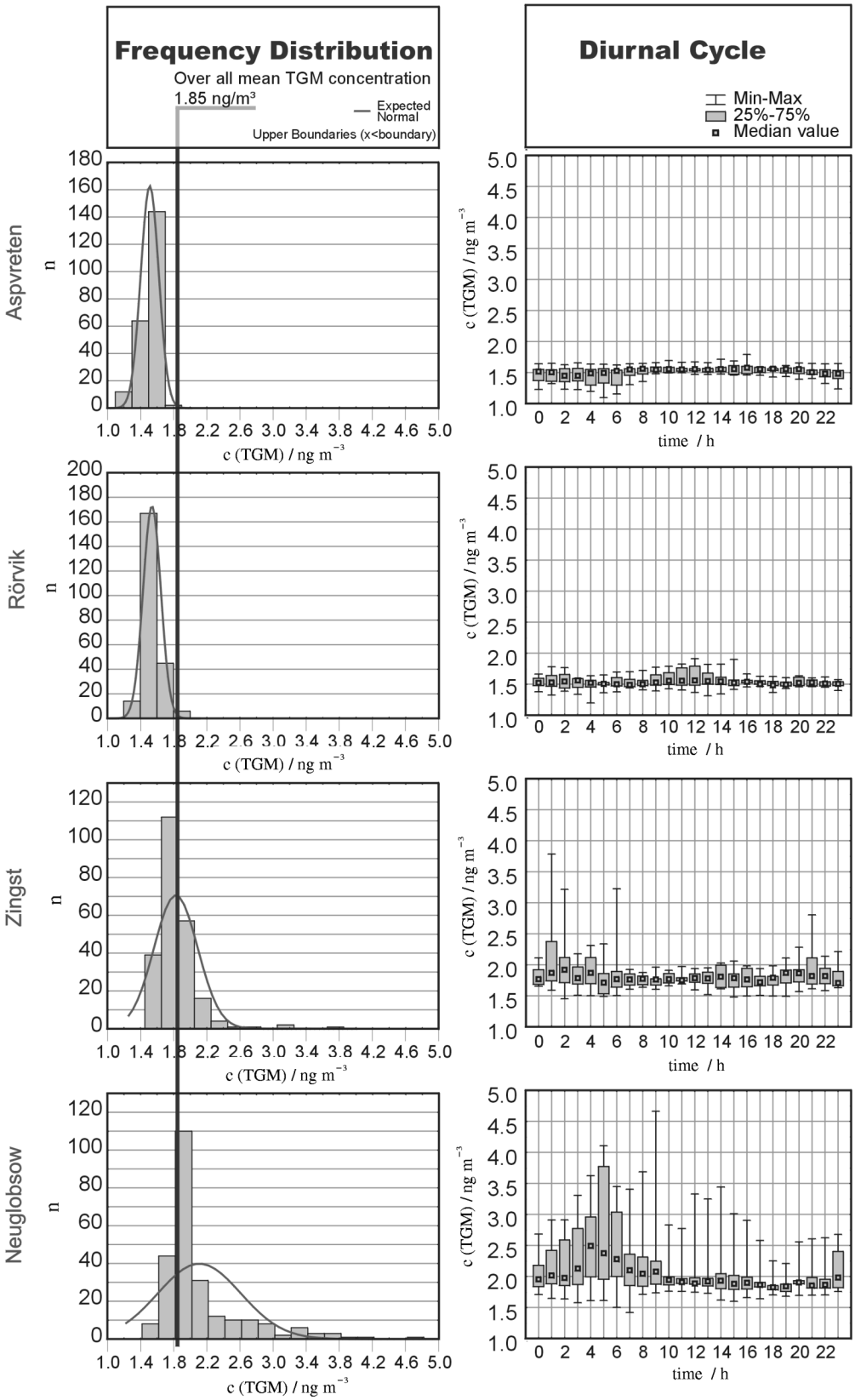

Figure 6.3: Combined graphical representations of the frequency distribution (left part) and the diurnal cycle (right part) of the 1 h average TGM concentrations measured during the 1995 Transect Experiment at each individual sampling site

Both time series measured at the Swedish sites were characterised by narrow frequency distributions with a standard deviation of less than 7%, and a maximum at 1.5 ng m^{-3}. Comparing these results with measurements carried out under the umbrella of the Nordic Network for Atmospheric Mercury during the years 1985 to 1989, and recent data from the years 1990 to 1992, two trends are supported. On one hand, the trend of declining TGM background concentration during recent years continues. During the years 1985-1989 and 1990-1992 (Iverfeldt et al., 1995, Iverfeldt et al., 1991b) the median concentrations of TGM, observed at the Swedish west coast, were 2.8, and 2.6 ng m^{-3} respectively. A reasonable extrapolation of the values observed at Rörvik over the whole year is not possible from the data reported here, but a trend to lower TGM concentrations today seems to be indicated. On the other hand, the absence of elevated TGM peak events at the Swedish sampling sites during the time of this study corresponds well with investigations carried out in the years 1991 and 1992 (Iverfeldt et al., 1995).

6.1.3 Results of the 1997 Transect Experiment

A second Transect Experiment was carried out in winter 1997 (March/April) over a three weeks period at the same sampling sites. Figure 6.4 summarizes the TGM time-series measured at these four sampling locations.

Similarly to the 1995 Transect Study the 1997 data show the most pronounced variability of measured TGM concentrations at the site Neuglobsow. The two Swedish sites are again characterized by fairly constant low levels of atmospheric mercury. The data set is also indicating that a "pollution event" has been detected at all four sites during April 25 to 27. Figure 6.5 shows the combined graphical representations of the frequency distribution and the diurnal cycle of the 1 h average TGM concentrations measured during the 1997 Transect Experiment at each individual sampling site.

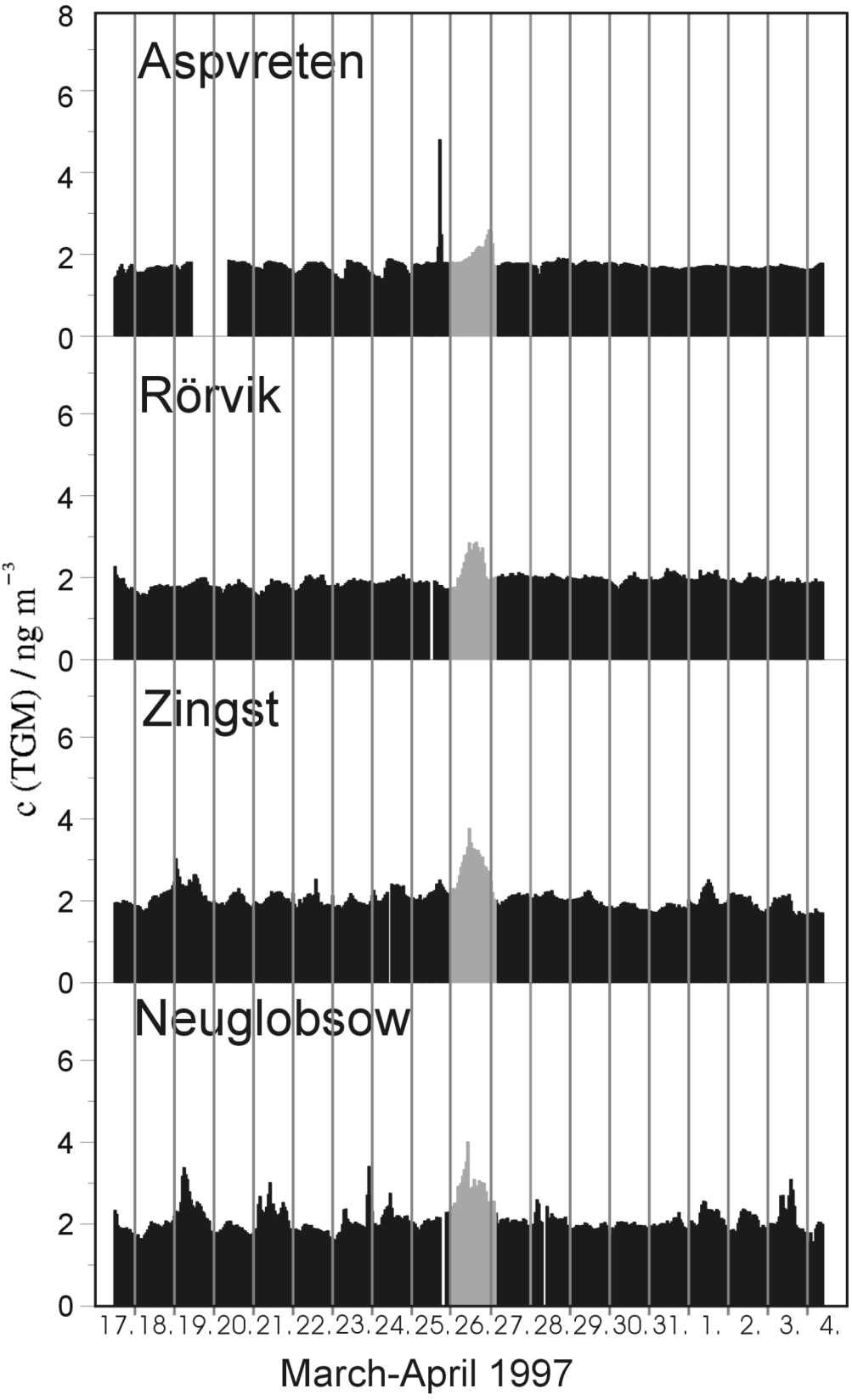

Figure 6.4: Time series of the 5 min average concentrations observed during the 1997 Transect Experiment, separately displayed for each sampling site

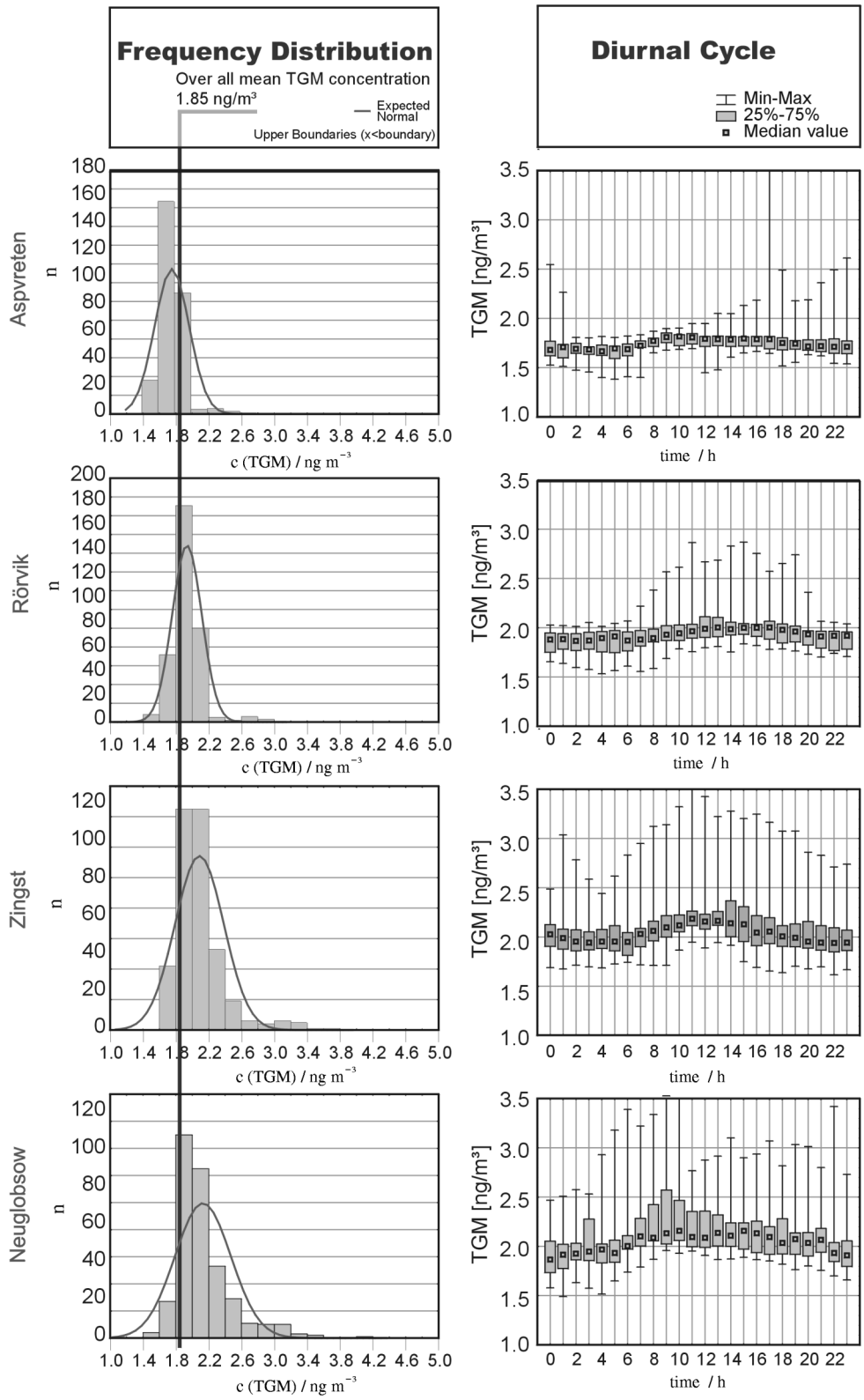

Figure 6.5: Combined graphical representations of the frequency distribution (left part) and the diurnal cycle (right part) of the 1 h average TGM concentrations measured during the 1997 Transect Experiment at each individual sampling site

6.1.4 Summary of 1995 and 1997 Transect Experiments

During both, the summer and the winter experiment a decreasing variability in the TGM concentration from south to north was obvious. This is depicted by the time series plots and is confirmed by the south to north decreasing standard deviation of the fitted Gaussian function within the frequency plots (left four graphs). The high variability, at least at the southernmost site (Neuglobsow) is dominated by a significant 24h periodicity (Figure 6.3 and Figure 6.5; right four graphs). A shift of the daily maximum TGM concentration from 5 a.m. during the summer experiment (Figure 6.3) to 9 a.m. during the winter (Figure 6.5) supports a correlation between the TGM concentration and meteorological, photochemical and perhaps biological processes as suggested by Lindberg 1996 (biosphere/atmosphere exchange processes).

Just as significant as the differences of the variability on the south to north transect, the TGM concentration levels differ between the four sites and also show seasonal differences. This is summarized in Figure 6.6.

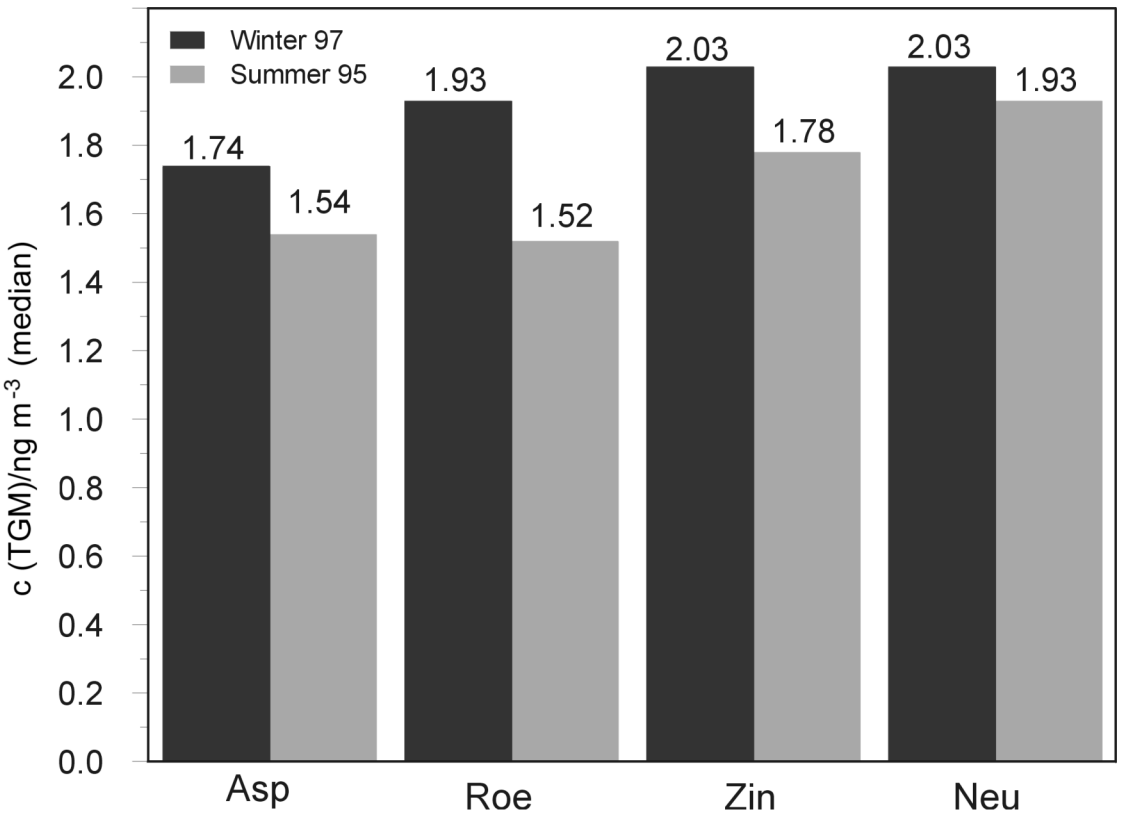

Figure 6.6: Regional distribution of the median TGM observations during summer 1995 and Winter 1997

During both experiments a south to north decreasing TGM gradient was found. A ΔTGM between the mean concentrations observed at the southernmost site Neuglobsow and the most northerly site Aspvreten of 0.38 (1997) and 0.60 (1995) ng m^{-3} was calculated. To avoid the influence of single peak events on the mean concentration levels, the more robust median TGM levels were also compared. During winter 1997 a north to south increasing median TGM concentration gradient of approximately 20% was found. During the summer 1995 experiment the gradient was less pronounced but with 14 % also significant. Comparing the median concentrations between the 1995 and 1997 experiments the systematically elevated levels at all sites during the winter experiment become obvious. This finding is in accordance to model results which predicts elevated concentrations during the late winter/ early spring (Petersen et al., 1995). During the 1997 experiment a contaminated air mass was simultaneously observed at the four sampling sites.

The basic statistics of the 1 hour average concentrations are summarized in Table 6.1.

Table 6.1: Summary of 1-hour Average Concentrations Measured during Transect 1995 and 1997 and Related Basic Statistics

1997 March - April					
Site	**Valid N (n)**	**Mean (ng m^{-3})**	**Minimum (ng m^{-3})**	**Maximum (ng m^{-3})**	**Std.Dev (ng m^{-3})**
Aspvreten	408	1.75	1.38	4.81	0.21
Rörvik	427	1.94	1.53	2.87	0.18
Zingst	427	2.09	1.62	3.79	0.30
Neuglobsow	425	2.13	1.49	4.03	0.34
1995 June-July					
Aspvreten	222	1.51	1.10	1.79	0.11
Rörvik	232	1.54	1.20	1.91	0.11
Zingst	233	1.83	1.45	3.79	0.26
Neuglobsow	250	2.11	1.42	4.66	0.50

The data sets shown here have recently been selected as experimental reference data for an international model intercomparison exercise under the UN-ECE Convention on Long-Range Transport of Air Pollutants (CLTRAP). The main selection criteria applied by EMEP Meteorological Synthezising Centre - East in Moscow (MSC-East) as the responsible organization were their high time resolution and well documented quality standards (WMO/EMEP/UNEP, 1999; MSC-East, 2001).

6.2 Aircraft Measurements of Atmospheric Mercury over Southern and Eastern Germany

Since almost all our knowledge is derived from ground based measurements, one of the lesser known aspects is the vertical and horizontal distribution of mercury in the troposphere. However, experimentally derived data on the three dimensional distribution and variability are an important input parameter and an accepted validation tool for atmospheric transport and deposition models.

Based on the generally accepted view that elemental mercury with an atmospheric residence time of about 1 yr is by far the dominating component of total atmospheric mercury (Lindqvist and Rodhe, 1985; Slemr et al., 1985; Schroeder and Jackson, 1987), rather even vertical and horizontal distribution of atmospheric mercury in the troposphere of a hemisphere is expected. Since all other gaseous mercury species and those attached to aerosols have a much shorter atmospheric residence time of up to a few days, enhanced mercury concentrations and pronounced concentration gradients are expected only in the vicinity of sources. These general suppositions are supported by model simulations of transport and chemistry of mercury in the atmosphere (Mason et al., 1994; Pai et al., 1997; Petersen et al., 1998).

The very few attempts to measure mercury concentrations onboard airborne platforms, however, have provided conflicting results so far. Slemr et al. (1985) measured TGM concentration above central Europe at altitudes varying from 6,000 to 12,000 m in a fairly small range from 1.2 to 3.1 ng m^{-3} without any pronounced vertical gradient. This is roughly in agreement with the suppositions outlined above, although the large scatter of the data precludes a more definitive conclusion. The large scatter of the individual measurement results was probably due to analytical problems, possibly caused by stainless steel sampling inlet. In contrast to this data set, Ionov et al. (1976), Kvietkus et al. (1985), Brosset (1987) and Kvietkus (1995) report the occurrence of pronounced gradients with decreasing TGM concentrations with increasing altitude. Ionov et al. (1976) reported a decrease in mercury

concentrations with increasing altitude which was similar to the concentration decrease of radon decay daughters and from this they estimated an atmospheric residence time of mercury to be about 10 days. Measurements of Brosset (1987) were made above sea west of Göteborg where no local sources are to be expected. They cover altitudes up to 3,000 m and the mercury concentrations decreased roughly proportional to the pressure decrease with altitude. Kvietkus et al. (1985) and Kvietkus (1995) reported measurements over different areas of the former Soviet Union. Mercury concentrations varied strongly depending on the location but generally decreased with increasing altitude of up to 3,500 m. A more detailed analysis of the vertical profile over the eastern Lithuania in June 1988 (Kvietkus, 1995) revealed the almost exact proportionality of measured mercury concentrations to the pressure at the sampling altitudes. A possible dependency of the detector response on ambient pressure is not discussed in either of these works. However, a recent study by Ebinghaus and Slemr (2000) has shown, that the response of the most commonly used Atomic Fluorescence Spectroscopy detectors is significantly dependent on the ambient pressure.

In this chapter mercury measurements onboard an aircraft during a level flight from Oberpfaffenhofen, southwest of Munich, to Halle and back, made on June 13, 1996 will be presented and discussed. In addition, vertical profiles of TGM concentrations were measured up- and downwind of a former chlor-alkali and acetaldehyde plant at Schkopau in East Germany (former GDR), which with an emission of more than 50 tons $year^{-1}$ is supposed to be the largest singular point source of mercury in Europe until 1990 (Helwig and Neske, 1990). Production at three of the four chlor-alkaline plants and at the acetaldehyde plant have since been terminated and the emissions in 1994 were estimated to 2 – 4 tons $year^{-1}$ (Krüger et al. 1999; Ebinghaus and Krüger, 1996).

6.2.1 Experimental Strategy and Flight Details

The flight was carried out with an aircraft Dornier 228 CALM of the German Aerospace Research Establishment (DLR) in Oberpfaffenhofen near Munich. A PTFE lined stainless steel tubing was used as a sampling inlet. The tubing was placed on top of the cabin about 1 m in front of the propellers. The tubing was bent and its opening faced the rear of the aircraft to prevent sampling of cloud droplets and coarse aerosols. Two automated mercury analysers (Tekran Model 2537A Mercury Vapor Analyzer, Tekran Inc., Toronto, Canada) were connected to the inlet by PFA tubing and operated with a time resolution of 5 min. Mercury released at approximately 700°C is detected by an atomic fluorescence detector (AFS). Both instruments were operated with a sampling flow rate of 1500 cm^3 (Standard Temperature and

Pressure, STP, i.e. 273.16 K and 1,013 mbar) min^{-1}, corresponding to a sample volume of 7,500 cm^3 (STP).

During take-off and landing the instruments were operated with air filtered by an activated carbon cartridge to avoid contamination of the sample lines and gold traps by kerosene vapor or engine exhaust.

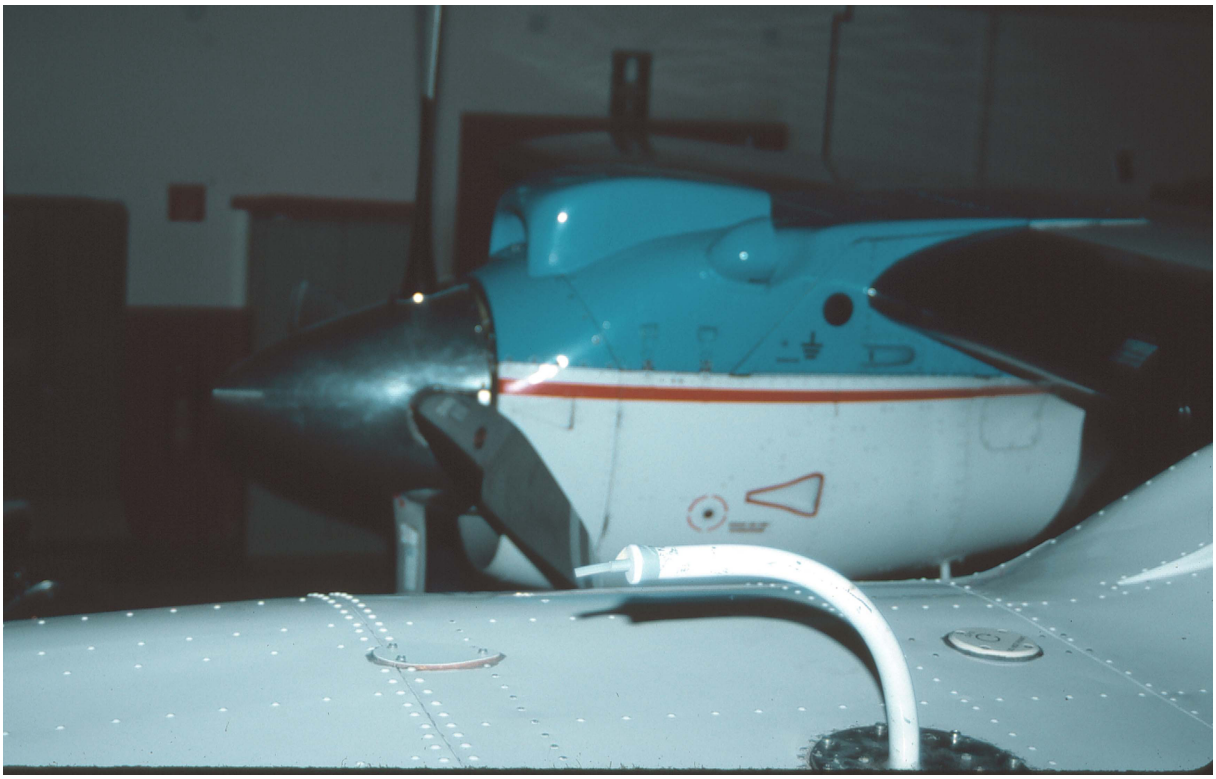

Figure 6.7: Sample inlet on top of the cabin of the Dornier 228 CALM research aircraft

A similar but manual technique with silver coated quartz wool collectors and double amalgamation procedure has been used for measurements at the summit of the Wank mountain (Slemr and Scheel, 1998). Usually 0.6 m^3 (STP) of air were taken within a sampling time of 2 h. At these conditions the detection limit was about 0.1 ng m^{-3}. Both techniques were intercompared at Mace Head in Ireland in 1995 and found to yield identical results (Ebinghaus et al., 1999).

Figure 6.8 shows the path of the flight made out on June 13, 1996. The aircraft started at Oberpfaffenhofen southwest of Munich, southern Germany, and turned north-east towards Halle/Leipzig over a distance of approximately 400 km on a constant cruising altitude of 900 m. 5 km away from the former chlor-alkali plant at Schkopau, the aircraft started to ascent

from 400 m to a maximum altitude of 3,800 m a.s.l. on the upwind side of the plant (51° 26' N; 11 ° 57' E). The descent from 3,800 m to 480 m was carried out 5 km downwind of the factory (51 ° 20,5' N; 11 ° 57,8' E). Horizontal sampling was again carried out on the way back to Munich at a constant cruising altitude of 2,500 m above the boundary layer. Simultaneous TGM measurements were made at the summit of the Wank mountain (1,780 m a.s.l.) at the northern rim of the Bavarian limestome Alps (Slemr and Scheel, 1998). The southernmost flight section of the return flight came to about 40 km close to the Wank mountain.

Figure 6.8: Path of the flight made on June 13 1996. Simultaneous TGM measurements were made at the summit of the Wank mountain

The aircraft instruments were operated at ambient pressure which changes with the flight altitude. Therefore, detailed laboratory studies have been carried out in order to obtain information about the pressure dependence of the Tekran analysers. Figure 6.9 shows schematically the plumbing of the instruments and the pressure control setup used to investigate the pressure dependence of the AFS detector response.

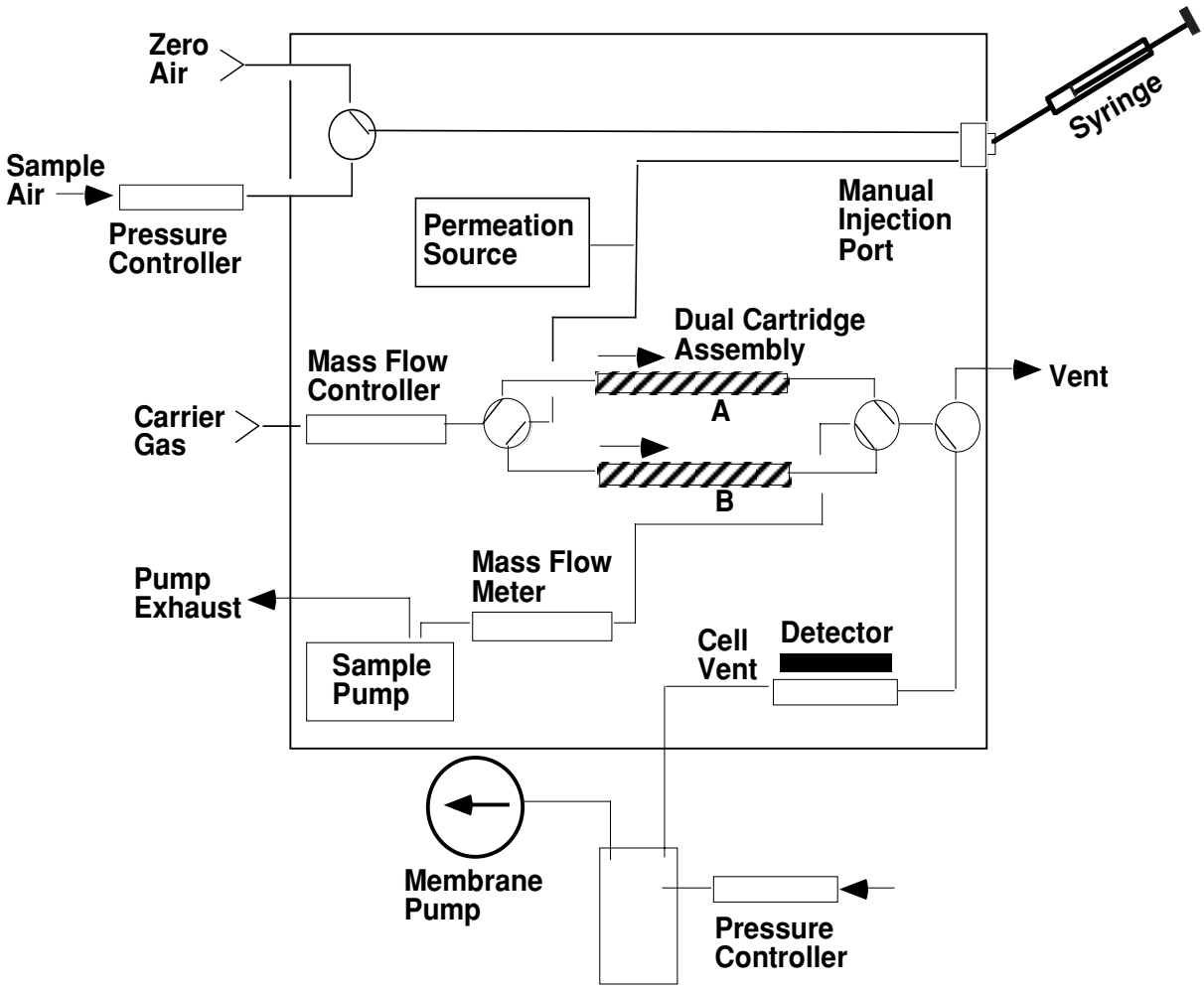

Figure 6.9: Plumbing of the Tekran instruments and the setup used to study the pressure dependence of the AFS detector. Parts within the box are internal parts of the Tekran instrument. External pressure control at the vent of the AFS detector was only used to investigate the pressure dependence of the AFS detector response

Changes in ambient pressure may influence the gold trap collection efficiency. The air sample mass flow rate is kept constant by a mass flow controller (flow meter with a closed loop feedback control of the pump speed). Constant mass flow means that the volume flow rate increases with decreasing pressure and the residence time of the air within the trap decreases. A shorter residence time of air within the trap may lead to decreasing collection efficiency (Slemr et al., 1979). Experiments with different ambient air pressures at the sample inlet showed that the pump speed control works properly down to an ambient pressure of 500 mbar. At lower pressures the pump speed comes to an upper limit and the sample flow rate starts to decrease. The pressure dependence of the collection efficiency has been tested by manual injections of 50 µl of Hg-saturated air (22.5° C) into the sample inlet at 981 mbar and between 530 and 550 mbar. The tests resulted in TGM concentrations of 108.1 ± 6.1 ng m^{-3} at 981 mbar (n=6) and of 108.1 ± 5.5 ng m^{-3} at about 540 mbar (n=6) showing no pressure dependence of the gold trap collection efficiency.

Figure 6.9 shows that the AFS detector of the Tekran instrument is usually vented at ambient pressure. Since the argon carrier gas flow is controlled by a mass flow controller, the volume flow will increase with decreasing ambient pressure. At constant thermal desorption parameters (time controlled), the higher volume flow rate will lead to shorter residence time of mercury atoms in the detector. In addition, decreasing pressure in the AFS detector may change the ratio of fluorescence to quenching in favor of more fluorescence. The combination of these and several other possible effects of pressure change on the response of the AFS detector is hardly predictable and has to be tested experimentally. As shown in Figure 6.9 the vent pressure was controlled by a pressure controller within the range of 620 and 980 mbar. The AFS detector response is shown in Figure 6.10 as a function of the vent pressure.

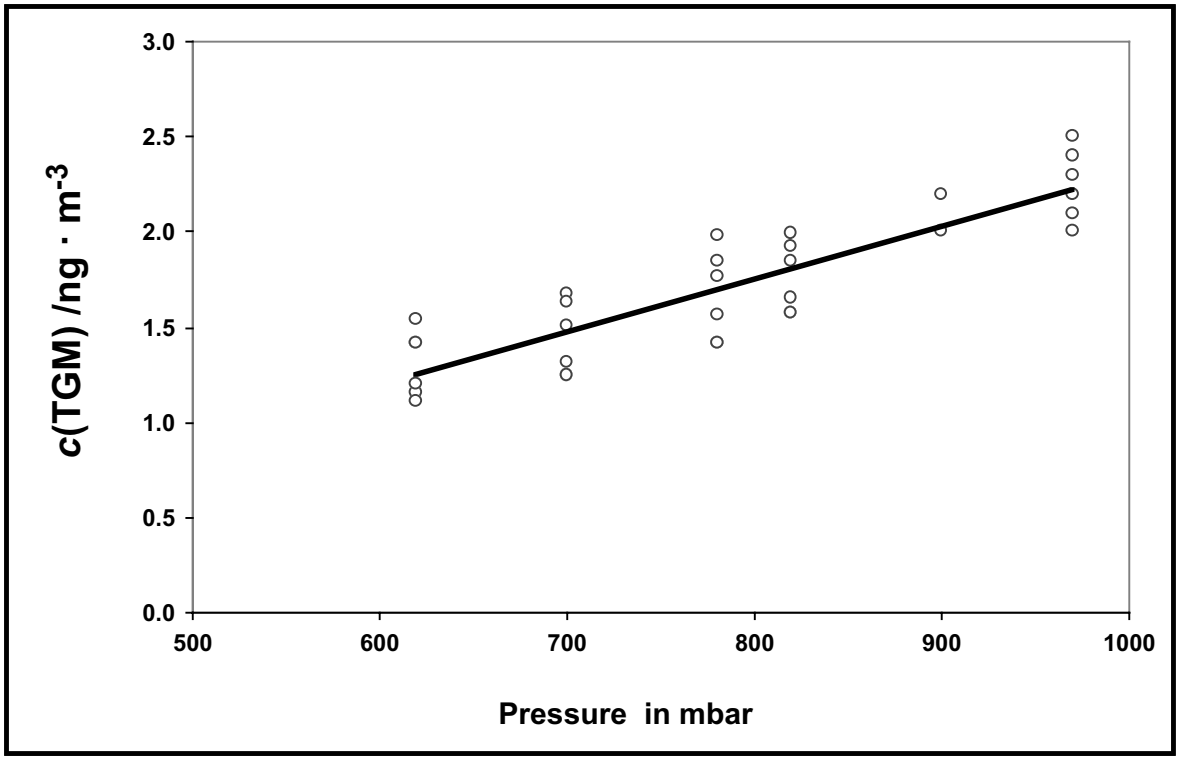

Figure 6.10: Response of the AFS detector as a function of its vent pressure. Ambient air was sampled in these tests and TGM concentration may have changed during these tests

An almost linear relation between the AFS detector response and ambient pressure was observed over the entire pressure range with a decrease of about 0.1 % /mbar. In these experiments indoor air was sampled and, thus, changes in mercury concentrations during the experiments could not be excluded. Therefore similar experiments were also made with known, manually injected quantities of elemental mercury vapor and a Model 2500 Tekran AFS detector. This detector is identical with the AFS detector used in the Model 2537 Analyzer. The regression line from these tests as depicted in Figure 6.11 was used for correction of the signals obtained during the flight.

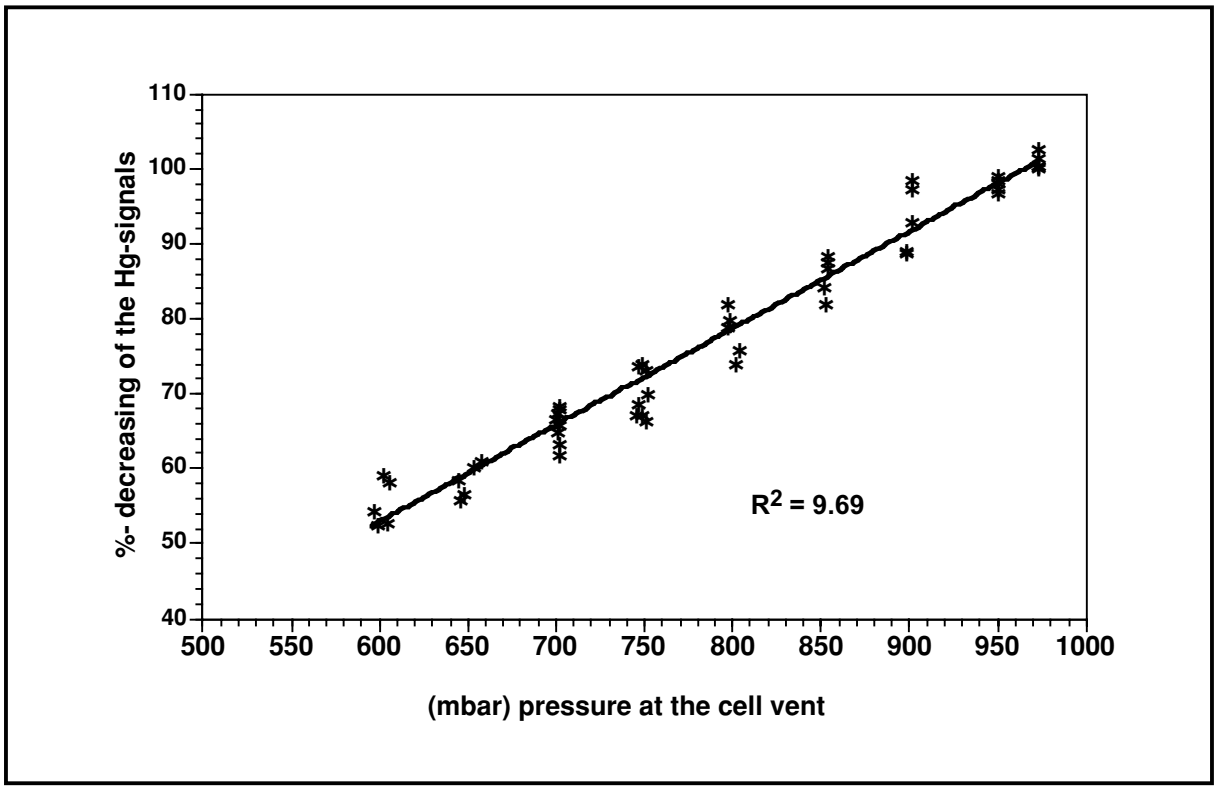

Figure 6.11: Response of the AFS detector as a function of its vent pressure. 50 µL of mercury saturated air at 20oC was injected during these tests. The regression line from this test was used to correct the measurements made during the aircraft measurements

The results of these tests in Figure 6.11 are in good agreement with those in Figure 6.10.

In summary, the response of the instruments used for TGM measurements onboard the aircraft was found to be pressure (altitude) dependent and the measurements have to be corrected for this dependence. All concentrations reported in this paper are given in ng m^{-3} (STP) units, where STP means standard temperature of 0°C and standard pressure of 1,013 mbar.

6.2.2 Results of two Horizontal Level Flights Legs

The synoptical weather situation on June 13, 1996, was dominated by a strong high pressure zone "Xaver" over Ireland. At its perimeter cool marine air masses of sub-polar origin were transported into Germany and in the evening the corresponding cold front arrived at the northern rim of the Alps. The exchange of warm and humid by cold air masses in northern Alps was accompanied by strong storm activities with plenty of precipitation. Radiosondes from Prague, Wahnsdorf (near Dresden), Meiningen (halfway between Erfurt and Würzburg) at midday showed an inversion at about 2,000, 2,000, and 1,550 m a.s.l., respectively, with well mixed cold humid air mass below and very dry air mass above. TGM concentrations measured during the horizontal cruises at constant altitudes of 900 and 2,500 m above sea level (a.s.l.) are shown in Figure 6.12. Each bar in this figure represents a 5 minute interval and a sample volume of 7,500 cm^3 (STP).

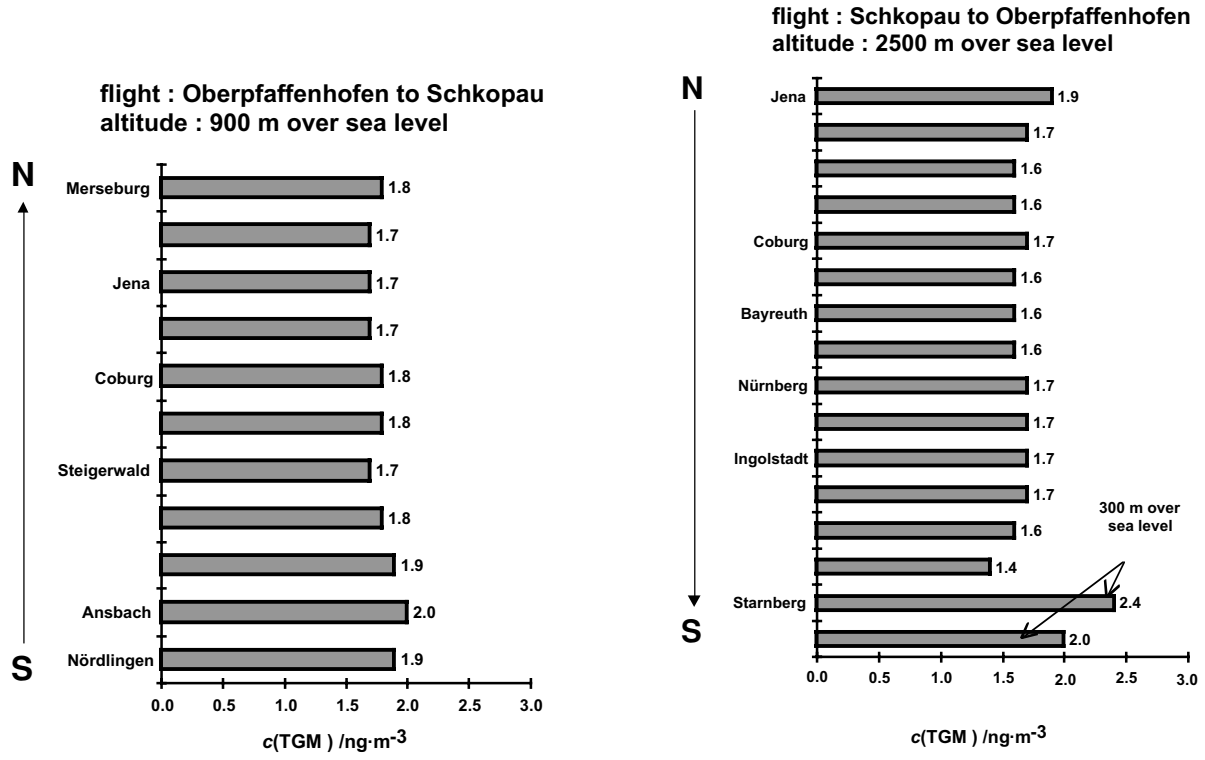

Figure 6.12: TGM concentrations measured during the level flight legs at 900 m and 2,500 m a.s.l. on 13 June 1996

At an altitude of 900 m a.s.l., TGM concentrations showed a slight gradient with decreasing concentration to the north. This may be due to the incomplete exchange of the air mass with low TGM concentrations replacing from the north the air mass with higher TGM

concentration. According to the radiosonde vertical soundings this entire flight leg was within the mixing layer in a humid air mass. During the return level flight at 2,500 m a.s.l., free tropospheric extremely dry air mass was encountered with an average TGM concentration of 1.64 ± 0.1 ng m^{-3} (n=22). The average TGM concentration at 900 m a.s.l. was with 1.77 ± 0.1 ng m^{-3} (n=17) slightly higher. This small difference can more likely be attributed to the different air masses rather than a systematical vertical gradient.

Two southernmost TGM measurements at the return flight with 2.20 ± 0.3 ng m^{-3} (n=2) differed substantially from the rest of the flight. But they agreed with the TGM concentration of 2.32 ± 0.1 ng m^{-3} (n=8) measured at the same time at the summit of the Wank mountain. These higher TGM concentrations south of Munich can be attributed to a warm humid air mass just south of the approaching cold front. Two day backward trajectories starting at the Wank mountain and at Frankfurt in central Germany were calculated for 840 and 925 mbar, respectively, corresponding approximately to the altitude of the Wank summit and the flight altitude of 900 m a.s.l., respectively. The backward trajectories starting at the Wank mountain point to slow transport of the air mass over France and Central Europe. In contrast, those starting at Frankfurt show a fast transport from the North Atlantic. Thus higher TGM concentrations south of the cold front are consistent with the different origin and transport of the air masses south and north of the cold front.

6.2.3 Results of Vertical Profiling Measurements up- and downwind a Partly Inactivated Chlor-Alkali Plant

At the northernmost point of the flight, approximately 5 km upwind and downwind of the chlor-alkali plant at Schkopau a spiral ascent from 400 to 3760 m a.s.l. and descent, respectively, were carried out. An aerial view of the plant is shown in Figure 6.13.

Figure 6.13: Aerial view of BSL Werk Schkopau from an altitude of approximately 2500 m a.s.l.

The vertical profiles of the TGM concentrations are shown in Figure 6.14. Upwind of the plant, the TGM concentration was with 1.76 ± 0.1 ng m^{-3} (n=14) independent of altitude. Downwind of the factory, higher TGM concentrations with 2.02 ± 0.2 ng m^{-3} (n=5) were observed below 1660 m a.s.l. than upwind of the factory. Above this altitude the TGM concentrations with 1.64 ± 0.1 ng m^{-3} (n=10) were comparable with those measured upwind. The vertical distribution of TGM concentrations downwind of the factory was consistent with radiosound profiles at Meiningen and Wahnsdorf indicating that the mixing layer at Halle may have reached an altitude of about 1,650 m a.s.l.

The difference between downwind and upwind TGM concentrations can be used to estimate roughly the mercury emissions at the factory. The width of the factory area normal to the wind direction was approximately 1.5 km. The factory is located at an altitude of 130 m a.s.l. and the mixing height is assumed to be 1,660 m a.s.l. Weather map yields a surface wind speed of approximately 10 m s^{-1} and an air temperature of 13 °C for the region Leipzig/Halle.

Assuming that TGM concentrations are evenly distributed over the width of the factory area and that the entire sounding spiral was within the factory plume, the mean difference of TGM concentrations in the mixing layer then results in emission of about 0.4 kg of mercury per day.

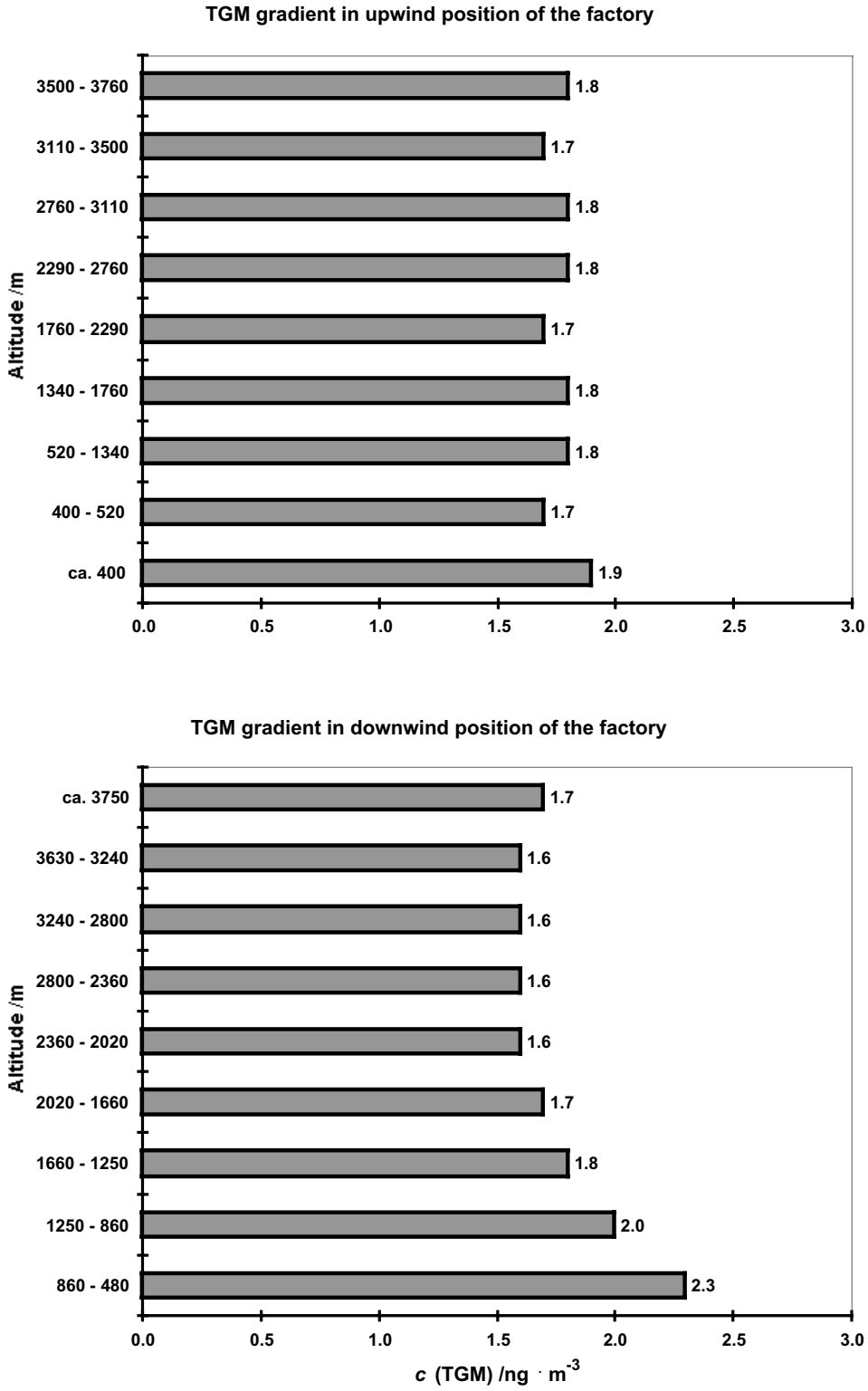

Figure 6.14: Vertical profiles of the TGM concentrations upwind and downwind of the chlor-alkali plant at Schkopau near Halle, 13 June 1996

In summary, aircraft TGM measurements made on June 13, 1996, show that a) TGM is evenly distributed within an air mass over long distances, b) TGM concentration may change with the change of air mass, and c) slight difference between TGM concentration in the mixing layer and the free troposphere may be due to the different air masses rather than a vertical gradient. These observations are consistent with long term TGM measurement at the summit of Wank mountain (Slemr, 1996; Slemr and Scheel, 1998). As reported by Slemr (1996), TGM concentrations are usually constant over a period of several days and change with the change of air mass. No pronounced diurnal variation of TGM concentrations (larger than the precision of the TGM measurements of 5.8%) was observed at the Wank summit, despite of the diurnal cycle of upslope winds during the day and downslope winds during the night. This observation points to the lack of pronounced vertical gradients in TGM concentrations (Slemr, 1996). Thus the observations of temporal TGM variability at one site are in excellent agreement with the aircraft observations of spatial TGM variability at a given time, reported here. The observations of temporal variability at the Wank summit and spatial variability are also consistent with the generally accepted, long residence time of elemental mercury, the dominating TGM component, in the atmosphere.

Our aircraft measurement of the spatial variability of TGM concentrations over Germany reported here, the observations of temporal variability at the Wank summit (Slemr, 1996) and older aircraft TGM measurements (Slemr et al., 1985) differ from almost all other aircraft TGM measurements which reported pronounced vertical gradients in TGM concentrations (Ionov et al., 1976; Kvietkus et al., 1985; Brosset, 1987; Kvietkus, 1995). Experimental details given by this reports do not allow any conclusion about the pressure dependence of the instruments used in these measurements. Further TGM measurements onboard aircrafts are needed.

From measurements of TGM concentrations upwind and downwind of the former chlor-alkali plant at Schkopau we derived an emission of about 0.4 kg mercury per day on June 13, 1996. The largest uncertainty of our estimate is probably connected with the assumption about the sampling of the plant plume. The diameter of a full turn during the spiral descent downwind of the plant was about 2.5 km, almost twice the 1.5 km diameter of the plant area. Consequently, TGM measurement includes also air outside of the plume. The sampling of the plume and its surrounding leads to an underestimation of the TGM concentration upwind/downwind difference and to an underestimation of the TGM emission. Krüger et al. (1999) investigated the mercury emissions by the plant in 1993 and 1994. By combining field measurements with inverse dispersion model simulations they estimated that 1.5 – 3.5 kg of mercury was emitted per day on June 14, 1994. In view of the uncertainty described above and the time lapse from 1994 to 1996, both estimates are in reasonable agreement.

7 Global Transport of Anthropogenic Contaminants to Polar Regions and Ecosystems

The polar ecosystems are generally considered to be one of the last pristine regions of the earth. The Arctic, for example is populated by few people, has minimal commercial fishing, little industrial activity, and is therefore imagined to be relatively unaffected by local human activity. These generalizations hold true for most of the Arctic except for highly industrialized regions of the Russian Arctic including the Kola Peninsula, Pechora and Ob/Yenisey river basins (Bard, 1999). In comparison with the Arctic, Antarctica is considered to be much less affected by any kind of anthropogenic influences resulting in even more pronounced pristine characteristics.

Growing evidence indicates, however, that there has been long-distance atmospheric transport of anthropogenic contaminants from mid- and low latitude sources to the polar regions (Bard, 1999 and references therein). Three major pollutant groups are of growing concern:

- acidifying gases (SO_x) from Eurasian smelters and industry (Barrie et al., 1989),
- heavy metals from fossil fuel combustion and mining (Akeredolu et al., 1994) and
- persistent organic pollutants (POPs) including pesticides used in agriculture and polychlorinated biphenyls leached from electronic transformers (Muir et al., 1992).

Long-range transport of atmospheric pollution has led to bioaccumulation of these compounds by plankton (Bidleman et al., 1989). Contaminants biomagnify through the marine food chain to levels in top predators, including humans, which may have adverse physiological effects (Dewailly et al., 1989; Bacon et al., 1992).

Generally, air pollution is not confined to local areas and can be atmospherically transported tens of thousands of kilometers to remote regions such as the polar ecosystems. The winter phenomenon of "ice crystal haze" observed by K.R. Greenaway during 1940s surveillance flights and later coined "Arctic haze" (Mitchell, 1956) was discovered not to be wind-blown dust, but air pollution from the mid-latitudes (Kerr, 1979; Barrie and Bottenheim, 1991). Arctic haze is a mixture of aerosols containing acidifying SO_x and NO_x, coarse particles of soot, heavy metals, polycyclic aromatic hydrocarbons (PAH), and polychlorinated biphenyls (PCB) (Iversen and Joranger, 1985; Halsall et al., 1997; Stern et al., 1997).

Arctic haze is concentrated in the lower troposphere (up to 3 km altitude) and is most pronounced during the coldest months of the year from December to April (Pacyna, 1995). The seasonal cycle of anthropogenic emissions (e.g. April–June agricultural pesticide application) cannot adequately explain the distinct annual cycle of Arctic air pollution.

Iversen and Joranger (1985) proposed that a quasi-stationary, large-scale, meteorological phenomenon known as "blocking" is responsible for the seasonality of the pole-ward transport of pollutants. Episodically, mid-latitude source areas undergo periods of atmospheric stagnation due to the blocking of the westerlies by anticyclones (Dastoor and Pudykiewicz, 1996). The resultant stagnant weather conditions reduce contaminant scavenging potential and thus permit accumulation of pollutants over the source areas. If a cyclonic sytem approaches the blocking high, a strong pressure gradient builds and forces northward transport of contaminated air. The transport path may persist long enough to permit the pollutants to be swept into the Arctic troposphere (Weller and Schrems, 1996). By using tracer aerosols it was demonstrated that particles could be transported from the source to the pole within 7 to 10 days (Raatz and Shaw, 1984). Other studies have demonstrated that polluted air masses can reach the Arctic within 48 to 72 hours (Oehme, 1991).

The occurrence of blocking highs corresponds well to observed seasonal variations of Arctic air pollution (Iversen and Joranger, 1985). Rapid changes in circulating systems are responsible for the episodic nature of Arctic aerosol pollution (Lejenäs and Holmén, 1996). The geographic position of blocking highs seasonally favors different sources. Eurasian sources, which are more available to the Arctic than North American emission sources, account for more than 50 % of Arctic air pollution (Barrie, 1986). During winter, the strong Siberian anticyclone drives air from central Eurasia into the Arctic which then moves either over North America or into major anti-cyclonic regions in the Aleutians and near southern Greenland (Barrie et al., 1992). During the spring, the Siberian high-pressure cell dissipates and western Eurasia makes the greatest contaminant contribution to the Arctic. During summer, there is a weak north to south transport alternating with input from the north Pacific and the north Atlantic (Barrie et al., 1992).

Volatile contaminants from mid- and low-latitudes reach the Arctic through a process known as "global distillation" (Goldberg, 1975). Many of the developing countries which still use environmentally persistent pesticides, for example, are located in the tropics. This region is characterized by elevated temperatures and heavy rainfall which promotes the rapid dissipation of contaminants through air and water (Tanabe et al., 1994). Contaminants evaporate from soils of these warm regions and become available for atmospheric transport poleward where they condense out in the colder air (known as the "cold finger" (Ottar, 1981) or "cold condensation" effect (Wania and Mackay, 1993). The sorption of high molecular weight organic vapors to atmospheric particulate matter is enhanced by low temperatures (Bidleman et al., 1989). The theory of "global fractionation" describes how the most volatile contaminants, such as PCB and HCH, travel to the highest latitudes, while less volatile compounds, such as DDT, are less readily distilled and tend to remain near their source region

(Simonich and Hites, 1995). Thus the volatile contaminants are apt to condense in the coldest Northern and Southern regions and since these areas are a comparably small proportion of the Earth's surface, these contaminants can concentrate to surprisingly high levels in the polar ecosystems.

Contaminants can be transported by one-hop or multi-hop pathways. One-hop describes the transport of a contaminant which enters the atmosphere in the source region, is directly transported to the polar regions and is deposited the Earth's surface without returning to the atmosphere. Contaminants transported by one-hop pathways include involatile organochlorines, e.g. DDT, less volatile PAHs, e.g. benzo[a]pyrene, acids; and heavy metals with the exception of mercury (Barrie et al., 1997). In contrast, multi-hop contaminants undertake multiple atmospheric hops. Such chemicals include mercury and the more volatile organochlorines and PAHs (Barrie et al., 1997).

Once contaminants reach the polar regions, their lifetime in the troposphere depends on local removal processes. Pollutant removal processes are inefficient in those regions especially during the winter due to low temperature, low solar radiation input, and low precipitation, thus low scavenging by wet deposition (Barrie, 1986; Weller and Schrems, 1996). As a result, compounds which would be photodegraded in warmer climates may persist in the polar regions. Eventually aerosol pollutants enter the terrestrial, aquatic and marine environments by gas-exchange across the air-seawater interface or deposition of particles with adsorbed pollutants. Detection of tropical pesticides and other contaminants in remote Canadian and Alaskan freshwater lake and aquatic animals supports the atmospheric transport theory (Lockhart et al., 1992; Wilson et al., 1995).

7.1 Global Distribution of Atmospheric Mercury

Long-range atmospheric transport of mercury, its transformation to more toxic methylmercury compounds and the substantial bioaccumulation mainly in the aquatic foodchain have motivated intensive research on mercury as a pollutant of global concern. A low aqueous solubility and chemical reactivity of elemental mercury (Hg^0), which is by far the dominating component of total gaseous mercury (Slemr et al., 1985; Schroeder and Jackson, 1985) are the major reasons for its long atmospheric residence time permitting long-range atmospheric transport of mercury to regions far from centers of anthropogenic activity, for example the Atlantic and Pacific Oceans and the Arctic (Boutron et al., 1998, Schroeder et al., 1995; Slemr, 1996, Mason et al., 1992; Ebinghaus et al., 1995).

The long average lifetime of elemental mercury in the atmosphere of about one year would allow homogenous mixing at least within one hemisphere however, complete global mixing would need longer time scales. Since anthropogenic sources of mercury emissions into the atmosphere are mainly located in the northern hemisphere a concentration gradient between the two hemispheres should be expected, provided that the lifetime estimate is correct.

Between 1977 and 1980 Franz Slemr and co-workers have carried out several ship cruises with TGM measurements over the Atlantic Ocean (Slemr et al., 1985). During these campaigns the traditional manual methods with a time resolution of approximately 24 hours have been applied.

Later on these measurements have been repeated in 1990 and 1994 with essentially the same measurement technique along the same route and during the same seasons. The data obtained by Slemr et al. (1985; 1996) are summarized in Table 7.1.

Table 7.1: Summary of TGM Concentration Measurements over the Atlantic Ocean between 1977 and 1980 (adopted from Slemr et al., 1985)

Cruise	Latitude	TGM concentration ng m^{-3} range	TGM concentration ng m^{-3} mean	Standard deviation ng m^{-3}	Number of samples
Northern hemisphere[a]					
October 1977	11 - 30°N	1.0 - 2.6	1.763	0.362	62
Nov./Dec. 1978	5 - 51°N	1.42 - 2.70	1.849	0.306	89
Jan./Feb. 1979	21 - 53°N	1.63 - 3.06	2.169	0.382	52
Oct./Nov. 1980	12 - 54°N	1.41 - 3.41	2.085	0.351	100
Oct./Nov. 1990	7 - 54°N	1.41 - 3.41	2.247	0.409	117
Oct./Nov. 1994	6 - 54°N	1.31 - 3.18	1.788	0.410	101
Southern hemisphere[b]					
October 1977	32°S - 11°N	0.8 - 1.7	1.187	0.249	64
Nov./Dec. 1978	23°S - 3°N	0.86 - 1.85	1.350	0.207	63
Jan./Feb. 1979	2°S - 4°N	1.07 - 2.09	1.259	0.216	37
Oct./Nov. 1980	34°S - 11°N	1.10 - 1.89	1.453	0.157	82
Oct./Nov. 1990	48°S - 7°N	0.86 - 2.44	1.497	0.295	158
Oct./Nov. 1994	46°S - 6°N	0.82 - 2.13	1.180	1.167	165

[a]North of the intertropical convergence zone (ITCZ)

[b]South of the ITCZ

A concentration gradient between the two hemispheres is obvious from the data obtained by Slemr et al. (1996) supporting the estimate of an average atmospheric lifetime of atmospheric mercury of about one year. This unique data set has also been used for the estimation of global trends in the atmospheric mercury concentrations. However, due to the technical limitations connected with the traditional manual methodology the standard deviation is fairly high. Additionally, the temporal and consequently the spatial resolution is very much limited by the average sampling time of about one day taking into account the average traveling velocity of *RV Polarstern* of about 15 knots.

In December 1999 we have installed an automated mercury vapor analyzer (Tekran Model 2537A) onboard the *RV Polarstern* during the cruise from Bremerhaven, Germany to Cape Town, Republic of South Africa. After a stopover of a few days in Cape Town, the ship went southwards for Neumayer station which takes about 12 days.

The course plot of the *RV Polarstern* during the cruise ANT XVII/ 1 is shown in Figure 7.1.

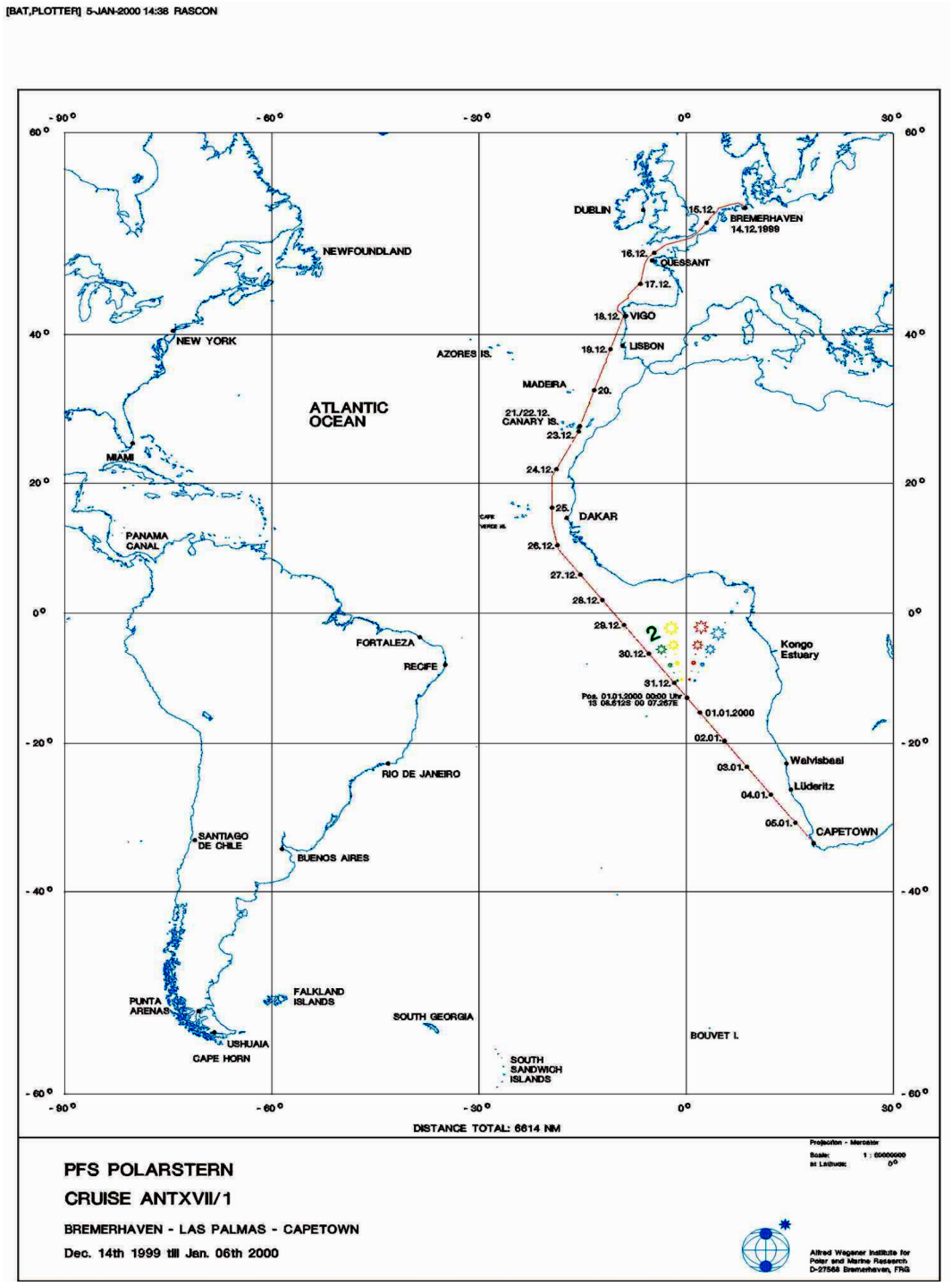

Figure 7.1: Cruise plot of *RV Polarstern* during ANTXVII/1, December 1999 to January 2000

The Tekran Analyzer has been installed in a laboratory container on top of the upper front deck of *RV Polarstern*. The sample inlet was mounted on a mast in front of the container to minimize the risk of contamination. Additionally, the sample inlet was protected from rain and sea water impact. The set up onboard is depicted in Figure 7.2.

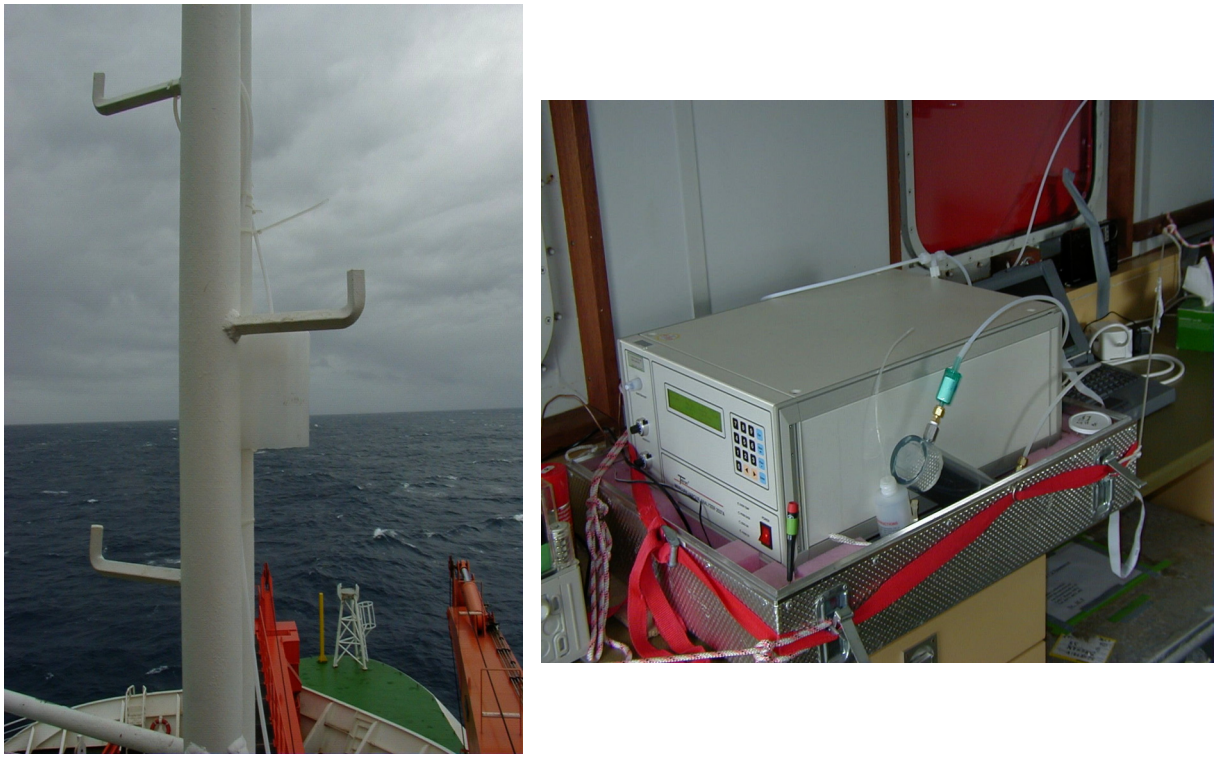

Figure 7.2: Analytical set up for TGM measurements during *RV Polarstern* cruise ANTXVII/1

The Tekran Analyzer was operated on a 15 minutes time base. Wind direction measurements were carried out routinely to identify contamination periods where the sample inlet could have been impacted by the plume of the ship. Especially before the stopovers in Vigo, Portugal, the Canary Islands and Cape Town this effect was observed.

The results of the TGM measurements onboard *RV Polarstern* are shown in Figure 7.3

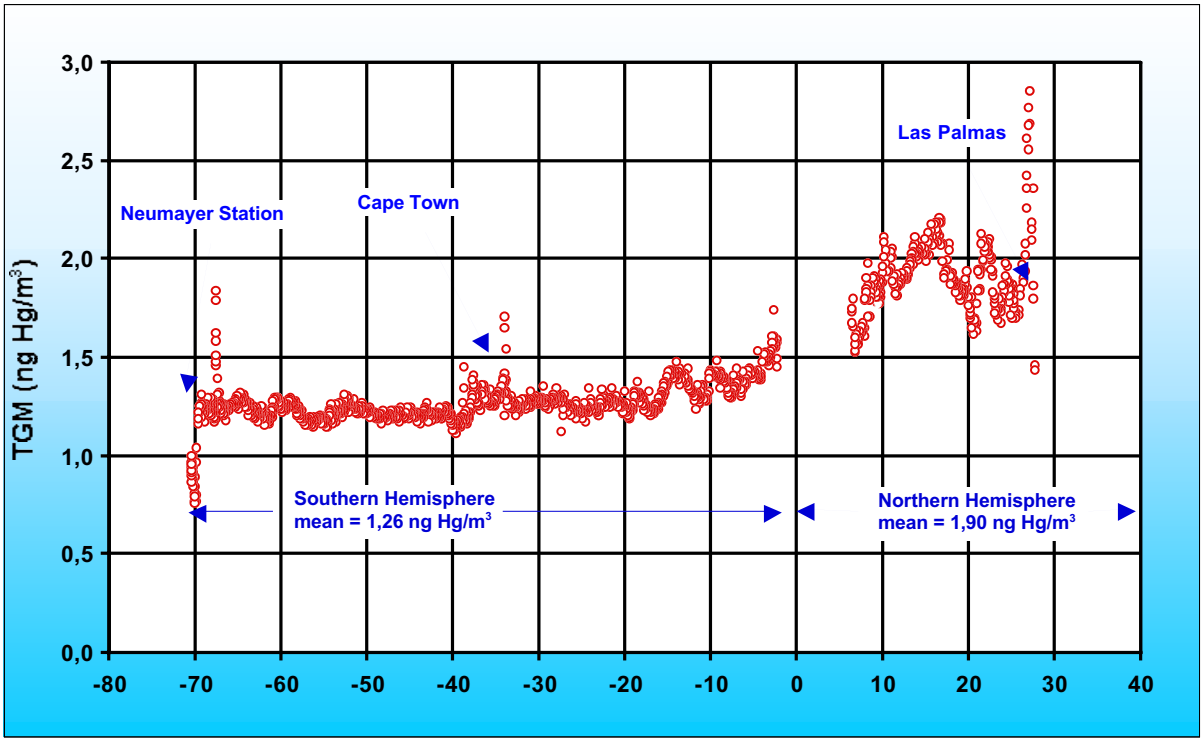

Figure 7.3: Interhemispheric TGM measurements onboard *RV Polarstern* between 30° North (Las Palmas) and 70° South (Neumayer Station), the x-axis gives the latitude in degrees

From Figure 7.3 a significant concentration gradient between the two hemispheres can be derived as earlier shown by Slemr et al. (1996). A Northern hemispheric mean of 1.9 ng m^{-3} corresponds with a Southern hemispheric mean value of 1.26 ng m^{-3}, which is about 34 % less. The mean TGM concentrations measured during the cruise in the Northern hemisphere are slightly higher than the long-term average concentrations measured at Mace Head which are around 1.75 ng m^{-3}. The variability of concentrations is quite large between Las Palmas (30° North) and the equator. Due to an instrument failure no measurement data are available between 5° North and 3° South.

Between 10 and 70° degrees South TGM concentrations are very evenly distributed and remain fairly constant at around 1.3 ng m^{-3}. Different variability and an interhemispheric concentration gradient of TGM support the lifetime estimate of about 1 year.

7.2 Phenomenon of Spring Time Mercury Depletion Events in Polar Regions

The background concentration of total gaseous mercury (TGM) in the lower troposphere of the northern hemisphere is generally around 1.8 ng m^{-3} and 1.3 ng m^{-3} in the southern hemisphere respectively (Slemr, 1996; this work). Long-term studies, such as the measurements at Mace Head and ship cruises show only very few and short periods with concentrations below these background values.

Recently, highly time-resolved TGM measurements in the Arctic have shown that lower tropospheric TGM levels are significantly depleted, while mercury concentrations in snow are concurrently increased during the three months after polar sunrise (Schroeder et al., 1998; Lu et al., 2001; Lindberg et al., 2001). A possible explanation may involve chemical or photochemical oxidation of Hg^0 to Hg^{2+} (resulting either in particle-associated mercury (Hg_{part}) and/or reactive gaseous mercury (RGM) species) and significantly enhanced deposition fluxes of mercury leading to unequivocally increased input of atmospheric mercury into the Arctic ecosystem (Schroeder et al., 1998). The Arctic TGM depletion is strongly correlated with ground-level ozone concentrations. These tropospheric ozone loss events in the Arctic are associated with enhanced bromine monoxide concentrations in the free troposphere (Platt and Wagner, 1998). It is hypothesized that Br atoms and/or BrO radicals are involved in a chemical reaction which destroys ozone (McElroy et al., 1999) and that the depletion of surface-level atmospheric boundary layer mercury (at times up to an altitude of ≈ 1 km) is due to a reaction between gaseous elemental mercury and BrO free radicals (Boudries and Bottenheim, 2000). Figure 7.4 shows the proposed reaction scheme for the decomposition of ozone and the subsequent transformation of gaseous elemental mercury into inorganic species that will deposit more rapidly onto terrestrial and/or marine surfaces.

Recent studies have reported short-term boundary layer ozone depletion events for the Antarctic (Wessel et al., 1998). At Neumayer and relative to the beginning of spring in both hemispheres the ozone depletion events occur 1-2 months earlier than in the Arctic, are less frequent and of shorter duration (Lehrer, 1999). Strong and sudden increases in the tropospheric BrO mixing ratio during spring were also found for the Antarctic obtained by Differential Optical Absorption Spectrometry (DOAS) measurements (Kreher et al., 1997) and observations from satellite instruments (Platt and Wagner, 1998; Hegels et al., 1998). *Friess* (2001) documented that the numerous strong and sudden enhancements of BrO detected during August and September 1999 and 2000 at Neumayer are caused by BrO located in the lower troposphere, released by well known autocatalytic processes on acidified sea salt surfaces. The strong depletion of near surface ozone is caused by catalytic cycles involving bromine (Fries, 2001).

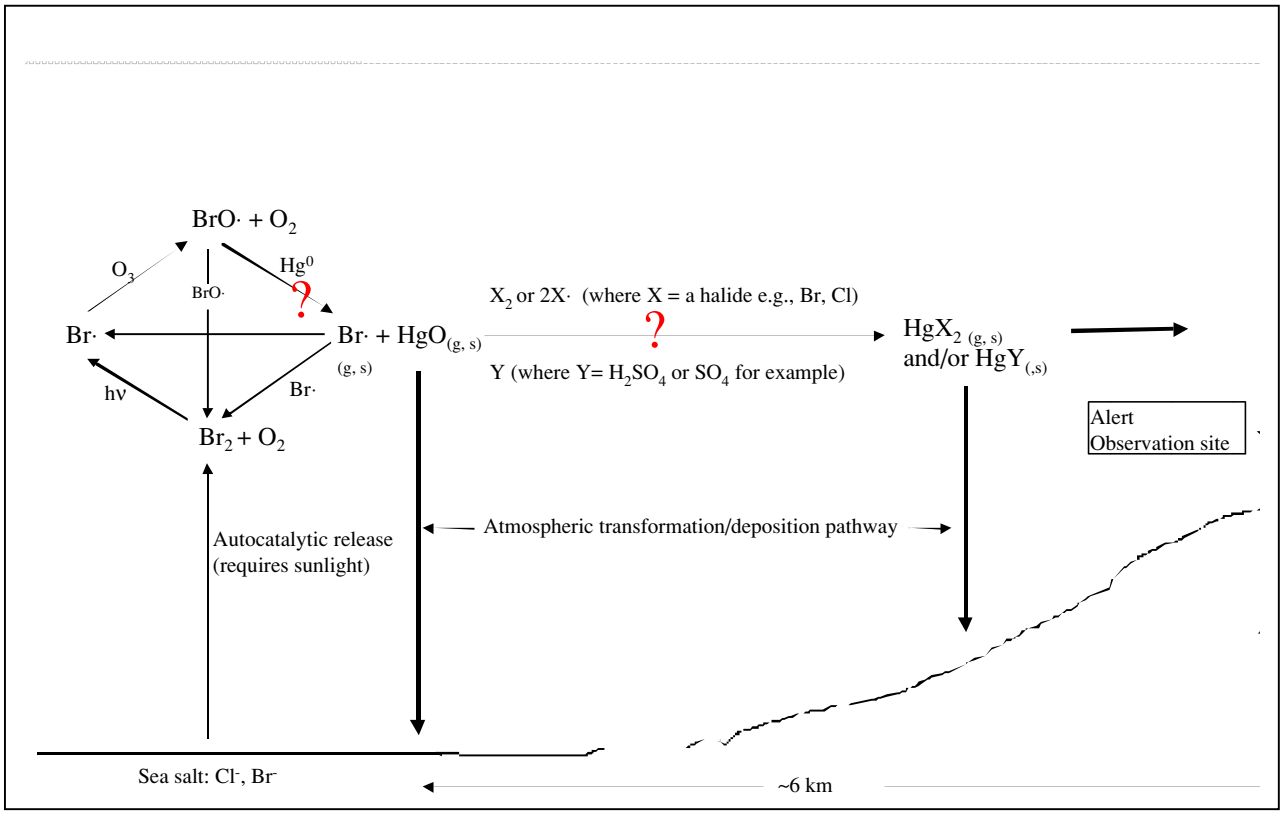

Figure 7.4: Proposed reaction scheme for the explanation of mercury depletion events in the Canadian Arctic according to Schroeder et al.

The reaction scheme shows that bromine molecules can be autocatalytically released from sea ice and sea salt when UV-intensity is sufficient. Sunlight also decomposes Br_2 into bromine radicals that immediately reacts with boundary layer ozone resulting in bromine oxide

radicals and oxygen molecules. These reactions have been described in the literature. It is then proposed that elemental mercury is oxidized by bromine oxide. Resulting mercuric oxide can be readily deposited or reacts with abundant halogens or sulfuric acid to form the respective mercuric halides or sulfates.

Although the exact speciation of the resulting mercury compound is not yet known it can assumed that gaseous elemental mercury is transformed into species with a much higher dry deposition velocity, such as RGM and/or particulate phase mercury. Consequently, during MDEs would lead to enhanced deposition fluxes into the Arctic ecosystem in the very sensitive period of polar spring. This hypothesis has been experimentally supported by the analysis of surface snow samples in Alaska and the Canadian Arctic (Lindberg, 2001; Lu et al., 2001).

7.3 TGM Measurements at the German Antarctic Research Station Neumayer

Data on atmospheric mercury concentrations in the Antarctic are extremely limited and no knowledge exists on the short-term variability during the time period after antarctic polar sunrise.

The measurements reported here comprise the first annual time-series of TGM concentrations in the Antarctic in order to investigate the occurrence of possible mercury depletion events (MDEs) in south polar regions. This study also provides the first-time high resolution data of total gaseous mercury concentrations in the Antarctic that can be compared with existing data sets of MDEs in the Arctic to reveal similarities and varieties in the temporal and quantitative sequence of mercury depletion events after polar sunrise.

In the period from January 2000 to January 2001 highly time-resolved measurements of TGM with a sample integration time of 15 minutes were carried out at the German Antarctic research station Neumayer, operated throughout the year by the Alfred Wegener Institute for Polar and Marine Research, Bremerhaven. The geographic location of Neumayer Station is illustrated in Figure 7.5.

Figure 7.5: Location of the German Neumayer Station. The distance to the South Pole is approximately 2000 km

The site is located at 70°39'S, 8°15'W, on the Ekströmisen, about 8 km from Atka Bay. At Neumayer the maximum solar incidence angle is 42.8°. The sun stays permanently above the horizon from November 19th to January 24th and permanently below the horizon from May 19th to July 27th. The analysers were installed at the Neumayer Air Chemistry Observatory (ACO), which is approximately 1.6 km south of the main site. The new observatory (since January 1995) was designed as a container building placed on a platform some metres above the snow. It is used as a large clean air laboratory to study one of the undisturbed parts of the earth's troposphere. Local pollution by vehicles and the base itself is a potential problem for many measurements concerning the background status of the Antarctic troposphere. But due to the fact that the prevailing wind directions are from the east and northern wind directions are very rare, contamination from the base can be excluded most of the time. Nevertheless, supplementary control of the contamination situation is done (wind direction, wind speed, condensation nuclei, snow drift, PAH concentration).

Figure 7.6 shows a view of the Neumayer Air Chemistry Observatory (ACO).

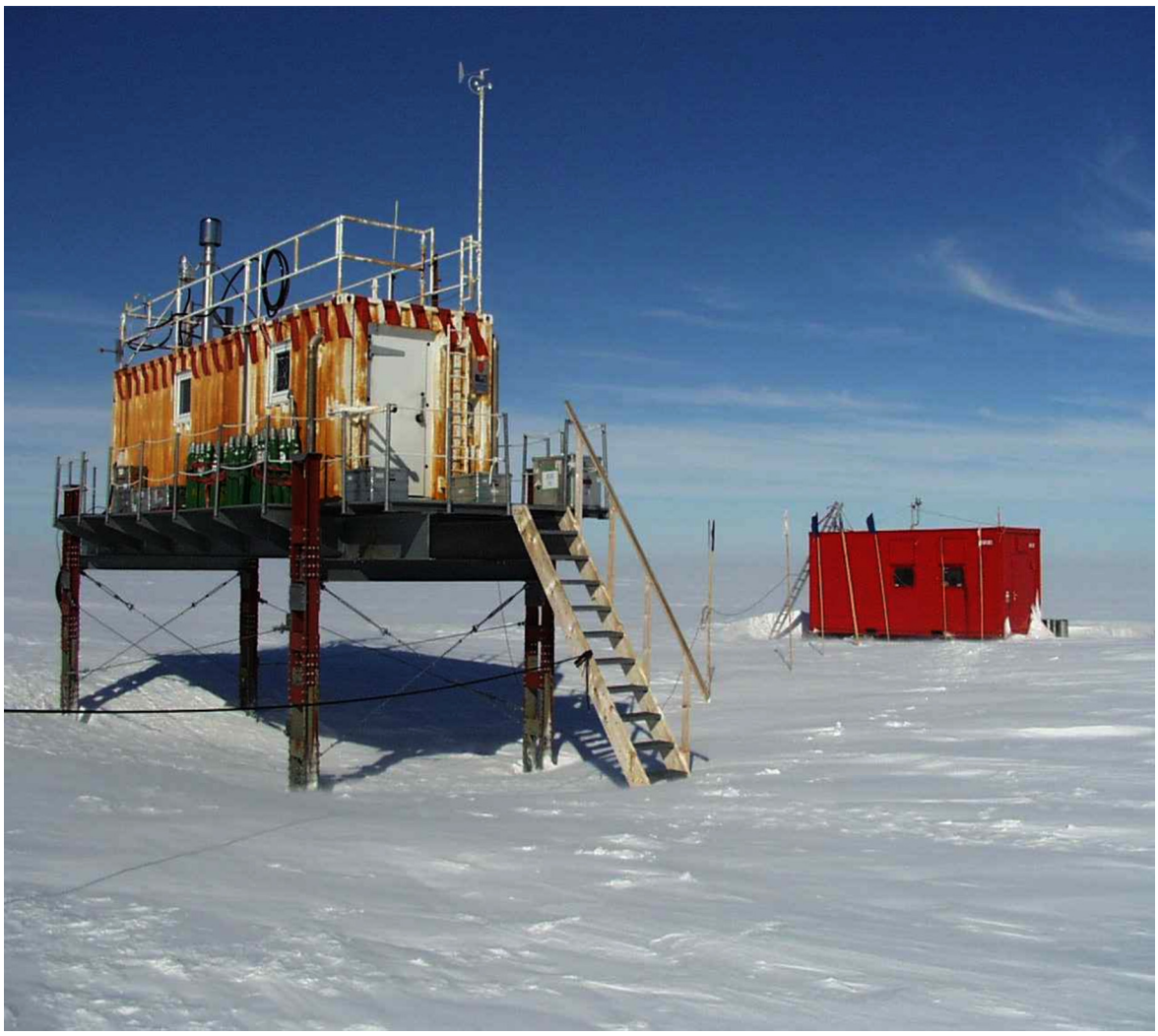

Figure 7.6: The Neumayer Air Chemistry Observatory (ACO) at Neumayer Station, the Tekran instruments were installed in the permanently operated container in front

Two Tekran gas-phase mercury vapour analysers (Model 2537A) were installed at Neumayer Station in January 2000. The set-up, accuracy and precision of this instrument has been assessed during field intercomparisons at an urban/industrial site (Schroeder et al., 1995) and at a remote marine background location (Ebinghaus et al., 1999). The Tekran analysers were operated with a 15-minute integrated sampling frequency. The sample inlet with a drift protection (no filter) was located 6 m above the snow surface on top of the ACO. The air was sampled at a flow rate of 1.0 L min^{-1} through a heated Teflon line about 10 m in length. Each Tekran analyser had its own Teflon tube running through the same heated sample line and ending up wuth a 0.45 µm PTFE filter in front of the inlet of the analyser. The analysers were calibrated every 25 hours with an internal automatic permeation source injection. Additional manual injections through the heated Teflon line were carried out to ensure the reproducibility

of the sampling line (see chapter 7.1.1). The detection limit for TGM in this operation mode is better than 0.1 ng m^{-3}.

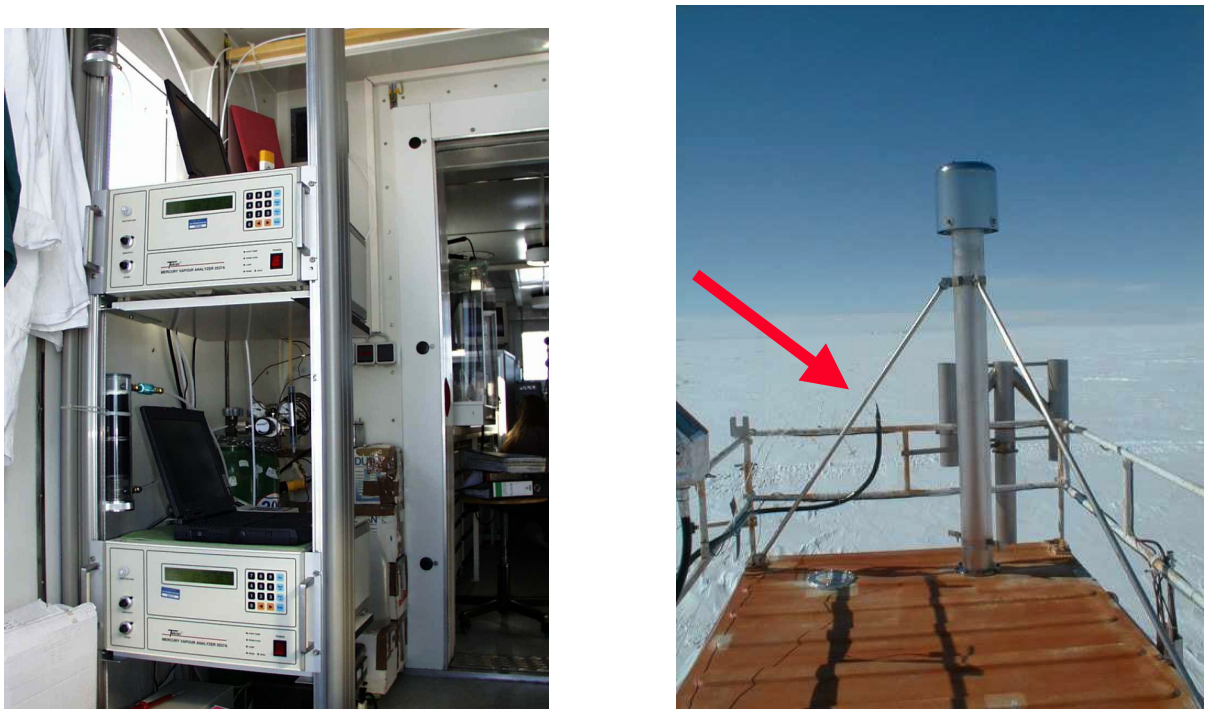

Figure 7.7: Installation of two Tekran instruments inside the trace gas observatory (left), the heated sampling inlet line (marked by the red arrow) was mounted on top of the container approximately 6 m above the snow surface

BrO total density values were generated at the University of Bremen using the DOAS algorithm on operational GOME Satellite (Global Ozone Monitoring Experiment) level-1 data as described in Richter et al. (1998). Both stratospheric and tropospheric BrO contribute to the observed columns. As the spatial and temporal variability of stratospheric BrO is small, all the enhanced BrO values above the Antarctic ice sheet are attributed to large tropospheric concentrations of BrO. Furthermore under both clear and cloudy sky conditions, BrO densities have been observed within the range of typical stratospheric values, whereas significantly enhanced BrO densities were only detected under clear sky conditions, when the spectrometers aboard the satellite were able to measure deep down into the troposphere (Friess, 2001).

Ozone mixing ratios were measured continuously by means of an Ansyco ozone analyser (Model O341M) based on UV-absorption with a detection limit of 1 ppbv.

To ensure the repeatability of the measurements the following sampling protocol was used at Neumayer: For quality assurance, two analysers were operated in parallel for one week. When the correspondence of the two Tekran analysers had been tested and quantified, one analyser started measuring TGM for the next three weeks, the other one was turned off. The next comparison will follow after three weeks as described above. After polar sunrise in August 2000, both analysers were operating in parallel during the time interval between Antarctic springtime and the end of the measurement period. Automated standard additions had been carried out every 8.75 hours over the entire measurement period to check the sensitivity of the signal and therefore the stability of the detector response and the internal permeation source. The accuracy of the measurements was verified by manual injections of a known volume of air from a saturated mercury vapour atmosphere at a known temperature. This procedure was applied before, during and after the analysers were running in the ACO at Neumayer between January 2000 and January 2001. The results are summarized in Table 7.2.

Table 7.2: Comparison of Mean TGM Concentrations Measured from Manual Injections of Mercury Saturated Air with the Calculated Theoretical Value of the Reference Material (Pure Elemental Mercury)

Date	Instrument	n	Calculated theoretical value in ng m^{-3}	Measured mean concentration with 95 % confidence limit in ng m^{-3}	t-test value	95 % t-distribution value (two-sided)
02.12.99 (GKSS)	Tekran 2537A (082) -direct Injection-	7	28.55	29.46 ± 1.46	1.52	2.45
14.02.00 (Neumayer)	Tekran 2537A (082) -Inj. in heated sample line-	3	11.33	11.35 ± 0.45	0.23	4.30
18.07.01 (GKSS)	Tekran 2537A (082) -direct Injection-	10	17.57	17.56 ± 0.37	0.07	2.26
19.07.01 (GKSS)	Tekran 2537A (083) -direct Injection-	10	17.57	17.36 ± 0.39	1.27	2.26

In each case the critical values obtained from a t-table at P = 95 % and the particular degrees of freedom is bigger than the calculated mean from the measured TGM concentrations. There are no significant differences between the theoretical and the measured values.
The results in Table 7.2 confirm the good accuracy of this method. To demonstrate the trueness of the results, further comparative measurements of TGM with two different methods were carried out before the instruments had been set up at Neumayer. One of the analyser was running on board of the *RV Polarstern* on the way from Germany to the Antarctic between December 1999 and January 2000 in order to understand the mercury distribution on a global scale with the background of an interhemispheric gradient (F. Slemr, personal communication). All TGM concentrations obtained onboard of *RV Polarstern* south of the ITCZ (inter tropical convergence zone) were plotted. This TGM measurement results can be compared with TGM data obtained at the same time with a different method at the Global Atmosphere Watch (GAW) station at Cape Point, South Africa, operated by the South African Weather Bureau and the Fraunhofer Institute for Atmospheric Environmental Research, Germany. It is one of the most important measurement sites in the southern hemisphere in order to get information about background concentrations of environmentally important trace gases. Previous studies (Slemr, 1996, Slemr et al., 1995) have shown that total gaseous mercury background concentrations over the Atlantic Ocean in the southern hemisphere are very homogeneous and are about 25 % lower than the northern hemispherical TGM background concentrations.

At this station TGM is collected manually on gold or silver coated quartz wool and analysed by cold vapour atomic fluorescence spectroscopy (CV-AFS). This technique was also validated by an international intercomparison conducted at Mace Head, Ireland, in 1995 (Ebinghaus et al., 1999 and chapter 3 of this work). The comparability of the results obtained in the time period between December 1999 and January 2000 onboard of *RV Polarstern* and at the GAW station Cape Point is shown in Figure 7.8.

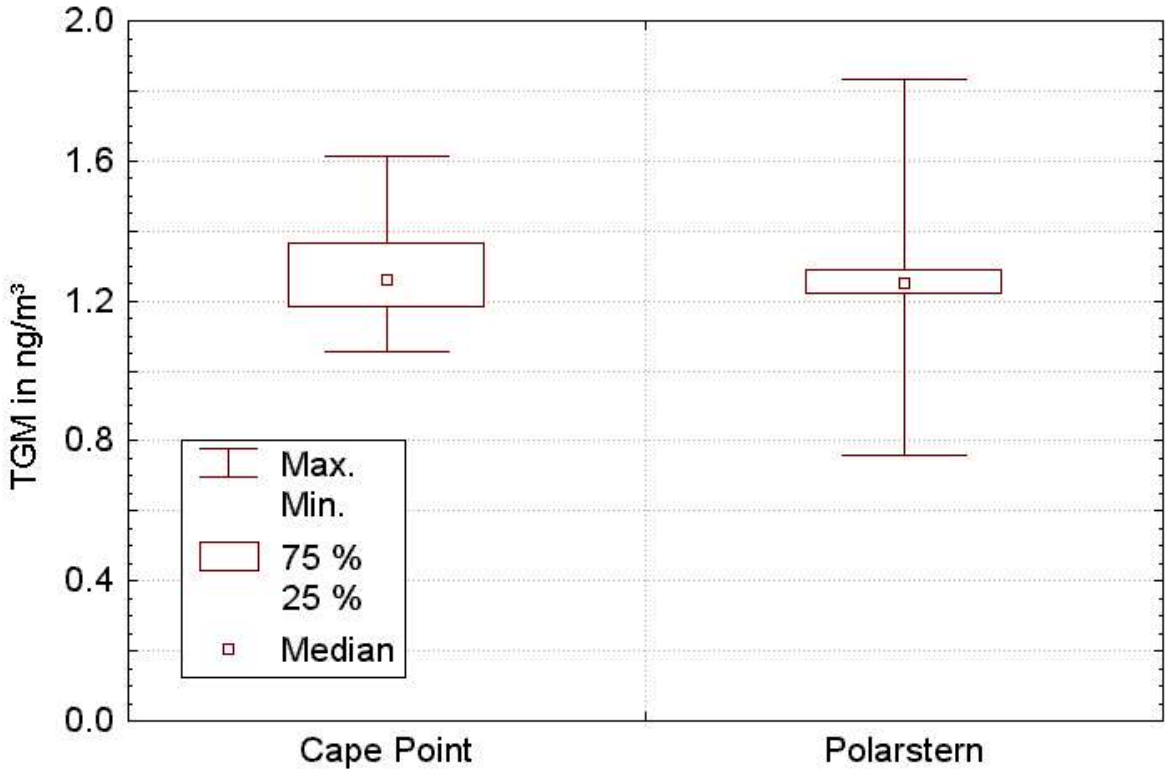

Figure 7.8: Box and Whisker plot representation of the background concentrations of total gaseous mercury measured with two different methods in the southern hemisphere

A robust statistics with a median instead of a mean value is used because the analytical data are contaminated by outliers and conform only broadly to a normal distribution. It can be shown that the results obtained on similar air masses with both methods are in good agreement and therefore it can be considered that the results from each method are true. This intercomparison also prove the homogenous distribution of atmospheric mercury in the southern hemisphere far away from centers of anthropogenic emissions.

Table 7.3 summarizes statistical data from the background concentrations of total gaseous mercury measured onboard of *RV Polarstern* and at Cape Point with two different methods in the southern hemisphere in the time period between December 1999 and January 2000.

Table 7.3: Comparability of the Data Obtained in the Southern Hemisphere onboard of *RV Polarstern* and at Cape Point

Site	n	Median	Min.	Max.	Lower	Upper Quartile	Interquartile Range
Cape Point station (34°S, 18°E)	59	1.26	1.05	1.61	1.18	1.37	0.19
RV Polarstern (2°S – 70°S)	1612	1.25	0.76	1.84	1.22	1.29	0.08

7.4 First Annual Time Series of TGM in Antarctica

The results of TGM measurements and ground-level ozone concentrations for the time period January 2000 to January 2001 are presented in Figure 7.9. The TGM concentrations were obtained from two separate Tekran analysers and mean values were used if both analysers were operating in parallel. The arithmetic mean of all TGM measurements during this time period was 1.06 ± 0.24 ng m^{-3} whereby the complete data set conform only broadly to a normal distribution (Ebinghaus et al., 2002). Ozone concentrations are mixing ratios by volume (1 ppbv = one part per billion by volume) under defined standard conditions.

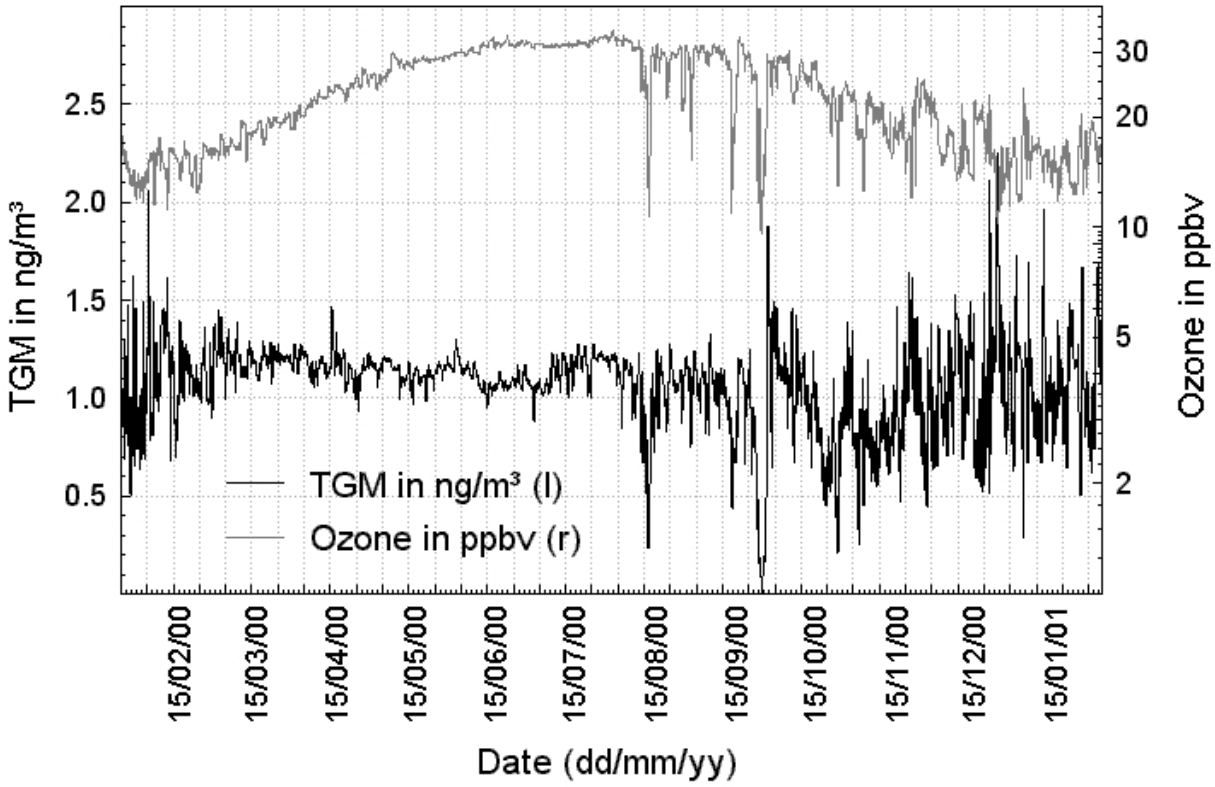

Figure 7.9: First annual time series of 1-hour averaged TGM and surface-level ozone concentrations at Neumayer, January 2000 – January 2001

The TGM data shown in Figure 7.9 can briefly be characterized for three different time periods:

- Between January and February 2000, and December to February 2000/01, TGM concentrations were highly variable. During this time period, TGM and ozone concentrations are frequently negatively correlated. High concentration peaks of more than 2.0 ng m^{-3} can be related to anthropogenic activities near the Air Chemistry Observatory (ACO) during summer campaigns.
- Between March and July 2000 the TGM concentrations remained at a fairly constant level of about 1.2 ng m^{-3} while ozone concentrations constantly increased. This background level of TGM is in good agreement with the average background concentrations in the southern hemisphere, presented in Figure 7.3.
- Between August and November 2000 several simultaneous depletion events of surface-level TGM and ozone were detected with minimum daily average TGM concentrations of about 0.1 ng m^{-3}.

In the following, emphasis should be given on this third period where mercury depletion events occur concurrently with ozone depletions in the troposphere during Antarctic springtime.

The correlation analysis of the complete TGM and ozone dataset from January 2000 to January 2001 yields a very low correlation coefficient of r = 0.09; hence, no linear relationship among these two variables is evident. But the TGM concentration pattern of the third period between August and October 2000 shows a strong positive correlation with ozone as depicted in Figure 7.10.

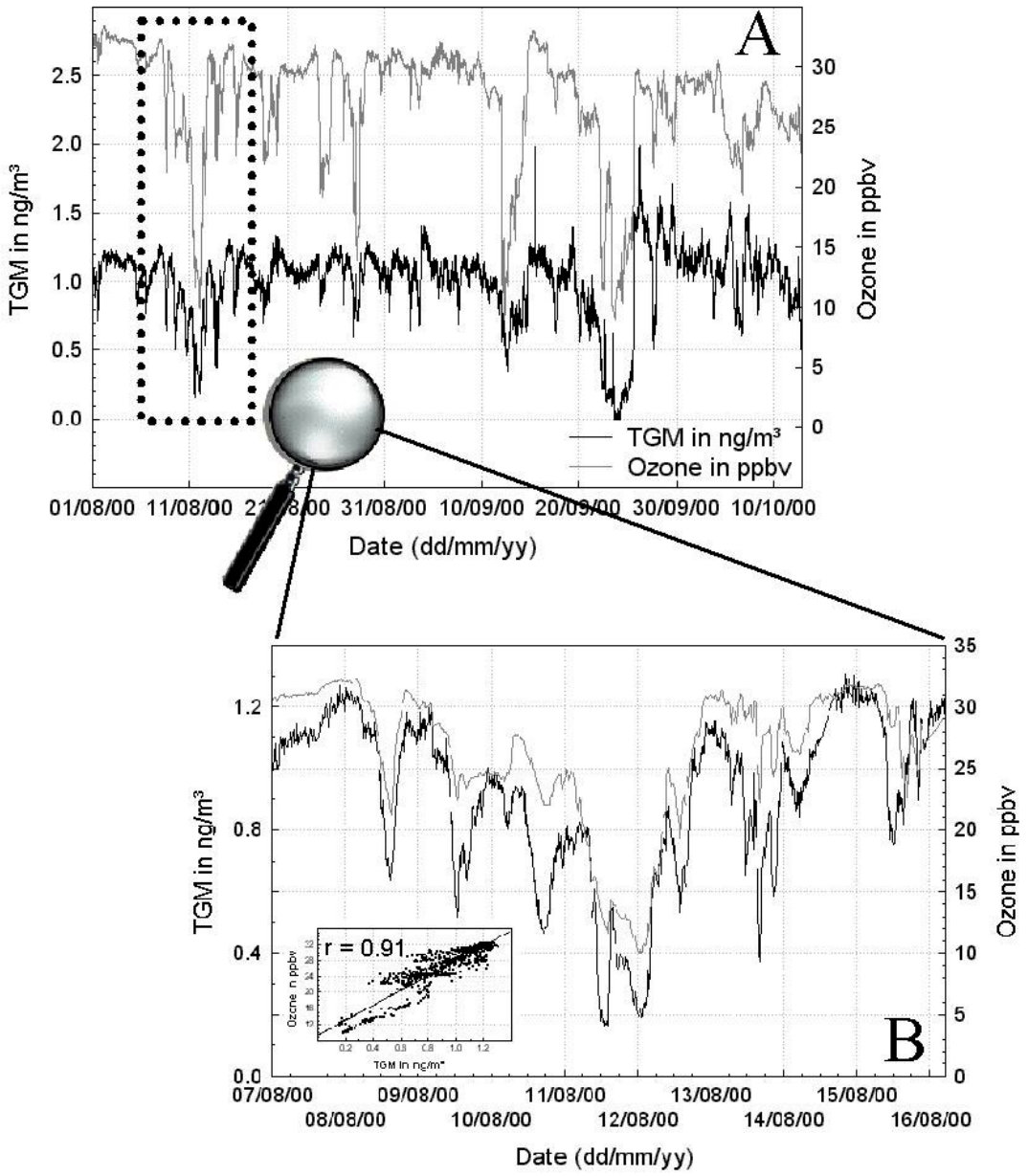

Figure 7.10: Ozone and TGM concentrations during the mercury depletion events (MDEs) from August – October 2000 (A) and for the first event at the beginning of August 2000 (B)

In Figure 7.10 TGM concentrations are mean values from two separate analysers in the highest time resolution (15 min). Ozone concentrations are 15-minute averaged ground level values. Both analysers (ozone and TGM) have been running at the Neumayer Air Chemistry Observatory and have measured concentrations in the planetary boundary layer.

When looking at the scatter plot of the depletion events from the 07th to the 16th of August 2000, a high correlation coefficient of r = 0.91 between ozone and TGM concentrations is obvious.

Statistical analysis of the time series of the entire depletion period between August and November 2000 has revealed a positive correlation coefficient of r = 0.75 (see maximum at lag = 0 in Figure 7.12) between ozone and TGM, which is complementary to the data reported for the Canadian Arctic (Schroeder et al., 1998). However, single depletion events of a few days (Figure 3B) even show a stronger correlation between TGM and surface-level ozone as discussed above.

It could also be shown that mercury depletion events (MDEs) coincide with enhanced occurrence of BrO radicals in the Antarctic atmosphere during springtime as measured from the satellite-based GOME instrument (Figure 7.11).

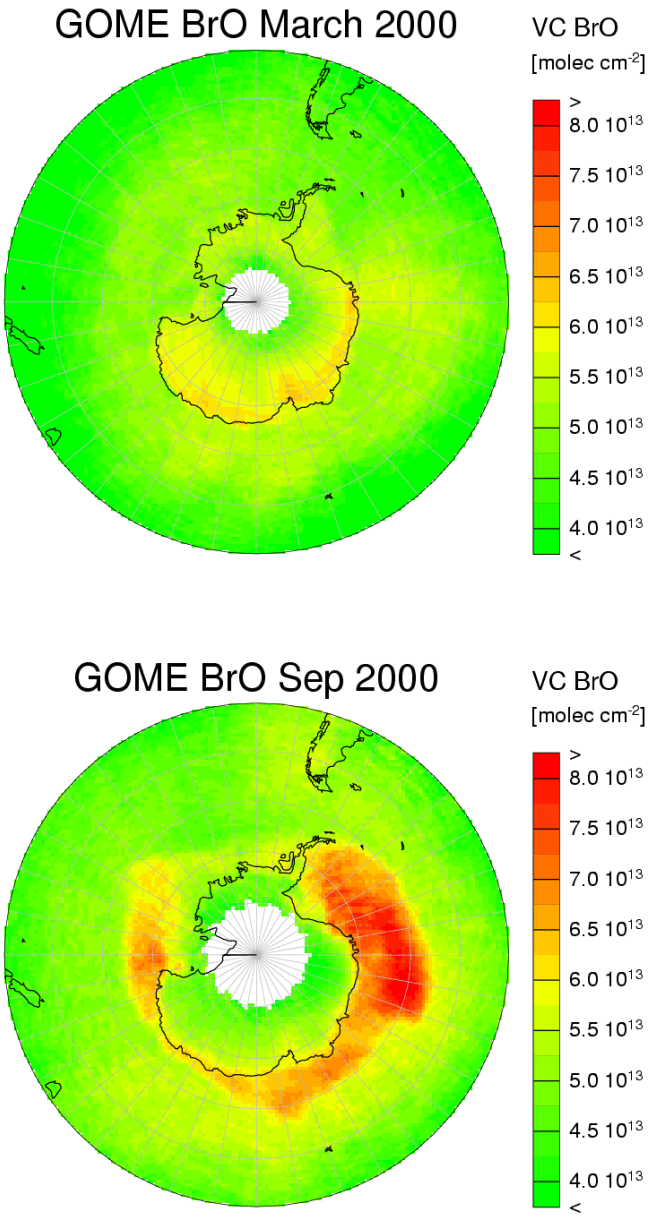

Figure 7.11: GOME (Global Ozone Monitoring Experiment) observations of the BrO vertical column density (expressed as VC BrO in molecules m^{-2}) over the Antarctic from March and September 2000

The GOME satellite pictures show clouds of enhanced BrO above the sea ice surfaces around the Antarctic continent after polar sunrise (September). The areas where elevated tropospheric BrO concentrations build up and decay are clearly visible in the coastal areas around the Antarctic continent (no satellite data are available for the white areas on the map).

It is suspected that air masses at ground originating from the sea ice surface, accompanied by BrO enhancements, could be a necessary prerequisite for the following MDEs at Neumayer Station.

Further statistical analysis has been carried out with the ozone and TGM data obtained during the depletion period between August and October 2000. The cross-correlation function of these two parameters has been calculated by shifting the 4 point moving averages of the measured ozone concentrations with a lag time of 15 minutes against the respective TGM concentration. As mentioned before 15 min is the maximum time resolution given by the operation parameters of the TGM analyzer.
The cross-correlation function is shown in Figure 7.12.

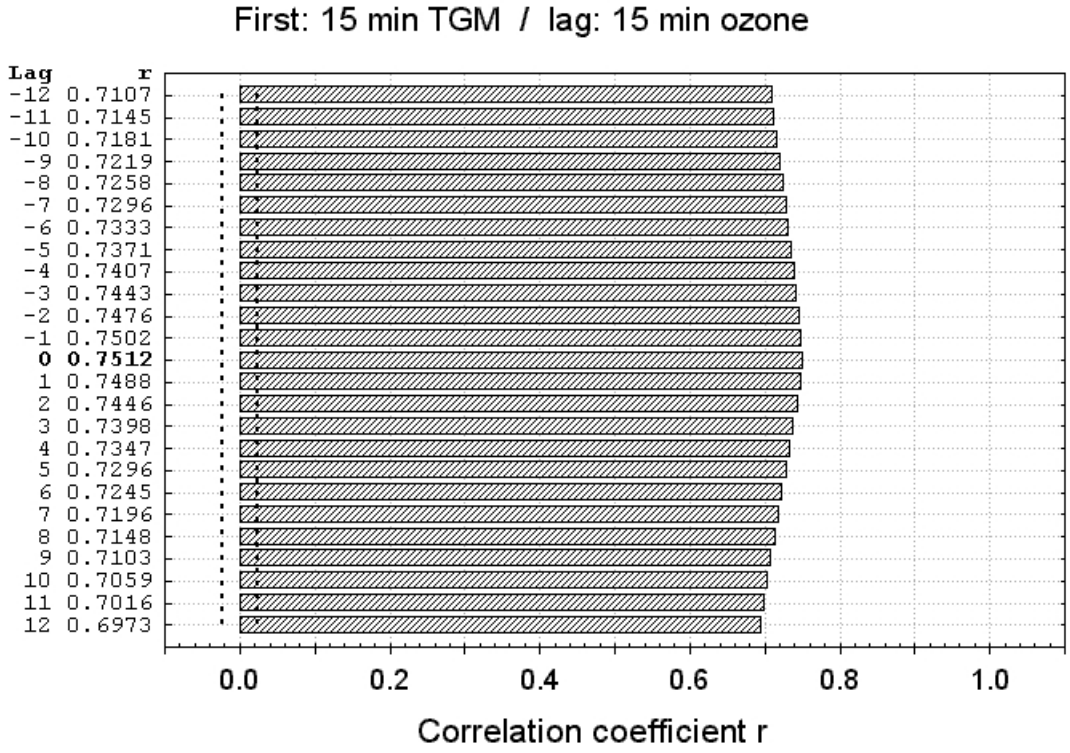

Figure 7.12: Cross-correlation function of TGM (mean values from two separate analysers in the highest time resolution (i.e. 15 min)) and 15-minute averaged ground level ozone concentrations during the mercury depletion events (MDEs)

The maximum in the cross-correlation function of ozone and TGM in the highest time resolution during the depletion events between August and October 2000 occurs at a lag of zero (correlation coefficient = 0.75) Thus it appears that the suggested reaction involving ozone, Br atoms and/or the resulting BrO radicals, along with vapour phase mercury:

- must be either a very fast (photochemically-induced/mediated) reaction which is completed on-site in less than 15 minutes within the sampled air-mass **or**
- has already occurred before the depleted air parcels are advected to the measurement location.

Furtheron it can be concluded from the cross correlation calculation that the ozone and TGM concentrations are not directly linked to each other but dependent on the reaction with another (third or fourth) parameter.

7.5 Comparison of Mercury Depletion Events in the Arctic and Antarctic

The first comparison of total gaseous mercury concentrations in the two polar regions is shown in Figure 7.13. The daily average concentrations of TGM at Neumayer 2000/01 with MDEs during Antarctic springtime (August-November) are compared with the mean daily average concentrations of the 1995 – 1999 TGM concentrations, measured at Alert, Nunavut, Canada (82°28'N, 62°30'W), showing the Arctic MDEs between March and June. Note that the Alert time scale is shifted for 182 days compared to the Neumayer time scale and that all data are exponentially smoothed. Table 7.4 shows the climatological seasons and their respective Julian Days for the North and South polar regions.

Table 7.4: Climatological Seasons and their Corresponding Julian Days for the Antarctic and the Arctic

Season	Julian Day Antarctic	Julian Day Arctic
Spring	244 - 334	60 - 151
Summer	335 - 59	152 - 243
Autumn	60 - 151	244 - 334
Winter	152 - 243	335 - 59

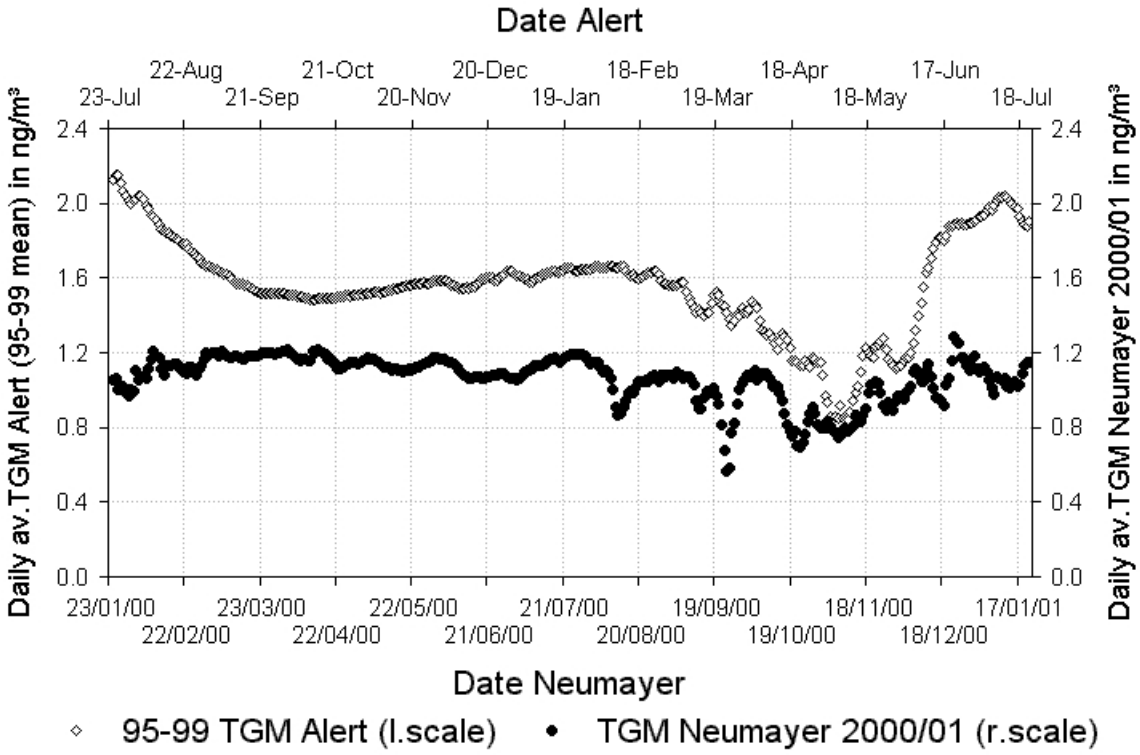

Figure 7.13: Comparison of the annual time-series of total gaseous mercury concentrations in the Antarctic (Neumayer) and Arctic (Alert). All data are exponentially smoothed

Figure 7.13 shows the comparison of mean daily average TGM concentrations measured at Alert in the high Canadian Arctic between 1995 and 1999 (gray line) and the respective data measured at Neumayer in the Antarctic in 2000/01 (black line).

At Neumayer the first MDEs occur about 1–2 months earlier than in the Arctic at Alert. We suggest that the earlier beginning of mercury depletion events after polar sunrise in the Antarctic is due to the following reasons:

- The different latitudinal positions of the two sampling sites. Neumayer is located at 70°S and the sun comes up for the first time on July 27th each year, whereas Alert has a position of 82°N and polar sunrise takes place later in the season.
- Most of the sea ice where enhanced BrO concentrations are found (Figure 7.11) is located north of Neumayer station at lower latitudes and can cover the ocean up to 55°S at the end of the Antarctic winter. The Arctic sea ice is found north of Alert at higher latitudes and around the North Pole. Therefore, the sea ice as a possible place where the photochemical reaction of ozone and Br atoms and/or the following reaction of BrO radicals and vapour phase mercury can take place, is exposed much earlier to the sun in the Antarctic than in the Arctic during springtime.

The annual time series measured at the Neumayer Station gives clear evidence that mercury depletion events do also occur in the Antarctic. Furthermore, it is evident that MDEs coincide with ozone depletion events in the lower troposphere and that the hypothesis is supported that free BrO radicals are involved.

MDEs can be supposed to result in an increased input of atmospheric mercury in the comparatively short springtime period in polar regions and are therefore an important feature in the global distribution of this pollutant. Further studies are necessary to explain the reaction mechanism and the kinetics of the MDEs identified during our measurements in the Antarctic. It is also important to combine these results with trajectory calculations in combination with sea ice maps in order to investigate the origin of the depleted air masses and the real place of the chemical reaction between ozone, reactive bromine and elemental mercury respectively.

7.6 Atmospheric Mercury Species at Neumayer Station and over the South Atlantic Ocean during Polar Summer

It has been shown that formation of reactive gaseous mercury species may play a key role during MDEs in North and South polar regions.

Inorganic RGM species (e.g., $HgCl_2$) are water-soluble and their dry deposition velocities and scavenging ratios are much higher than those for Hg^0. Therefore, RGM species have a much shorter atmospheric lifetime than Hg^0 and they can be expected to be removed closer to their sources (Lindberg and Stratton, 1998; Schroeder and Munthe, 1998; Bullock, 2000). However, American and Canadian researchers recently found very high levels of RGM and TPM species in the Arctic environment. Drastically increased levels of TPM and RGM were measured during Mercury Depletion Events (MDEs) in the time during and after polar sunrise at Alert, Nunavut/Canada (Lu et al., 2001) and Point Barrow, Alaska/USA (Lindberg et al., 2001; Lindberg et al., 2002).

The halogen (preferentially bromine) atoms react with ozone, forming halogen oxide radicals (BrO• and / or ClO•), which in turn can oxidise elemental mercury to Hg(II) species. The halogen atoms may also directly oxidise elemental mercury to Hg(II). RGM is formed which could be HgO, $HgBr_2$ and / or $HgCl_2$ (Lindberg et al., 2002). However, HgO (i.e., mercuric oxide) is incorrectly classified as a reactive gaseous mercury species; its vapour pressure is too low for it to be in the gaseous phase even in temperate locations let alone the Arctic, nor is it particularly reactive chemically.

Recent research on MDEs at Arctic and Antarctic sites has revealed clear evidence that long-lived gaseous elemental mercury is transformed to TPM and / or RGM during polar springtime but have also set up new questions:

- why do MDEs abruptly end at polar summer
- is RGM produced in an on-site reaction or
- can RGM only be produced in the marine boundary layer, and
- do high levels of RGM in polar regions only occur simultaneously with depleted concentrations of tropospheric ozone?

Sudden increases in the tropospheric BrO• mixing ratio during spring were found in the Antarctic using ground-based differential optical absorption spectrometry (DOAS) measurements and observations from satellite-borne instruments as discussed in chapter 7.4. Friess (2001) documented, from trajectory calculations for Neumayer Station, that air masses coming from the sea ice surface accompanied by BrO enhancements are found to be a necessary prerequisite for the observations of surface ozone depletion events. A similar link to MDEs has not yet been established and an open question is: why do MDEs stop abruptly during polar summer, even though solar intensity is still high or even increasing, compared with spring?

Up to the present, RGM measurements in the Antarctic were performed only once - at Terra Nova Bay from November 2000 to January 2001 (Sprovieri et al., 2002). RGM concentrations ranged from 10 to 330 pg m^{-3} and revealed the high oxidation potential in the atmosphere during Antarctic summer. The measurements reported in this work comprise the first data-set of different atmospheric mercury species in Antarctica and over the South Atlantic Ocean.

In the period from 23rd of December 2000 to 05th of February 2001, highly time-resolved measurements of atmospheric mercury species were carried out at Neumayer station. After completing the measurement program at Neumayer in February 2001, the instruments for the determination of TGM, GEM, and RGM were operated on board the *RV Polarstern* on the cruise from Neumayer to Punta Arenas, Chile, during February 2001 (for the cruise plot see Figure 7.19). The Tekran analysers were placed inside an air chemistry research container on the upper deck about 12 m above sea level.

Two Tekran gas-phase mercury vapour analysers (Model 2537A) were installed at Neumayer Station in January 2000 for the determination of an annual time-series of atmospheric mercury concentrations in the Antarctic (Ebinghaus et al., 2002). Until December 2000 the two Tekran analysers were operated with a 15-minute integrated sampling frequency at a flow rate of 1.0 L min^{-1}. This measurement program was enhanced throughout the ANT-XVIII (18th Antarctic program of the German Alfred Wegener Institute for Polar and Marine Research)

summer campaign (December 2000 to February 2001) and for the ship cruise from Neumayer to Punta Arenas (February 2001) by extensive measurements of atmospheric mercury species. RGM was measured with a Tekran 1130 mercury speciation unit which gave one Tekran 2537A mercury vapour analyser the ability to simultaneously monitor both elemental (GEM) and reactive gaseous mercury (RGM) species in ambient air at the pg m^{-3} level. A schematic diagram of the integrated system of the Tekran 1130 speciation unit connected to the Tekran 2537A is shown in Figure 7.14. A specially KCl-coated quartz annular denuder captured reactive gaseous mercury while allowing elemental mercury to pass through. At Neumayer the heated denuder module with the sample inlet was located 2 m above the snow surface, mounted on an aluminium mast about 5 m beside the ACO.

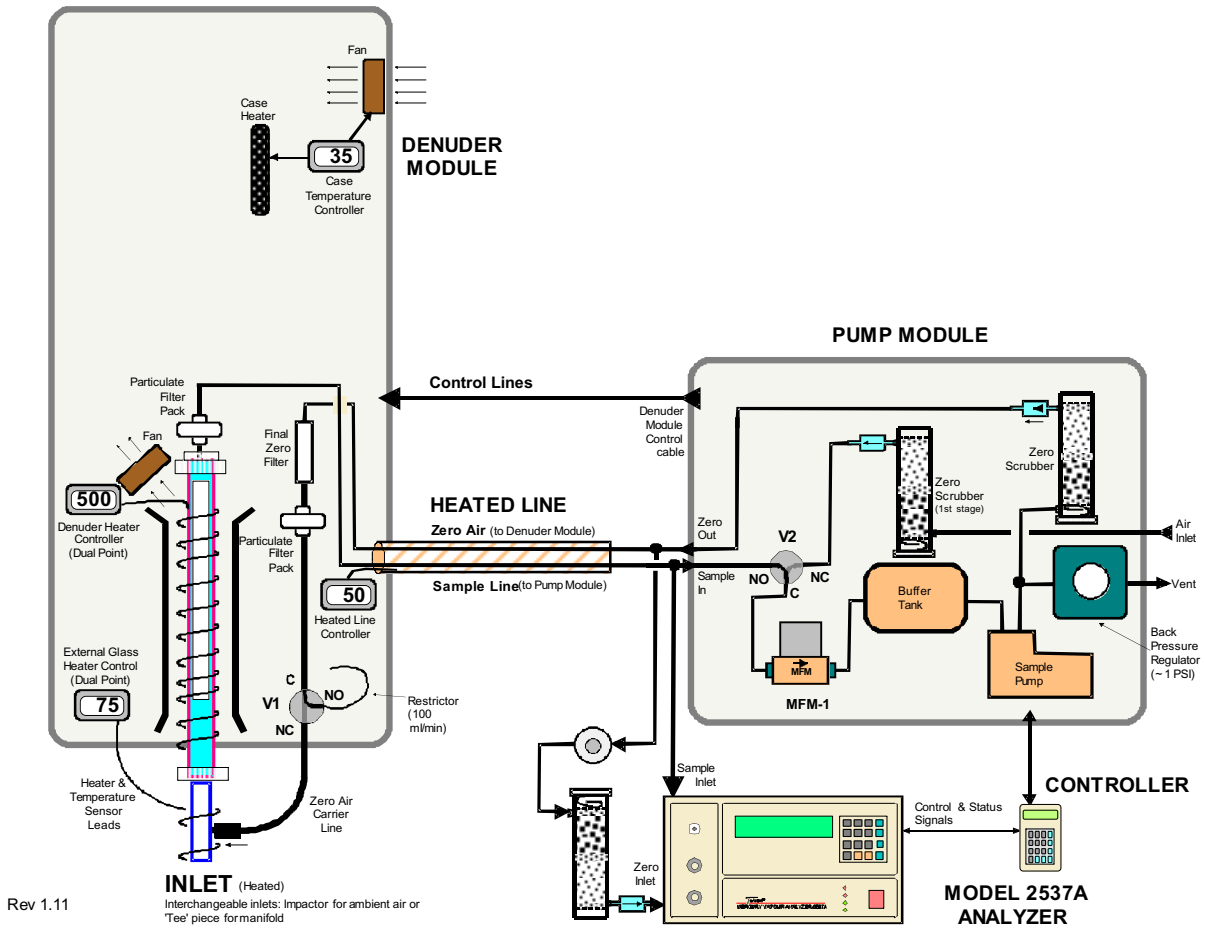

Figure 7.14: Schematic diagram for the integrated system of the Tekran 1130 speciation unit connected to the Tekran 2537A

During the 60 min sampling (adsorption) phase for RGM, the Model 2537A provided 5-min integrated samples for GEM concentrations at a flow rate of 1.5 L min^{-1}. An additional pump module integrated in the 1130 speciation unit pulled 6 L/min ambient air and increased the total flow rate for the denuder to 7.5 L min^{-1}. During the analysis (desorption) phase, the denuder was flushed with zero air and heated to 500°C to thermally reduce RGM to the elemental form. Downstream of the denuder a 0.45 µm PTFE filter, in front of the sample inlet of the Tekran 2537A, prevented the fine particulate phase mercury (particle size < 2.5 µm) from penetrating into the gold traps. The second Tekran 2537A continued to measure TGM and was operated with a 5-minute integrated sampling frequency. The sample inlet with a drift protection (no filter) was located 6 m above the snow surface on top of the ACO. The air was sampled at a flow rate of 1.5 L min^{-1} through a heated sample line about 10 m in length ending up with a 0.45 µm PTFE filter in front of the inlet of the analyser. The analysers were calibrated every 25 hours with an internal automatically-triggered permeation source injection.

Total particulate-phase mercury (TPM) was measured using an AESminiSamplR® developed by the Meteorological Service of Canada (see chapter 2.3). The airborne particulate matter was collected at 2 m height on two AESminiSamplR® devices sampling in parallel. The total sample volume ranged between 4-6 m^3 of ambient air with an integration time of 48 h.

A direct calibration method for RGM measurements with the Tekran speciation unit 1130 does not yet exist. It is difficult if not impossible to find a representative certified reference material for a reproducible calibration of gaseous Hg^{II}-species on a KCl-coated denuder. Field intercomparison studies of different methods for the determination of RGM were performed at Mace Head, Ireland (see chapter 3) and Sassetta, Italy (Ebinghaus et al., 1999; Munthe et al., 2001). They revealed a good precision for the denuder method and no significant breakthrough. It was also reported that the thermal desorption and reduction of RGM to Hg^0 has an efficiency of nearly 100%. Comparable results were also obtained for different methods like multistage filter packs, refluxing mist chambers, and KCl-coated denuders (Sheu and Mason, 2001).

The analytical gold trap in the detection system for TPM analysis was calibrated according to the detailed description given in chapter 2.

7.7 Investigations on the Chemical Composition of Operationally Defined TGM

In recent years, controversial discussions about the chemical composition of TGM at high levels of RGM and / or TPM have led to different interpretations of the parameter TGM measured with a Tekran Model 2537A analyser. Because RGM has been shown to adsorb on many materials, the question was whether, at high levels of RGM, the gaseous divalent inorganic mercury species (commonly assumed to be $HgCl_2$) could pass through the sample line and the particulate filter in front of the sample inlet of a Tekran 2537A to sum up, with the Hg^0, to TGM? We used both a Tekran speciation unit 1130 connected to a Tekran 2537A to provide GEM and RGM concentrations, and a traditional Tekran 2537A with a heated sample line and a particulate filter in front of the analyser to measure TGM concentrations. All 2-h averaged atmospheric mercury species concentrations during the complete summer period (December 00 – February 01) containing RGM-concentrations > 0.15 ng m^{-3} are presented in Figure 2. The lower graph represents the residuals of TGM – (GEM + RGM) showing that the deviations are generally lower than 10% (< 0.11 ng/m^3) of the mean TGM level (≈ 1.1 ng/m^3) even at higher levels of RGM up to 0.4 ng/m^3. This figure gives clear evidence that, under Antarctic conditions with low air humidity, high levels of reactive gaseous mercury can pass through a heated Teflon line and a particulate filter to be amalgamated on gold cartridges and subsequently detected as Hg^0 in a Tekran 2537A.

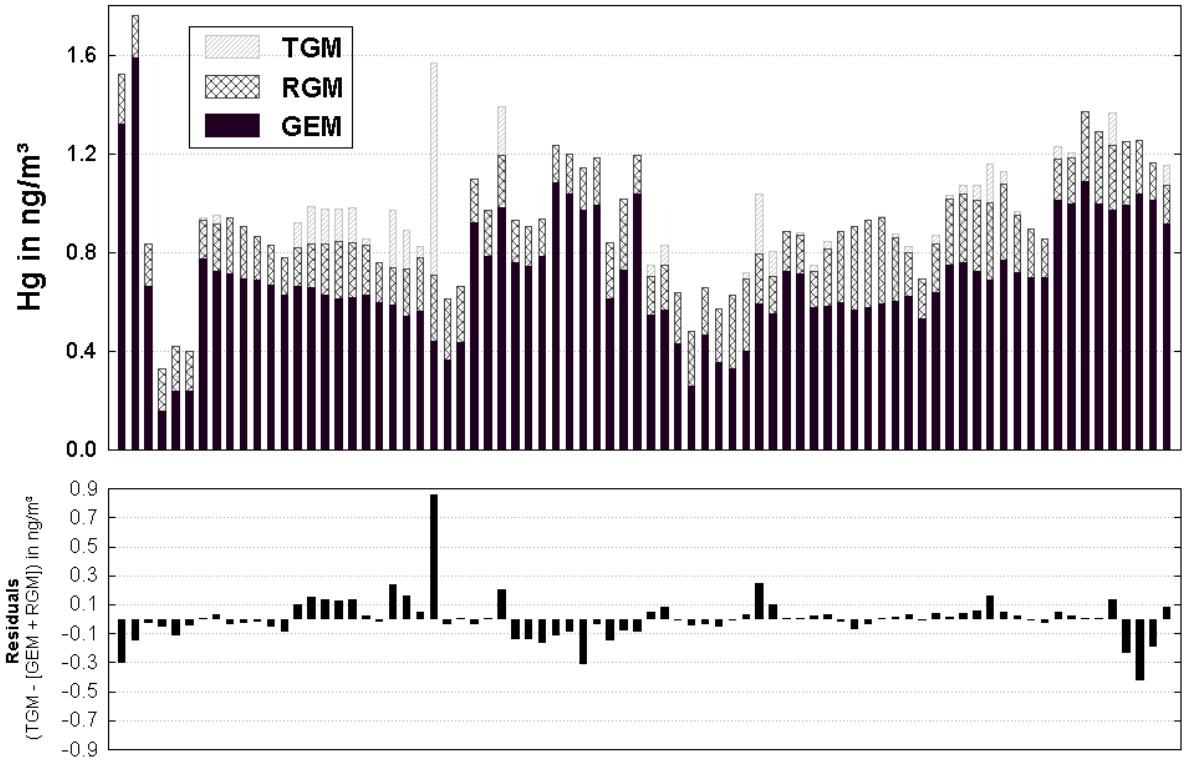

Figure 7.15: Selected 2-hour averaged mercury species concentrations during the summer period (Dec 00 – Feb 01) containing RGM levels (> 0.15 ng/m^3) and the respective residuals of TGM – (GEM + RGM)

In addition, Table 7.5 shows the arithmetic mean of the 2-h averaged TGM, GEM, and the calculated sum of GEM + RGM concentrations for the complete measurement period during Antarctic summer. The three data sets are normally distributed (Kolmogorov-Smirnov test) and their standard deviations based on the same variance of the entire population (F test for P =0.95).

Table 7.5: Arithmetic Mean of 2-hour Averaged TGM, GEM, and the Calculated Sum of GEM + RGM Concentrations during Antarctic Summer (December 00 – February 01) at Neumayer Station

Parameter	Instrument	n	Arithmetic mean and standard deviation ($ng\ m^{-3}$)	Max. ($ng\ m^{-3}$)	Min. ($ng\ m^{-3}$)
TGM	Tekran 2537A	515	1.08 ± 0.29	2.34	0.27
GEM	Tekran 2537A + speciation unit 1130	528	0.99 ± 0.27	1.89	0.16
GEM + RGM	Tekran 2537A + speciation unit 1130	504	1.07 ± 0.23	1.95	0.33

Table 7.5 shows that the mean TGM concentration during the Antarctic summer period differs significantly from the mean GEM concentration (result of the t test: $t = 5.37 > t[P = 0.95, f = 1041] = 2.60$). Moreover, a comparison of the mean values of the TGM concentrations and the calculated sum of GEM + RGM concentrations reveal no significant difference between these two aggregate concentrations for this summer period (t test: $t = 0.75 < t[P = 0.95, f = 1017] = 2.60$). These statistical results exemplify that it is possible to measure TGM with a heated sample line and a Tekran 2537A as the commonly defined 'sum parameter' of both gaseous mercury species (GEM + RGM) in ambient air, even at periods with relatively high RGM concentrations.

7.8 The End of Mercury Depletion Events during Antarctic Springtime

Antarctic MDEs coincided with ozone depletion events in the lower troposphere and supported the hypothesis that BrO free radicals are involved, as shown by Ebinghaus and co-workers (2002).

It was hypothesized that depletion of atmospheric boundary layer mercury (at times up to an altitude of ≈ 1 km) was due to a reaction between gaseous elemental mercury and BrO free radicals or halogen atoms. The MDEs ended at the beginning of November, but a possible explanation for their sudden termination was left open. The results of the TGM measurements and ground-level ozone concentrations for the time period from January 2000 to January 2001 are presented in Figure 7.9. In addition Figure 7.16 gives the weekly correlation coefficients (r) for surface-level ozone and TGM concentrations as bars in the bottom graph. The correlation analysis for the fall and dark winter months (March – July) yields very variable correlation coefficients; hence, considering the complete winter time, no significant linear relationship among these two variables is evident. The TGM concentration pattern between August and October 2000 shows a strong positive correlation with ozone (max. correlation coefficient $r > 0.9$) as discussed earlier. MDEs suddenly end at the beginning of November when TGM and ozone concentrations start being negatively correlated (max. $r \approx -0.8$) until the beginning of February 2001 (end of the mercury measurements at Neumayer Station). Regarding the ozone chemistry, this is a first indication that the atmospheric processes for the oxidation of mercury during springtime MDEs should be based on a different mechanism compared with the Antarctic summer period from November to February.

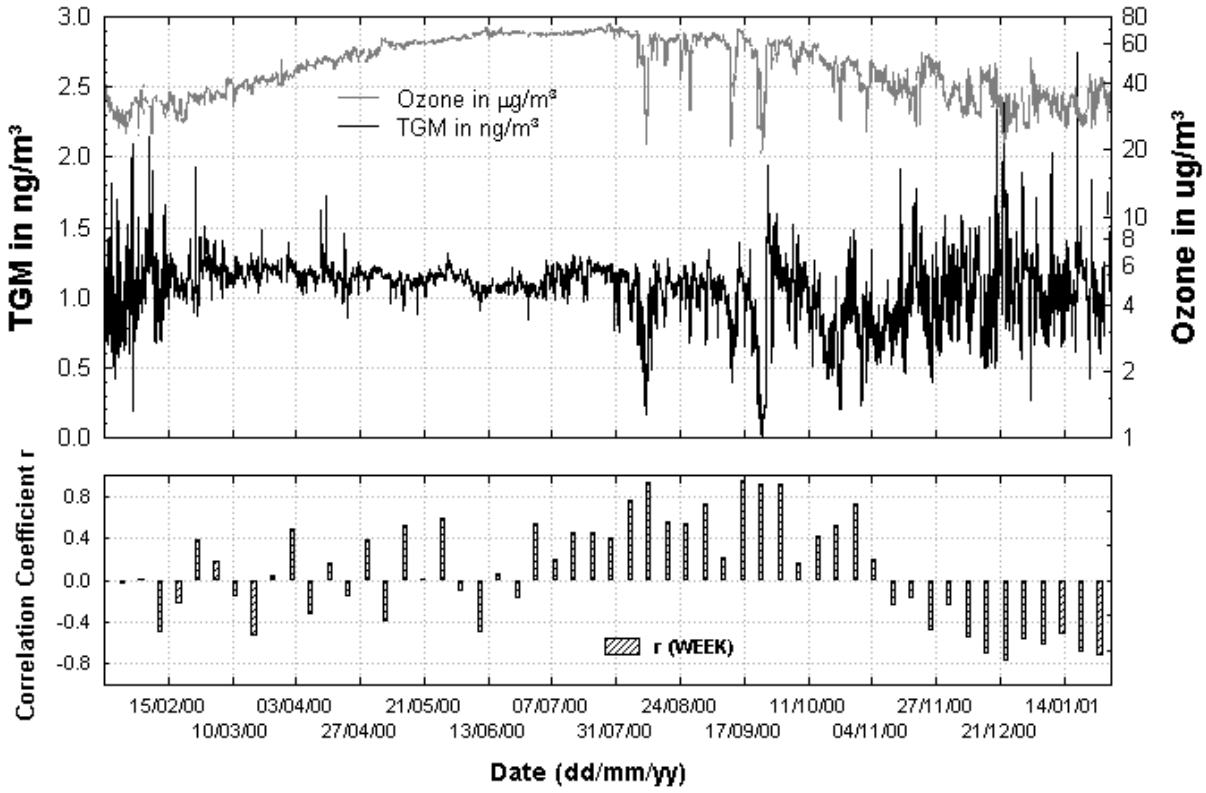

Figure 7.16: Annual time series of 1-hour averaged TGM and surface-level ozone concentrations at Neumayer, January 2000 – February 2001 and their weekly mean correlation coefficients r. The TGM concentrations were obtained from two separate Tekran analysers and mean values were used if both analysers were operating in parallel

One remaining question is: why do MDEs suddenly end at the beginning of November 2000 during Antarctic springtime ? Figure 7.17 shows the smoothed trend of the 12-hour averaged TGM concentrations since May 2000. The gray bars represent the number of coordinates from every five-day (120-h) backward trajectories which were located over sea ice with more than 40% ice coverage. All backward trajectories were based on the results of the Global Model of the German Weather Service and were obtained for Neumayer Station every 12 hours. The trajectories were calculated for surface pressure and consist of 21 coordinates (every 6 hours) representing the backward transport of the surface air masses. The weekly sea ice analysis charts were obtained from the web page of the National Ice Center from the National Oceanic and Atmospheric Administration (NOAA) in Washington. Our category with sea ice coverage > 40% is based on the classification of the National Ice Center. A number of 21 would be related to an air mass that originated from the sea ice having a maximum contact time with sea ice over the Southern Atlantic Ocean (coverage > 40%) before reaching Neumayer, whereas no contact with sea ice with more than 40% ice coverage would result in a number of

0. The dashed line represents the astronomic sunshine duration (ASSD) for 24 hours at Neumayer Station. During the year 2000/01 the sun stayed permanently above the horizon from November 10th to January 25th (ASSD = 24 h) and permanently below the horizon from May 17th to July 17th (ASSD = 0 h).

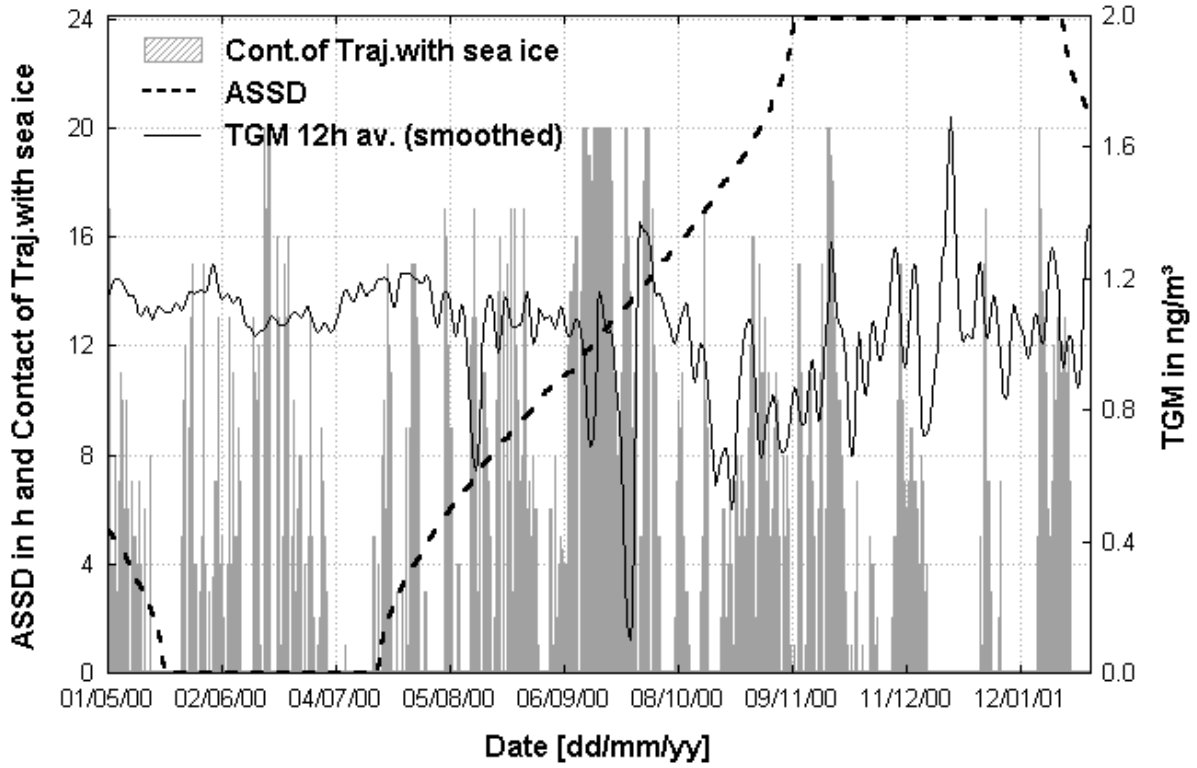

Figure 7.17: Comparison of the 12-hour averaged TGM concentrations (smoothed) and the duration of sea ice contact of the surface air parcels obtained from trajectory calculations ending at Neumayer at 12:00 and 24:00 UT. The dashed line represents the astronomical sunshine duration (ASSD) for each day

Figure 7.17 gives clear evidence that shortly after polar sunrise (polar sunrise = 17th of July 2000), at the beginning of August, the first strong MDEs occurred at Neumayer. This coincides with the arrival of air masses that resided most of the time over the ocean, covered with more than 40% sea ice, before reaching Neumayer Station. This good agreement between the TGM measurements during MDEs, and the results from trajectory calculations in combination with sea ice charts, supports the theory that reactive bromine, which destroys ozone and can oxidize elemental mercury in a subsequent reaction, is released from sea salt surfaces, which are provided either by sea ice surfaces or by uptake of sea salt aerosols.

These reactions must end when the sea ice in the Weddell Sea around Neumayer starts to vanish at the end of November, thus reducing, within a short time, the size of the surrounding sea ice which in winter covers an area of around one and one-half times the area of the continent (around 20 million km^2 in October, 3 million km^2 in February). The consequences are shown in Figure 7.17. Although photochemical reactions would be supported by strong solar radiation in the time after 01^{st} of November, the occurrence of strong MDEs decreased and the duration of air mass contact with sea ice decreased as well. Release of reactive bromine species from sea salt surfaces, as a precursor for surface ozone destruction and the oxidation of atmospheric mercury (Hg^0) after polar sunrise can only take place within a short time period ending with the disappearance of the sea ice around the Antarctic continent.

TGM concentrations during Antarctic summer were still highly variable; however, these transformations are supposed to be due to other atmospheric reactions, as explained in the following chapter.

7.9 Mercury Species Concentrations during Antarctic Summer

The results of mercury species measurements for the time period December 2000 to February 2001 are presented in Figure 7.18. The arithmetic mean of all TGM measurements between 23^{rd} of December 2000 and 05^{th} of February 2001 was (1.08 ± 0.29) ng m^{-3} and is in the range of typical background concentrations of TGM for the southern hemisphere as reported in (Ebinghaus et al., 2002; Sprovieri et al., 2002). Mercury levels in the remote southern hemisphere are generally lower than in the northern hemisphere and in the Arctic. Several studies (Slemr, 1996; Slemr et al., 2002; Ebinghaus et al., 2002) have shown that total gaseous mercury background concentrations over the Atlantic Ocean in the southern hemisphere are very homogeneous and are about 25% lower than the northern hemispherical TGM background concentration. Nevertheless, the data measeured at Neumayer station revealed that TGM and GEM concentrations during the sunlit summer period varied more than during the dark winter months and depletions with concentrations < 0.3 ng m^{-3} were frequently observed.

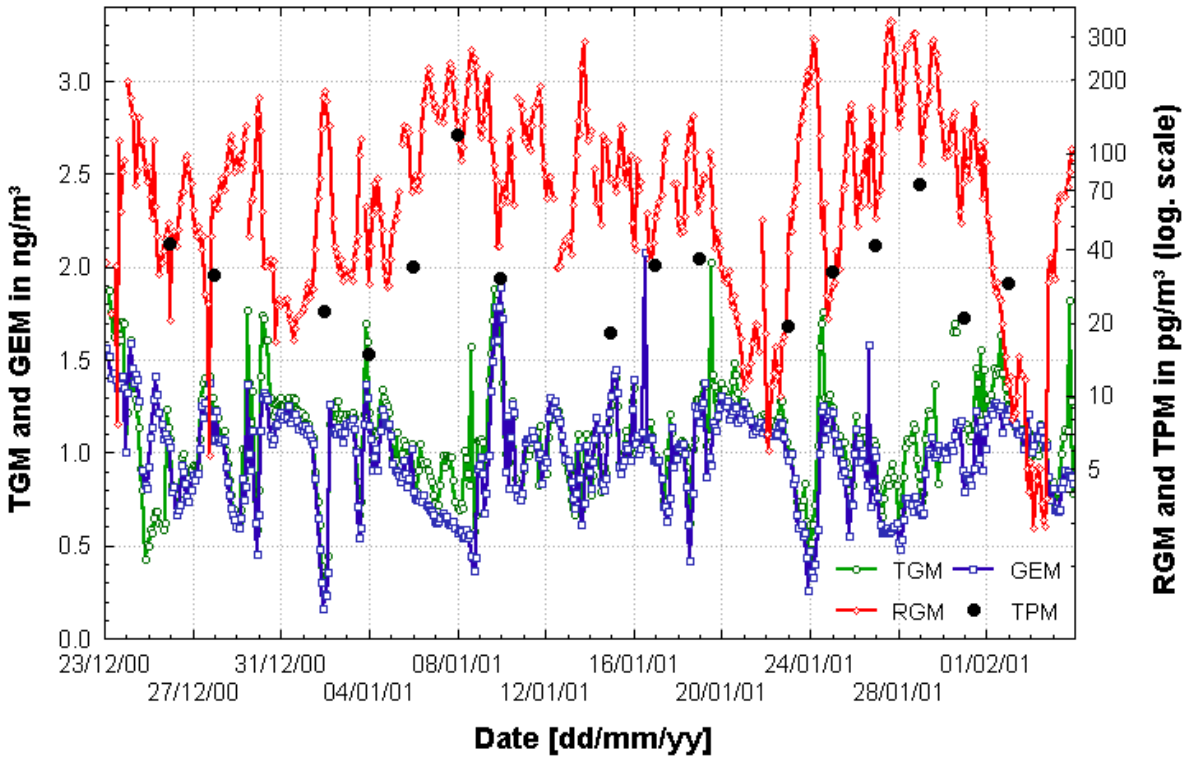

Figure 7.18: Atmospheric mercury species concentrations at Neumayer Station between 23rd of December 2000 and 05th of February 2001. TGM, RGM and GEM levels are 2-hourly mean concentrations. TPM concentrations were obtained from 48-h integrated samples. Missing data in the RGM concentrations were due to the automatic calibration cycles for the Tekran analyser

RGM concentrations during this summer period varied between 5 pg m^{-3} to maximum levels of more than 300 pg m^{-3}. These peak concentrations are comparable to those measured in the vicinity of strong anthropogenic sources such as coal-fired power plants and waste incinerators (Sheu and Mason, 2001). Comparable values have been reported for the depletion period in the Arctic at Point Barrow, Alaska/USA (Lindberg et al., 2002) and for the non-depletion period (November – December 2000) in the Antarctic at Terra Nova Bay (Sprovieri et al., 2002) with maximum values of 900 pg m^{-3} and 300 pg m^{-3} respectively.

Previous RGM measurements at a rural European site over a two-month time period showed average values of 5 to 90 pg m^{-3} (Ryaboshapko et al., 2001). This is in good agreement with very homogeneous RGM levels with a median of 6 pg m^{-3} (n = 75; lower quartile = 4 pg m^{-3}, upper quartile = 16 pg m^{-3}) obtained on board of the *RV Polarstern* in February 2001 over the south Atlantic Ocean (see Figure 7.19).

As shown in Figure 7.18, TPM concentrations at Neumayer were in the range of 15 to 120 pg m^{-3} showing roughly the time trend of the RGM concentrations only at a lower level and having a much lower time resolution because of the long sampling time of 48 hours. Our data clearly indicate an important change in the speciation of atmospheric mercury during Antarctic summer at Neumayer Station, producing high levels of RGM and / or TPM at this remote site.

7.10 Mercury Species Concentrations over the South Atlantic Ocean

In order to reconfirm the homogenous distribution of atmospheric mercury in the remote southern hemisphere and to point out the exceptionally high RGM levels found at Neumayer Station during Antarctic summer, additional mercury species measurements were carried out on board of the RV "Polarstern" after finishing the measurement campaign at Neumayer. The results of the ship cruise from Neumayer to Punta Arenas are presented in Figure 7.19. TGM, GEM, and RGM remained very stable at low levels without high variations over the entire measurement. The mean TGM concentration was (1.1 ± 0.2) ng m^{-3} and is in good agreement with average southern hemispherical background TGM concentrations from previous studies (Slemr, 1996; Slemr et al., 2002; Ebinghaus et al., 2002). The first RGM measurements ever obtained on board of a ship in the southern hemisphere yielded very low concentrations in the range of 1 to 30 pg m^{-3}; thus, revealing no significant differences between GEM and TGM during the whole cruise. The few outliers at the beginning of the cruise were due to contamination from the ship stopping several times because of heavy sea ice. No obvious trend over the south Atlantic Ocean or influence from the South American continent can be seen. These supplementary measurements confirm the hypothesis that the very high RGM concentrations at Neumayer Station measured in the time between December 2000 and February 2001) should be influenced by local production of oxidised gaseous mercury species over the Antarctic continent or shelf ice at polar summer.

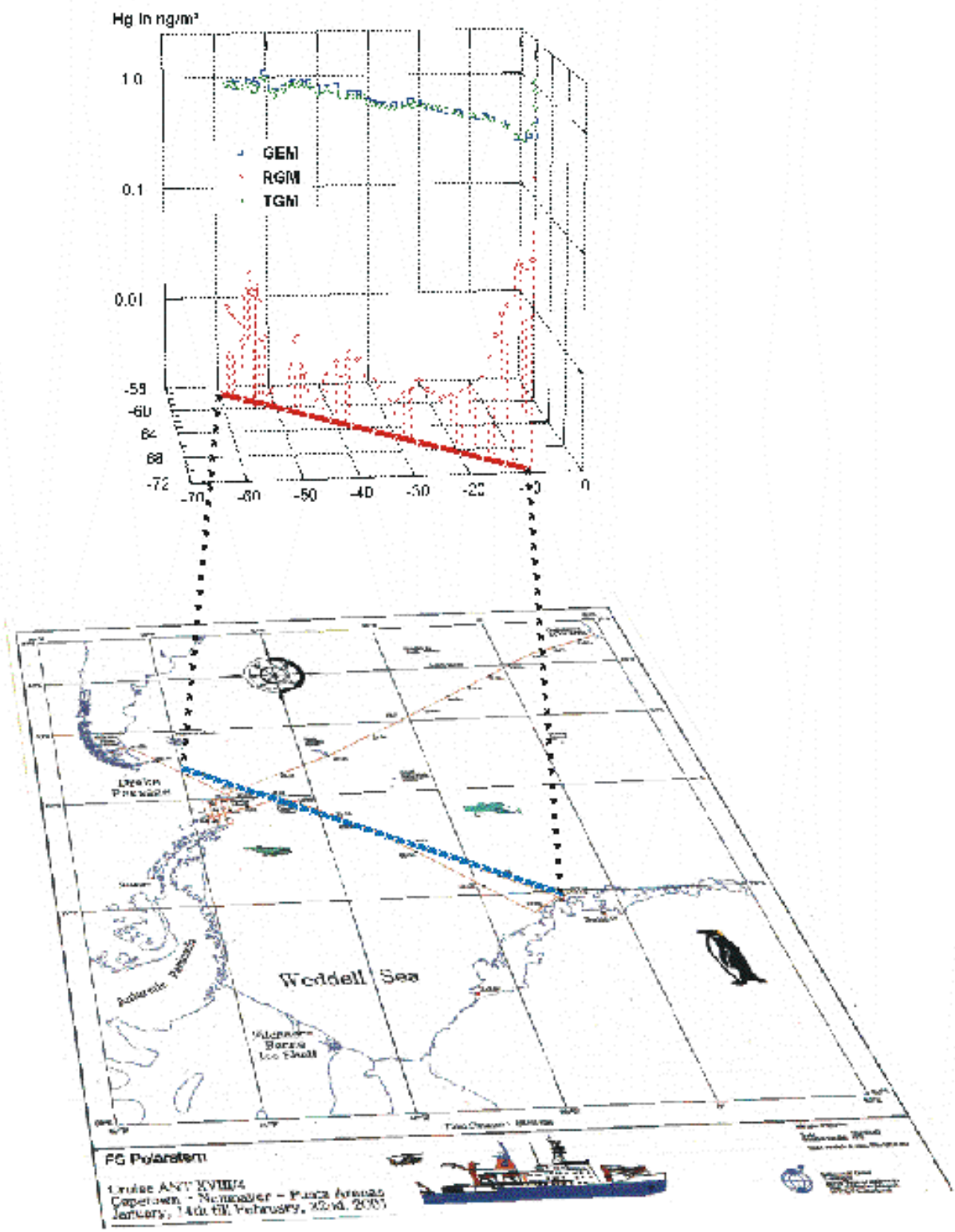

Figure 7.19: Two-hourly averaged atmospheric mercury species concentrations over the south Atlantic Ocean measured on board of the *RV Polarstern* during cruise ANTXVIII/4 (Neumayer – Punta Arenas, February 2001)

7.11 Implications on the Dynamics and Chemistry of Atmospheric Mercury Transformations during Antarctic Summer

As shown in the previous chapters, the summer-time oxidation of elemental mercury and transformation to more reactive gaseous species at Neumayer is based on a different reaction mechanism compared with the gas-phase oxidation of elemental Hg by BrO and the prior destruction of surface-level ozone during springtime depletions (Lindberg et al., 2002; Ebinghaus et al., 2002). To examine potential influences of meteorological factors, anthropogenic emissions or solar radiation, a representative short time period of 2-hour mean atmospheric mercury species concentrations and surface-level ozone concentrations, together with selected additional meteorological and chemical parameters, is presented in Figure 7.20. During this Antarctic summer time period event, highly variable mercury concentrations were observed, with significant negatively correlated surface-level ozone and TGM (r = -0.61) or GEM concentrations (r = -0.58). At the same time, RGM concentrations are positively correlated with ground-level ozone concentrations (r = 0.30).

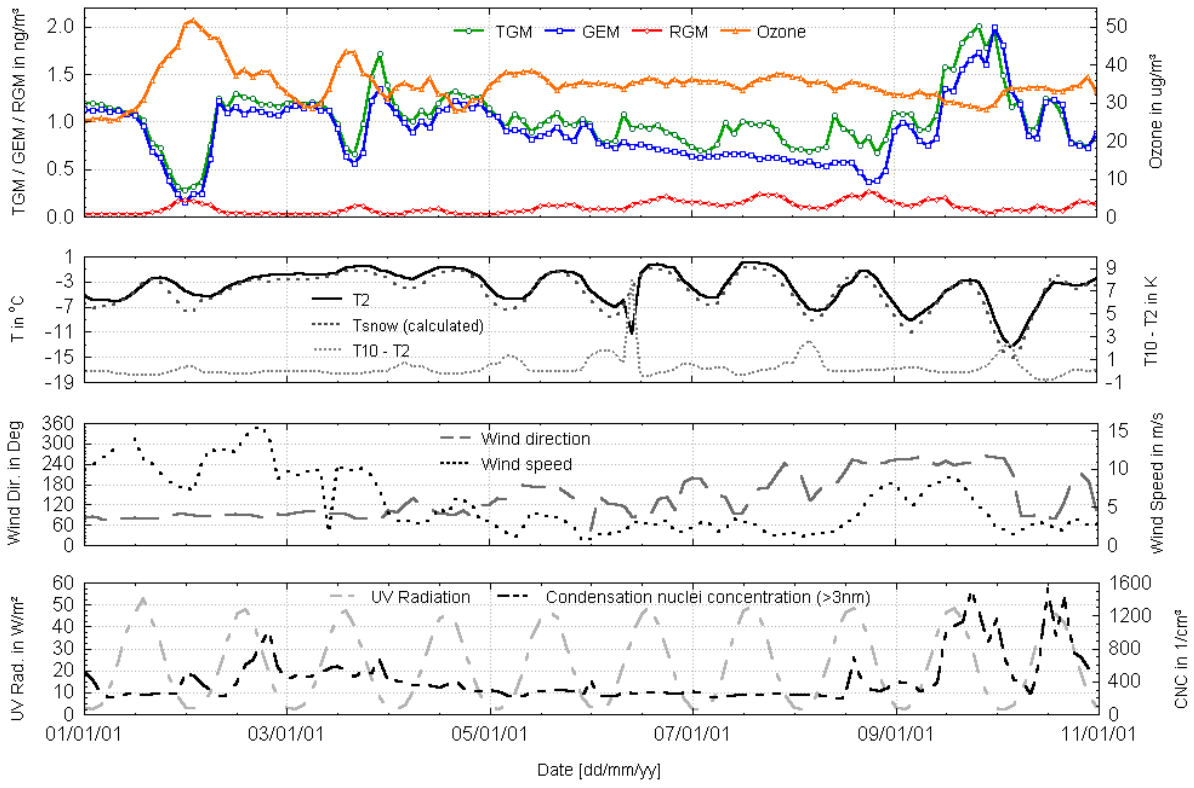

Figure 7.20: Two-hourly averaged atmospheric mercury species TGM, GEM, RGM, and ozone concentrations together with selected meteorological and chemical parameters for a single event during Antarctic summer. T10 and T2 represent the air temperature at 2 m and 10 m height

During this short event (01st – 11th of January 2001), TGM and GEM concentrations decreased temporarily from normal background levels of 1.1 – 1.2 ng m^{-3} to < 0.4 ng m^{-3}, whereas RGM levels increased simultaneously from 30-40 pg m^{-3} to more than 200 pg m^{-3} and surface-level ozone concentrations exceeded normal background concentrations (30 µg m^{-3} during Antarctic summer, representing the minimum of the annual ozone concentrations caused by photolysis of ozone from higher UV-B radiation to more than 50 µg m^{-3}. T2 and T10 represent the temperature measured at 2 meters and 10 meters height. The strength of the inversion in terms of the stability of the lower troposphere can be estimated by the temperature difference T10 – T2.

In particular, during 01st and 02nd of January a strong decrease of TGM and GEM was observed. For this depletion and all following events no significant correlation to any of the given additional parameters could be found. We hypothesize that the oxidation of elemental mercury to divalent atmospheric mercury species and a concurrent production of ozone has already occurred before the air parcels were advected to the measurement location. On the basis of several recent studies giving evidence that ozone is photochemically produced at the South Pole (SP) surface during Antarctic summer, together with a high atmospheric oxidizing power on the Antarctic plateau (Davis et al., 2001; Crawford et al., 2001), we propose a gas-phase oxidation of elemental mercury by potential oxidants like OH, HO_2, O(^{1}D and ^{3}P), NO_3 etc. associated with high levels of NO resulting from photodenitrification processes in the snowpack which serve as an ozone precursor (conversion of NO to NO_2, followed by photolysis of NO_2). This hypothesis is confirmed by the latest results from the ISCAT program (Investigation of Sulfur Chemistry in the Antarctic Troposphere) revealing high concentrations of TPM in aerosol samples together with a simultaneous production of ozone at South Pole in November 2000 – January 2001 (Arimoto, 2002). Furthermore, Sommar et al. (2001) have recently investigated the reactivity and kinetics of hydroxyl radicals towards Hg^0 in the gas phase, finding that the reaction is slightly exothermal and Zhou et al. (2001) showed that the snowpack photochemical production of HONO could affect the concentrations of hydroxyl radicals in the Arctic boundary layer.

Additional cross-correlation analysis of TGM and ozone concentrations at the highest time resolution (5 minutes) for different events where Hg^0 concentrations decreased and surface-level ozone increased, always lead to a maximum negative correlation in the cross-correlation function at a lag of zero. These results confirm that the suggested reaction in the atmosphere producing ozone and oxidizing elemental mercury must be faster than 5 min or was already completed. The second explanation is probably more plausible because Hg^0 minima are infrequent during this time, very short-lived, and no significant correlation with other parameters like UV-radiation and wind speed measured on-site at Neumayer Station were

detected. The actual place of the oxidation reaction of elemental mercury in the atmosphere and the origin of the depleted air masses should be relatively close to Neumayer Station. Extremely high RGM levels were measured at this site and RGM species are not known to undergo long-range transport because of their relatively short atmospheric lifetime (Lindberg and Stratton, 1998; Schroeder and Munthe, 1998).

Additional atmospheric measurement data of potential precursor compounds (NO_y, CO, and OH radicals) and isentropic trajectory calculations are necessary to explain the reaction mechanism and the origin of the air masses reaching Neumayer during Antarctic summer with concurrent high concentrations of RGM and surface-level ozone.

High CNC-levels (condensation nuclei concentration) measured on the 09th and 10th of January 2001 at the end of this event were associated with extremely high TGM and GEM concentrations exceeding normal background concentrations by more than 50% (> 1.5 ng m^{-3}). Higher concentrations of elemental mercury during Antarctic summer can be due to anthropogenic emissions. From late December to mid February an increased number of visiting scientists is operating in the vicinity of the main station and it is well known that human activities produce large concentrations of condensation nuclei (Jaenicke et al., 1992). They cannot be totally excluded at Neumayer although the ACO is located 1.6 km south of the main station and vehicles are not allowed to approach the ACO.

Re-emission of Hg(0) from Arctic snow-pack following the spring-time depletion period has been reported recently (Lalonde et al., 2001). However, Hg^0 peaks at Neumayer are infrequent, very short-lived, and no significant correlation with UV-radiation or temperature can be seen. Therefore we would exclude re-emission of Hg^0 from the snow and / or water surface by photoreduction and volatilisation to the atmosphere as an explanation for the effects we observed.

8 Summary and Conclusions

The work presented here summarizes field and laboratory studies that have been carried out to investigate the chemistry and environmental behavior of atmospheric mercury on different spatial and temporal scales. The spatial scales cover local, regional, hemispheric and global dimensions.

Research on the local scale distribution and deposition of atmospheric mercury has been carried out within a 5 km radius around a partly inactivated caustic soda plant in eastern Germany.

Regional distribution studies have been compiled during two horizontal transect experiments at 4 measurement sites covering a distance of approximately 800 km. Additionally, aircraft measurements have been carried out at different altitudes over a horizontal distance of about 400 km and vertically between 400 and almost 4000 meter a.s.l.

The hemispherical and global distribution of atmospheric mercury has been investigated during cruises with the *RV Polarstern* and during two measurement campaigns at the Antarctic research station Neumayer.

Temporal scales covered by this work include short-term variations of atmospheric mercury concentrations within less than one hour, variations that typically occur within time steps of a few hours to several days and long-term studies that have been carried out over a time period of seven years and are ongoing.

Short-term variability can be seen for example during pollution events in the concentration data of the transect studies and in the Mace Head data set. Mercury depletion events (MDEs) typically last for several hours before the concentration levels out again at normal background values. In the absence of pollution and depletion events a very homogeneous temporal (and spatial) distribution of atmospheric mercury could be shown for several days up to weeks. Finally, one of the world's most comprehensive long-term data set of atmospheric mercury is presented covering the time period from 1995 to 2001 allowing a trend estimate for the northern hemisphere.

This chapter summarizes major findings and conclusions but also open questions and research needs for the future in relation to the work carried out within this thesis.

Air / surface exchange processes and their role in the atmospheric cycling of mercury

The atmospheric cycling of mercury is driven by the volatility of the elemental form, oxidation and adsorption processes and the subsequent deposition of ionic species to the underlying surface. Once deposited, oxidized mercury species can be converted into the elemental form and are available for evasion fluxes again.

The exchange of gaseous mercury at any interface is driven by a concentration gradient. If one compartment has a higher Hg(0) concentration than another, a net emission will take place, while net deposition will occur if the competing compartment is clean compared to the overlying atmosphere. The consequence is that for example soils located close to large atmospheric mercury sources are clearly sinks while these sources are active. In the long run however, these soils may turn into important sources when the original emissions are discontinued and therefore direct flux measurements will be important at such sites.

It seems appropriate to propose the existence of a "compensation point". This would mean that soils below a certain Hg(0) concentration or probably soil gas concentration tend to absorb mercury, while soils above that concentration emit mercury depending on the Hg(0) concentration in the overlying air. This assumption would also be valid even if the mechanisms of emission and absorption may not be the same. A similar compensation point concept has also been reported for vegetation.

Globally, hundreds of such sites that have been impacted by atmospheric mercury deposition still exist and their contribution to regional mercury emissions could be significant. The concept of a compensation point is not only restricted to soils and vegetation. It can also be assumed that inland waters or marine systems may be converted from net deposition sinks into net emission sources depending on the concentration gradient between the dissolved and the gaseous phase.

The discussion about the relative significance of natural and anthropogenic emissions is complicated by processes that we classify here as indirect anthropogenic re-emissions. This term is chosen to describe secondary re-emission of mercury from anthropogenic sources following partial initial deposition of primary anthropogenic mercury emissions. It is not possible to quantify the natural and anthropogenic fraction in the total amount of re-emitted mercury. In general it can be assumed that direct anthropogenic and direct natural emission are in the same order of magnitude however, the estimation of the mercury amount emitted from natural sources still contains large uncertainties: Global volcanic emissions were estimated from the Hg/S ratio and account for approximately 20 to 90 t y^{-1}, which is about 1-5% of the annual emissions from human activities.

The role of vegetation in the overall picture seems to be ambiguous and needs further investigation, since all processes are apparently very specific to both the site and plant species. A recent study gave first evidence that mercury emissions originating from forest fires may have been significantly underestimated. Based on characteristic CO/CO_2 and CO/Hg emission ratios inside the plume of forest fire that destroyed about 9000 ha of a mixed vegetation it was estimated that biomass burning could contribute to about 50 % of natural mercury emissions globally.

Results from the geological heat flux approach suggest that mercury transfer through mid-ocean ridges could be on the order of 1900 to 3800 t y^{-1}, while the whole oceanic crust would emit 7300 to 14700 t y^{-1} of mercury. These results in combination with other sources of submarine mercury like hydrothermal vents, seismic activity and erosion of ocean ridges as well as submerged parts of the continents could give the impression that atmospheric deposition might be negligible in the total oceanic mercury budget. However, other authors assume that deposition is the major source of mercury (re)emitted to the atmosphere from ocean surfaces. These findings contradict each other to a degree that the role of crustal degassing for oceanic mercury and subsequent emission into the atmosphere can not be evaluated yet.

To obtain a more complete and accurate picture on the global biogeochemical cycling of mercury including the relative importance of natural sources these pathways and their terrestrial counterparts definitely have to be investigated much more thoroughly before the large discrepancies in global mercury budgets can be resolved. Actual flux measurements could be a major tool to help to answer these questions in the future and are presently increasing in quantity and quality worldwide.

Atmospheric mercury distribution on local scale

Major anthropogenic sources of atmospheric mercury are industrial activities such as caustic soda production and fossil fuel combustion. The relative importance of these sources has been discussed in detail in chapter 1.1. During active production, emissions from these types of sources are normally estimated by emission ratio calculations or the amount of energy produced.

If these sources are no longer active it can be assumed that they still emit mercury however, classical approaches for emission estimates are not applicable because the necessary input parameter are not available.

An example how to handle the difficult question of mercury emissions from a (partly) inactivated production plant is given for the industrial complex "BUNA" close to Halle and Merseburg in Eastern Germany. It could be shown that by a combination of field measurements with numerical modeling, emissions of mercury from inactive plants could be estimated with an uncertainty of a factor of two. These numerically derived emission estimates have later been verified satisfactorily by measurement data obtained onboard of a research aircraft.

Both approaches revealed emission estimates of the inactivated industrial complex on the order of 2 to 4 kg per day reflecting the importance of more or less diffuse emissions from formerly active mercury sources. The relative importance of the individual sources on the plant area could be identified.

An attempt has been made to derive a mercury mass-balance on a local scale around the BUNA complex. It could be estimate that 30 % of the emitted mercury is deposited in the local vicinity of the plant, whereas 70 % are available for long-range transport at least on a regional scale. This estimate points to the fact that local emissions contribute to the regional or even hemispherical mercury burden. The potential for long-range transport is strongly dependent on the mercury species emitted.

Atmospheric mercury distribution on regional scale

Observational data on the spatial and temporal distribution of atmospheric mercury are very limited. Available data sets are mainly based on ground-based measurements at single locations for different time periods. Within this work measurement campaigns have been carried out to investigate the (quasi-)real time distribution of atmospheric mercury in the horizontal and in the vertical dimension. The two transect experiments consisted of simultaneous measurements of atmospheric mercury at four sites covering a distance of about 800 km. Aircraft measurements revealed data from two horizontal flight legs at different altitudes (below and above the boundary layer) over a distance of 400 km, and from spiral ascents and descents between 400 and 4000 m. The diameter of the spirals was about 5 km. Consequently, an air mass of an entire volume of about 8000 km^3 has been investigated during the flight by sampling over a time period of less than 6 hours.

No experimentally derived information on the regional distribution of atmospheric mercury for central Europe was available for the time after 1990 when the Nordic Network for Mercury in Air and Precipitation in Scandinavia had been terminated. In this work two field experiments were carried out for two weeks in summer 1995 and for three weeks in winter 1997 at four European sites along a 800 km line between Stockholm and Berlin. A total

number of 30,000 individual concentration measurements data were obtained during these two episodes representing the most comprehensive data set on the regional distribution of atmospheric mercury in Europe to date. In both experiments the short-term variability of measured concentrations has a decreasing amplitude in the diurnal cycle from the more southerly (German) to the more northerly (Swedish) sites. Significantly elevated concentrations have only been observed at the German sites. A very interesting observation was made after heavy rainfall at the most southerly site Neuglobsow. Immediately after the rain has started after a few warm days without any precipitation, the TGM concentration were significantly enhanced.

This finding gave first evidence and led to the hypothesis that rain may enhance mercury emission fluxes from soils however, other possible reasons could not principally be excluded. The influence of irrigation on evasional fluxes of mercury has later been reconfirmed by us and independent groups during an intercomparison exercise for mercury flux measurement methods at Steamboat Springs, Nevada, which is not part of the work presented here.

In general, the variability at the site Neuglobsow is dominated by a significant 24 h periodicity. The observed shift of the daily maximum TGM concentration from 5 a.m. during summer to 9 a.m. during winter supports the hypothesis that ambient air concentrations of mercury are influenced by meteorological, photochemical and biosphere/atmosphere exchange processes.

Just as significant as differences in regional variability of atmospheric mercury concentrations is the seasonal variability with generally higher concentrations in winter. This observation is consistent with our long-term data set obtained at Mace Head and with independent model results as well.

The transect data sets presently serve as experimental reference data for an international model intercomparison exercise under the UN-ECE Convention on Long-Range Transport of Air Pollutants (CLTRAP) which is coordinated by EMEP Meteorological Synthesizing Center East in Moscow, Russia.

Numerical models generally use a constant vertical mixing ratio of atmospheric mercury as an initial parameter however, reliable experimental data on the vertical distribution to support or to validate this important boundary condition hardly existed and gave conflicting results.

Within the mixing layer the horizontal distribution of atmospheric mercury is very homogeneous over a distance of 400 km with slightly decreasing concentrations to the north. This could be explained by an incomplete exchange of an air mass with low TGM concentrations replacing from the north the air mass with higher TGM concentrations. A similar homogeneous distribution was observed during the level flight above the mixing layer

over the same distance. Major conclusions of our aircraft measurements are: a) atmospheric mercury is evenly distributed within an air mass over long distances, b) concentrations may change with the change of air masses, and c) slight differences between atmospheric mercury concentrations in the mixing layer and the free troposphere may be due to different air masses rather than a vertical gradient.

The aircraft measurements reported in this work differ from almost all older aircraft measurements of atmospheric mercury concentrations but are in good agreement with the generally accepted long residence of elemental mercury in the atmosphere. In addition, older reports gave no experimental details allowing any conclusion about the pressure dependence of the instruments used in these measurements. It can be concluded that further TGM measurements onboard aircrafts are needed. In the meantime aircraft studies on atmospheric mercury have been increasingly carried out in North America however, their results are not available in the scientific literature to date.

Long-term monitoring of atmospheric mercury at Mace Head, Ireland

The Mace Head atmospheric research station is ideally placed to study western inflow boundary conditions of atmospheric trace gases travelling from the Atlantic Ocean into northwestern Europe. Between September 1995 and December 2001 no trend in the atmospheric mercury concentrations could be seen at this location. If shorter time scales are used, a 4 % increase is detected between 1995 and 1997 in the entire data set. A similar increase of about 4 % was found for filtered clean sector data (representing air masses that are clearly of marine origin) for the time period 1995 to 1999.

The annual average concentration levels at Mace Head derived from the entire measurement data between 1995 and 2001 remain fairly constant at 1.74 ng m^{-3}. Comparison with 4 short-term monitoring data sets of two Swedish sites that measured TGM in 1998/99 with similar instrumentation reveals that the atmospheric mercury concentration data obtained at Mace Head are on an average higher than those measured at the continental sites. We observed that the Mace Head data are about 0.2 to 0.3 ng m^{-3} higher than those of the two Scandinavian background stations. Transport from North America across the Atlantic may well occur, but such large scale processes should not only affect the Mace Head station, but also the Swedish sites close to Stockholm and Gothenburg, respectively. No local anthropogenic emission source exists near Mace Head. Higher concentrations at Mace Head may partly be explained by emissions of mercury from the ocean surface or by oxidative removal processes of TGM while the air masses are traveling from west to east. However, it should be noted that in

general the concentration levels measured at Mace Head are on an average lower than those found at continental European sites that are influenced by anthropogenic mercury emissions.

A south to north concentration gradient of atmospheric mercury between highly industrialized Eastern Germany and Central Sweden has been previously reported and could be attributed to regional anthropogenic emissions especially from the area around Halle/Leipzig/Bitterfeld in Eastern Germany. The reason for the observed west-to-east decreasing gradient from Mace Head to remote sites in Scandinavia is not yet clear.

Another interesting aspect is the comparison of the Mace Head data with those obtained at Alert (82.5ºN; 62.3ºW) in the Canadian Arctic. Both data sets start in 1995 (January and September respectively) and are ongoing. The long-term average at both sites is around 1.7 ng m^{-3} over the years, both sites do not show a trend of concentrations over time. However, at Alert the phenomenon of the so-called "Mercury Depletion Events (MDEs)" can be observed each year after polar sunrise. By a complex sequence of photolytically mediated chemical and physical processes (which are not yet completely understood) atmospheric mercury concentrations drop below the background value several times for several hours up to days. Recently, MDEs have also been detected at Barrow, Alaska (71º 19'N;156º 37'W) the Eastern part of Hudson Bay (Kuujjuarapik, 55º30'N; 77º73'W) and at a coastal site in the Antarctic (Neumayer, 70º39'S, 8º15'W), as described in this work.

Although Mace Head is only 2 degrees latitude south of the Canadian station Kuujjuarapik, MDEs have never been observed in our data set between 1995 and 2001. We propose that the total absence of sea ice at this coastal location may be a possible explanation for the significantly different environmental chemistry of atmospheric mercury at these two sites.

Monitoring of atmospheric mercury at Mace Head is planned to continue until at least October 2004.

Global distribution and Antarctic springtime depletion of atmospheric mercury

A significant concentration gradient of atmospheric mercury has been measured onboard the *RV Polarstern* between the two hemispheres with a higher northern hemispheric mean. This finding is in good agreement with earlier work that also report a significant change in TGM concentration while passing the inner tropical convergence zone (ITCZ).

The southern hemispheric mean is of value 1.3 ng m^{-3} and about 30 % lower than the corresponding value for the northern hemisphere. The variability of concentrations was quite large beween 30º North and the equator. Between 10º and 70º South atmospheric mercury concentration are evenly distributed.

Data on atmospheric mercury concentrations in the Antarctic are extremely limited and no knowledge existed on the short-term variability during the time period after Antarctic polar sunrise so far. The measurements reported in this work comprise the first annual time series of atmospheric mercury measurements in the Antarctic. It could be shown for the first time that mercury depletion events (MDEs) do occur in the South polar regions and that these events are positively correlated with ground level ozone concentrations during Antarctic spring. MDEs are supposed to lead to an increased input of atmospheric mercury into the polar ecosystem in the ecologically sensitive springtime period. It could also be demonstrated that MDEs coincide with enhanced occurrence of BrO radicals in the Antarctic atmosphere. Statistical analysis has been carried out to obtain information on the reaction kinetics and the reaction partners involved in MDEs. At Neumayer station the first MDEs occur 1–2 months earlier than in the Canadian Arctic and the role of the latitudinal positions and sea ice coverage were evaluated. At Alert polar sunrise takes place later in the season. Most of the sea ice where enhanced BrO concentrations are found is located north of Neumayer station at lower latitudes. In comparison, the Arctic sea ice is found north of Alert at higher latitudes and around the North Pole. It can be concluded, that the sea ice as a possible place where the photochemical reaction of ozone and Br atoms and/or the following reaction of BrO radicals and vapor phase mercury can take place, is exposed much earlier to the sun in the Antarctic than in the Arctic during springtime.

Atmospheric mercury species distribution over the south Atlantic ocean and in the Antarctic during polar summer

Springtime depletion events (MDEs) suddenly end during Antarctic summer. A possible explanation of this phenomenon is presented in this work, showing that air masses originating from the sea ice surface are a necessary prerequisite for the observation of depletions of atmospheric mercury at polar spring. Measurements of atmospheric mercury species during Antarctic summer at Neumayer during December 2000 – February 2001 show that fast photochemical oxidation of gaseous elemental mercury leads to variable Hg^0 concentrations during this period, with extremely high concentrations up to more than 300 pg/m^{-3} of reactive gaseous mercury (RGM). In contrast to this, mercury species measurements were also performed on board of the *RV Polarstern* for the first time. These measurements revealed constantly low RGM values and homogeneous background concentrations of TGM over the south Atlantic Ocean. These new findings suggest, that there is evidence for an enhanced oxidation potential of the Antarctic lower troposphere over the continent which needs to be considered for the interpretation of dynamic transformations of mercury during summertime and possibly other redox reactions as well.

Beside solar radiation, the origin of the air parcels and their contact with sea ice are important factors and could be a major requirement for the sudden end of MDEs at Neumayer Station. It appears that below a certain percentage of sea ice coverage north of the site, the probability of observing air masses depleted in mercury concentration is drastically decreased.

Furtheron, an explanation is proposed how different oxidation mechanisms can lead to high RGM levels during Antarctic summer while they are accompanied with negatively correlated surface-level ozone concentrations; which is exactly the opposite behavior when compared with the springtime depletion period.

Tropospheric mercury concentrations in polar regions are very sensitive to species transformations caused by photochemically-driven oxidation processes during the sunlit time of the year. After the end of MDEs in November 2000 we found a different behaviour of TGM and surface-level ozone during Antarctic summer. Ozone was not destroyed but could have rather been produced via a photochemical reaction of ozone precursors like NO and NO_2 over the Antarctic continent. This phenomenon could be associated with an enhanced oxidation potential affecting the transformation of various chemicals (e.g. Hg^0) leading to different exchange processes between the atmosphere, snow, and ice.

The dynamic species transformations of atmospheric mercury during Antarctic summer presented here illustrate the complexity of photochemical reactions in polar regions and have revealed the limitations in our understanding of the chemical cycling in remote regions with seasonnally variable sea-ice coverage. Further studies on possible reaction mechanisms and kinetics of these phenomena are necessary to assess the resulting input into the polar biosphere. At present it is not clear (i.) how much of the deposited mercury can be reemitted from snow pack after photochemically induced reduction, (ii.) what the ultimate fate of deposited mercury is during and after snowmelt, (iii.) how much mercury remains in the terrestrial (tundra) environment and what fraction enters the polar oceans.

The major question that remains to be answered is a mass balance for the polar regions: what percentage of the atmospheric mercury that is deposited during polar springtime remains in the ecosystem and is finally entering the foodchain ?

9 References

Advokaat, E.M. and Lindberg, S.E. (1996): Effect of rainfall exclusion on air/surface exchange rates of mercury over forest soils, In: Ebinghaus, R., Petersen, G., Tümpling, U. v. (eds.), 1996: Fourth International Conference on Mercury as a Global Pollutant, Book of Abstracts, Hamburg August, 4–8, 1996, p. 458 (GKSS Forschungszentrum Geesthacht GmbH, Max-Planck-Str., D-21502 Geesthacht, Germany).

Airey, D. (1982): Contributions from coal and industrial materials to mercury in air, rainwater and snow. Sci Tot. Environ. 25, 19–40.

Akeredolu. F., Barrie, L.A., Olson, M.P., Oikawa, K.K., Pacyna, J.M. (1994): The flux of anthropogenic trace metals into the Arctic from mid-latitudes in 1989, Atmospheric Environment, 28 (8), 1557–1572.

Amyot, M., Mierle, G., Lean, D.R.S., McQueen, D.J. (1995): Volatilization of Hg from lakes mediated by solar radiation, Proc. 1995 Canadian Mercury Network Workshop, York University, Toronto, Ontario, Canada.

Arimoto, R. (2002): New Mexico State University, Carlsbad, personal communication.

Amyot, M., Mierle, G., Lean, D.R.S. and McQueen, D.J. (1994): Sunlight-induced formation of dissolved gaseous mercury in lake waters, Environ. Sci. Technol. 28, 2366–2371.

Axenfeldt, F., Münch, J., Pacyna, J. (1991): Europäische Test-Emissionsdatenbasis von Quecksilberkomponenten für Modellrechnungen. In: Petersen, G. (Ed.) Belastung von Nord-und Ostsee durch ökologisch gefährliche Stoffe am Beispiel atmosphärischer Quecksilberverbindungen. Abschlussbericht des Forschungsvorhabens 10402726 des Umweltforschungsplanes des Bundesministers für Umwelt, Naturschutz und Reaktorsicherheit. Im Auftrag des Umweltbundesamtes, Berlin, External Report GKSS 92/E/111, GKSS Research Centre Geesthacht, Max-Planck-Str., D-21502 Geesthacht, Germany.

Bacon, C.E., Jarman, W.M., Cossa, D.P. (1992): Organochlorine and polychlorinated biphenyl levels in pinniped milk from the Arctic the Antarctic, California and Australia, Chemosphere, 24 (6), 779–791.

Baeyens, W. and Leermakers, M. (1996): Particulate, dissolved and methylmercury budgets for the Scheldt estuary (Belgium and The Netherlands), In: Baeyens W., Ebinghaus, R. and Vasiliev, O. (eds): Global and Regional Mercury Cycles: Sources, Fluxes and Mass Balances. NATO-ASI-Series, 2. Environment - Vol. 21, Kluwer Academic Publishers, Dordrecht, The Netherlands, pp. 285–301.

Baeyens, W., Leermakers, M., Dedeurwaerder, H. and Lansens, P. (1991): Modelization of the mercury fluxes at the air-sea interface, Water, Air, Soil Pollut. 56, 731–744.

Bahlmann, E. (1997): Untersuchungen einer GC/AFS Kopplung zur Bestimmung flüchtiger Quecksilberspezies in der Elbe, Magisterarbeit Universität Lüneburg.

Baker, P.G.L., Brunke, E.G. Slemr, F., Crouch, A.M. (2001): Measurement of atmospheric mercury at a baseline station in South Africa, Atmos Environ, in press.

Bard, S.M. (1999): Global transport of anthropogenic contaminants and consequences for the Arctic marine ecosystem, Marine Pollution Bulletin, 38 (5), 356–379.

Bargagli, R., Barghigiani, C., Siegel, B.Z. and Siegel, S.M. (1989): Accumulation of mercury and other metals by the lichen, *Parmelia sulcata*, at an Italian minesite and a volcanic area, Water, Air, Soil Pollut. 45, 315–327.

Barnett, M.O., Harris, L.A., Turner, R.R., Henson, T.J., Melton, R.E., Stevenson, R.J. (1995): Characterization of mercury species in contaminated floodplain soils, Water, Air, Soil Pollut. 80, 1105–1108.

Barrie, L.A. (1986): Arctic Air Pollution: An overview of current knowlegde, Atmospheric Environment, 20 (4), 643–663.

Barrie, L.A., Olson, M.P., Oikawa, K.K. (1989): The flux of anthropogenic sulphur into the Arctic from mid-latitudes in 1979/80, Atmospheric Environment, 23 (11), 2505–2512.

Barrie, L.A, Bottenheim, J.W. (1991): Sulphur and nitrogen in the Arctic atmosphere. In: Pollution of the Arctic Atmosphere, (ed.) Sturges, W.T., Ch. 6, Elsevier, Barking, U.K.

Barrie, L.A., Gregor, D., Hargrave, B., Lake, R., Muir, D., Shearer, R., Tracey, B., Bidleman, T. (1992): Arctic contaminants: Sources, occurrences and pathways, Science of the Total Environment, 122, 1–74.

Barrie, L.A., Macdonald, R., Bidleman, T., Diamond, M., Gregor, D., Semkin, R., Strachan, W., Alaee, M., Backus, S., Bewers, M., Gobeil, C., Halsall, C., Hoff, J., Li, A., Lockhart, L., Mackay, D., Muir, D., Pudykiewics, J., Reimer, K., Smith, J., Stern, G., Schroeder, W.H., Wageman, R., Wania, F., Yunker, M. (1997): Ch. 2, Sources, Occurrence and Pathways. In: Canadian Arctic Contaminants Assessment Report, (eds) Jensen, J., Adare, K., Shearer, R., Indian and Northern Affairs, Ottawa, Canada.

Beine, H.J. (1997) Measurements of CO in the high Arctic. AGU Fall meeting 1997.

Berdowski J.J.M., Baas J.,Bloos J.-P.J., Visschedijk A.J.H., and Zandveld P.Y.J., (1997) The European Emission Inventory of Heavy Metals and Persistent Organic Pollutants. TNO , Report UBA-FB, UFOPLAN. Ref,No. 104.02 672/03, Apeldoorn, 239p.

Bidleman, T., Patton, G.W., Walla, M.D., Hargrave, B.T., Vass, W.P., Erichson, P., Rowler, B., Scott, V., Gregor, D.J. (1989): Toxaphene and other organochlorines in Arctic ocean fauna: evidence for atmospheric delivery, Arctic, 42 (4), 307–315.

Biester, H. and Scholz, C. (1997): Determination of Mercury phases in Contaminated Soils - Hg-Pyrolysis versus Sequential Extractions, Environ. Sci. Technol. 31, 233–239.

Bloom, N.S. (1988): Determination of picogram levels of methylmercury by aqeous phase ethylation, followed by cryogenic gas chromatography with cold vapor atomic fluorescence detection, Can. J. Fish Aq. Sci., 46, 1131.

Bloom, N.S., Watras, C.J. (1988): Observations of methylmercury in precipitation, Sci Total Environ, 87/88, 199–207.

Bloom, N.S., Prestbo, E.M., Tokos, J.S., Van der Geest, E., Kuhn, E.S. (1996): Distribution and origins of mercury species in the Pacific Northwest atmosphere, in: Ebinghaus, R., Petersen, G., von Tümpling, U. (eds), 4th International conference on Mercury as a Global Pollutant, Book of Abstracts, Hamburg, August 4–9, 1996, p. 90, (GKSS Forschungszentrum Geesthacht GmbH, Max-Planck-Str., D-21502 Geesthacht, Germany).

Boudris, H.; Bottenheim, J.W. *Geophys. Res. Lett.* **2000**, *27* (*4*), 517–520.

Boutron, C.F.; Vandal, G.M.; Fitzgerald, W.F.; Ferrari, C.P. *Geophys. Res. Lett.* **1998**, *25*, 3315–3318.

Braman, R.S. and Johnson, D.L. (1974): Selective absorption tubes and emission technique for the determination of ambient forms of mercury in air, Environ. Sci. Technol., 8, 996–1003.

Branches, F.J.P., Erickson, T.B., Aks, S.E., and Hryhorczuk, D.O. (1993): The price of gold: mercury exposure in the Amazon rain forest, Clin Toxicol, 31, 295–306.

Brosset, C., Lord, E. (1991): Mercury in precipitation and ambient air – a new scenario, *Water Air Soil Poll*, 56, 493–506.

Brosset, C. and Lord, E. (1991): Mercury in precipitation and ambient air. A new scenario, *Water, Air and Soil Pollution*, 56, 493–506.

Brosset, C. (1987): The behavior of mercury in the physical environment. Water Air Soil Pollut. **34**, 145–166.

Brosset, C. (1982): Total airborne mercury and its possible origin, Water Air Soil Poll., 17, 37–50.

Bullock, O.R.., Jr.(2000): Science of the Total Environment, 259, 145.

Brunke, E.G., Labuschagne C., Slemr, F. (2001): Gaseous mercury emissions from a fire in the Cape Peninsula, South Africa, during January 2000, Geophys. Res. Letters, in press.

Burke, J., Hoyer, M., Keeler, G., and Scherbatskoy, T., (1995) Wet deposition of mercury and ambient mercury concetration at a site in the lake Champlain basin, Water, Air, and Soil Pollution, 80:353–362.

Camargo, J.A. (1993): Nature 365, 302

Carpi, A., Lindberg, S.E. (1997): The sun-light mediated emission of elemental mercury from soil amended with municipal sewage sludge, Environ Sci Technol, 31, 2085–2091.

Carpi, A. and Lindberg, S.E. (1998): Application of a Teflon™ dynamic flux chamber for quantifying soil mercury flux: tests and results over background soil, Atmos. Environ., 32, 873–882.

Carpi, A., Lindberg, S.E., Prestbo, E.M. and Bloom, N.S. (1997): Methyl mercury contamination and transport in municipal sewage sludge amended soil, submitted to J. Environ. Qual.

Centre for Toxic Metals Newsletter (1999), 5, Issue 2, page 2.

Cleary, D. (1996): Mercury contamination in the developing world: Problems and solutions, In: Ebinghaus, R., Petersen, G., Tümpling, U. v. (eds.), 1996: Fourth International Conference on Mercury as a Global Pollutant, Book of Abstracts, Hamburg August, 4–8, 1996, p. 3 (GKSS Forschungszentrum Geesthacht GmbH, Max-Planck-Str., D-21502 Geesthacht, Germany).

CIMELCO (1991): Proyecto Binacional Puyango-Tumbes, Consorcio Cimelco Construtores, Tumbes, Peru.

Coggins, A.M. (2000): Long term measurements of total gaseous mercury (TGM) at Mace Head and atmospheric deposition of heavy metals in ombrogenous peats in the West of Ireland, PhD Thesis, National University of Ireland, Galway, Ireland.

Cooke, W.F., Jennings, S.G., and Spain, T.G. (1997): Black carbon measurements at Mace Head, 1989–1996. J. Geophys. Res., 102, 25,339–25,346.

Cossa, D., Coquery, M., Gobeil, C. and Martin, J.M. (1996): Mercury fluxes at the ocean margins, In: Baeyens, W., Ebinghaus, R., Vasiliev, O. (eds.): Global and Regional Mercury Cycles: Sources, Fluxes and Mass Balances. NATO-ASI-Series, Vol. 21, Kluwer Academic Publishers, Dordrecht, The Netherlands, 229–247.

Cossa, D. and Gobeil, C. (1996): Speciation and mass balance of mercury in the lower St. Lawrence estuary and Saguenay Fjord (Canada), In: Ebinghaus, R., Petersen, G., Tümpling, U. v. (eds.), 1996: Fourth International Conference on Mercury as a Global Pollutant, Book of Abstracts, Hamburg August, 4 – 8, 1996, p. 458 (GKSS Forschungszentrum Geesthacht GmbH, Max-Planck-Str., D-21502 Geesthacht, Germany).

Coquery, M. (1995): Mercury speciation in surface waters of the North Sea, Neth. J. of Sea Res., 34, 245–259.

Crawford, J.H., Davis, D.D.; Chen, G.; Buhr, M.; Oltmans, S.; Weller, R.; Mauldin, L.; Eisele, F.; Shetter, R.; Lefer, B.; Arimoto, R.; Hogan, A. (2001): Evidence for photochemical production of ozone at the South Pole surface, Geophysical Research Letters, 28, 19, 3641–3644.

Dastoor, A.P., Pudykiewicz, J. (1996): A numerical global meteorological sulfur transport model and its application of Arctic air pollution, Atmospheric Environment, 30 (9), 1501–1522.

Davis, D.; Novak, J.B.; Chen, G.; Buhr, M.; Arimoto, R.; Hogan, A.; Eisele, F.; Mauldin, L.; Tanner, D.; Shetter, R.; Lefer, B.; McMurry, P. (2001): Unexpected High Levels of NO Observed at South Pole, Geophysical Research Letters, 28, 19, 3625–3628.

Dewailly, E., Ayotte, P., Bruneau, S., Laliberte, C., Muir, D.C.G., Norstrom, R.J. (1993): Breast milk contamination by PCDDs, PCDFs and PCBs in Arctic Québec: A preliminary assessment, Chemosphere, 24 (7–10), 1245–1249.

Dumarey , R., Temmermann, E., Dams, R. and Hoste, J. (1985): The accuracy of the vapor-injection calibration method for the determination of mercury by amalgamation/cold vapour atomic absorption spectrometry, Analytica Chimica Acta, 170, 337 – 340

Dyvik F. (1995): Mercury as trace contaminant in non ferrous metal production. Occurrence, distribution, waste and gas treatment and mercury free sulphuric acid production by the use of the Boliden/Norzink process for gas. In : Proceedings of Academy of certified Hazardous materials Managers, Conf. and Annual meeting, August 1–4, Rochester, N.Y., pp 15.

Ebinghaus, R., Kock, H.H., Temme, Ch., Einax, J.W., Löwe, A.G., Richter, A., Burrows, J.P., Schroeder, W.H. (2002): Antarctic springtime depletion of atmospheric mercury, Environmental Science and Technology, 36, 1238–1244.

Ebinghaus, R., Kock, H.H., Coggins, A.M., Spain, T.G., Jennings, S.G., Temme, Ch. (2002): Long-term measurements of atmospheric mercury at Mace Head, Irish west coast between 1995 and 2001, submitted to Atmospheric Environment.

Ebinghaus, R., Kock, H.H., Hempel, M. (2000): Bestimmung von Quecksilber in Umgebungsluft mit Hilfe von zeitlich hochauflösenden On-line Verfahren, Gefahrstoffe – Reinhaltung der Luft, 60, 5, 205 – 211.

Ebinghaus, R., Jennings, S.G. , Schroeder, W.H. , Berg, T., Donaghy, T., Guentzel, J., Kenny, C., Kock, H.H., Kvietkus, K., Landing, W., Munthe, J., Prestbo, E.M., Schneeberger, D., Slemr, F., Sommar, J., Urba, A., Wallschläger, D., Xiao, Z. (1999): International field intercomparison measurements of atmospheric mercury species at Mace Head, Ireland, Atmos. Environ., 33 , 3063–3073.

Ebinghaus, R. and Krüger, O. (1996): Emission and Local Deposition Estimates of Atmospheric Mercury in North Western and Central Europe, In: W. Baeyens, R.Ebinghaus, and O.Vasiliev (eds.): Global and Regional Mercury Cycles: Sources, Fluxes and Mass Balances. NATO-ASI-Series, 2. Environment – Vol. 21, Kluwer Academic Publishers, Dordrecht, The Netherlands, 135 - 159.

Ebinghaus, R., Kock. H.H. (1996): Neuere Verfahren zur Analytik von Quecksilber in Luft, Gefahrstoffe – Reinhaltung der Luft, 56, 179 –183.

Ebinghaus, R., Kock, H.H., Jennings, S.G. and Spain, T.G. (1996): Continuous measurements of total gaseous mercury at Mace Head, Ireland, Fourth International Conference on Mercury as a Global Pollutant, Book of Abstracts, (edited by Ebinghaus, R., Petersen, G. and von Tümpling, U.), GKSS Forschungszentrum, Max-Planck-Str., D-21502 Geesthacht, Germany.

Ebinghaus, R., Kock, H.H., Jennings, S.G., McCartin, P., Orren, M.J. (1995): Measurements of Atmospheric Mercury Concentrations in Northwestern and Central Europe --- Comparison of Experimental Data and Model Results, Atmos Environ, Vol. 29, No. 22, pp. 3333 – 3344.

Ebinghaus, R. and Wilken, R.D. (1993): Transformations of mercury species in the presence of Elbe river bacteria, Appl. Organomet. Chem. 7, 127–135.
Edner, H. et al. (1991): Lidar search for atmospheric atomic mercury in Icelandic geothermal fields, J. Geophys. Res. 96D, 2977–2986.

Eppel, D.P., Petersen, G., Misra, P.K., Bloxam, R. (1991): A numerical model for simulating pollutant transport from a single point source, Atmos. Environ., 25a, (7), 1391 – 1401.

Expert Panel on Mercury Atmospheric Processes (1994): Mercury atmospheric processes: a synthesis report, workshop proceedings, EPRI/TR-104214, Tampa, Florida, September 1994.

Fairbridge, R.W. (1966): The encyclopedia of oceanography, Reinhold Publishing Corporation, New York.

Ferrara, R. et al. (1994): Atmospheric mercury emission at Solfatara volcano (Pozzuoli, Phlegraean Fields – Italy), Chemosphere 29, 1421–1428.

Ferrara, R., Maserti, B.E., Petrosino, A., Bargagli, R. (1988): Mercury levels in rain and air and the subsequent wash-out mechanism in a central Italian region, Atmos. Environ., 20, 125–128.

Finlayson-Pitts, B.J. and Pitts, J.N. (1986): Atmospheric chemistry: fundamentals and experimental techiques, John Wiley & Sons, New York.

Fitzgerald, W.F., Engstrom, D.R., Mason, R.P., Nater, E.A. (1998): The case for atmospheric mercury contamination in remote areas, Environ. Sci. Technol., 32, 1–7.

Fitzgerald, W.F. (1996): Mercury emissions from volcanoes, in: Ebinghaus, R., Petersen, G., von Tümpling, U. (eds), 4th International conference on Mercury as a Global Pollutant, Book of Abstracts, Hamburg, August 4–9, 1996, p. 87, (GKSS Forschungszentrum Geesthacht GmbH, Max-Planck-Str., D-21502 Geesthacht, Germany).

Fitzgerald, W.F. and Mason, R.P. (1996): The global mercury cycle: oceanic and anthropogenic aspects, in: Baeyens, W., Ebinghaus, R., Vasiliev, O. (eds) Global and Regional Mercury Cycles: Sources, fluxes and mass balances, NATO ASI Series 2. Environment Vol. 21, Kluwer, Dordrecht, The Netherlands, pp 85–108.

Fitzgerald, W.F. (1995): Is mercury increasing in the atmosphere? The need for an atmospheric mercury network (AMNET), Water Air Soil Poll, 80, 245–254

Fitzgerald, W.F., Mason, R.P., Vandal, G.M. and Dulac, F. (1994): Air-water cycling of mercury in lakes, in: Watras, C.J. and Huckabee, J.W. (eds.): Mercury pollution: integration and synthesis, 203–220, Lewis Publishers, Boca Raton.

Fitzgerald, W.F. (1993). Global biogeochemical cycling of mercury, in: Allan, R.J. and Nriagu, J.O. (eds.): Proc. 9th Int. Conf. Heavy Met. Environ. 1, 320–323, Toronto, 12.–17.9.1993, CEP Consultants Ltd., Edinburgh.

Fitzgerald, W.F., Mason, R.P. and Vandal, G.M. (1991): Atmospheric cycling and air-water exchange of mercury over mid-continental lacustrine regions, Water, Air, Soil Pollut. 56, 745–767.

Fitzgerald, W.F. (1986): Cycling of mercury between the atmosphere and oceans. In : The role of air-sea exchange in geochemical cycling, NATO, AIS, Reidel Publishing Co., dordrecht, The Netherlands, 363–408.

Fitzgerald, W.F., Gill, G.A. and Kim, J.P. (1983): An equatorial pacific ocean source of atmospheric mercury, *Science*, 224, 597–599.

Fitzgerald, W.F. und Gill, G.A. (1979): Subnanogram determination of mercury by two-stage gold amalgamation and gas-phase detection applied to atmospheric analysis, Analytical Chemistry, 51, 1714–1720.

Friess, U. (2001): Spectroscopic measurements of atmospheric trace gases at Neumayer-Station, Antarctica; Ph.D. Thesis, University of Heidelberg, Heidelberg, Germany, 2001.

Goldberg, E.D. (1975): Synthetic organohalides in the sea, Proceedings of the Royal Society of London, Series B, 189, 277–289.

Gustin, M.S., Taylor, G.E., Leonard, T.L. and Keislar, R.E. (1996): Atmospheric mercury concentrations associated with geologically and anthropogenically enriched sites in Central Western Nevada, Environ. Sci. Technol. 30, 2572–2579.

Gustin, M.S., Lindberg, S.E., Austin, K., Coolbaugh, M., Vette, A., Zhang, H. (2001): Assessing the contribution of natural sources to regional atmospheric mercury budgets, Science of the Total Env, in press.

Hall, B., Schager, P., Lindqvist, O. (1991): Chemical reactions of mercury in combustion flue gases, Water Air Soil Pollut, 56, 3–14.

Halsall, C.J., Barrie. L.A., Fellin, P., Muir, D.C.G., Billeck, B., Lockard, L., Rovinski, F.Ya., Konovov, E.Ya. (1997): Spatial and temporal variations of polycyclic aromatic hydrocarbons in the Arctic atmosphere, Environmental Science and Technology, 31 (12), 3593–3599.

Hanson, P.J., Lindberg, S.E., Tabberer, T.A., Owens, J.G., Kim, K.H. (1995): Foliar exchange of mercury vapor: evidence for a compensation point, Water Air Soil Poll, 80, 373–382.

Hao, W.D., Ward, D.E., Olbu, G., Baker, S.P. (1996): Emissions of CO2, CO, and hydrocarbons from fires in diverse African savanna ecosystems, J. Geophys. Res., 101, 23577–232584.

Hegels, E.; Crutzen, P.J.; Klüpfel, T.; Perner, D.; Burrows, P.J. (**1998):** Geophys. Res. Lett. 25, 3127–3130.

Helwig, A., Neske, P. (1990): Zur komplexen Erfassung von Quecksilber in der Luft. In: Aktuelle Aufgaben der Messtechnik in der Luftreinhaltung, *VDI Berichte* 838, 457–466, VDI Verlag Düsseldorf, Germany.

Horvat, M. (1996): Mercury analysis and speciation in environmental samples, pp. 1–31, In: W. Baeyens, R. Ebinghaus and O.Vasiliev (eds.): Global and Regional Mercury Cycles: Sources, Fluxes and Mass Balances. NATO-ASI-Series, 2. Environment – Vol. 21, Kluwer Academic Publishers, Dordrecht, The Netherlands.

Horvat, M., Bloom, N.S. and Liang L. (1993): A comparison of distillation with other current isolation methods for the determination of methyl mercury compounds in low level environmental samples: Part 2, water, Anal. Chimica Acta, 282, 153.

Ikingura, J.R. and Mutakyahwa (1995): Sources of mercury contamination and exposure in Tanzania. Proc. Int. Conf. on mining and environment in Easter and Southern Africa, 23–27 Oct., 1995, Mwanza, Tanzania.

Ikingura, J. (1994): Mercury contamination from gold-mining in Tanzania. In: Evaluation of the role and distribution of mercury on ecosystems with special emphasis on tropical regions. SCOPE, Rio de Janeiro, (unpublished).

Iverfeldt, Å. (1995): Mercury chemistry in air and its atmospheric residence time, Proc. 1995 Canadian Mercury Netwok Workshop, York University, Toronto, Ontario, Canada.

Iverfeldt Å. (1991) Mercury in forest canopy throughfall water and its relation to atmospheric deposition. Water Air Soil Pollut. 56, 553–564.

Iverfeldt Å. (1991a) Occurrence and turnover of atmospheric mercury over the Nordic countries . Water Air Soil Pollut. 56, 251–265.

Iverfeldt, A., Munthe, J., Brosset, C., Pacyna, J. (1995): Long-term changes in concentration and deposition of atmospheric mercury over Scandinavia, Water Air Soil Poll., 80, 227–233.

Iversen, T., Joranger, E. (1985): Arctic air pollution and large scale atmospheric flows, Atmospheric Environment, 19 (12), 2099–2108.

Ionov, V.A., Nazarov, I.M. and Fursov, V.Z. (1976) Mercury transport in the atmosphere, Reports Acad. Science USSR **228**, 456–459.

Jacobs, L.A., Klein, S.M. and Henry, E.A. (1995): Mercury cycling in the water column of a seasonally anoxic urban lake (Onondaga Lake, NY), Water, Air, Soil Pollut. 80, 553–562.

Jaenicke, R.; Dreiling, V.; Lehmann, E.; Koutsenoguii, P.K.; Stingl, J. (1992): Condensation nuclei at the German Antarctic Station "Georg von Neumayer", Tellus, 44B, 311–317.

Jaisinki, S.M. (1995): The materials flow of mercury in the United States. Resour. Conser. Recycl, 15, 145–179.

Jennings, S.G. McGovern, F. and Cooke, W.F. (1993): Carbon mass concentration measurements at Mace Head, on the west coast of Ireland, *Atmos. Environ.* 27A, 1229–1239.

Jensen, A., and Iverfeldt, A. (1994) Atmospheric bulk deposition of mercury to the southern Baltic sea area, In:Watras, C.J. and Huckabee, J.W. (eds) *Mercury Pollution: Integration and synthesis*, Lewis Publishers, Ann Arbor, Michigan, PP. 221–229.

Junge, C.E. (1977): Basic considerations about trace gas constituents in the atmosphere as related to the fate of global pollution, in: Fate of pollutants in the air and and water environments, part 1, vol 8. Wiley, New York, pp 7–23.

Keeler, G., Glinsorn, G. and Pirrone, N. (1995) Particulate mercury in the atmosphere.: Its signifcance, transoport, transformations and sources. Water Air and Soil Pollution, 80, 159–168.

Kerr, R.A. (1979): Global pollution: is the Arctic Haze actually industrial smog ?, Science, 205, 290–293.

Kim, K.H., Lindberg, S.E. and Meyers, T.P. (1995): Micrometeorological measurements of mercury vapor fluxes over background forest soils in Eastern Tennessee, Atmos. Environ. 29, 267–282.

Kim, K.H. and Lindberg, S.E. (1995): Design and initial tests of a dynamic enclosure chamber for measurements of vapor-phase mercury fluxes over soils, Water Air Soil Pollut. 80, 1059–1068.

Kim, J.P. and Fitzgerald, W.F. (1986) Sea-air partitioning of mercury in the equatorial Pacific ocean. Science, 231, 1131–1133.

Klusman, R.W. and Matoske, C.P. (1983): Adsorption of mercury by soils from oil shale development areas in the Piceance Basin of Northwestern Colorado, Environ. Sci. Technol. 17, 251–256.

Klusman, R.W. and Webster, J.D. (1981): Meteorological noise in crustal gas emission and relevance to geochemical exploration, J. Geochem. Explor. 15, 63–76.

Kovalevsky, A.L. (1986): Mercury-biogeochemical exploration for mineral deposits, Biogeochem. 2, 211–220.

Koppmann, R., Khedim, A., Rudolph, J., Poppe, D., Andreae, M.O., Helas, G., Welling, W., Zenker, T. (1997): Emissions of organic trace gases from savanna fires in southern Africa during the 1992 Southern African Fire Atmospheric Research Initiative and their impact on the formation of tropospheric ozone, J. Geophys. Res., 102, 18879–18888.

Kreher, K.; Johnston, P.V.; Wood, S.W.; Platt, U. (**1997):** *Geophys. Res. Lett.*, *24*, 3021–3024.

Krüger, O., Ebinghaus, R., Kock, H.H., Richter-Politz, I. and Geilhufe, Ch. (1999) Inverse modelling of gaseous mercury emissions at the contaminated industrial site BSL Werk Schkopau. In: *Mercury Contaminated Sites – Characterization, Risk Assessment and Remediation,* eds. R. Ebinghaus, R.R. Turner, D. Lacerda, O. Vasiliev, W. Salomons, Springer Environmental Science, Springer Verlag, Heidelberg, pp. 377–392.

Kuivala, A. (1984): Paper presented at the 32nd meeting of GDMB Zinkfachausschuss in Kokkola, Finland.

Kvietkus, K., Shakalis, I. and Rosenberg, G. (1985) Results of measurements of mercury concentrations in the atmosphere on horizontal and vertical profiles, Phys. Atmosphere, No. 10 69–72.

Kvietkus, K. (1995) Investigation of the gaseous and particulate mercury concentrations along horizontal and vertical profiles in the lower troposphere. In *Proceedings of the 10th World Clean Air Congress,* eds. P. Anttila, J. Kämäri, M. Tolvanen, Espoo, Finland, May 28 – June 2, 284.

Kvietkus, K., Xiao, Z., Lindqvist, O. (1995): Water, Air, Soil Pollut., 80, 1209–1216.

Lacerda , L.D. (1997): Evolution of mercury contamination in Brazil, Water Air Soil Poll, 97, 247–255.

Lacerda, L.D., Prieto, R.G., Marins, R.V., Azevedo, S.L.N., Pereira, M.C. (1995): Anthropogenic mercury emissions to the atmosphere in Brazil, in Proc. Int Conf on Heavy Metals in the environment, Hamburg, vol 1, pp 379–382.

Larjava, K. (1993): Doctorate Thesis, Technical Research Centre of Finland, Espoo, Finland.

Lee, D.S., Dollard, G.J., and Pepler, S. (1998) Gas phase mercury in the atmosphere of the United Kingdom, Atmos. Environ., 32, 855–864.

Lehrer, E. (1999): Polar tropospheric ozone loss; Ph.D. Thesis, University of Heidelberg, Heidelberg, Germany.

Lejenäs, H., Holmén, K. (1996): Characteristics of the large-scale circulation during episodes with high and löow concentrations of carbon dioxide and air pollutants at an Arctic monitoring site in winter, Atmospheric Environment, 30 (17), 3045–3057.

Lenschow, D.H., Stephens, P.L. (1982): The role of thermals in the boundary layer, Boundary layer meteorolgy, 19, 509 – 532.

Lindberg, S. E.; Brooks, S.; Lin, C.-J.; Scott, K.J.; Landis, M.S.; Stevens, R.K.; Goodsite, M.; Richter A. (2002): Dynamic Oxidation of gaseous Mercury in the Arctic Troposphere at Polar Sunrise, Environ. Sci. Technol., 36, 1245–1256.

Lindberg, S.E.; Brooks, S.; Lin, C-J.; Scott, K.J.; Landis, M.S.; Stevens, R.K. (2001): Formation of reactive gaseous mercury in the arctic: evidence of oxidation of Hg0 to gas-phase Hg-II compounds after arctic sunrise. Water, Air, Soil, Pollut., Focus 2001, 1, 295–302.

Lindberg, S. E., P. J. Hanson, T.P. Meyers, and K-Y Kim (1998): Micrometeorological studies of air/surface exchange of mercury over forest vegetation and a reassessment of continental biogenic mercury emissions. Atmos. Envir., 32, 895–908.

Lindberg, S.E., Hanson, P.J. Meyers, T.P., Kim, K.-Y. (1998): Micrometeorological studies of air/surface exchange of mercury over forest vegetation and a reassessment of continental biogenic mercury emissions, Atmos Environ, 32, 895–908.

Lindberg, S.E., Stratton, W.J. (1998): Atmospheric mercury speciation: Concentrations and behaviour of reactive gaseous mercury in ambient air, Environ Sci Technol, 32, 49–57.

Lindberg, S. E., T.P. Meyers, and C. Miles. 1997. Everglades mercury air/surface exchange study (E-MASE): Application of Field Methods and Models to Quantify Mercury Emission from Wetlands at the Everglades Nutrient Removal Project (ENR), First Annual Report to South Florida Water Management District.

Lindberg, S.E., Meyers, T.P., Munthe, J. (1996): Evasion of mercury vapor from the surface of a recently limed acid forest lake in Sweden, Water Air Soil Poll, 85, 2265–2270.

Lindberg, S.E. (1996): Forests and the global biogeochemical cycle of mercury: the importance of understanding air/vegetation exchange processes, in: Baeyens, W., Ebinghaus, R., Vasiliev, O. (eds) Global and Regional Mercury Cycles: Sources, fluxes and mass balances, NATO ASI Series 2. Environment Vol. 21, Kluwer, Dordrecht, The Netherlands, pp 359–380.

Lindberg, S.E., K-H. Kim, T.P. Meyers, and J.G. Owens (1995): A micrometeorological gradientapproach for quantifying air/surface exchange of mercury vapor: Tests over contaminated soils. Envir. Sci. Technol. 29:126–135.

Lindberg, S.E., Meyers, T.P., Taylor, G.E., Turner, R.R., Schroeder, W.H. (1992): Atmospheric /surface exchange of mercury in a forest: results of modeling and gradient approaches, J Geophys Res, 97, 2519–2528.

Lindberg, S.E., Jackson, D.R., Huckabee, J.W., Janzen., S.A., Levin, M.J., Lund, J.R. (1979): Atmospheric emission and plant uptake of mercury from agricultural soils near the Almadén mercury mine, J Environ Qual, 8, 572–578.

Lindberg, S.E. and Turner, R.R. (1977): Mercury emission from chlorine-production and solid waste deposits, Nature (London), 268, 133–136.

Lindqvist, O., , K., Aastrup, M., Andersson, A., Bringmark, L., Hovsenius, G., Hakanson, L., Iverfeldt, A., Meili, M. and Timm, B. (1991): Mercury in the Swedish Environment-Recent research on causes, consequences and corrective methods. Water Air Soil Pollut. 55, pp 261.

Lindqvist, O. and Rodhe, H. (1985) Atmospheric mercury – a review, Tellus 37B, 136–159.

Lindqvist, O.; Jernelöv, A.; Johansson, K. and Rodhe, H. (1984): Mercury in the Swedish environment, global and local sources, SNV PM 1816, Swedish Environmental Protection Agency, S-171 85 Solna, Sweden.

Lockhart, W.L.; Wilkinson, P.; Billeck, B.N.; Hunt, R.V.; Wagemann, R.; Brunskill, G.J. (1995): Water, Air and Soil Pollution, 80, 603–610.

Lockart, W.L., Stewart, R.E.A. (1992): Biochemical stress indicators in marine mammals. In: (eds.) Murray, J.L., Shearer, R.G. Synopsis of research conducted under the 1991/92 Northern Contaminants Program, Environmental Studies, 68, 158–164.

Logan, J.A. (1985) Tropospheric ozone: seasonal behaviour, trends, and anthropogenic influence, J. Geophys. Res., 86, 7210–7254.

Lu, J. Y.; Schroeder, W. H.; Barrie, L. A.; Steffen, A.; Welch, E.H.; Martin, K.; Lockhart, W. L.; Hunt, R.V. G. Boila and A. Richter. Magnification of atmospheric mercury deposition to polar regions in springtime: the link to tropospheric ozone depletion chemistry, Geophys. Res. Lett. 2001, 28, 3219–3222.

Lu, J.Y., Schroeder, W.H., Berg, T., Munthe, J., Schneeberger, D., Schaedlich, F. (1998): A device for sampling and determination of total particulate mercury in ambient air, Anal. Chem. Vol. 70, No 11, 2403–2408.

Martinez-Cortizas, A., Pontevedra-Pombal, X., Garcia-Rodeja, E., Novoa-Munoz, J.C., Shotyk, W. (1999): Mercury in Spanish peat bog: Archive of climate change and atmospheric metal deposition, Science, 284, 939–929.

Mason, R.P., Lawson, N.M. and Sullivan, K.A. (1997): The concentration and speciation of mercury in Chesapeake Bay precipitation, Atmos. Environ. 31, No. 21, 3541–3550.

Mason, R.P. and Fitzgerald, W.F. (1996): Sources, sinks and biogeochemical cycling of Mercury in the Ocean. In: W. Baeyens, R.Ebinghaus, and O.Vasiliev (eds.): Global and Regional Mercury Cycles: Sources, Fluxes and Mass Balances. NATO-ASI-Series, 2. Environment – Vol. 21, Kluwer Academic Publishers, Dordrecht, The Netherlands, 249–272.

Mason, R.P., Morel, F.M.M. and Hemond, H.F. (1995): The role of microorganisms in elemental mercury formation in natural waters. Water, Air Soil poll. 80, 775– 787.

Mason, R.P., Fitzgerald, W.F. and Morel, F.M.M. (1994a) The biogeochemical cycling of mercury: anthropogenic influences. Geochim. Cosmochim. Acta 58, 3191–3198.

Mason, R.P., O'Donnell, J. and Fitzgerald, W.F. (1994): Elemental mercury cycling within the mixed layer of the equatorial Pacific Ocean , in: Watras, C.J. and Huckabee, J.W. (eds.): Mercury pollution: integration and synthesis, 83–97, Lewis Publishers, Boca Raton.

Mason, R.P. and Fitzgerald, W.F. (1993): The distribution and biogeochemical cycling of mercury in the equatorial Pacific Ocean, Deep-Sea Res. 40, 1897–1924

Mason, R.P., Fitzgerald, W.F. and Vandal, G.M. (1992) The source and composition of mercury in Pacific Ocean rain. J. Atmos. Chem. **14**, 489 – 500.

Mason, R.P. and Fitzgerald, W.F. (1991): Mercury speciation in open ocean waters, Water, Air, Soil Poll., 56, 779–789.

McElroy, C.T.; McLinden, C.A.; McConnell, J.C. (**1999):** *Nature*, *397*, 338–341.

McNerney, J.J. and Buseck, P.R. (1973): Geochemical exploration using mercury vapor, Econ. Geol. 68, 1313–1320.

Meji, R, (1991): The fate of mercury in coal-fired power plants and the influence of wet flue-gas desulphurization . Water Air Soil Pollution. 56, 21–33.

Ming, G. (1994): In: Evaluation on the role and distribution of mercury in ecosystems with special emphasis on tropical regions, SCOPE, Rio de Janeiro (unpublished).

Mitchell, M. (1956): Visual range in the polar regions with particular reference to the Alaskan Arctic, Journal of Atmospheric and Terrestrial Physics, Special Supplement, 195–211.

Muir, D.C.G., Wageman, R., Hargrave, B.T., Thomas, D.J. Peakall, D.B., Norsstrom, R.J. (1992): Arctic marine ecosystem contamination, Science of the Total Environment, 122, 75–134.

Mukherjee, A.B., Sally, Innanen and M. Verta (1995): An update of the mercury inventory and atmospheric mercury fluxes to and from Finland Water, Air and Soil Pollution, 80, 255–264.

Munthe, J., I.Wängberg, N.Pirrone, A.Iverfeldt, R.Ferrara, P.Costa, R.Ebinghaus, X.Feng,K.Gardfelt, G.Keeler, E.Lanzillotta. S.E.Lindberg, J.Lu, Y.Mamane, E.Nucaro, E.Prestbo, S.R.Schmolke, W.H.Schroeder, J.Sommer, F.Sprovieri, R.K.Stevens, W.Stratton, G.Tuncel, A.Urba; (2001) Intercomparison of methods for sampling and analysis of atmospheric mercury species. Atmos. Environment, Vol 35/17, 3007–3017.

Munthe, J., Hultberg, H., Iverfeldt, Å. (1995): Mechanisms of deposition of methylmercury and merury to coniferous forests, Water Air Soil Poll, 80, 363–371.

Munthe, J. (1992): The aqueous oxidation of elemental mercury by ozone, Atmos Environ, 26A, 1461–1468.

Nico, L.G., Taphorn, D.C. (1994): Mercury in fish from gold-mining regions in upper Cuyuni River system, Venzuela, Fresenius Environ. Bull., 3, 287–292.

Nriagu, J.O.; Pacyna, J.M. (1988): Quantitative assessment of worldwide contamination of air, water and soils by trace metals, Nature, 333, 134–139.

Nriagu, J. (1994): Mechanistic steps in the photoreduction of mercury in natural waters, Sci. Total Environ., 154, 1–8.

Nriagu, J.O. (1989): A global assessment of natural sources of atmospheric trace metals, Nature 338, 47–49.

Nriagu, J.O. and Pacyna, J.M. (1988): Quantitative assessment of worldwide contamination of air, water and soils by trace metals. Nature, 33, 134–139.

Obolensky, A.A.(1996): Natural Mercury sources in the environment: contribution of Siberia In: W. Baeyens, R.Ebinghaus, and O.Vasiliev (eds.): Global and Regional Mercury Cycles: Sources, Fluxes and Mass Balances. NATO-ASI-Series, 2. Environment – Vol. 21, Kluwer Academic Publishers, Dordrecht, The Netherlands, 453-462.

Oehme, M. (1991): Dispersion and transport paths of toxic persistent organochlorines to the Arctic levels and consequences, Science of the Total Environment, 106, 43–53.

Oltmans, S.J. and Levy, H. II (1994) Surface ozone measurements from a global network. *Atmos. Environ.* 28**,** 9–24.

Ottar, B. (1981): The transfer of airborne pollutants to the Arctic region, Atmospheric Environment, 15, 1439–1445.

Pacyna, J.M. (2001): personal communication.

Pacyna, J.M., Pacyna E.G. (2000): Assessment of emissions/discharges of merucry reaching the Arctic environment, NILU Report OR7/2000, Norsk institutt for luftforskning, N-2027, Kjeller, Norway.

Pacyna, J.M. (1996): Emission inventories of atmospheric mercury from anthropogenic sources. In: W. Baeyens, R.Ebinghaus, and O.Vasiliev (eds.): Global and Regional Mercury Cycles: Sources, Fluxes and Mass Balances. NATO-ASI-Series, 2. Environment – Vol. 21, Kluwer Academic Publishers, Dordrecht, The Netherlands, 161–178.

Pacyna, J.M., Sofiev, M.A., Ebinghaus, R., Henden, E., Petersen, G., Schroeder, W.H., Slemr, F., Sokolov, V. and Yagolnitzer, M. (1996): Atmospheric mercury working group report, pp. 523–530, In: W. Baeyens, R. Ebinghaus and O.Vasiliev (eds.): Global and Regional Mercury Cycles: Sources, Fluxes and Mass Balances. NATO-ASI-Series, 2. Environment – Vol. 21, Kluwer Academic Publishers, Dordrecht, The Netherlands.

Pacyna., J.M. (1995): The origin of Arctic air pollutants: lessons learned and future research, Science of the Total Environment, 160, 39–53.

Pai, P., Karamandchandani, P., Seigneur, Ch. (1997): Simulation of the regional atmospheric transport and fate of mercury using a comprehensive Eulerian model, Atmos Environ, 31, 2717–2732.

Patrick, W.H. (1994): From wastelands to wetlands, J. Environ. Qual. 23, 892–896.

Petersen, G., Munthe, J., Pleijel, K., Bloxam, R. and Kumar, A.V. (1998) A comprehensive Eulerian modelling framework for airborne mercury species: development and testing of a tropospheric chemistry module. Atmos. Environ., 32-5, 829–843.

Petersen, G., Munthe J., Bloxam, R. (1996): Numerical modeling of regional transport, chemical transformations and deposition fluxes of airborne mercury species, in: Baeyens, W., Ebinghaus, R., Vasiliev, O. (eds) Global and Regional Mercury Cycles: Sources, fluxes and mass balances, NATO ASI Series 2. Environment Vol. 21, Kluwer, Dordrecht, The Netherlands, pp 191–218.

Petersen, G., Iverfeldt, Å., Munthe, J. (1995): Atmospheric mercury species over central and northern Europe. Model calculations and comparison with observations from the Nordic air and precipitation network for 1987 and 1988, Atmos Environ, 29 (1), 47–67.

Pfeiffer, W.C. Lacerda, L.D. (1988): Mercury inputs into the Amazon Region, Brazil, Environ. Technol. Lett., 9, 325–330.

Pirrone, N., Keeler, G.J., Nriagu, J.O. (1996): Regional differences in worldwide emissions of mercury to the atmosphere. Atmos. Environ. 30, 3379.

Platt, U.; Wagner, T. (**1998):** *Nature*, *395*, 486–490.

Porcella, D.B., Chu, P. and Allan, M.A. (1996): Inventory of North American mercury emissions to the atmosphere: Relationship to the global mercury cycle. In: W. Baeyens, R.Ebinghaus, and O.Vasiliev (eds.): Global and Regional Mercury Cycles: Sources, Fluxes and Mass Balances. NATO-ASI-Series, 2. Environment – Vol. 21, Kluwer Academic Publishers, Dordrecht, The Netherlands, 179–190.

Porcella, D.B. (1995): The atmospheric mercury pool, Proc. 1995 Canadian Mercury Netwok Workshop, York University, Toronto, Ontario, Canada.

Porcella, D.B. (1994): Mercury in the environment: biogeochemistry, in: Watras, C.J. and Huckabee, J.W. (eds.): Mercury pollution: integration and synthesis, 3–19, Lewis Publishers, Boca Raton

Poissant, L. and Casimir, A. (1996): Water-air and soil-air exchange rate of total gaseous mercury measured in Southern Québec (Canada), In: Ebinghaus, R., Petersen, G., Tümpling, U. v. (eds.), 1996: Fourth International Conference on Mercury as a Global Pollutant, Book of Abstracts, Hamburg August, 4–8, 1996, p. 136 (GKSS Forschungszentrum Geesthacht GmbH, Max-Planck-Str., D-21502 Geesthacht, Germany)

Prestbo, E.M., Bloom, N.S., Hall, B. (1995): Mercury speciation in coal combustion flue gas: methodology, intercomparison, artifatcs and atmospheric implications, Water Air Soil Pollut, 80, 145–158.

Priester, M. (1993): Tecnologia de meio ambiente para mini-mineraçao e sua difusao. A experienca de um projeto GTZ para evitar emissoes de mercurio na mineraçao primária de ouro no sul da Colombia. In: Mathis, A., Rehaag, R., (orgs), Consequencias da Garimpagem no Ambito Social e Ambiental da Amazonia. FASE/Buntstift e.V./Katalise, Belém, 102-112.

Prospero, J.M., Charlson, R.J., Mohnen, V., Jaenicke, R., Delany, A.C., Moyers, J., Zoller, W., Rahn, K. (1983): The atmospheric aerosol system: an overview, Rev Geophys Space Phys, 21, 1607–1629.

Raatz, W.E., Shaw, G.E. (1984): Long-range tropospheric transport transport of pollution aerosols into the Alaskan Arctic, Journal of Climatology and Applied Meteorology, 7 (23), 1052–1064.

Ramel, C. (1996): SCOPE project "Evaluation of the Role and Distribution of Mercury on Ecosystems with Special Emphasis on Tropical Regions". In: W. Baeyens, R.Ebinghaus, and O.Vasiliev (eds.): Global and Regional Mercury Cycles: Sources, Fluxes and Mass Balances. NATO-ASI-Series, 2. Environment – Vol. 21, Kluwer Academic Publishers, Dordrecht, The Netherlands, 505–513.

Rantalahti, R. (1996): Outokumpu Oy, Harjavalta– Personal communication.

Rasmussen, P.E. (1994): Current methods of estimating atmospheric mercury fluxes in remote areas, Environ. Sci. Technol. 28, 2233–2241.

Rea, A.W.; Keeler, G.J.; and Scherbatskoy, T. (1996): The deposition of mercury in throughfall and litterfall in the Lake Champlain Watershed: a short-term study. Atmos. Environ., 30, 3257–3263.

Reich, S. (1995): Untersuchungen zur Speziesanalytik von Quecksilber in Meerwasser, Diplomarbeit, Fachhochschule Hamburg.

Richter, A.; Wittrock, F.; Eisinger, M.; Burrows, J.P. (**1998):** Geophys. Res. Lett., 25, 2683–2686.

Richter-Politz, I. (1991): personal communication.

Ryaboshapko, A., Bullock, R., Ebinghaus, R., Ilyin, I., Lohman, K., Munthe, J., Petersen, G., Seigneur, C., Wängberg, I. (2002): Comparison of Mercury Chemistry Models, Atmospheric Environment, in press.

Ryaboshapko, A., Ilyin, I., Bullock, R., Ebinghaus, R., Lohman, K., Munthe, J., Petersen, G., Seigneur, Ch., Wängberg, I. (2001): Intercomparison Study of Numerical Models for Long-Range Atmospheric Transport of Mercury, Co-operative Programme for Monitoring and Evaluation of the Long-Range Transmission of Air Pollutants in Europe, EMEP Technical Report 2/2001, Meteorological Synthezising Centre East, Moskau, Russia.

Schmolke, S.R., Schroeder, W.H., Kock, H.H., Schneeberger, D., Munthe, J., Ebinghaus, R. (1999): Simultaneous measurements of total gaseous mercury at four sites on a 800 km transect: spatial distribution and short-time variability of total gaseous mercury over central Europe, Atmos. Environ., 33, 1725–1733.

Schmolke, S.R., Wängberg, I., Schager, P., Kock, H.H., Otten, S., Ebinghaus, R., Iverfeldt, Å. (1997): Estimates of the air/sea exchange of mercury derived from the Lagrangian experiment, summer 1997, 1st Ann. Meet. EU MAST III Project BASYS, Sept 29–Oct 1, Warnemünde, Germany.

Schroeder, W.H. (2000): Personal Communications, Meteorological Service of Canada, Downsview, Ontario, Canada.

Schroeder, W.H.; Anlauf, K.G.; Barrie, L.A.; Lu, J.Y.; Steffen, A.; Schneeberger, D.R.; Berg, T. (1998): Arctic springtime depletion of mercury, Nature, 394, 331–332.

Schroeder, W.H. and Munthe, J. (1998): Atmospheric Mercury – An overview, Atmos. Environ. 32, 809–822.

Schroeder, W.H. and Schneeberger, D. (1996): High temporal resolution measurements of total gaseous mercury at Alert, Northwest Territories, Canada. In: Ebinghaus, R., Petersen, G., Tumpling, U. (eds) 4th Int. Conf. on mercury as a global pollutant, Hamburg, Aug 4–8, 1996,

Schroeder, W. H., Ebinghaus, R., Shoeib, M., Timoschenko, K. and Barrie, L. A. (1995a) Atmospheric Mercury Measurements in the Northern Hemisphere from 56 ° to 82.5 °N Latitude. Water Air Soil Pollut., 80, 1227–1236.

Schroeder, W.H., Keeler, G., Kock, H., Roussel, P., Schneeberger, D. and Schaedlich, F. (1995b): International field intercomparison of atmospheric mercury measurement methods, Water Air Soil Pollut., 80, 611–620.

Schroeder, W.H., Lamborg, C., Schneeberger, D., Fitzgerald, W.F. and Srivastava, B. (1995c): Comparison of a manual method and an automated analyzer for determining total gaseous mercury in ambient air, In: R.-D. Wilken, U. Förstner and A. Knöchel (eds.): Proceedings of the 10th International Conference on Heavy Metals in the Environment, CEP Consultants Ltd., Publisher, Edinburgh, U.K., Vol. 2, pp. 57–60.

Schroeder, W.H., Lindqvist, O., Munthe, J. and Xiao, Z.F. (1992): Volatilization of mercury from lake surfaces, Sci. Total Environ. 125, 47–66.

Schroeder, W.H., Munthe, J. and Lindqvist, O. (1989): Cycling of mercury between water, air and soil components of the environment. Water Air Soil Pollut. 48, 337–347.

Schroeder, W.H., Lane, D.A. (1988): The fate of airborne toxic pollutants, Environ. Sci. Technol., 22,240–246.

Schroeder, W.H. and Jackson, R.A. (1987) Environmental measurements with an atmospheric mercury monitor having speciation capabilities, Chemosphere 16, 183 –199.

Sheu, G.-R.; Mason, R.P. (2001): An Examination of Methods for the Measurements of Reactive Gaseous Mercury in the Atmosphere, Environ. Sci. Technol., 35, 1209–1216.

Simonich, S.L., Hites, R.A. (1995): Global distribution of persistent organochlorine compounds, Science, 269, 1851–1854.

Slemr, F.; Brunke, E.; Labuschagne, C.; Ebinghaus, R.; Munthe, J., (2002): Worldwide trends in Atmospheric Mercury Concentrations, *Poster at EUROTRAC-2 Symposium 2002*, 11–15 March, 2002, Gamisch-Partenkirchen, Germany.

Slemr, F. and Scheel, H.E. (1998) Trends in atmospheric mercury concentrations at the summit of the Wank mountain, southern Germany, Atmos. Environ. **32**, 845–853.

Slemr, F. (1996): Trends in atmospheric mercury concentrations over the Atlantic Ocean and the Wank summit and the resulting constraints on the budget of atmospheric mercury, in: Baeyens, W., Ebinghaus, R., Vasiliev, O. (eds) Global and Regional Mercury Cycles: Sources, fluxes and mass balances, NATO ASI Series 2. Environment Vol. 21, Kluwer, Dordrecht, The Netherlands, pp 33–84.

Slemr, F., Robertson, P. and Brunke, E. (1996) Monitoring of atmospheric mercury at Cape Point and Wank. In: Proceedings of the 4th International Conference on Mercury as a Global Pollutant, eds. R. Ebinghaus, G. Petersen and U. v. Tümpling, August 4 - 8, 1996, Hamburg, p. 127.

Slemr, F.; Junkermann, W.; Schmidt, R.W.H.; Sladkovic, R. (**1995):** Geophys. Res. Lett., 22, 16, 2143–2146.

Slemr, F., Langer, E. (1992): Increase in global atmospheric concentrations of mercury inferred from measurements over the Atlantic Ocean, Nature, 355, 434–437.

Slemr, F., Schuster, G., Seiler, W. (1985): Distribution, speciation and budget of atmospheric mercury, J Atmos Chem, 3, 407–434.

Slemr, F., Seiler, W., Eberling, C. and Roggendorf, P. (1979) The determination of total gaseous mercury in air at background levels, Anal. Cim. Acta **110**, 35–47.

Sommar, J.; Gardfeldt, K.; Strömberg, D.; Feng, X. (2001): A kinetic study of the gas-phase reaction between the hydroxyl radical and atomic mercury, Atmos. Environ., 35, 3049–3054.

Spain, T.G. (1995): University College Galway, personal communication.

Sprovieri, F.; Pirrone, N.; Hedgecock, I.M.; Landis, M.S., Stevens, R.K. (2002): Intensive Atmospheric Mercury Measurements at Terra Nova Bay in Antarctica; Journal of Geophysical Research (in press).

Stern G.A., Muir, D.C.G., Segstro, M., Dietz, R., Heide-Jørgensen, M.-P. (1994): PCBs and other organochlorine contaminants in white whales (*Delphinaterus leucas*) from west Greenland: variations with age and sex, Meddelelser om Grønland, Bioscience, 39, 243–257.

Stock, A.; Cucuel, F. (1934): Die Bestimmung des Quecksilbergehalts der Luft, Berichte der Deutschen Chemischen Gesellschaft, 67, 122–127.

Stratton, W.J., Lindberg, S.E. (2001): Atmospheric mercury speciation: Laboratory and field evaluation of a mist chamber method for measuring reactive gaseous mercury, Environ. Sci. Technol. 35, 170–177.

Stratton, W.J., Lindberg, S.E. (1995): Use of a refluxing mist chamber for measurement of gas-phase water-soluble mercury(II) species in the atmosphere, Water Air Soil Poll, 80, 1269–1278.

Swaine, D.J. (1990): Trace elements in coal. UK, Butterworth and Co. Ltd., pp 276.

Tanabe, S., Iwata, H., Tatsukawa, R. (1994): Global contamination by persistent organochlorines and their ecotoxicological impact on marine mammals, Science of the Total Environment, 154, 163–177.

Tekran (1998): Tekran home page; Model 2537A – Principles of operation;
http://tekran.com/2537/2737poi.html.

Timoschenko, K. and Ebinghaus, R. (1994) Air chemistry: Determination of atmospheric mercury and aerosol black carbon, *Reports on Polar Research* **134**, 48–52.

Torres, E.B. (1992): Environmental and health surveillance of mercury in small scale gold processing industries in the Philippines. In: Proc. Int. Symp. Epidemiol. Stud. Environ. Pollut. and health effects of methylmercury, Nat. Inst. for Minamata Disease, Kumamoto, 56–65.

Turner, R. R., and S. E. Lindberg. (1978): Behavior and transport of mercury in a river-reservoir system downstream of an inactive chloralkali plant. Environ. Sci. Technol. 12:918–923.

Vandal, G.; Fitzgerald, W.F.; Rolfhus, K.; Russ, C. and Lamborg, C. (1996): Sources and Cycling of mercury and methylmercury in Long Island Sound: Preliminary Results, In: Ebinghaus, R., Petersen, G., Tümpling, U. v. (eds.), 1996: Fourth International Conference on Mercury as a Global Pollutant, Book of Abstracts, Hamburg August, 4–8, 1996, p. 458 (GKSS Forschungszentrum Geesthacht GmbH, Max-Planck-Str., D-21502 Geesthacht, Germany) .

Vandal, G.M., Fitzgerald, W.F., Rolfhus, K.R. and Lamborg, C.H. (1995): Modeling the elemental mercury cycle in Pallette Lake, Wisconsin, USA, Water, Air, Soil Pollut. 80, 529–538

Vandal, G.M., Mason, R.P. and Fitzgerald, W.F. (1991): Cycling of mercury in temperate lakes. Water Air Soil Poll. 56, 791–803.

Varekamp, J.C. and Buseck, P.R. (1986): Global mercury flux from volcanic and geothermal sources, Appl. Geochem. 1, 65–73

Varekamp, J.C. and Buseck, P.R. (1983): Hg anomalies in soils: a geochemical exploration method for geothermal areas, Geothermics 12, 29–47

Wallschläger, D., Kock, H.H., Schroeder, W.H., Lindberg, S.E., Ebinghaus, R. and Wilken, R.D. (2001): Estimating gaseous mercury emissions from contaminated floodplain soils to the atmosphere with simple field measurement techniques, Environ. Sci. Technol., in press.

Wallschläger, D., Kock, H.H., Schroeder, W.H., Lindberg, S.E., Ebinghaus, R. and Wilken, R.D. (2000). Mechnism and significance of mercury volatilization from contaminated floodplains of the German river Elbe, Atmos. Environment, 34 (22), 3745–3755.

Wallschläger, D. and Wilken, R.D. (1997): The influence of floodplains on mercury availability, in: Dwyer, J.F. et al. (eds.): Environmental toxicology and risk assessment: Modeling and risk assessment (6th vol.), 179–196, ASTM STP 1317, American Society for Testing and Materials, West Conshohocken

Wallschläger D., Wilken, R.-D. (1996): The Elber River: A special example for a European river contaminated heavily with mercury, in: Baeyens, W., Ebinghaus, R., Vasiliev, O. (eds) Global and Regional Mercury Cycles: Sources, fluxes and mass balances, NATO ASI Series, 2. Environment – Vol. 21, Kluwer, Dordrecht, The Netherlands, pp 317–328.

Wallschläger, D. (1996): Speziesanalytische Untersuchungen zur Abschätzung des Remobilisierungspotentials von Quecksilber aus kontaminierten Elbauen, Ph.D. thesis, University of Bremen and GKSS Research Center, Geesthacht,

Wallschläger, D., Hintelmann, H., Evans, R.D. and Wilken, R.D. (1995): Volatilization of dimethylmercury and elemental mercuryfrom river Elbe floodplain soils, Water, Air, Soil Pollut. 80, 1325–1329.

Wania, F., Mackay D. (1993): Global fractionation and cold condensationof low-volatility organochlorine compounds in polar regions, Ambio, 22. 10–18.

Warneck, P. (1988): *Chemistry of the natural atmosphere*, Academic Publ., New York.

Watras, C.J. et al. (1994): Sourcesa and fates of mercury and methylmercury in Wisconsin lakes, in: Watras, C.J. and Huckabee, J.W. (eds.): Mercury pollution: integration and synthesis, 153–177, Lewis Publishers, Boca Raton.

Weller, R., Schrems, O. (1996): Photooxidants in the marine Arctic troposphere in summer, Journal of Geophysical Research, 101 (D4), 9139–9147.

Wessel, S.; Aoki, S.; Winkler, P.; Weller, R.; Herber, A.; Gernandt, H.; Schrems, O. (**1998**,): *Tellus 50B*, 34–50.

Wilken, R.D. and Hintelmann, H. (1991): Mercury and methylmercury in sediments and suspended particles from the river Elbe, North Germany, Water, Air, Soil Pollut. 56, 427–437.

Wilson, R., Allen-Gil, S., Griffin, D., Landers, D. (1995): Organochlorine contaminants in fish from an Arctic lake in Alaska, USA, Science of the Total Environment, 160/161, 511–519.

Windmöller, C.C., Wilken, R.-D., Jardim, W. (1996):) Mercury Speciation in Contaminated
Soils by Thermal Release Analysis, Water, Air, Soil Pollut. 89, 399–416.

WMO/EMEP /UNEP (1999): Workshop on modelling of Atmospheric Transport and Deposition of Persistent Organic Pollutants and Heavy Metals, Geneva, Switzerland, 16 to 19 November 1999

Xiao, Z., Sommar, J., Wie, S., Lindqvist, O. (1997): Sampling and determination of gas-phase divalent mercury in the air using a KCl coated denuder, Fresenius J Anal Chem, 358, 386–391.

Xiao, Z., Munthe, J., Schroeder, W.H. and Lindqvist O. (1991): Vertical fluxes of mercury over forest soil and lake surfaces in Sweden. Tellus 43B, 267–279.

Youden, W.J. and Steiner, E.H. (1975): Statistical Manual of the Association of Official Analytical Chemists. AOAC, Arlington, VA.

Yshuan,Y.S.(1994):In:Evaluation of the role and distribution of mercury in ecosystems with special emphasis on tropical regions, SCOPE, Rio de Janeiro (unpublished).

Zapata , J.Q. (1994): Environmental impacts study of gold mining in Nueva Esperanza in the Madeira River Bolivian-Brazilian border. In: Environmental mercury pollution and its health effects in Amazon River Basin. Nat. Inst Minamata Disease and Inst Biophysics of the Univ Federal do Rio de Janeiro, Rio de Janeiro, 23–24,

Zhou, X.; Beine, H.J.; Honrath, R.E.; Fuentes, J.D.; Simpson, W.; Shepson, P.B.; Bottenheim, J.W. (2001): Geophys. Res. Lett., 28, 4087–409.

10 Acknowledgements

This work would not have been possible without the excellent research opportunities at the GKSS Research Centre in Geesthacht, my scientific home institute since 1991. I would like to thank my directors for the chance and challenge to summarize ten years of research work related to the environmental chemistry of atmospheric mercury in this habilitation thesis.

Special thanks go to the Dean of the Department of Environmental Sciences of the University of Lüneburg Prof. Dr. Wolfgang Ruck and his predecessor Prof. Dr. Werner Härdtle for their promotion. This work was performed during my ongoing lectures at the University of Lüneburg.

Numerous colleagues have contributed to different aspects of this work however, only one person was involved in all studies that are presented here:

Hans Herbert Kock's input to this work can hardly be overestimated and I would like to express my special gratitude to Hans for his untiring support in the realization of all research projects that we have carried out – the first (sometimes diffuse) ideas with initial and constructive discussions, the work carried out in the lab and in the field and finally the publication of the scientific results.

The cooperation with my colleagues from the field of numerical modeling was very fruitful and I have learnt a lot during many discussions about modeling aspects related to the environmental behavior of atmospheric mercury. I am very grateful to Gerhard Petersen, who has significantly influenced the research direction of my work, for his long-lasting support and many stimulating discussions. I also thank Olaf Krüger for the model runs carried out during the BUNA studies.

Stefan Schmolke, Volker Thele and Franz Slemr (Max-Planck-Institute for Chemistry) have significantly contributed to the transect and air craft studies and I would like to thank them for their time and work.

The work at Mace Head was and is possible because of the excellent cooperation with Gerry Spain and Gerry Jennings. I always enjoyed my stays in Ireland and appreciated the scientific input and hospitality of our Irish partners.

I would like to thank Christian Temme (University of Jena), Astrid Löwe (Alfred Wegener Institute) and Bill Schroeder (Meteorological Service of Canada) for their individual contributions to the work onboard *RV Polarstern* and at Neumayer Station. Christian went down to Antarctica with Polarstern twice and carried out the field work during polar summer. Astrid was one of the "Überwinterer" and took care of our measurements for about one year. Bill Schroeder, as the initiator of worldwide research on MDEs in the North and South Polar regions, contributed to this work by many helpful discussions and his enormous knowledge on atmospheric mercury.

Bernd Neidhart supported me throughout the past five years with his friendly promotion and his confidence. He gave me the opportunity and the degree of freedom that enabled me to conduct my research work at GKSS and this thesis in parallel and I am very grateful for this.

I am deeply indebted to my wife Christine for her encouragement, stimulation and the time she shared with me.

This work is dedicated to my late father Franz Josef and my mother Rosalie.

11 List of Abbreviations and Acronyms

ACO: Air Chemistry Observatory

AMAP: Arctic Monitoring and Assessment Program

AQFWD: Air Quality Framework Directive

A.S.L.: Above Sea Level

ASSD: Astronomic Sunshine Duration

AWI: Alfred Wegener Institute for Polar and Marine Research

BC: Black Carbon Aerosol (Soot)

CNC: Condensation Nuclei Concentration

CLTRAP: Convention on Long-Range Transport of Air Pollutants

CVAAS: Cold-Vapor Atomic Absorption Spectrometry

CVAFS: Cold-Vapor Atomic Fluorescence Spectrometry

DGM: Dissolved Gaseous Mercury

DMM: Dimethylmercury

DOAS: Differential Optical Absorption Spectrometry

DOC: Dissolved Organic Carbon

DWD: Deutscher Wetterdienst (German Weather Service)

ECMWF: European Centre for Medium Range Weather Forecasting

EFPC: East Fork Poplar Creek

EMEP: European Monitoring and Evaluation Program

EPO: Equatorial Pacific Ocean

ER: Emission Ratio

GAW: Global Atmosphere Watch

GEM: Gaseous Elemental Mercury

GOME: Global Ozone Monitoring Experiment

HELCOM: Baltic Marine Environment Protection Commission (Helsinki Commission)

IOGM: Inorganic Oxidized Gaseous Mercury

ISCAT: Investigation of Sulphur Chemistry in the Antarctic Troposphere

ITCZ: Intertropical Convergence Zone

MBR: modified Bowen-ratio method

MDE(s): Mercury Depletion Event(s)

MSC: Meteorological Synthesizing Center

MTL: Mercury in Temperate Lakes Project

NOAA: National Oceanic and Atmospheric Administration

OSPAR: The Convention for the Protection of the Marine Environment of the North-East Atlantic (Oslo-Paris-Commission)

RGM: Reactive Gaseous mercury

STP: Standard Temperature and Pressure

TGM: Total Gaseous mercury

TPM: Total Particulate Mercury

UN-ECE: United Nation - Economic Commission for Europe

UNEP: United Nation Environment Program

VC: Vertical Column Density

WBW: Walker Branch Watershed

WD: Wind Direction

WMO: World Meteorological Organization

List of Figures

7.12	Cross-correlation function of TGM (mean values from two separate analysers in the highest time resolution (i.e. 15 min)) and 15-minute averaged ground level ozone concentrations during the mercury depletion events (MDEs)
7.13	Comparison of the annual time-series of total gaseous mercury concentrations in the Antarctic (Neumayer) and Arctic (Alert). All data are exponentially smoothed
7.14	Schematic diagram for the integrated system of the Tekran 1130 speciation unit connected to the Tekran 2537A
7.15	Selected 2-hour averaged mercury species concentrations during the summer period (Dec 00 – Feb 01) containing RGM levels (> 0.15 ng/m^3) and the respective residuals of TGM – (GEM + RGM)
7.16	Annual time series of 1-hour averaged TGM and surface-level ozone concentrations at Neumayer, January 2000 – February 2001 and their weekly mean correlation coefficients r. The TGM concentrations were obtained from two separate Tekran analysers and mean values were used if both analysers were operating in parallel
7.17	Comparison of the 12-hour averaged TGM concentrations (smoothed) and the duration of sea ice contact of the surface air parcels obtained from trajectory calculations ending at Neumayer at 12:00 and 24:00 UT. The dashed line represents the astronomical sunshine duration (ASSD) for each day
7.18	Atmospheric mercury species concentrations at Neumayer Station between 23rd of December 2000 and 05th of February 2001. TGM, RGM and GEM levels are 2-hourly mean concentrations. TPM concentrations were obtained from 48-h integrated samples. Missing data in the RGM concentrations were due to the automatic calibration cycles for the Tekran analyser
7.19	Two-hourly averaged atmospheric mercury species concentrations over the south Atlantic Ocean measured on board of the *RV Polarstern* during cruise ANTXVIII/4 (Neumayer – Punta Arenas, February 2001)
7.20	Two-hourly averaged atmospheric mercury species TGM, GEM, RGM, and ozone concentrations together with selected meteorological and chemical parameters for a single event during Antarctic summer. T10 and T2 represent the air temperature at 2 m and 10 m height

List of Tables